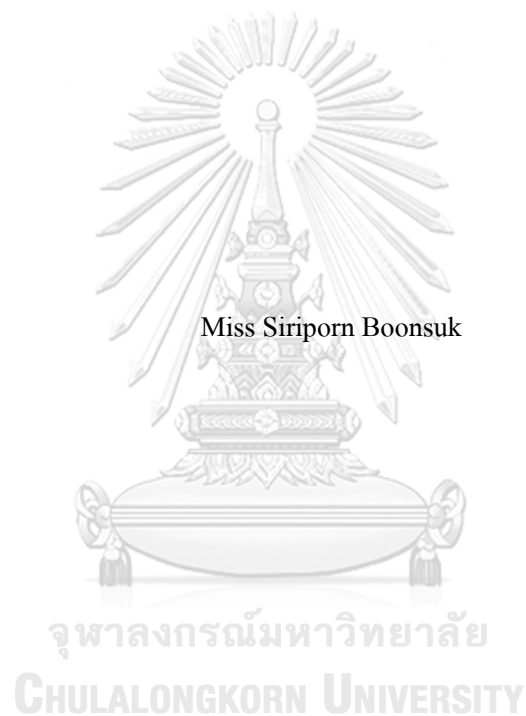


DESIGN AND PERFORMANCE EVALUATION OF INTEGRATED SYSTEM OF
HYDROTREATING AND HYDROGEN GENERATION FOR BIO-HYDROGENATED
DIESEL FUEL PRODUCTION FROM PALM OIL



A Thesis Submitted in Partial Fulfillment of the Requirements
for the Degree of Master of Engineering in Chemical Engineering

Department of Chemical Engineering

Faculty of Engineering

Chulalongkorn University

Academic Year 2018

Copyright of Chulalongkorn University

การออกแบบและประเมินสมรรถนะของกระบวนการรวมไฮโดรทรีตติงและการผลิตไฮโดรเจน
สำหรับการผลิตเชื้อเพลิงชนิดไบโอไฮโดรเจนดีเซลจากน้ำมันปาล์ม



วิทยานิพนธ์นี้เป็นส่วนหนึ่งของการศึกษาตามหลักสูตรปริญญาวิศวกรรมศาสตรมหาบัณฑิต
สาขาวิชาวิศวกรรมเคมี ภาควิชาวิศวกรรมเคมี
คณะวิศวกรรมศาสตร์ จุฬาลงกรณ์มหาวิทยาลัย
ปีการศึกษา 2561
ลิขสิทธิ์ของจุฬาลงกรณ์มหาวิทยาลัย

Thesis Title	DESIGN AND PERFORMANCE EVALUATION OF INTEGRATED SYSTEM OF HYDROTREATING AND HYDROGEN GENERATION FOR BIO-HYDROGENATED DIESEL FUEL PRODUCTION FROM PALM OIL
By	Miss Siriporn Boonsuk
Field of Study	Chemical Engineering
Thesis Advisor	Professor Suttichai Assabumrungrat, Ph.D.
Thesis Co Advisor	Assistant Professor Worapon Kiatkittipong, D.Eng.

Accepted by the Faculty of Engineering, Chulalongkorn University in Partial
Fulfillment of the Requirement for the Master of Engineering

..... Dean of the Faculty of Engineering
(Associate Professor Supot Teachavorasinskun, D.Eng.)

THESIS COMMITTEE

..... Chairman
(Pongtorn Charoensuppanimit, Ph.D.)

..... Thesis Advisor
(Professor Suttichai Assabumrungrat, Ph.D.)

..... Thesis Co-Advisor
(Assistant Professor Worapon Kiatkittipong, D.Eng.)

..... Examiner
(Rungthiwa Methaapanon, Ph.D.)

..... External Examiner
(Assistant Professor Kanokwan Ngaosuwan, D.Eng.)

สิริภรณ์ บุญสุข : การออกแบบและประเมินสมรรถนะของกระบวนการรวมไฮโดรทรีตติงและการผลิตไฮโดรเจนสำหรับการผลิตเชื้อเพลิงชนิดไบโอดีเซลจากน้ำมันปาล์ม. (DESIGN AND PERFORMANCE EVALUATION OF INTEGRATED SYSTEM OF HYDROTREATING AND HYDROGEN GENERATION FOR BIO-HYDROGENATED DIESEL FUEL PRODUCTION FROM PALM OIL) อ.ที่ปรึกษาหลัก : ศ. ดร.สุทธิชัย อัสสะบารุงรัตน์, อ.ที่ปรึกษาร่วม : ผศ. ดร.วราพล เกียรติกิตติพงษ์

งานวิจัยนี้ได้ศึกษาถึงการจำลองกระบวนการควบรวมระหว่างกระบวนการไฮโดรทรีตติงและการผลิตไฮโดรเจนด้วยปฏิกิริยาไดออกซิเจนชั้นที่แตกต่างกัน (ได้แก่ ปฏิกิริยาดีคาร์บอนซิเลชันไฮโดรดีคาร์บอนิเลชันและปฏิกิริยาไฮโดรไดออกซิเจนชั้น) กระบวนการควบรวมถูกนำเสนอในสองรูปแบบคือ 1) การควบรวมระหว่างกระบวนการไฮโดรทรีตติงแบบขั้นตอนเดียวและกระบวนการผลิตไฮโดรเจนด้วยการรีฟอร์มมิงโพรเพนด้วยไอน้ำ (เรียกว่า “กระบวนการรวมแบบขั้นตอนเดียว”) และ 2) การควบรวมระหว่างกระบวนการไฮโดรทรีตติงแบบสองขั้นตอนร่วมกับกระบวนการผลิตไฮโดรเจนด้วยการรีฟอร์มมิงกลีเซอรอลด้วยไอน้ำ (เรียกว่า “กระบวนการรวมแบบสองขั้นตอน”) ผลการวิจัยพบว่าการเลือกปฏิกิริยาไดออกซิเจนชั้นด้วยปฏิกิริยาดีคาร์บอนซิเลชันมีความต้องการใช้พลังงานขั้นต่าที่น้อยที่สุดและให้ประสิทธิภาพของกระบวนการทั้งหมดสูงที่สุดสำหรับการควบรวมกระบวนการทั้งสองรูปแบบเนื่องจากมีความต้องการไฟฟ้าต่ำกว่าเพื่อกักอัดไฮโดรเจน นอกจากนี้กระบวนการควบรวมแบบขั้นตอนเดียวมีความต้องการใช้พลังงานขั้นต่าที่น้อยกว่ากระบวนการรวมในสองขั้นตอนอย่างมีนัยสำคัญ เพราะมีความต้องการระบบให้ความเย็นและความร้อนต่ำกว่ามาก ในกรณีของวัตดูดิบไตรโอเลอิน ไฮโดรเจนส่วนเกินสามารถทำได้เฉพาะเส้นทางปฏิกิริยาดีคาร์บอนซิเลชันเท่านั้นด้วยกระบวนการควบรวมแบบสองขั้นตอน ในทางตรงกันข้าม ในกรณีของไตรปาล์มมีดินซึ่งเป็นวัตดูดิบชนิดอิมตัว ไฮโดรเจนส่วนเกินสามารถทำได้จากเส้นทางปฏิกิริยาดีคาร์บอนซิเลชันและปฏิกิริยาไฮโดรดีคาร์บอนิเลชันในทั้งสองกระบวนการควบรวม กล่าวโดยสรุปเส้นทางปฏิกิริยาดีคาร์บอนซิเลชันของกระบวนการควบรวมแบบขั้นตอนเดียวให้ประสิทธิภาพของกระบวนการทั้งหมดสูงที่สุด ซึ่งไตรปาล์มมีดินให้ประสิทธิภาพของกระบวนการทั้งหมดสูงที่สุดที่ร้อยละ 89.3 ขณะที่ไตรโอเลอินให้ร้อยละ 86.7 เนื่องจากไตรปาล์มมีดินต้องการปริมาณไฮโดรเจนน้อยกว่าไตรโอเลอิน

สาขาวิชา วิศวกรรมเคมี
ปีการศึกษา 2561

ลายมือชื่อนิสิต
ลายมือชื่อ อ.ที่ปรึกษาหลัก
ลายมือชื่อ อ.ที่ปรึกษาร่วม

5970464221 : MAJOR CHEMICAL ENGINEERING

KEYWORD: HYDROTREATING, BIO-HYDROGENATED DIESEL, PROPANE STEAM REFORMING, GLYCEROL STEAM REFORMING, HYDROGEN GENERATION, HEAT INTEGRATION, PERFORMANCE EVALUATION

Siriporn Boonsuk : DESIGN AND PERFORMANCE EVALUATION OF INTEGRATED SYSTEM OF HYDROTREATING AND HYDROGEN GENERATION FOR BIO-HYDROGENATED DIESEL FUEL PRODUCTION FROM PALM OIL. Advisor: Prof. Suttichai Assabumrungrat, Ph.D. Co-advisor: Asst. Prof. Worapon Kiatkittipong, D.Eng.

This research studied the simulations of the integrated systems between of hydrotreating and hydrogen generation with various selectivity of deoxygenation (DO) pathways (i.e. decarboxylation (DCO₂), hydrodecarbonylation (HDCO), and hydrodeoxygenation (HDO)). Two integrated systems were proposed i.e. 1) integrated system between single-step hydrotreating and propane steam reforming (as called “*single-step integrated system*”) and 2) integrated system between two-step hydrotreating (hydrolysis+DO) and glycerol steam reforming (as called “*two-step integrated system*”). Results revealed that, among DO pathways, DCO₂ exhibited the lowest total minimum energy requirement (total MER) and the highest total efficiency for both integrated systems mainly due to lower electricity requirement to compress H₂. In addition, *single-step integrated system* offered significantly lower total MER than that of *two-step integrated system* because it required much lower cooling and heating utilities. In the case of triolein feed, H₂ surplus can be achieved only for DCO₂ pathway with *two-step integrated system*. On the contrary, in the case of tripalmitin, saturated feedstock, H₂ surplus can be achieved from DCO₂ and HDCO in both integrated systems. In summarize, DCO₂ pathway of *single-step integrated system* offers the highest total efficiency which tripalmitin, as expected, offeres the highest total efficiency (89.3%) while triolein offeres 86.7% since less amount H₂ is required.

Field of Study: Chemical Engineering

Academic Year: 2018

Student's Signature

Advisor's Signature

Co-advisor's Signature

ACKNOWLEDGEMENTS

First of all, I would like to respect and fully appreciate my advisor, Professor Suttichai Assabumrungrat, and my co-advisor, Assistant Professor Worapon Kiatkittipong, for their suggestions that are useful to my work.

In my thesis, I would also be grateful to the thesis committee commendation, Dr. Pongtorn Charoensuppanimit, Dr. Rungthiwa Methaapanon, and Assistant Professor Kanokwan Ngaosuwan, for the valuable guidance to this research. My special thanks belong to Associate Professor Doonyapong Wongsawaeng for improving my thesis.

Moreover, I am grateful to the scientists, my seniors, and my friends, who are the members of Center of Excellence on Catalysis and Catalytic Reaction Engineering and special thanks to the friends who are the members of control lab for work area, advice, counseling including friendship and encouragement. I would like to give my special thanks to Mr. Natthaporn Saithong, a good friend who provide ideas on my work.

Finally, I would like express my deepest gratitude to my beloved parents, who always support me on everything and who helped make my study successful.



Siriporn Boonsuk

TABLE OF CONTENTS

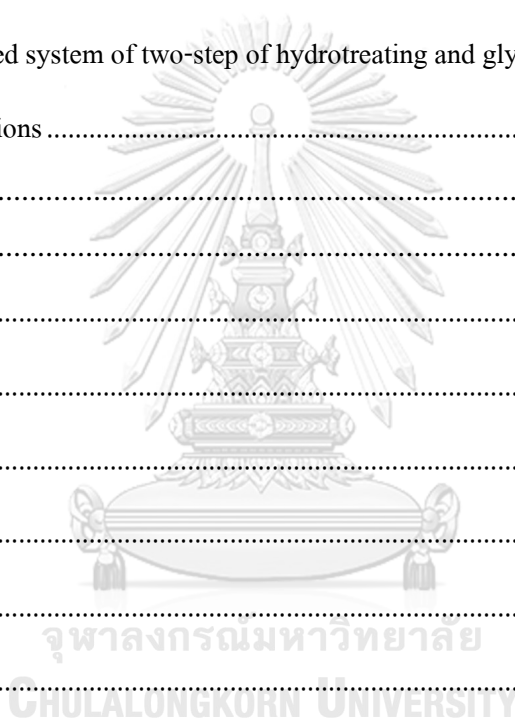
	Page
ABSTRACT (THAI)	iii
ABSTRACT (ENGLISH)	iv
ACKNOWLEDGEMENTS	v
TABLE OF CONTENTS	vi
LIST OF FIGURES	xi
LIST OF TABLES	xx
NOMENCLATURE	xxiii
CHAPTER I INTRODUCTION	1
1.1 Motivation	1
1.2 Objective	3
1.3 Scope of work	3
1.4 Methodology	3
1.5 Expected output	5
1.6 Research plan	8
CHAPTER II THEORY	9
2.1 Oil feedstocks	9
2.2 Bio-hydrogenated diesel	11
2.3 Hydrotreating	14
2.3.1 Hydrogenation	14
2.3.2 Hydrogenolysis	15
2.3.3 Hydrolysis	16
2.3.4 Deoxygenation	16
2.3.5 Hydroisomerization	18

2.4 Steam reforming process	19
2.4.1 Propane steam reforming	19
2.4.2 Glycerol steam reforming	20
CHAPTER III LITERATURE REVIEWS	21
3.1 Bio-hydrogenated diesel fuel production	21
3.1.1 Single-step of hydrogenolysis of triglycerides/ deoxygenation of free fatty acids process	21
3.1.2 Two-step: hydrolysis of triglycerides and deoxygenation of free fatty acids process	39
3.2 Hydrogen production.....	47
3.2.1 Propane steam reforming process	47
3.2.2 Glycerol steam reforming process	49
3.3 Integrated system of hydrotreating and hydrogen generation process	53
3.3.1 Multiple processes of integrated system of hydrotreating and hydrogen generation	53
3.3.2 Single process of integrated system of hydrotreating and hydrogen generation	57
3.4 Pressure swing adsorption technology	61
3.5 Catalysts for hydrotreating of triglycerides/ free fatty acids process	64
(1) Noble metal catalyst	64
(2) Non-noble metal and non-sulfide catalyst.....	65
(3) Bimetallic sulfide catalyst	66
3.6 Thermodynamic of hydrotreating.....	67
CHAPTER IV PROCESS SIMULATION	69
4.1 Thermodynamic property methods	69
4.2 Bio-hydrogenated diesel fuel production	70

4.2.1 Single-step of hydrogenolysis of triglycerides/ deoxygenation of free fatty acids process	70
4.2.1.1 Modelling validation of hydrogenolysis of triglycerides/ deoxygenation of free fatty acids	70
4.2.1.2 Process and operating condition selection of single-step of hydrotreating ..	75
4.2.1.3 Process description of single-step of hydrotreating	75
4.2.2 Two-step: hydrolysis of triglycerides and deoxygenation of free fatty acids process	81
4.2.2.1 Modelling validation of hydrolysis of triglycerides and deoxygenation of free fatty acids	81
4.2.2.2 Process and operating condition selection of two-step of hydrotreating	81
4.2.2.3 Process description of two-step of hydrotreating	82
4.3 Hydrogen production.....	89
4.3.1 Propane steam reforming process	89
4.3.1.1 Modelling validation of propane steam reforming	89
4.3.1.2 Process and operating condition selection of propane steam reforming.....	91
4.3.1.3 Process description of propane steam reforming	92
4.3.2 Glycerol steam reforming process	96
4.3.2.1 Modelling validation of glycerol steam reforming	96
4.3.2.2 Process and operating condition selection of glycerol steam reforming	98
4.3.2.3 Process description of glycerol steam reforming.....	99
4.4 Integrated system of hydrotreating and hydrogen generation	103
4.4.1 Integrated system of single-step of hydrotreating and propane steam reforming	103
4.4.1.1 Base case condition of integrated system	103
4.4.1.2 Material balance condition of integrated system	103

4.4.2 Integrated system of two-step of hydrotreating and glycerol steam reforming	112
4.4.4.1 Base case condition of integrated system	112
4.4.2.2 Material balance condition of integrated system	112
CHAPTER V RESULTS AND DISCUSSION	122
5.1 Performance evaluation of integrated system of hydrotreating and hydrogen generation.	122
5.1.1 Net H ₂ of integrated system	125
5.1.1.1 Net H ₂ of integrated system of single-step of hydrotreating and propane steam reforming.....	126
5.1.1.2 Net H ₂ of integrated system of two-step of hydrotreating and glycerol steam reforming	128
5.1.2 Energy requirement of integrated system	131
5.1.2.1 Energy requirement of integrated system of single-step of hydrotreating and propane steam reforming	132
5.1.2.2 Energy requirement of integrated system of two-step of hydrotreating and glycerol steam reforming.....	134
5.1.3 Electricity requirement of integrated system	136
5.1.3.1 Electricity requirement of integrated system of single-step of hydrotreating and propane steam reforming	137
5.1.3.2 Electricity requirement of integrated system of two-step of hydrotreating and glycerol steam reforming.....	138
5.1.4 Minimum energy requirement of integrated system	140
5.1.4.1 Minimum energy requirement of integrated system of single-step of hydrotreating and propane steam reforming.....	143
5.1.4.2 Minimum energy requirement of integrated system of two-step of hydrotreating and glycerol steam reforming	143
5.1.5 Total minimum energy requirement of integrated system	143

5.1.6 Thermal efficiency of integrated system.....	147
5.1.7 Total efficiency of integrated system.....	148
5.2 Comparison of the results of integrated system of hydrotreating and hydrogen generation	152
CHAPTER VI CONCLUSION AND RECOMMENDATIONS	156
6.1 Conclusion.....	156
6.1.1 Integrated system of single-step of hydrotreating and propane steam reforming	156
6.1.2 Integrated system of two-step of hydrotreating and glycerol steam reforming	157
6.2 Recommendations	158
REFERENCES	159
APPENDIX.....	168
APPENDIX A	169
APPENDIX B	173
APPENDIX C	175
APPENDIX D	176
APPENDIX E.....	182
APPENDIX F	188
APPENDIX G	197
APPENDIX H	198
VITA.....	206



LIST OF FIGURES

	Page
Figure 1.1 The pathways of integrated system of hydrotreating and hydrogen generation for bio-hydrogenated diesel fuel production.	6
Figure 1.2 Block diagram of integrated system of single-step of hydrotreating and hydrogen generation.....	7
Figure 1.3 Block diagram of integrated system of two-step of hydrotreating and hydrogen generation.....	7
Figure 2.1 Example of unsaturated triglycerides ($C_{55}H_{98}O_6$) ¹³	9
Figure 2.2 Ecofining™ process producing alternative diesel fuel ¹⁷	12
Figure 2.3 Ecofining process diagram ¹⁸	12
Figure 2.4 Revamped hydrotreater for raw tall diesel co-processing ¹⁹	13
Figure 2.5 NExBTL process to produce green diesel ²⁰	13
Figure 2.6 NExBTL Process Chemistry ²⁰	14
Figure 2.7 Hydrotreating of triglycerides pathways ²	14
Figure 2.8 Partial hydrogenation of triglycerides ²⁴	15
Figure 2.9 Freezing point and number of cetane of carbon number in n-paraffins and methyl branched paraffins ¹⁴	19
Figure 3.1 TGs reaction's possible routes in hydrotreating of vegetable oils ^{7, 32}	22
Figure 3.2 Process flow diagram of renewable diesel production with hydrotreating of palm oil ³²	23
Figure 3.3 Hydrotreating process ⁶	23
Figure 3.4 Renewable jet fuel production ¹	24
Figure 3.5 Process flow diagram of green diesel production model ³⁴	25
Figure 3.6 BHD production process diagram ³⁵	26
Figure 3.7 Process flow diagram of BHD production ³⁸	27
Figure 3.8 Process flow diagram of hydrotreated vegetable oil ³⁹	27
Figure 3.9 Gibbs free energies of total hydrogenation into hydrocarbons with various temperatures at pressure of 70 bar ⁴⁰	28

Figure 3.10 Concentrations of C ₁₇ and C ₁₈ hydrocarbon at 70 bar for tristearate (calculation) and rape-seed oil (experiments) hydrogenation ⁴⁰	29
Figure 3.11 Profile of C ₁₅ /C ₁₆ , C ₁₇ /C ₁₈ from equilibrium and experimental at 350 °C with various pressures of reactor ³³	30
Figure 3.12 Profiles of mass fractions of equilibrium at 350 °C and 12.5:1 of H ₂ :CPO with various pressures of reactor and 20:1 of H ₂ : CPO at 350 °C from experimental data ³³	30
Figure 3.13 Hydrogen consumption at 350 °C, 2 h ⁻¹ of LHSV with various pressures of reactor and H ₂ :CPO ratios ³³	31
Figure 3.14 Hydrodeoxygenation of stearic acid mechanism pathways, using Ni catalyst ⁴¹	32
Figure 3.15 The reaction temperatures effect on conversion of stearic acid using nickel supported catalyst, 0.18 kmol/m ³ of concentration of stearic acid and 8 bar of initial hydrogen pressure ⁴¹	33
Figure 3.16 The network of reaction for deoxygenation of stearic acid ⁴²	34
Figure 3.17 Total pressure effects on deoxygenation of stearic acid using 5 wt.% Ni-γ-Al ₂ O ₃ at 300 °C of temperature. Symbols: (o) stearic acid, (□) heptadecane, (*) stearyl alcohol, and (+) octadecane ⁴²	35
Figure 3.18 Biodiesel production process with hydrolysis of triolein using plug flow reactor ⁴³	40
Figure 3.19 FFAs yields obtained from rapeseed oil in subcritical waters in various conditions ⁴⁴	40
Figure 3.20 Molar (%) of stearic acid (■), heptadecane (●), stearylalcohol (□), and octadecane (Δ) in the HDO reaction of TOFA. Conditions of reaction: 300 °C of temperatue and total pressure in hydrogen of 30 bar ⁴²	41
Figure 3.21 Continuous hydrolysis and fed-batch decarboxylation system ⁴⁵	42

Figure 3.22 Concentrations of TG, DG, and MG with various times at 250 °C of temperature, water feed rate of 20 mL/min, and oil feed rate of 10 mL/min ⁴⁵	42
Figure 3.23 Concentrations of FFA and GLY with various times at 250 °C of temperature, water feed rate of 20 mL/min, and oil feed rate of 10 mL/min ⁴⁵	43
Figure 3.24 Molar flow rates of CO ₂ and CO and mol (%) of effluent H ₂ obtained from deoxygenation of canola oil derived FFA for fed-batch at 300 °C and 19 bar, using 5% Pd/C catalyst with dodecane solvent and 7.0 mL/min of feed rate ⁴⁵	43
Figure 3.25 Diagram of the hydrolysis, DCO ₂ , and isomerization/hydrocracking process ⁴⁷	45
Figure 3.26 Moles of hydrogen generated per mole of propane (open symbol) and SESR (solid symbol) of propane with various pressures and 6 of WPMR ⁴⁸	47
Figure 3.27 Moles of hydrogen generated per mole of propane with various WPMR and temperature at atmospheric pressure (A) ⁴⁸	48
Figure 3.28 Products composition with various temperatures at atmospheric pressure and 12 of WPMR (A) ⁴⁸	48
Figure 3.29 PSR performance on gas distribution from Ni/YSZ and 1.0% M/Ni/YSZ catalysts (M =Ru, Rh, Pd, and Ag), and selectivity of gas at 650 °C ⁴⁹	49
Figure 3.30 H ₂ selectivity in GSR using three catalysts ¹⁰	50
Figure 3.31 Conversions of glycerol and steam with various temperatures ¹⁰	51
Figure 3.32 Molar number of thermodynamic equilibrium of GSR: (a) conversion and (b) gas products ¹⁰	52
Figure 3.33 Hydrogen mole generated per glycerol mole unit in the GSR reactor with various WGMR and temperatures at atmospheric pressure ⁵¹	53

Figure 3.34 Yields of synthesis gas in the equilibrium GSR reactor with various temperatures and WGMR at atmospheric pressure: (a) CO, (b) CH ₄ ⁵¹	53
Figure 3.35 Diagram of aviation fuel production ⁵²	54
Figure 3.36 Process flow diagram for base case condition of combined process ¹⁶	55
Figure 3.37 Process flow diagram for hydrogen generation via GSR ¹⁶	55
Figure 3.38 Process flow diagram for hydrotreating of stearic acid ¹⁶	55
Figure 3.39 Process structure of the simulation model ⁵³	56
Figure 3.40 Vegetable oils hydroprocessing unit ⁵⁴	57
Figure 3.41 Possible reaction of green diesel production from vegetable oil using PtNi/Al ₂ O ₃ +Pd/C combined ⁵⁵	58
Figure 3.42 Range of adsorption force of compounds ⁵⁷	61
Figure 3.43 Isotherm of adsorption between partial pressure of molecule of gas and equilibrium of loading onto material of adsorbent ⁵⁷	62
Figure 3.44 Process diagram of PSA system ⁵⁷	62
Figure 3.45 Results of CO ₂ /CO ratio with various sampling times using 5% Pd/C and 5% Pt/C catalysts, operating condition at 300 °C of temperature, 6 bar of pressure for stearic acid deoxygenation ²⁶	64
Figure 4.1 Reaction temperature effect on conversion of stearic acid using nickel supported catalyst, 0.18 kmol/m ³ of concentration of stearic acid and 8 bar of initial hydrogen pressure between experiment and simulation from kinetic model of Kumar and co-workers ⁴¹	71
Figure 4.2 Product selectivity of hydrotreating of stearic acid using nickel supported catalyst at 95% conversion of stearic acid, 0.18 kmol/m ³ of concentration of stearic acid, 280 °C and 290 °C of reaction temperature and 8 bar of initial hydrogen pressure between experiment and simulation from kinetic model of Kumar and co-workers ⁴¹	72

- Figure 4.3** Product selectivity of hydrotreating of stearic acid using nickel supported catalyst at 95% and 99.91% conversion of stearic acid with 154 and 360 min of reaction time, respectively, 0.18 kmol/m³ of concentration of stearic acid, 290 °C of reaction temperature, and 8 bar of hydrogen pressure for simulation from kinetic model of Kumar and co-workers⁴¹.....73
- Figure 4.4** Product selectivity of hydrotreating of stearic acid over 5% Ni- γ -Al₂O₃ at 360 min of reaction time, 99% of stearic acid conversion, 0.035 M (mole/L) of concentration of stearic acid, 300 °C of reaction temperature, 30 bar of hydrogen pressure between experiment and simulation from kinetic model of Jenistova and co-workers⁴².....74
- Figure 4.5** Process flow diagram of single-step of hydrotreating.77
- Figure 4.6** Conversion of triolein and the moles number of liquid products per unit mole of triolein for hydrolysis reaction at temperature of 270 °C and pressure of 70 bar, 1.0 of water per triolein volumetric ratio from kinetic model of Minami⁴⁴ with condition of Gomez-Castro⁴³.....81
- Figure 4.7** Process flow diagram for two-step of hydrotreating.84
- Figure 4.8** Product gas composition with dry basis for equilibrium reactor of PSR, 12 of WPMR, 677 °C of temperature and atmospheric pressure between thermodynamic data of Wang and co-workers⁴⁸ and equilibrium simulation.89
- Figure 4.9** Product gas composition with dry basis and conversion of propane for equilibrium reactor of PSR performance using various catalysts of Ni/YSZ, 1% Ru/Ni/YSZ, 1% Rh/Ni/YSZ, and 1% Pd/Ni/YSZ, 9 of WPMR, 650 °C of temperature and atmospheric pressure between experiment of Im and co-workers⁴⁹ and equilibrium simulation.....90

Figure 4.10 Mole number of H ₂ per unit mole of propane using various catalysts of Ni/YSZ, 1% Ru/Ni/YSZ, 1% Rh/Ni/YSZ, and 1% Pd/Ni/YSZ, 9 of WPMR, 650 °C of temperature and atmospheric pressure between experiment of Im and co-workers ⁴⁹ and equilibrium simulation.	91
Figure 4.11 Process flow diagram of propane steam reforming.	93
Figure 4.12 Product gas composition with dry basis for equilibrium reactor of GSR using un-promoted and promoted Ni catalysts, 6 of WGMR, 700 °C of temperature, and atmospheric pressure between experiment of Profeti and co-workers ⁵⁰ and equilibrium simulation.	96
Figure 4.13 Conversion of glycerol and the mole number of H ₂ per unit mole of glycerol, using catalyst C3, 9 of WGMR, 450, 550, and 650 °C of temperature, and atmospheric pressure between experiment of Wang and co-workers ¹⁰ and equilibrium simulation.	97
Figure 4.14 Comparing H ₂ selectivity of GSR, 9 of WGMR, 450, 550, and 650 °C of temperature, and atmospheric pressure between experiment of Wang and co-workers ¹⁰ and equilibrium simulation.	98
Figure 4.15 Process flow diagram of glycerol steam reforming.	100
Figure 4.16 Process flow diagram of integrated system of single-step of hydrotreating and propane steam reforming without recycle.	105
Figure 4.17 Process flow diagram of integrated system of single-step of hydrotreating and propane steam reforming with recycle consideration.	106
Figure 4.18 Complete process flow diagram of integrated system of single-step of hydrotreating and propane steam reforming.	107
Figure 4.19 Process flow diagram of integrated system of two-step of hydrotreating and glycerol steam reforming without recycle.	114

Figure 4.20 Process flow diagram of integrated system of two-step of hydrotreating and glycerol steam reforming with recycle consideration.	115
Figure 4.21 Complete process flow diagram of integrated system of two-step of hydrotreating and glycerol steam reforming.	116
Figure 5.1 Net H ₂ of integrated system with various selectivity of deoxygenation reaction pathways. Single-step of hydrotreating and PSR from (a) tripalmitin and (b) triolein. Two-step of hydrotreating and GSR from (c) tripalmitin and (d) triolein. ..	126
Figure 5.2 H ₂ flow rate for each of net H ₂ of integrated system with selectivity of deoxygenation reaction pathways. Single-step of hydrotreating and PSR from (a) tripalmitin and (b) triolein. Two-step of hydrotreating and GSR from (c) tripalmitin and (d) triolein.	130
Figure 5.3 Energy requirement of integrated system with various selectivity of deoxygenation reaction pathways. Single-step of hydrotreating and PSR from (a) tripalmitin and (b) triolein. Two-step of hydrotreating and GSR from (c) tripalmitin and (d) triolein.	131
Figure 5.4 Energy requirement for each equipment of integrated system of single-step of hydrotreating and PSR with selectivity of deoxygenation reaction pathways from tripalmitin and triolein.	132
Figure 5.5 Energy requirement for each equipment of integrated system of two-step of hydrotreating and GSR with selectivity of deoxygenation reaction pathways from tripalmitin and triolein.	135
Figure 5.6 Electricity requirement of integrated system with various selectivity of deoxygenation reaction pathways. Singl-step of hydrotreating and PSR from (a) tripalmitin and (b) triolein. Two-step of hydrotreating and GSR from (c) tripalmitin and (d) triolein.	137
Figure 5.7 Electricity requirement for each equipment of integrated system of single-step of hydrotreating and PSR with selectivity of deoxygenation reaction pathways from tripalmitin and triolein.	138
Figure 5.8 Electricity requirement for each equipment of integrated system of two-step of hydrotreating and GSR with selectivity of deoxygenation reaction pathways from tripalmitin and triolein.	139

Figure 5.9 Composite curves of optimum MER of integrated system. Single-step of hydrotreating and PSR with HDCO pathway from (a) tripalmitin and (b) triolein. Two-step of hydrotreating and GSR with HDO pathway from (c) tripalmitin and (d) triolein.....	141
Figure 5.10 MER of integrated system with various selectivity of deoxygenation reaction pathways. Single-step of hydrotreating and PSR from (a) tripalmitin and (b) triolein. Two-step of hydrotreating and GSR from (c) tripalmitin and (d) triolein. ..	142
Figure 5.11 Total MER of integrated system with various selectivity of deoxygenation reaction pathways. Single-step of hydrotreating and PSR from (a) tripalmitin and (b) triolein. Two-step of hydrotreating and GSR from (c) tripalmitin and (d) triolein.....	144
Figure 5.12 Total MER for each of energy requirement of integrated system with selectivity of deoxygenation reaction pathways. Single-step of hydrotreating and PSR from (a) tripalmitin and (b) triolein. Two-step of hydrotreating and GSR from (c) tripalmitin and (d) triolein.....	146
Figure 5.13 Thermal efficiency of integrated system with various selectivity of deoxygenation reaction pathways. Single-step of hydrotreating and PSR from (a) tripalmitin and (b) triolein. Two-step of hydrotreating and GSR from (c) tripalmitin and (d) triolein.....	148
Figure 5.14 Total efficiency of integrated system with various selectivity of deoxygenation reaction pathways. Single-step of hydrotreating and PSR from (a) tripalmitin and (b) triolein. Two-step of hydrotreating and GSR from (c) tripalmitin and (d) triolein.....	150
Figure A.1 Density of tripalmitin and triolein with various temperatures at pressure 1.0 bar.	169
Figure A.2 Enthalpy of tripalmitin, tristearin and triolein with various temperatures at pressure 1.0 bar and 50 bar.	170
Figure A.3 Heat of deoxygenation reaction of palmitic acid and stearic acid at temperature of 300 °C and pressure of 50 bar.	171
Figure A.4 Heat of hydrolysis reaction of triglycerides at high temperature and high pressure.	171

Figure D.1 Sensitivity composition of separation with various temperatures of CL-2 from tripalmitin.....	177
Figure D.2 Sensitivity composition of separation with various temperatures of CL-7 from tripalmitin.....	177
Figure D.3 Sensitivity composition of separation with various temperatures of CL-2 from triolein.	178
Figure D.4 Sensitivity composition of separation with various temperatures of CL-7 from triolein.	178
Figure D.5 Sensitivity composition of separation with various temperatures of CL-5 from tripalmitin.....	180
Figure D.6 Sensitivity composition of separation with various temperatures of CL-9 from tripalmitin.....	180
Figure D.7 Sensitivity composition of separation with various temperatures of CL-5 from triolein.	181
Figure D.8 Sensitivity composition of separation with various temperatures of CL-9 from triolein.	181
Figure H.1 Heat exchanger network and heat flow after heat integration of integrated system of single-step of hydrotreating and PSR from tripalmitin; (1) hot stream = red; (2) cold stream = blue.	201
Figure H.2 Heat exchanger network and heat flow after heat integration of integrated system of single-step of hydrotreating and PSR from triolein; (1) hot stream = red; (2) cold stream = blue.....	205

LIST OF TABLES

	Page
Table 1.1 Research timeline.....	8
Table 2.1 Composition of vegetable oils ¹⁴	10
Table 2.2 Triglycerides composition (%) of palm oil ¹⁵	10
Table 3.1 Reaction model in equilibrium reactor ³²⁻³³	22
Table 3.2 Estimated rate constant for HDO of stearic acid, using 5 wt.% of different catalysts at temperature 300 °C and 30 bar of total pressure ⁴²	35
Table 3.3 Literature review of modelling and design of plant for single-step of hydrogenolysis of TGs/ deoxygenation of FFAs process for bio-hydrogenated diesel fuel production.....	36
Table 3.4 Literature review of modelling and design of plant for two-step: hydrolysis of TGs and deoxygenation of FFAs process for bio-hydrogenated diesel fuel production.....	46
Table 3.5 Literature review of modelling and design of plant for integrated system of hydrotreating and hydrogen generation for bio-hydrogenated diesel fuel production.....	59
Table 3.6 Literature review of PSA technology for hydrogen recovery and purification.....	63
Table 3.7 Performance of different catalysts with various deoxygenation pathways.....	67
Table 3.8 Literature review of thermodynamic of hydrotreating.....	68
Table 4.1 Formation rates of different components with different temperatures, pre-exponential factor (A_0), and activation energy (E) ⁴¹	70
Table 4.2 Estimated rate constant for HDO of stearic acid using 5 wt.% Ni- γ -Al ₂ O ₃ catalyst at temperature of 300 °C with various total pressures ⁴²	73
Table 4.3 Stream description of single-step of hydrotreating demonstrated in Figure 4.5.....	78

Table 4.4 Equipment description of single-step of hydrotreating demonstrated in Figure 4.5.	80
Table 4.5 Stream description of two-step of hydrotreating demonstrated in Figure 4.7.	85
Table 4.6 Equipment description of two-step of hydrotreating demonstrated in Figure 4.7.	87
Table 4.7 Stream description of PSR demonstrated in Figure 4.11.	94
Table 4.8 Equipment description of PSR demonstrated in Figure 4.11.	95
Table 4.9 Stream description of GSR demonstrated in Figure 4.15.	101
Table 4.10 Equipment description of GSR demonstrated in Figure 4.15.	102
Table 4.11 Unit specification of integrated system of single-step of hydrotreating and PSR demonstrated in Figure 4.18.	108
Table 4.12 Unit specification of integrated system of two-step of hydrotreating and GSR demonstrated in Figure 4.21.	117
Table 5.1 Performance of integrated system of hydrotreating and hydrogen generation with deoxygenation reaction pathways from tripalmitin and triolein.	123
Table 5.2 Comparative performance of integrated system among different deoxygenation reaction pathways using tripalmitin and triolein as feedstock.	124
Table 5.3 Number of equipment unit of each integrated system.	151
Table 5.4 Summarization of the comparative results of integrated system of hydrotreating and hydrogen generation to the literature review for bio-hydrogenated diesel fuel production.	154
Table E.1 Calculator specification of flow rate calculation of M-H ₂ O-1 stream.	182
Table E.2 Calculator specification of flow rate calculation of H ₂ O-4 stream.	183
Table E.3 Calculator specification of flow rate calculation of H ₂ -3 stream.	184
Table E.4 Design specification with various temperatures of HT-5 equipment.	185

Table E.5 Calculator specification of flow rate calculation of H2O-5 stream.....	186
Table E.6 Calculator specification of flow rate calculation of H2-4 stream.....	187
Table F.1 The results of integrated system of single-step of hydrotreating and PSR with various selectivity of DO reaction pathways from tripalmitin.	189
Table F.2 The results of integrated system of single-step of hydrotreating and PSR with various selectivity of DO reaction pathways from triolein.....	191
Table F.3 The results of integrated system of two-step of hydrotreating and GSR with various selectivity of DO reaction pathways from tripalmitin.....	193
Table F.4 The results of integrated system of two-step of hydrotreating and GSR with various selectivity of DO reaction pathways from triolein.	195
Table G.1 Lower heating value of fuel.	197
Table H.1 Energy loads in each of heat exchangers of integrated system of single-step of hydrotreating and PSR from tripalmitin.	199
Table H.2 Summarization of temperature and heat recovery for each of heat exchangers after heat integration of integrated system of single-step of hydrotreating and PSR from tripalmitin.	200
Table H.3 Energy loads in each of heat exchangers of integrated system of single-step of hydrotreating and PSR from triolein.	203
Table H.4 Summarization of temperature and heat recovery for each of heat exchangers after heat integration of integrated system of single-step of hydrotreating and PSR from triolein.	204

NOMENCLATURE

BHD	Bio-hydrogenated diesel
CPO	Crude palm oil
DCO	Decarbonylation
DCO ₂	Decarboxylation
DG	Diglycerides
DO	Deoxygenation
EOS	Equation of state
FAMEs	Fatty acid methyl esters
FFAs	Free fatty acids
GSR	Glycerol steam reforming
HDCO	Hydrodecarbonylation
HDO	Hydrodeoxygenation
HEPD	N-heptadecane
HEXD	N-hexadecane
MG	Monoglyceride
NRTL	Non-random two liquid
OCTD	N-octadecane
OCTDL	L-octadecanol
PEND	N-pentadecane
PFAD	Palm fatty acid distilled
PR	Peng-Robinson equation of state
PSA	Pressure swing adsorption
PSR	Propane steam reforming

NOMENCLATURE (*Continued*)

PSRK	Predictive Soave-Redlich-Kwong equation of state
RK	Redlich-Kwong
SA	Stearic acid
SESR	Sorption enhanced steam reforming
SR	Steam reforming
SRM	Steam reforming of methane
STP	Standard temperature and pressure
TGs	Triglycerides
TOFA	Tested tall oil fatty acids
UCO	Used cooking oil
WGMR	Water to glycerol molar ratio
WPMR	Water to propane molar ratio

CHAPTER I INTRODUCTION

1.1 Motivation

Since the effects of greenhouse gas emission is a matter of concern, combustion of fossil fuels should be reduced.¹ The important key for future energy is the development of alternative fuel from bioresources.² However, to meet the energy needs of all industries and transportation, a sustainable and friendly energy source is needed.³

To reduce the consumption of fossil fuels and greenhouse gas emissions, alternative resources such as vegetable oils and biomass can be used to produce biofuel.³ Carbon dioxide (CO₂) in the carbon cycle can be reduced with using biodiesel, leading to the potential alternative fuels. Typically, triglycerides (TGs) are changed by transesterification with methanol and fatty acid methyl esters (FAMEs) can be produced. However, the use of FAMEs has the disadvantage of compatibility with conventional diesel engines.⁴

Bio-hydrogenated diesel (BHD), known as renewable diesel or green diesel, is a promising alternative fuel because it is similar to diesel derived from petroleum rather than biodiesel from esters. BHD can be produced from animal fat or vegetable oil through catalytic hydrotreating technology. One of the most potential raw material for the production of renewable fuels in Thailand is palm oil. Compared with other vegetable oils, palm oil uses less hydrogen (H₂) in the hydrotreating reaction as it has lower unsaturated free fatty acids (FFAs).⁵⁻⁸ Using palm fatty acid distillate (PFAD), which is a by-product from palm oil refineries, as a raw material consumes less hydrogen than TGs as a raw material. On the other hand, when using palm oil (consisting mostly of TGs) as a raw material, the by-product, i.e., propane or glycerol can be produced via hydrogenolysis or hydrolysis, respectively. These by-products can be employed for hydrogen production.

Due to the environmental regulations, higher qualities of transportation fuels are required. A large amount of hydrogen is used for hydrotreating and watertreatment processes in oil refineries, particularly crude oil including bio-

hydrogenated diesel fuel production. Propane steam reforming (PSR) can be employed to convert propane to hydrogen using Ni supported on Al_2O_3 catalysts, which is widely used for large industrial reformers.⁹ Similarly, glycerol steam reforming (GSR) can convert glycerol to hydrogen with the use of Ni-Mg-Al based catalysts.¹⁰

In this work, the process performance of the integrated system of bio-hydrogenated diesel fuel production and hydrogen production was evaluated. The two main approaches investigated in this study are: 1) hydrogenolysis / deoxygenation / PSR and 2) hydrolysis / deoxygenation / GSR.

For hydrogenolysis / deoxygenation / PSR, the hydrogenolysis and deoxygenation reactions take place in a single reactor. Palm oil and hydrogen were fed into the reactor for hydrotreating process. The reactions included hydrogenation of unsaturated TGs, hydrogenolysis of TGs to FFAs, and deoxygenation of FFAs. Propane and hydrocarbons were obtained from the deoxygenation process while three different by-products, i.e., carbon dioxide (CO_2), carbon monoxide (CO), and water (H_2O) can be obtained from three different reaction pathways, i.e., decarboxylation (DCO_2), hydrodecarbonylation (HDCO), and hydrodeoxygenation (HDO). Propane was fed to the hydrogen generation process in order to convert to hydrogen via PSR and water gas shift reaction. The generated hydrogen was fed back to hydrotreating for bio-hydrogenated diesel fuel production.

For hydrolysis / deoxygenation / GSR, TGs was hydrolyzed by water to FFAs and glycerol was obtained as a by-product. Glycerol was fed to the hydrogen generation process to produce hydrogen via GSR and water gas shift reaction. FFAs were deoxygenated via three different reaction pathways, i.e., decarboxylation (DCO_2), hydrodecarbonylation (HDCO), and hydrodeoxygenation (HDO) to obtain hydrocarbons products.

Both the hydrotreating and hydrogen generation process required operation at high temperature and consequently high energy consumption. Process heat integration would be necessary for an efficient operation of the integrated system. Based on the proposed integrated system, the valuable products were bio-hydrogenated diesel and other hydrocarbon fuels.

1.2 Objective

To design and evaluate the performance of the integrated system of hydrotreating and hydrogen generation system for bio-hydrogenated diesel fuel production from palm oil.

1.3 Scope of work

- 1.3.1 Select the appropriate thermodynamic model in Aspen Plus as simulation software for hydrotreating of bio-hydrogenated diesel fuel production and hydrogen generation process of hydrogen production.
- 1.3.2 Determine suitable major operating parameters and simulate each process: single-step of hydrogenolysis of TGs/ deoxygenation of FFAs process, and two-step: hydrolysis of TGs and deoxygenation of FFAs process, PSR process and GSR process.
- 1.3.3 Design the integrated system of hydrotreating and hydrogen generation processes.
- 1.3.4 Consider the deoxygenation reaction pathways via decarboxylation (DCO_2), hydrodecarbonylation (HDCO), and hydrodeoxygenation (HDO) to simulate the process performance.
- 1.3.5 Evaluate and compare the performance of the integrated system on the following aspects: net H_2 , energy requirement, electricity requirement, minimum energy requirement (MER), total MER, thermal efficiency, and total efficiency.
- 1.3.6 Apply the concept of heat integration to further improve the performances of the integrated system.

1.4 Methodology

1. Study physical and chemical properties of raw material as feedstock for bio-hydrogenated diesel fuel production process and compare composition of palm oil to vegetable oil.

2. Study reaction and operating parameters for bio-hydrogenated diesel fuel production.

- Reaction: hydrotreating via hydrogenolysis reaction, hydrolysis reaction, and hydrogenation reaction. Deoxygenation reaction pathways consisting of decarboxylation (DCO₂), hydrodecarbonylation (HDCO), and hydrodeoxygenation (HDO).

- Key operating conditions: property of catalysts and supports, amount of catalysts, temperature of reaction, pressure of reaction, type of feed stock, feed rate, H₂/oil molar ratio, H₂O to oil molar ratio.

3. Study reaction and operating parameters for hydrogen production.

- Reaction: PSR, GSR and water gas shift reactions, equilibrium chemical reaction.

- Key operating conditions: property of catalysts and supports, amount of catalysts, temperature of reaction, pressure of reaction, reactor type, steam to carbon ratio.

4. Select the appropriated thermodynamic model in Aspen Plus as a simulation software for hydrotreating of bio-hydrogenated diesel fuel production and hydrogen generation process of hydrogen production.

5. Determine the suitable major operating parameters of each process: single-step of hydrogenolysis of TGs / deoxygenation of FFAs process, and two-step: hydrolysis of TGs and deoxygenation of FFAs process, PSR process and GSR process.

6. Design the integrated system of hydrotreating and hydrogen generation via 1) hydrogenation / hydrogenolysis / deoxygenation / PSR and 2) hydrolysis / hydrogenation / deoxygenation / GSR.

7. Simulate the integrated system of single-step of hydrotreating and PSR and two-step of hydrotreating and GSR with various selectivity of deoxygenation reaction pathways (DCO₂: HDCO: HDO) from tripalmitin and triolein.

8. Report the overall mass and energy balance, weight (%) and purity of hydrocarbon range diesel products.

9. Evaluate the performance of the integrated system on:

- Net H₂
- Energy requirement
- Electricity requirement
- Minimum energy requirement (MER)
- Total Minimum energy requirement (MER)
- Thermal efficiency
- Total efficiency

10. Improve the integrated system and apply the concept of heat integration to reduce energy consumption.

11. Compare and summarize the results.

1.5 Expected output

The work should provide a conceptual design for the sustainable and performance integrated system for bio-hydrogenated diesel fuel and hydrogen productions with low total minimum energy requirement and high total efficiency.

The pathways of the integrated system of hydrotreating and hydrogen generation for bio-hydrogenated diesel fuel production with a simple diagram is shown in Figure 1.1. A block diagram of the integrated system of single-step of hydrotreating and hydrogen generation is shown in Figure 1.2 and a block diagram of the integrated system of two-step of hydrotreating and hydrogen generation is shown in Figure 1.3.

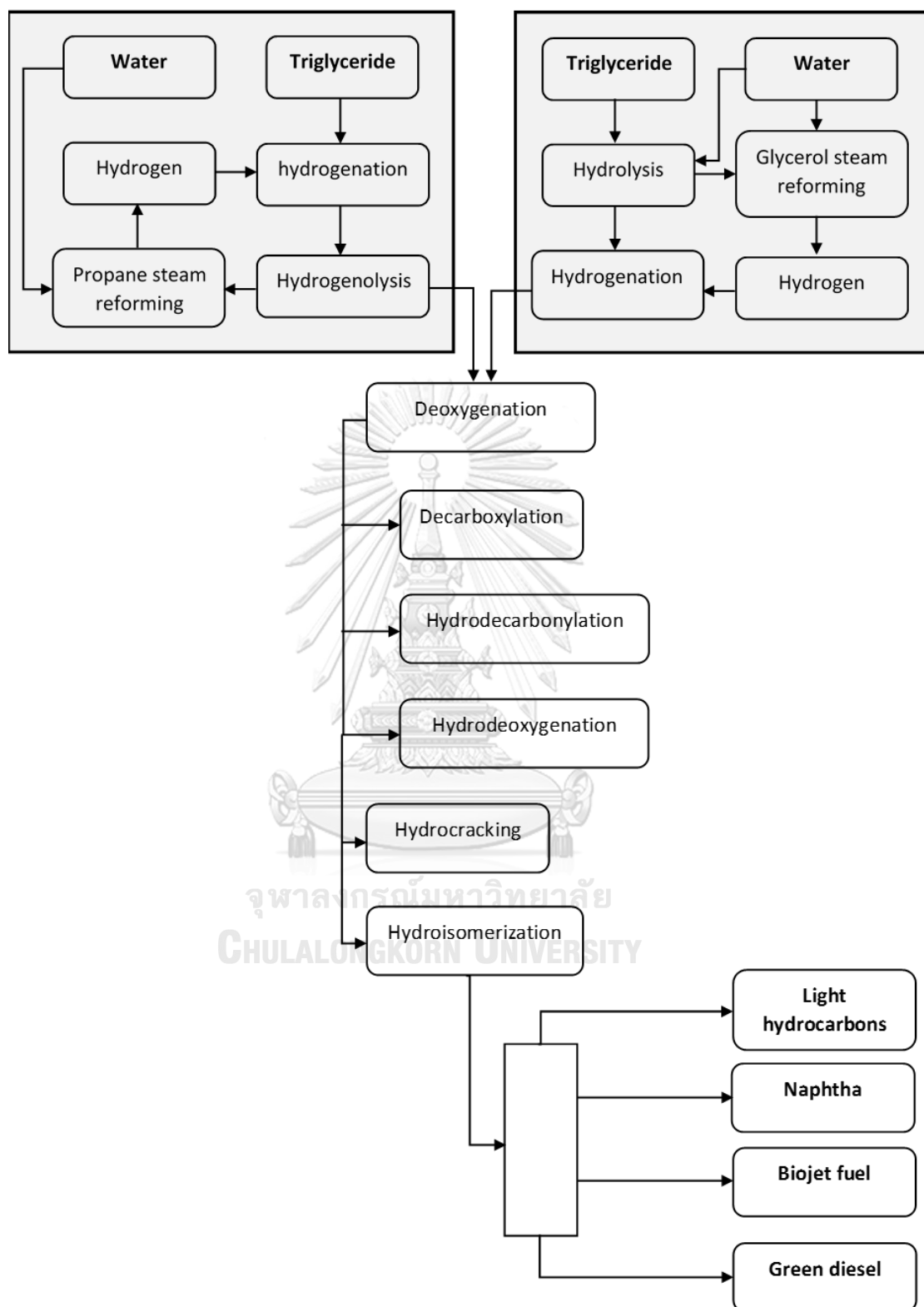


Figure 1.1 The pathways of integrated system of hydrotreating and hydrogen generation for bio-hydrogenated diesel fuel production.

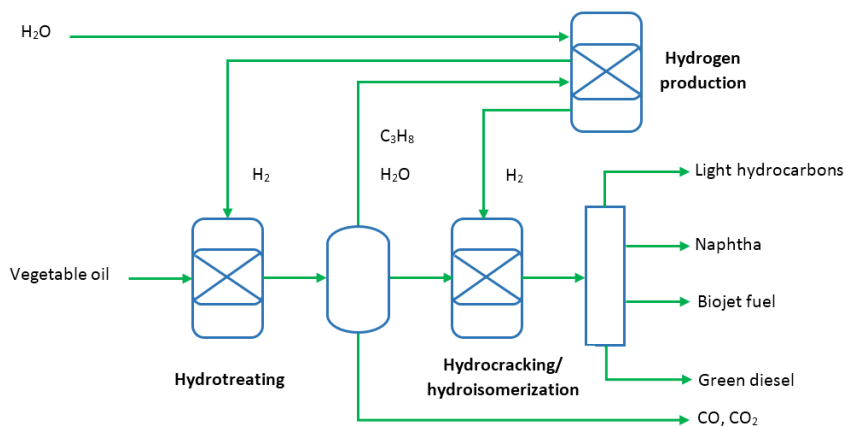


Figure 1.2 Block diagram of integrated system of single-step of hydrotreating and hydrogen generation.

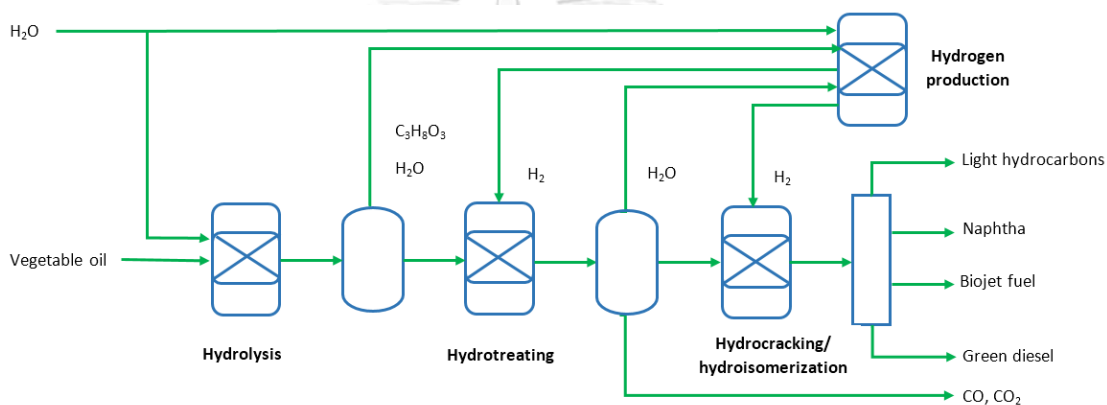


Figure 1.3 Block diagram of integrated system of two-step of hydrotreating and hydrogen generation.

1.6 Research plan

Table 1.1 Research timeline.

Step	Title	Research timeline (Month)																											
		2017												2018															
		05	06	07	08	09	10	11	12	01	02	03	04	05	06	07	08	09	10	11									
1	Study BHD production and find suitable major operating parameters																												
2	Study hydrogen production and find suitable major operating parameters																												
3	Validate model and select the appropriate thermodynamic model in Aspen Plus																												
4	Design the processes and the integrated system																												
5	Evaluate performance of the integrated system																												
6	Improve the performance of the integrated system by heat integrate																												
7	Comparison and summarize the results																												

CHAPTER II THEORY

Concepts of fundamental of hydrotreating of bio-hydrogenated diesel fuel production and hydrogen generation process of hydrogen production were presented in this chapter which gave the basic knowledge to understand this work.

2.1 Oil feedstocks

Triglycerides (TGs) are the main ingredients of vegetable oil, which are derived from glycerol and three fatty acids. Different types of TGs are saturated and unsaturated types. The saturated TGs have higher melting points than the unsaturated ones. They tend to solidify at room temperature. On the other hand, unsaturated TGs tend to be liquid at room temperature because of their lower melting point¹¹⁻¹². An example of unsaturated TGs shown in Figure 2.1¹³.



Figure 2.1 Example of unsaturated triglycerides ($C_{55}H_{98}O_6$)¹³.

The selection of oil as a feedstock depends on local availability. One of the most potential raw materials for the production of renewable fuels in Thailand is palm oil. The composition of vegetable oils is described by the content of fatty acids as shown in Table 2.1¹⁴. The TGs composition (%) of palm oil is shown in Table 2.2¹⁵. Most palm oils are palmitic acid (C16:0) and oleic acid (C18:1), which contain a lower fraction of unsaturated FFAs compared to another vegetable oil.

Table 2.1 Composition of vegetable oils¹⁴.

Source	Structure	Molecular weight (MW)		Typical composition, wt. %				
		Fatty acid	Triglyceride	Jatropha	Palm	Canola	Soybean	Sunflower
Capric	C10:0	172.3	554.8	0.0	0.0	0.6	0.0	0.0
Lauric	C12:0	200.3	639.0	0.0	0.0	0.0	0.0	0.0
Myristic	C14:0	228.4	723.2	0.0	2.5	0.1	0.0	0.0
Palmitic	C16:0	256.4	807.3	15.9	40.8	5.1	11.5	6.5
Palmitoleic	C16:1	254.4	801.3	0.9	0.0	0.0	0.0	0.2
Stearic	C18:0	284.5	891.5	6.9	3.6	2.1	4.0	5.8
Oleic	C18:1	282.5	885.4	41.1	45.2	57.9	24.5	27.0
Linoleic	C18:2	280.4	879.4	34.7	7.9	24.7	53.0	60.0
Linolenic	C18:3	278.4	873.3	0.3	0.0	7.9	7.0	0.2
Arachidic	C20:0	312.5	975.6	0.0	0.0	0.2	0.0	0.3
Eicosenoic	C20:1	310.5	969.6	0.2	0.0	1.0	0.0	0.0
Behenic	C22:0	340.6	1059.8	0.0	0.0	0.2	0.0	0.0
Erucic	C22:1	338.6	1053.8	0.0	0.0	0.2	0.0	0.0
Estimated MW:				869.7	847.0	876.9	871.9	876.7

Table 2.2 Triglycerides composition (%) of palm oil¹⁵.

TGs	Composition, %
PLL	2.71
MLP	0.67
OOL	1.87
POL	10.97
PLP	10.54
OOO	3.62
POO	23.15
POP	31.42
PPP	5.15
SOO	2.49
POS	5.64
PPS	1.08
SOS	0.70

Abbreviations: M - Myristic acid, P - Palmitic acid, S - Stearic acid, O - Oleic acid and L - Linoleic acid

2.2 Bio-hydrogenated diesel

Bio-hydrogenated diesel (BHD), also known as green diesel, is an alternative renewable energy from vegetable oils. The molecular structure of BHD is similar to that of petroleum diesel.

BHD obtained from the deoxygenation reaction consists of C₁₇ and C₁₈ n-paraffins with high cetane content. However, cold flow properties are not good as there is a high melting point between 20 and 28 °C. Thus, its quality must be upgraded through the second step in the selected hydroisomerization and cracking. This process improves the quality of diesel and also produces jet fuel¹⁶.

Technology/ Commercial processes of bio-hydrogenated diesel fuel production

Green fuels production technology from TGs has been used in refineries of petroleum with the type of catalyst, reactor type, and equipment of separation that can be operated for hydrotreatment of vegetable oils. Currently, the optimal production was studied in order to define the suitable catalyst and the optimal favorable operating conditions with using vegetable oil as a raw material for hydrotreating process to produce green fuels. Furthermore, there are some drawbacks of the process because hydrogen requires large consumption of various raw materials, which increases the cost of production. However, there are advantages of this technology in order to produce renewable fuels.¹⁴

UOP Honeywell Co.¹⁷ offered an alternative diesel fuel, which was produced from the Ecofining™ process as shown in Figure 2.2. Green diesel of Honeywell meets the diesel performance standards with good cold flow properties, which can be produced from a variety of renewable feedstocks by hydrotreating and isomerization.

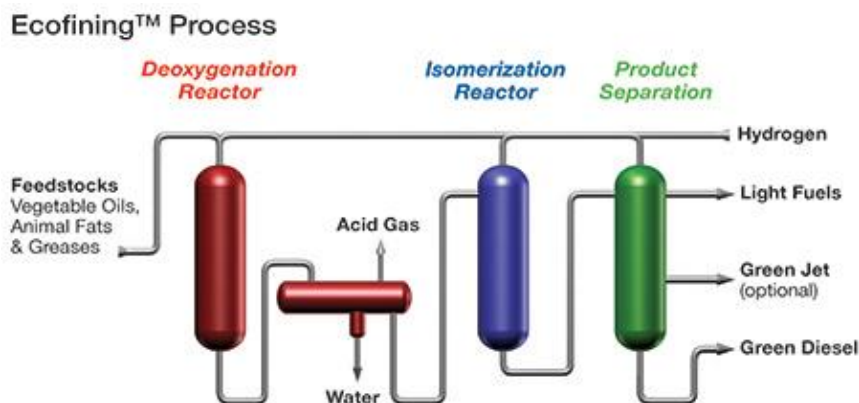


Figure 2.2 Ecofining™ process producing alternative diesel fuel¹⁷.

KALNes and co-workers, UOP¹⁸ reported green diesel production by Ecofining system which is an integration of two-stage of hydrotreating process. The Ecofining system block flow diagram is shown in Figure 2.3. In the process, the renewable oil is saturated and completely deoxygenated in the R1 reactor with minimum hydrogen partial pressure and the yield of volumetric products as hydrocarbon is greater than 100%.

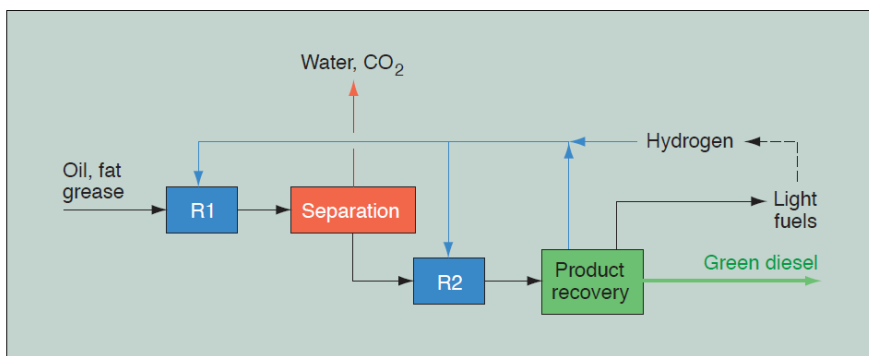


Figure 2.3 Ecofining process diagram¹⁸.

Haldor Topsøe has also produced BHD and jet fuel from oil as raw tall by developing a new hydrotreating technology. Tall oil from Kraft paper mills is a raw material, which is non-edible and has no effect on global food shortage¹⁴. Production of renewable diesel shown in Figure 2.4¹⁹.

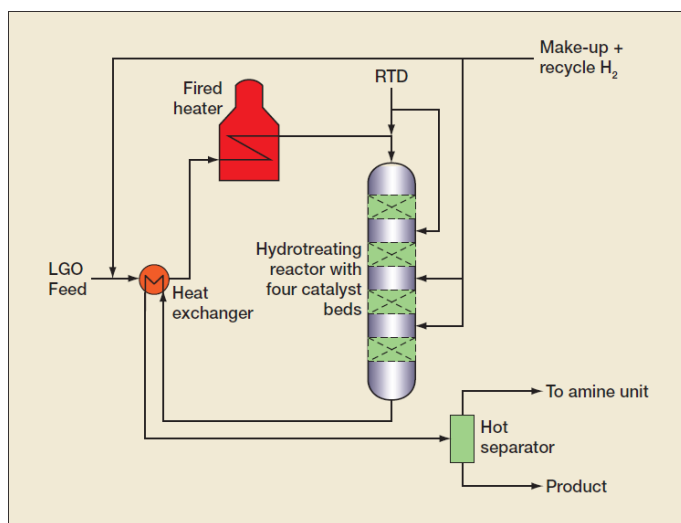


Figure 2.4 Revamped hydrotreater for raw tall diesel co-processing¹⁹.

The Neste Oil Co.²⁰ developed a technology of diesel fuel production from animal fats and vegetable oils in order to produce high quality products. The NExBTL process to produce green diesel is shown in Figure 2.5. The NExBTL Process Chemistry is shown in Figure 2.6.

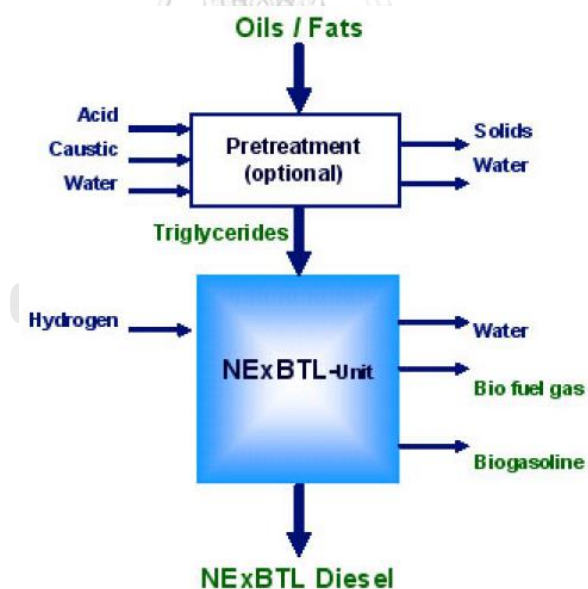


Figure 2.5 NExBTL process to produce green diesel²⁰.

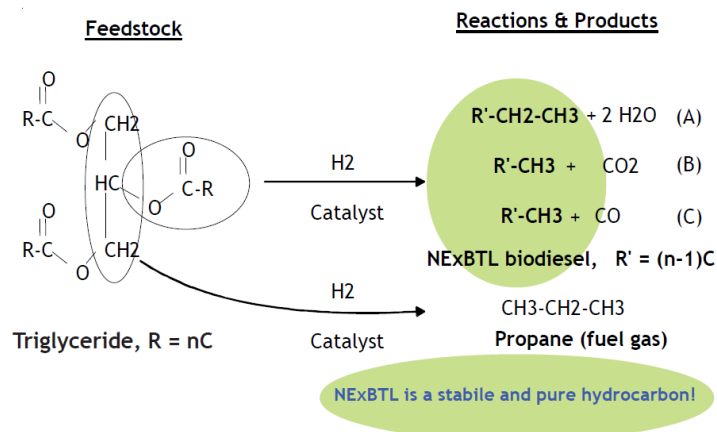


Figure 2.6 NExBTL Process Chemistry²⁰.

2.3 Hydrotreating

Hydrotreating processes include hydrogenation, hydrogenolysis, deoxygenation via HDO, HDCO and DCO₂, hydrocracking, and hydroisomerization²¹. Vegetable oils are reacted with hydrogen during the hydrotreating method in order to remove oxygen from the feedstock and generate bio-hydrogenated diesel fuel. Hydrotreating of triglycerides pathways are shown in Figure 2.7².

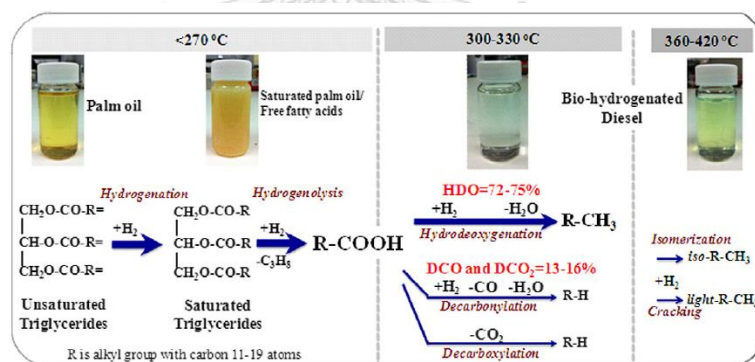


Figure 2.7 Hydrotreating of triglycerides pathways².

2.3.1 Hydrogenation

Hydrogenation of vegetable oils occurred in a multiple-phase catalytic reactor on supported Ni catalysts or palladium or platinum²²⁻²³. The hydrogenation reaction is an exothermic reaction of the unsaturated TGs or double bonds of the side chains, which are converted into saturated TGs resulting in enhanced oxidation stability.¹⁴ Partial hydrogenation of TGs is shown in Figure 2.8²⁴.

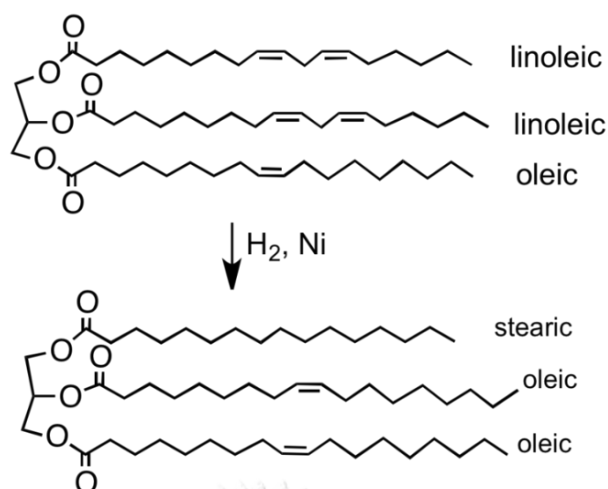


Figure 2.8 Partial hydrogenation of triglycerides²⁴.

Hydrogenation of triolein to tristearin



Hydrogenation of trilinolein to tristearin



Hydrogenation of trilinolenin to tristearin



Hydrogenation of oleic acid to stearic acid



Hydrogenation of linoleic acid to stearic acid



Hydrogenation of linolenic acid to stearic acid



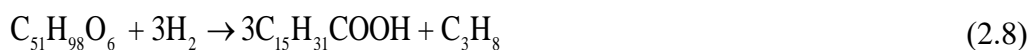
2.3.2 Hydrogenolysis

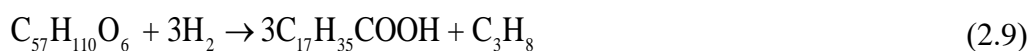
Hydrogenolysis is a chemical reaction whereby the molecule of a carbon-carbon is broken down by hydrogen²⁵. Hydrogenolysis of TGs is an exothermic reaction, which breaks down TGs into FFAs and propane by-product in the presence of hydrogen¹⁴. Examples of the reaction are shown below.

Hydrogenolysis of trimyristin to myristic acid

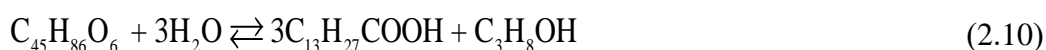


Hydrogenolysis of tripalmitin to palmitic acid



Hydrogenolysis of tristearin to stearic acid**2.3.3 Hydrolysis**

Hydrolysis of TGs hydrolyzed TGs by water into 3 fatty acids and a glycerol by-product. Examples of reaction are shown below.

Hydrolysis of trimyristin to myristic acid**Hydrolysis of tripalmitin to palmitic acid****Hydrolysis of tristearin to stearic acid****Hydrolysis of triolein to oleic acid****Hydrolysis of trilinolein to linoleic acid****Hydrolysis of trilinolenin to linolenic acid****2.3.4 Deoxygenation**

Deoxygenation of FFAs in a liquid phase reaction removes oxygen from the molecule of FFAs, which occurs through different reactions such as decarboxylation (DCO₂), hydrodecarbonylation (HDCO), and hydrodeoxygenation (HDO). Carboxyl groups in the fatty acid were removed to produce n-alkane with decarboxylation by releasing a CO₂ molecule, while carboxyl groups in the fatty acid were removed to produce alkenes with decarbonylation (DCO) by releasing CO and H₂O molecules. Both of DCO₂ and DCO are endothermic reactions²⁶. Furthermore, when there is hydrogen, deoxygenation of saturated fatty acid occurs through hydrodeoxygenation, an exothermic reaction that removes oxygen by releasing water to produce n-alkanes, and hydrodecarbonylation, an endothermic reaction that eliminates carboxyl group to produce n-alkanes by releasing CO and H₂O molecules²⁶.

However, CO₂, CO, H₂, and H₂O produced from the liquid phase will undergo phase of the gas reactions, which includes methanation of CO₂ and CO. A water-gas-

shift side reaction occurs during the process of deoxygenation^{14, 26-27}. The selectivity of the FFAs to undergo a particular deoxygenation reaction pathway is dictated by catalysts used and process conditions. The main reaction is shown below.

Route of decarboxylation

Route 1



Route 2



Water-gas shift



Decarboxylation



Decarboxylation of myristic acid



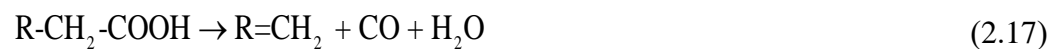
Decarboxylation of palmitic acid



Decarboxylation of stearic acid



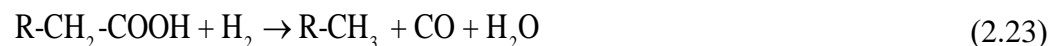
Route of decarbonylation



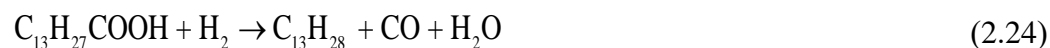
Route of hydrodecarbonylation

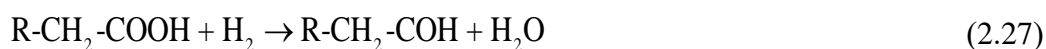
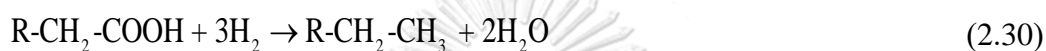
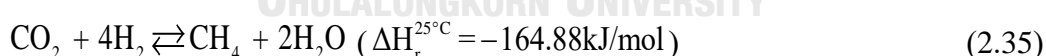
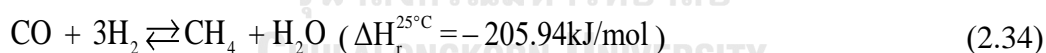


Hydrodecarbonylation



Hydrodecarbonylation of myristic acid



Hydrodecarbonylation of palmitic acid**Hydrodecarbonylation of stearic acid****Route of hydrodeoxygenation****Hydrodeoxygenation****Hydrodeoxygenation of myristic acid****Hydrodeoxygenation of palmitic acid****Hydrodeoxygenation of stearic acid****Water-gas shift****Methanation****2.3.5 Hydroisomerization**

Isomerization of a molecule exhibits a different arrangement but with the same atoms, e.g., A-B-C \rightarrow B-A-C²⁸. Hydroisomerization is the main constraint for obtaining most methyl-branched paraffins. With the use of catalysts such as zeolites or other acid supports, the targets can be achieved. The normal paraffins have a higher number of cetane in the range of boiling point of the diesel than that of their branched isomers. On the other hand, freezing points of iso-paraffins are lower than those of n-paraffins. Then, paraffins with quality in the diesel range should exhibit good cold flow properties and good combustion properties¹⁴.

Green diesel has a higher cetane number than diesel derived from petroleum, which is a quality of diesel that can be used in a powerful engine. Therefore, improvement of cold flow properties is essential for green diesel production. Figure 2.9 shows the freezing point and the number of cetane of carbon number in n-paraffins and methyl branched paraffins¹⁴.

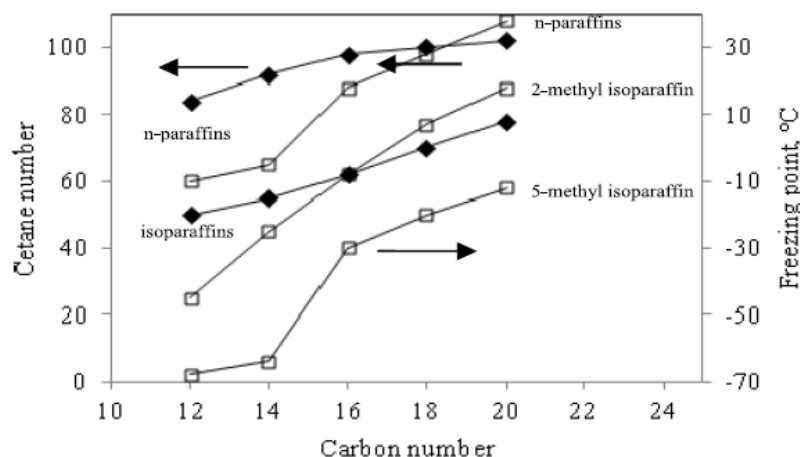


Figure 2.9 Freezing point and number of cetane of carbon number in n-paraffins and methyl branched paraffins¹⁴.

2.4 Steam reforming process

Steam reforming is a solution for hydrogen generation from hydrocarbon fuels such as natural gas where steam reacts with fuel in a reformer at high temperature. In order to produce hydrogen, the industry widely uses steam reforming of methane (SRM). Theoretically, 4 moles of H₂ can be generated per unit mole of methane via SRM. The commercial catalyst is Ni for the reforming of natural gas²⁹.

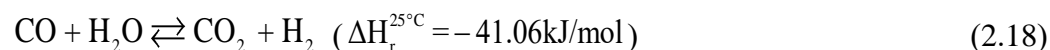
2.4.1 Propane steam reforming

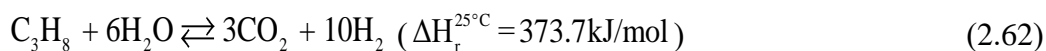
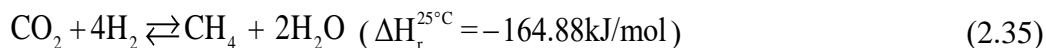
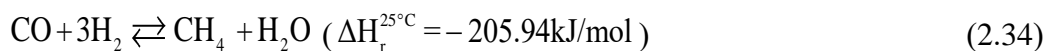
The alternative hydrogen production process uses propane and water as the reactants. Theoretically, 10 moles of H₂ can be generated per unit mole of propane via the overall propane steam reforming as shown below.

Propane steam reforming

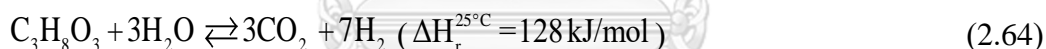
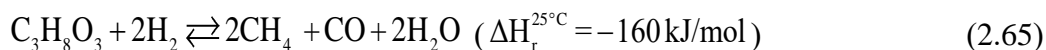


Water-gas shift



Overall PSR**Methanation****2.4.2 Glycerol steam reforming**

Glycerol steam reforming (GSR) uses glycerol and water as the reactants to produce hydrogen. Conventional GSR is an extremely endothermic reaction, requiring operation at high temperature. Glycerol reforming is a combination of decomposition of glycerol and water gas shift reaction. Theoretically, 7 moles of H_2 can be generated per unit mole of glycerol via the overall glycerol steam reforming as shown below^{16, 30-31}.

Glycerol decomposition**Water-gas shift****Overall GSR****Methanation****Glycerol hydrogenolysis**

CHAPTER III LITERATURE REVIEWS

In this chapter, literature reviews are divided into six parts. The first part consists of reviews of bio-hydrogenated diesel fuel production via hydrogenolysis and hydrolysis of vegetable oil. Secondly, a review of hydrogen production process via steam reforming using glycerol and propane as a reactant is presented. The third part is a review of the integration system of hydrotreating and hydrogen generation process. The fourth part is a review of pressure swing adsorption technology. The fifth part consists of a review on the use of catalysts for hydrotreating of TGs/ FFAs. Lastly, a review of thermodynamic of hydrotreating is presented.

3.1 Bio-hydrogenated diesel fuel production

3.1.1 Single-step of hydrogenolysis of triglycerides/ deoxygenation of free fatty acids process

Plazas-Gonzalez and co-workers³² studied simulation of green diesel production with hydrotreating of palm oil using a NiMo/ γ -Al₂O₃ catalyst. TGs reaction's possible routes in hydrotreating of oils is shown in Figure 3.1^{7, 32}. Peng Robinson with RK-ASPEN was used as a thermodynamic model and the reaction model shown in Table 3.1³²⁻³³ presented an equilibrium reactor. The process flow diagram of renewable diesel production with hydrotreating of palm oil is shown in Figure 3.2³², which was operated at 2,500 kg/h of initial feed of TGs and H₂/oil molar ratio of 20. For the initial temperature at 350 °C, increasing C₁₈ and C₁₆ with increasing pressure from 20 to 90 bar favors the reduction reactions (HDO) of stearic acid and palmitic acid, respectively. Then, a pressure of 40 bar was used to operate due to a higher interest in compounds. At 40 bar of pressure, the C₁₆ and C₁₈ of products are reduced with increasing temperature at 20 bar from 250 to 450 °C. Then, 300 °C of temperature was used to operate. At 40 bar and 350 °C, the C₁₆ and C₁₈ of products increased with the increase in the H₂/oil molar ratio from 10:1 to 25:1, with the 20:1 molar ratio being optimum for operation. For hydrotreating of oil, the optimal operating condition is in the range of 30 to 60 bar of pressure, 300 to 400 °C of temperature, and 20:1 of H₂/oil molar ratio, which obtained 97% purity of green diesel.

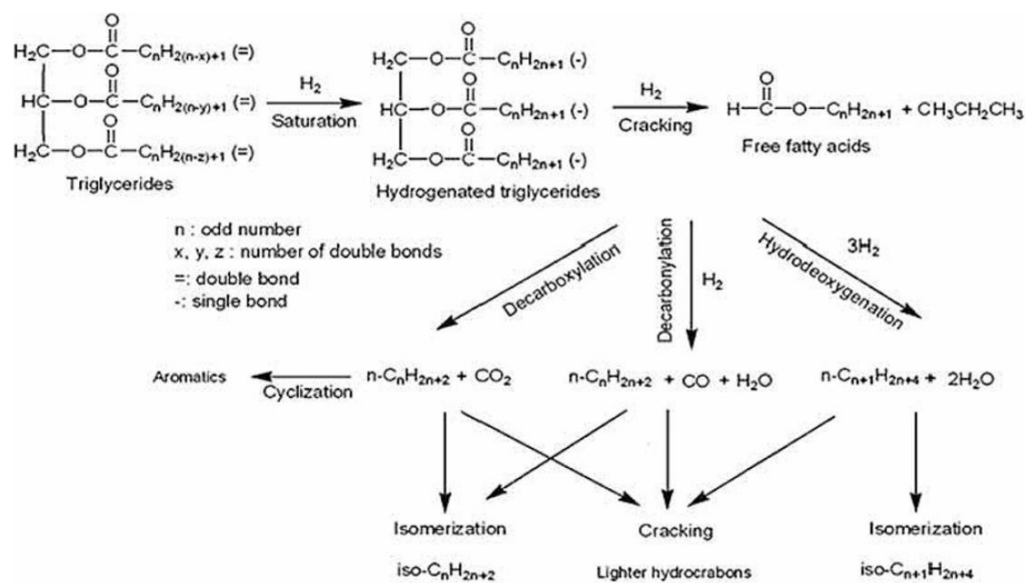


Figure 3.1 TGs reaction's possible routes in hydrotreating of vegetable oils^{7, 32}.

Table 3.1 Reaction model in equilibrium reactor³²⁻³³.

#	Stoichiometric reaction	Type
1	Triolein + 3H ₂ ⇌ 3 oleic acid + propane	Initial reactions
2	Tripalmitin + 3H ₂ ⇌ 3 palmitic acid + propane	
3	Trilinolein + 3H ₂ ⇌ 3 linoleic acid + propane	
4	Tristearin + 3H ₂ ⇌ 3 stearic acid + propane	
5	Oleic acid + H ₂ ⇌ stearic acid	Hydrogenation
6	Linoleic acid + 2H ₂ ⇌ stearic acid	
7	Stearic acid ⇌ n - C ₁₇ + CO ₂	Decarboxilation
8	Palmitic acid ⇌ n - C ₁₅ + CO ₂	
9	Oleic acid ⇌ C ₁₇ + CO ₂	
10	Stearic acid + H ₂ ⇌ n - C ₁₇ + CO + H ₂ O	Decarbonilation
11	Palmitic acid + H ₂ ⇌ n - C ₁₅ + CO + H ₂ O	
12	Oleic acid + H ₂ ⇌ C ₁₇ + CO + H ₂ O	
13	Stearic acid + 3H ₂ ⇌ n - C ₁₈ + 2H ₂ O	Reduction
14	Palmitic acid + 3H ₂ ⇌ n - C ₁₆ + 2H ₂ O	
15	Oleic acid + 3H ₂ ⇌ C ₁₈ + H ₂ O	
16	Stearic acid + 2H ₂ ⇌ octadecan-1-ol + H ₂ O	Alcohol formation
17	Palmitic acid + 2H ₂ ⇌ hexadecan-1-ol + H ₂ O	

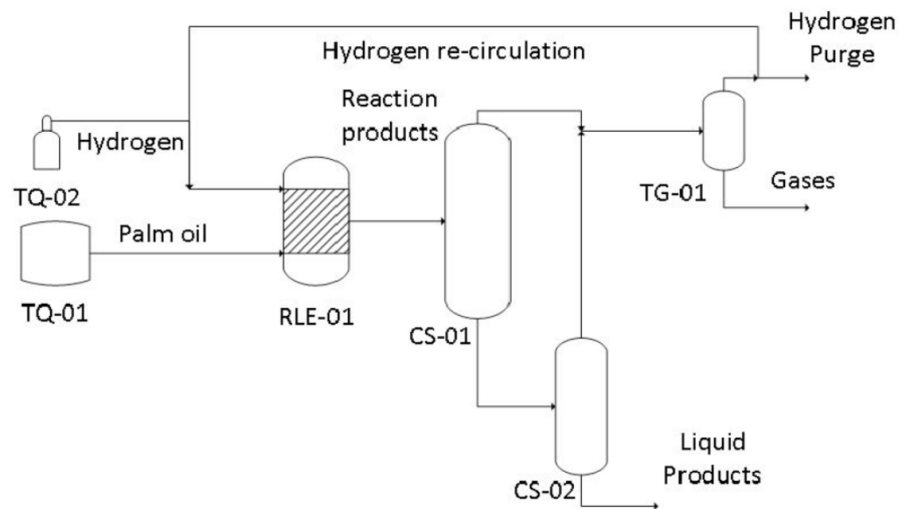


Figure 3.2 Process flow diagram of renewable diesel production with hydrotreating of palm oil³².

Kantama and co-workers⁶ studied techno-economic and heat-integrated for green diesel production from PFAD. The process consisted of three steps: catalytic hydrotreating, separating, and upgrading. For the operating condition of hydrotreating using a Pd/C catalyst, 375 °C of temperature and 40 bar of pressure, 76.13% conversion of PFAD was achieved in the conversion reactor. For isomerization, the reactor operates at 340 °C of temperature and 30 bar of pressure. The NRTL-RK property method was used in the process simulation. Furthermore, the studied results proved to be attractive for investment with 950 \$m⁻³ of green diesel price. The hydrotreating process is shown in Figure 3.3.

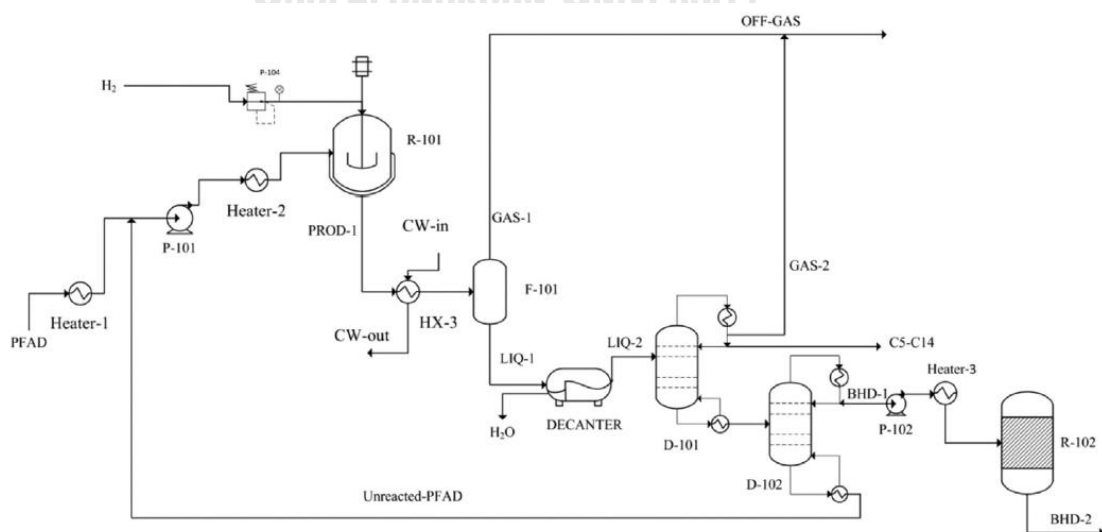


Figure 3.3 Hydrotreating process⁶.

Kantama and co-workers⁶ also studied heat integration to determine the minimum energy consumption with using pinch analysis and design a heat exchanger network with 10 °C of ΔT_{\min} .

Chu and co-workers¹ studied process modeling of renewable jet fuel production from camelina, carinata, and used cooking oil (UCO) in order to evaluate the demand of H₂ and the requirement of energy and electricity. The operating condition of the HDO process model was 400 °C of reaction temperature and 92 bar of reaction pressure using nickel-molybdenum (NiMo). The assumptions of DO for the HDO process model was 0.9994 of conversion of deoxygenation and 0.68, 0.03, and 0.29 of extent of DCO₂, HDCO, and HDO, respectively. The processes were simulated using RStoic reactor model and NRTL&Peng-Robinson of property method in an Aspen Plus simulator. The catalyst and the reaction condition determine the selectivity of cracking. A kerosene yield of 53% and a diesel yield of 13% were obtained, with 26 to 30 kg of H₂ consumption per ton of oil, which depends on the degree of unsaturation of feedstocks. The thermal energy demand from UCO, carinata oil, and camelina oil was 2.8, 5.2 and 5.7 GJ/ton oil, respectively, which is the energy required for oil extraction from carinata oil and camelina oil. The electricity demand from UCO, carinata oil, and camelina oil was 73, 170 and 227 kWh/ton oil. The renewable jet fuel production is shown in Figure 3.4.

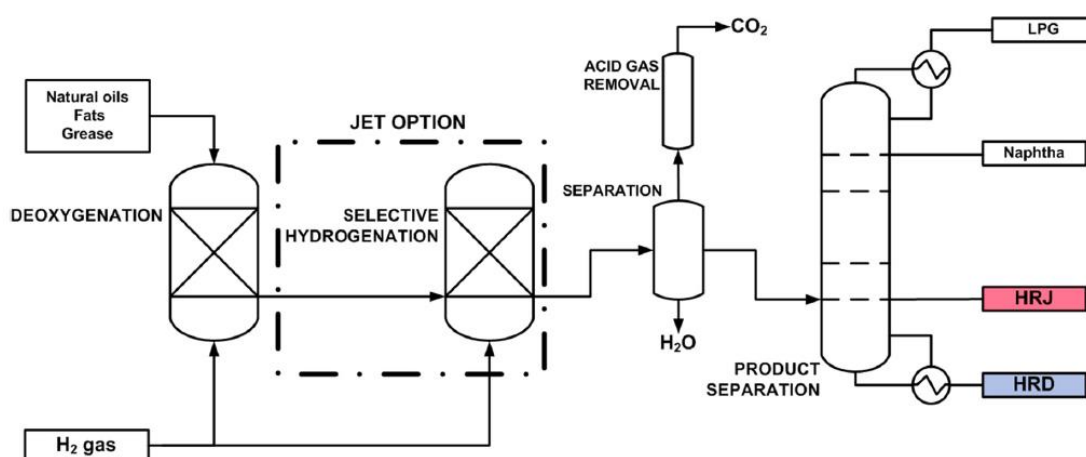


Figure 3.4 Renewable jet fuel production¹.

Cheah and co-workers³⁴ studied analysis of techno economic of green diesel production through the decarboxylation reaction from rubber seed oil using a Pd/C

catalyst. The operating condition was 375 °C of temperature and 40 bar of pressure in a packed bed reactor. The study achieved 90% conversion of deoxygenation with 95% to DCO₂ and 5% to HDCO reactions. The Aspen HYSYS program was used for simulation and the non-random two liquid (NRTL) property method was used for the thermodynamic model. Furthermore, the studied results specified that the production cost was sensitive to feedstocks price and H₂ gas price. The process flow diagram of the green diesel production model is shown in Figure 3.5.

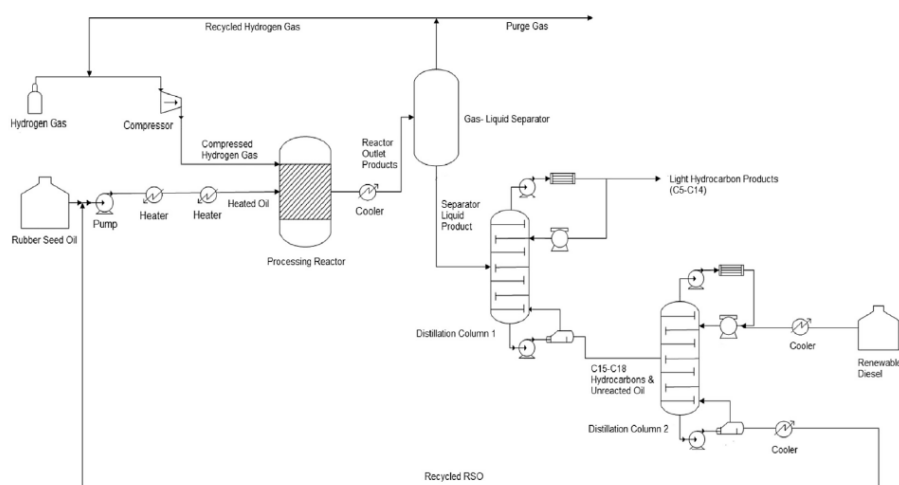


Figure 3.5 Process flow diagram of green diesel production model³⁴.

Miller and co-workers³⁵ studied techno-economic of BHD production from canola and camelina using the Aspen Plus model and the BK-10 property set for the thermodynamic model. The major process consisted of a hydrotreating unit and a distillation unit. The RYield model reactor was used to simulate hydrotreating using a Pd/C catalyst at the operating condition of 400 °C and 152 bar (15.2 MPa). The distillation train was simulated by PetroFrac unit operation. The high solubility and the low resistance to mass transport of alkane occurred in supercritical hexane which increased production costs. Furthermore, the BHD production is highly sensitive to the price of solvent, recovery of solvent and the cost of feedstock. The BHD production process diagram is shown in Figure 3.6.

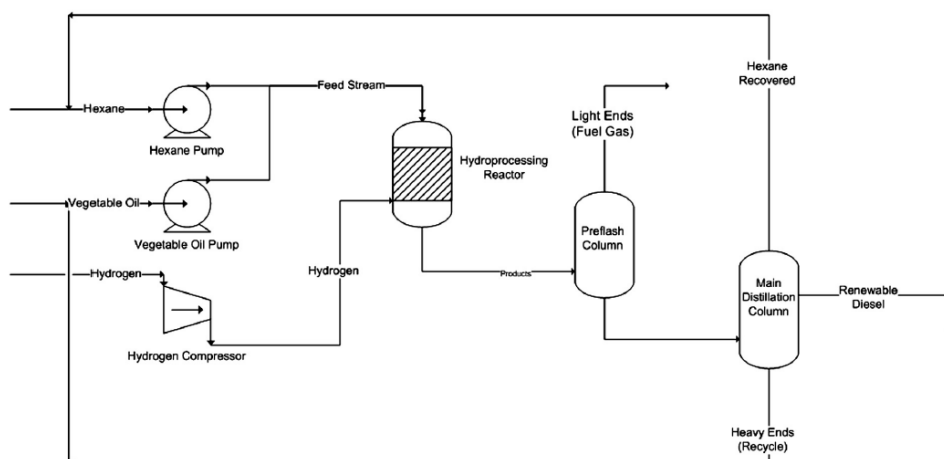


Figure 3.6 BHD production process diagram³⁵.

Azizan and co-workers³⁶ studied BHD production with equilibrium analysis of triolein. The R-Gibbs reactor was used for analysis and the thermodynamic model used the Peng-Robinson property method in Aspen HYSYS. The studied result indicated that the 5:1 feed molar ratio of H_2 to triolein was optimum with 70 bar of pressure, which can produce highly desired products. C_{18} hydrocarbon was selected to decrease with increasing temperature. Methane and propane were by-products from side reactions.

Perez-Cisneros and co-workers³⁷ studied hydrotreating of vegetable oils and petro-diesel blends for green diesel production with a process of reactive distillation. Perturbed-Chain Statistical Associating Fluid Theory (PC-SAFT) was used for the thermodynamic model in Aspen Plus to simulate the reactive distillation process. The mixture products from the hydrotreating process contained unreacted TGs, water, alkanes, and gaseous compounds such as H_2 , propane, CO_2 , and CO .

Glisic and co-workers³⁸ studied waste vegetable oil for BHD production and performed techno-economic analysis. The thermodynamic model used RK-Aspen EOS in UniSim software when the process operated at high pressures and high temperatures. Peng-Robinson EOS was employed at near atmospheric pressure. RYield reactor operation was simulated at 390 °C of temperature and 138 bar of pressure, using $CoMo/Al_2O_3$ and H_2/oil feed molar ratio of 46 with 95.6% conversion. The process flow diagram of the BHD production is shown in Figure 3.7.

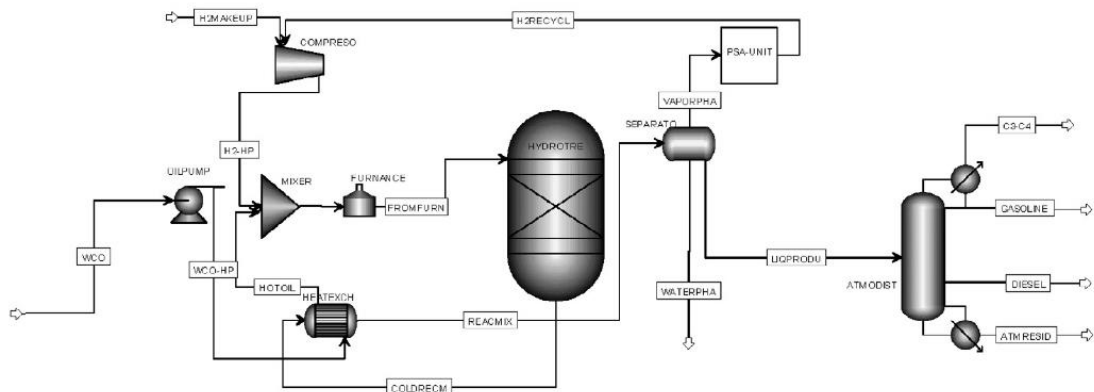


Figure 3.7 Process flow diagram of BHD production³⁸.

Hilbers and co-workers³⁹ studied hydrotreated vegetable oil process design for green diesel production. UniSim was used for the design and NRTL-RK was chosen as the thermodynamic property package. Hydrotreatment of vegetable oil consisted of pretreatment, reaction, and separation. The reactors in series (R1-2) was operated at 300-350 °C of temperature and 35 bar of pressure. The study achieved 97% conversion of hydrotreatment using the NiMo/ γ -Al₂O₃ catalyst. For the second reactor (R2), which was a trickle-bed reactor using the bifunctional Ni-Mo catalyst on ZSM-5 zeolite, operation at 380 °C of temperature and 35 bar of pressure yielded 100% conversion of isomerization with hydrogen feed. The process flow diagram of hydrotreated vegetable oil is shown in Figure 3.8.

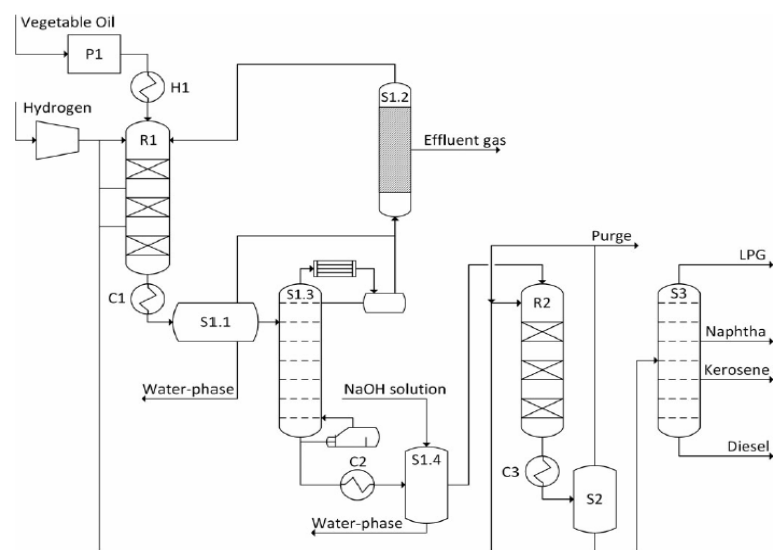


Figure 3.8 Process flow diagram of hydrotreated vegetable oil³⁹.

Smejkal and co-workers⁴⁰ studied thermodynamic of hydrotreating vegetable oil. The Joback's contribution method and tabulated values by Peng-Robinson EOS were used to calculate and estimate the accuracy of the Gibbs free energies of total hydrogenation into hydrocarbons with various temperatures at pressure of 70 bar as shown in Figure 3.9. The deviation is acceptable indicating the accuracy of the thermodynamic parameters, and the forecast is reasonable.

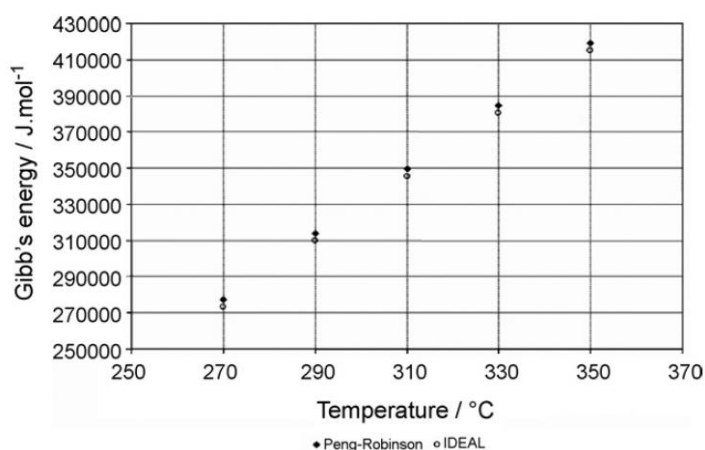


Figure 3.9 Gibbs free energies of total hydrogenation into hydrocarbons with various temperatures at pressure of 70 bar⁴⁰.

The sum of calculations from tristearate and hydrogenation of rape-seed oil from experiments was compared with the concentrations of C₁₇ and C₁₈ hydrocarbon products at 70 bar and temperature from 270 to 350 °C as shown in Figure 3.10. NiMoS on alumina was used as a catalyst. To obtain the extent of reaction corresponding with 7 moles of H₂ per unit mole of tristearate, H₂ to oil ratio of 100 was supplied. The temperature of 300 °C shows acceptable agreement between the experiment and the model.

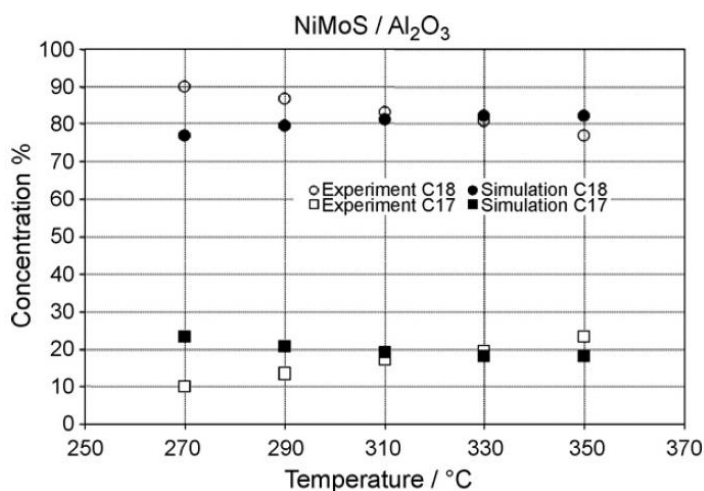


Figure 3.10 Concentrations of C₁₇ and C₁₈ hydrocarbon at 70 bar for tristearate (calculation) and rape-seed oil (experiments) hydrogenation⁴⁰.

Guzman and co-workers³³ studied hydrotreating of crude palm oil (CPO) using the NiMo/ γ -Al₂O₃ catalyst. Two process variables were investigated: 15 - 90 bar of hydrogen pressure and 0 - 14 days of time on stream (TOS). Equilibrium reactor in Aspen Plus was used based on stoichiometric approach, and the employed thermodynamic model of phase equilibrium was PSRK.

Results of simulation with two different H₂:CPO ratios equal to 12.5:1 and 20:1 at 350 °C were compared with H₂:CPO ratio of 20:1 from the experiment as shown in Figure 3.11. The simulation results at 12.5:1 of H₂:CPO ratio were in agreement with the experiment data. If these reactions are in a chemical equilibrium, they show that there is no effective hydrogen, but these reaction conditions can be limited by diffusion of hydrogen or diffusion of TGs to the active sites with the mass fraction profile shown in Figure 3.12.

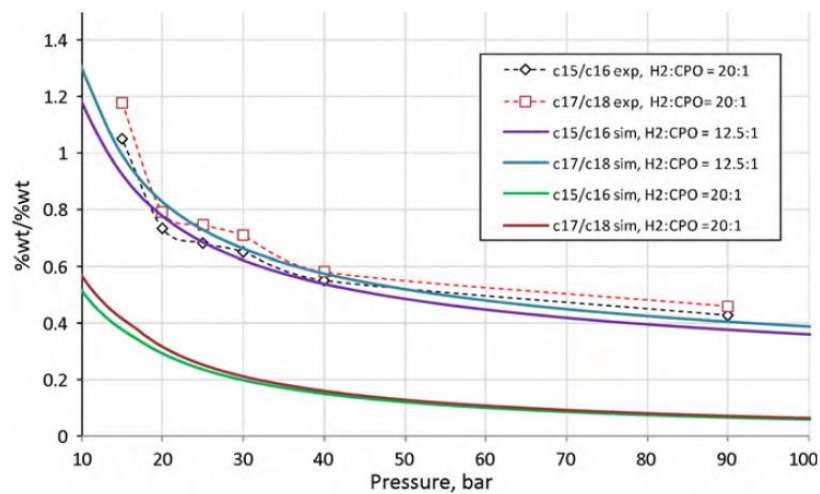


Figure 3.11 Profile of C₁₅/C₁₆, C₁₇/C₁₈ from equilibrium and experimental at 350 °C with various pressures of reactor³³.

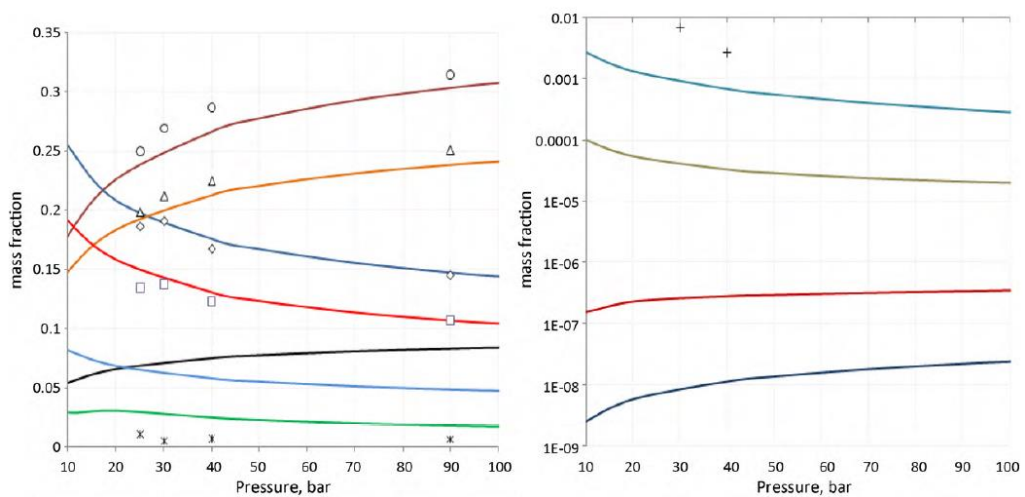


Figure 3.12 Profiles of mass fractions of equilibrium at 350 °C and 12.5:1 of H₂:CPO with various pressures of reactor and 20:1 of H₂:CPO at 350 °C from experimental data³³.

The hydrogen consumption from the effect of pressure was calculated from the simulation as shown in Figure 3.13. The results of CO and CO₂ gas products of HDCO and DCO₂ reaction routes, respectively, decreased with pressure. The hydroprocessing of CPO at approximately 40 bar of pressure, which DCO₂ and HDCO are favored, consumed less hydrogen following the lower pressure.

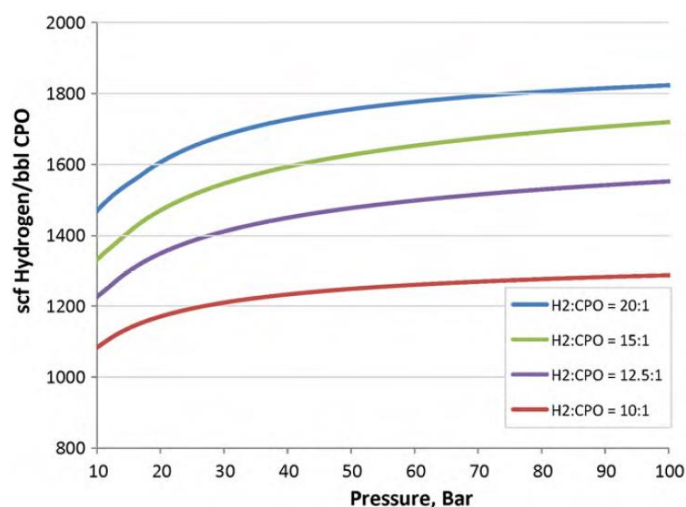


Figure 3.13 Hydrogen consumption at 350 °C, 2 h⁻¹ of LHSV with various pressures of reactor and H₂:CPO ratios³³.

Kumar and co-workers⁴¹ studied the hydrodeoxygenation of stearic kinetics, using acid over nickel metal on different supports, at the initial hydrogen pressure of 8 bar in the 260 - 290 °C of temperature range and 13 - 14.5 bar of pressure, which was operated in a batch reactor. A 100% conversion at 360 min was obtained from the operation at 290 °C of temperature and 14.5 bar of pressure. Hydrodeoxygenation of stearic acid mechanism pathways, using the Ni catalyst, is shown in Figure 3.14.

Moreover, the first order kinetic model was used in liquid phase components using the excess H₂. Thus, formation rates of the different components were expressed as shown in Table 4.1 in the next chapter by following the differential Equations 3.1 - 3.6.

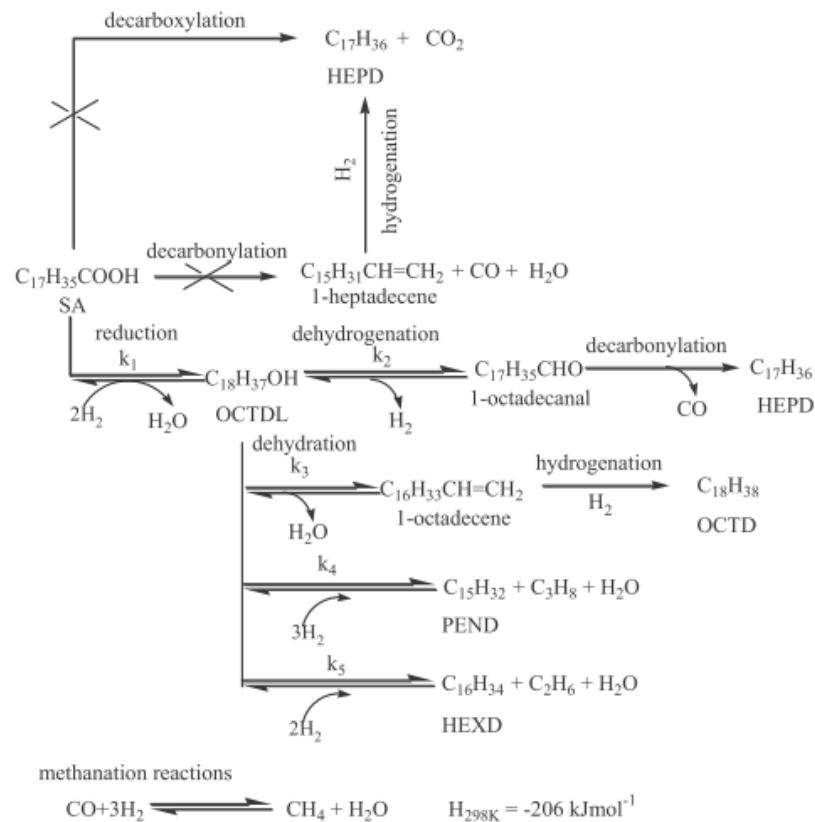


Figure 3.14 Hydrodeoxygenation of stearic acid mechanism pathways, using Ni catalyst⁴¹.

Rate of stearic acid consumption:
$$\frac{dC_{\text{SA}}}{dt} = -k_1 C_{\text{SA}} \quad (3.1)$$

HEPD production rate:
$$\frac{dC_{\text{HEPD}}}{dt} = k_2 C_{\text{OCTDL}} \quad (3.2)$$

OCTD production rate:
$$\frac{dC_{\text{OCTD}}}{dt} = k_3 C_{\text{OCTDL}} \quad (3.3)$$

PEND production rate:
$$\frac{dC_{\text{PEND}}}{dt} = k_4 C_{\text{OCTDL}} \quad (3.4)$$

HEXD production rate:
$$\frac{dC_{\text{HEXD}}}{dt} = k_5 C_{\text{OCTDL}} \quad (3.5)$$

OCTDL production rate:
$$\frac{dC_{\text{OCTDL}}}{dt} = k_1 C_{\text{SA}} - (k_2 + k_3 + k_4 + k_5) C_{\text{OCTDL}} \quad (3.6)$$

Figure 3.15 shows the effect of reaction temperatures on stearic acid conversion. Stearic acid conversion increases with increasing reaction temperatures. At 290 °C (563 K) of temperature, even after 240 min of reaction, almost complete

SA conversion was obtained with the selectivity to HEPD being the primary product in the presence of the nickel catalyst on γ -Al₂O₃ support.

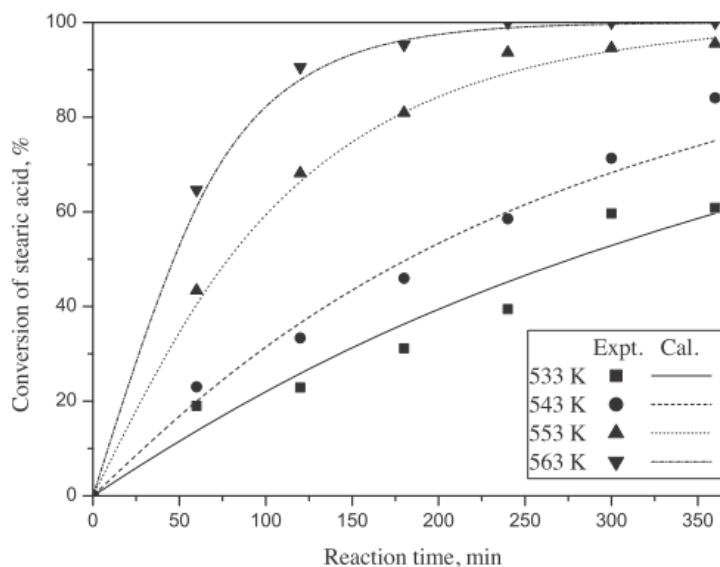


Figure 3.15 The reaction temperatures effect on conversion of stearic acid using nickel supported catalyst, 0.18 kmol/m³ of concentration of stearic acid and 8 bar of initial hydrogen pressure⁴¹.

Jenistova and co-workers⁴² proposed a kinetic model of deoxygenation of stearic acid using Ni supported on γ -Al₂O₃ catalyst. The results showed a 99% conversion in 360 min and 97% of selectivity to heptadecane which was operated at 300 °C of temperature and 30 bar of total pressure using 5% Ni- γ -Al₂O₃. The pressure effect was included in the kinetic model and the kinetic model applied for data with Ni- γ -Al₂O₃ as well as Pd/C, Ni-H-Y-80, and Ni/SiO₂ catalysts. The network of reaction for deoxygenation of stearic acid is shown in Figure 3.16. Langmuir-Hinshelwood type of kinetics was expressed in Equations 3.7 - 3.8 and hydrogen pressure is used to replace the dissolved hydrogen concentration. The reaction rate of the second step is not dependent on the hydrogen pressure as shown in Equation 3.9. Thus, the formation rate of various components of stearic acid (A), stearyl alcohol (B), heptadecane (C), and octadecane (D) is represented by the ordinary differential equation according to Equations 3.10 - 3.13.

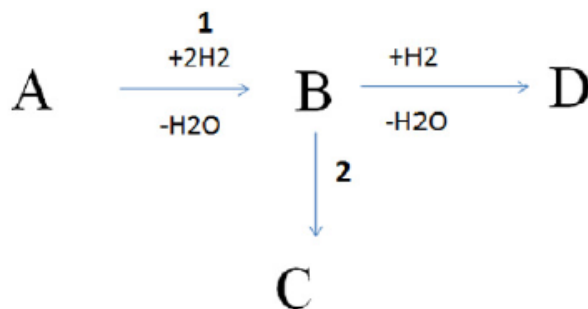


Figure 3.16 The network of reaction for deoxygenation of stearic acid⁴².

$$r_1 = \frac{k_1' c_A p_{H_2}}{(1 + K_A c_A)(1 + K_H p_{H_2})} \quad (3.7)$$

$$r_3 = \frac{k_3' c_B p_{H_2}}{(1 + K_A c_A)(1 + K_H p_{H_2})} \quad (3.8)$$

$$r_2 = \frac{k_2' c_B}{1 + K_A c_A} \quad (3.9)$$

A production rate: $\frac{dC_A}{dt} = -r_1$ (3.10)

B production rate: $\frac{dC_B}{dt} = r_1 - r_2 - r_3$ (3.11)

C production rate: $\frac{dC_C}{dt} = r_2$ (3.12)

D production rate: $\frac{dC_D}{dt} = r_3$ (3.13)

The estimated rate constants are listed in Table 4.2 with different catalyst types listed in Table 3.2. In Table 4.2, a single hydrogen pressure was used for the experimental data, so that lumped parameters k_1' and k_3' in this Table include the dependence on hydrogen pressure. The model well described the kinetic data.

Table 3.2 Estimated rate constant for HDO of stearic acid, using 5 wt.% of different catalysts at temperature 300 °C and 30 bar of total pressure⁴².

Catalyst	$k_1 \text{ min}^{-1}$	Rel. St. error (%)	$k_2 \text{ min}^{-1}$	Rel. St. error (%)	$k_3 \text{ min}^{-1}$	Rel. St. error (%)	$K_A [-]$	Rel. St. error (%)
5 wt% Ni-H-Y-80	1.4×10^{-3}	4.8	6.25	4.3	3.16×10^{-1}	4.2	4.01×10^1	3
5 wt% Ni/SiO ₂	1.85×10^{-3}	22.9	4.48×10^{-1}	25.6	5.46×10^{-4}	36.5	2.55×10^2	26.6
5 wt% Pd/C	4.66×10^{-4}	7.2	2.9	32.4	2.57×10^{-3}	31.5	2.06×10^2	8.8

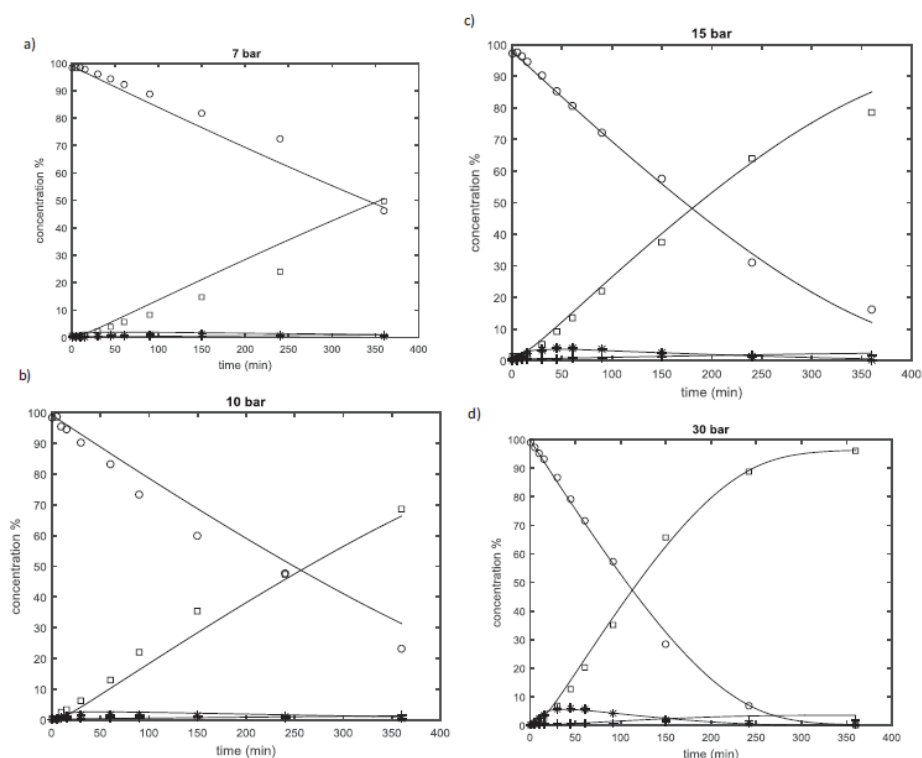


Figure 3.17 Total pressure effects on deoxygenation of stearic acid using 5 wt.% Ni- γ -Al₂O₃ at 300 °C of temperature. Symbols: (o) stearic acid, (\square) heptadecane, (*) stearyl alcohol, and (+) octadecane⁴².

Figure 3.17 shows the total pressure effects on deoxygenation of stearic acid. Stearic acid conversion increased with increasing total pressure. The solid lines were consistent with calculations.

The literature review of modelling and design of plant for single-step of hydrogenolysis of TGs/ deoxygenation of FFAs process for bio-hydrogenated diesel fuel production can be summarized in Table 3.3.

Table 3.3 Literature review of modelling and design of plant for single-step of hydrogenolysis of TGs/ deoxygenation of FFAs process for bio-hydrogenated diesel fuel production.

Feedstock	Simulation model	Thermodynamic model	Reactor model	Reaction condition	Catalyst	Performance	Reference
Palm oil	Aspen Plus	Peng Robinson with RK-Aspen	REquil	T=300 °C P=40 bar, H ₂ /oil=20:1	NiMo/ γ -Al ₂ O ₃	97% purity of BHD	Plazas-Gonzalez and co-workers, 2018 ³²
PFAD	Aspen Plus	NRTL-RK	RStoic	T=375 °C P=40 bar, T=340 °C P=30 bar	Pd/C	Conversion 76.13%	Kantama and co-workers, 2015 ⁶
Camelina oil, carinata oil, UCO	Aspen Plus	NRTL PENG-ROB	RStoic	T=400 °C P=92 bar	NiMo	Conversion 99.94%	Chu and co-workers, 2017 ¹
Rubber seed oil	Aspen HYSYS	NRTL	Conversion	T=375 °C P=40 bar	Pd/C	Conversion 90%	Cheah and co-workers, 2017 ³⁴
Canola oil, camelina oil	Aspen Plus	BK10	RYield	T=400 °C P=152 bar	Pd/C	-	Miller and co-workers, 2014 ³⁵

Table 3.3 Literature review of modelling and design of plant for single-step of hydrogenolysis of TGs/ deoxygenation of FFAs process for bio-hydrogenated diesel fuel production. (*Continued*).

Feedstock	Simulation model	Thermodynamic model	Reactor model	Reaction condition	Catalyst	Performance	Reference
Triolein	Aspen HYSYS	PENG-ROB	R-Gibbs reactor	T=50-450 °C P=40 bar	-	-	Azizan and co-workers, 2016 ³⁶
Triolein, oleic acid	Aspen Plus	PC-SAFT	RD	T=240-414 °C P=30 atm	Sulfide CoMo/Al ₂ O ₃ and NiMo/Al ₂ O ₃	Conversion 100%	Perez-Cisneros and co-workers, 2017 ³⁷
WVO	UniSim	RK-Aspen PENG-ROB	RYield	T=390 °C P=138 bar	CoMo/Al ₂ O ₃	Conversion 95.6%	Glisic and co-workers, 2016 ³⁸
Palm oil	UniSim	NRTL-RK	Trickle-bed	T=300-350 °C P=35 bar, T=380 °C P=35 bar	NiMo/γ-Al ₂ O ₃ Ni-Mo catalyst on a ZSM-5 zeolite	Conversion 97% Conversion 100%	Hilbers and co-workers, 2015 ³⁹
Tristearate, Rape-seed oil	Aspen Plus, Experimental	PENG-ROB	Fixed-bed reactor	T=270-350 °C P=70 bar	NiMo/Al ₂ O ₃ hydrotreating, Ni/Al ₂ O ₃ hydrogenation	Agreement	Smejkal and co-workers, 2009 ⁴⁰

Table 3.3 Literature review of modelling and design of plant for single-step of hydrogenolysis of TGs/ deoxygenation of FFAs process for bio-hydrogenated diesel fuel production. (*Continued*).

Feedstock	Simulation model	Thermodynamic model	Reactor model	Reaction condition	Catalyst	Performance	Reference
Crude palm oil	Aspen Plus, Experimental	PSRK	REquil Trickle-bed reactor	T=350 °C P=15-90 bar	NiMo/Al ₂ O ₃	Agreement with 20:1 (Exp.) and 12.5:1 (Cal.) of H ₂ :oil ratio	Guzman and co-workers, 2010 ³³
Stearic acid	Experimental	Kinetics model	Batch reactor	T=260, 270, 280, 290 °C P=13, 13.5, 14, 14.5 bar	Ni/ γ -Al ₂ O ₃	Conversion 60, 84, 98, 100% at 360 min	Kumar and co-workers, 2014 ⁴¹
Stearic acid	Experimental	Kinetics model	Semi-batch reactor	T=300 °C P=7, 10, 15, 30 bar	Ni/ γ -Al ₂ O ₃ Ni-H-Y-80 Ni/SiO ₂ Pd/C	Conversion 99%	Jenistova and co-workers, 2017 ⁴²

3.1.2 Two-step: hydrolysis of triglycerides and deoxygenation of free fatty acids process

Gomez-Castro and co-workers⁴³ reported 99.83% conversion of triolein for hydrolysis which was simulated by a first order kinetic model at 70 bar and 270 °C of reaction and triolein is hydrolyzed with water in a 1/1 volumetric ratio in order to shift the equilibrium to the desired products. Then, hydrolysis of triolein with water is shown in three steps of reaction:



where OLAC corresponds to oleic acid and TRIO, DIO, and MONO stand for triolein, diolein, and monoolein, respectively. The overall hydrolysis reaction can then be specified as:



The hydrolysis reaction considers first order for the kinetic model:

$$\frac{dC_{\text{OLAC}}}{dt} = k_{\text{H}} C_{\text{TRIO}} \quad (3.18)$$

where the value of k_{H} has been taken as 0.0026 s^{-1} at 270 °C (Minami and Saka⁴⁴) with 63,553.05 J/mol of activation energy of hydrolysis reaction. Water is fed in excess for the process. The Redlich-Kwong-Aspen equation of state (RK-ASPEN) was the thermodynamic model for the simulation of the hydrolysis reactor. Figure 3.18 demonstrates the biodiesel production process with hydrolysis of triolein. For the first reaction using a plug flow reactor, the stream leaves from the reactor into a decanter, where the phase of oil and the aqueous phase were separated. The UNIFAC model was used for simulating the decanter in order to predict two phases of liquid formation. The aqueous phase was obtained from the decanter, which contained glycerol and water.

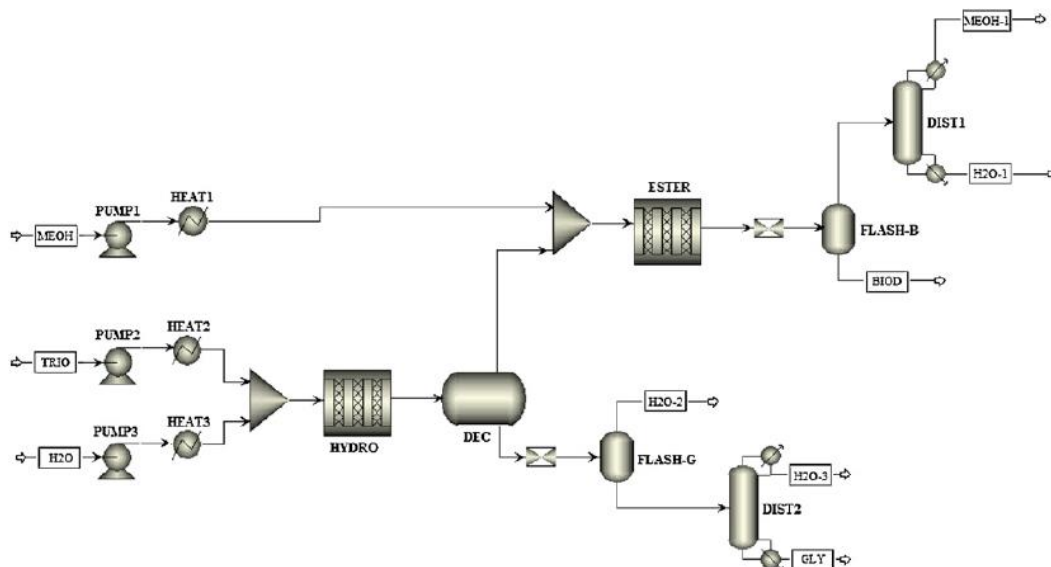


Figure 3.18 Biodiesel production process with hydrolysis of triolein using plug flow reactor⁴³.

Minami and co-workers⁴⁴ studied kinetics in the hydrolysis reaction of TGs in subcritical water without any catalyst in a tubular reactor from rape seed oil, which operated at 270 °C of temperature and 200 bar (20 MPa) of pressure. Figure 3.19 shows FFAs yields obtained from rapeseed oil in subcritical waters in various conditions. However, higher temperatures may lead to a higher rate of FFA formation, with around 90 wt.% of FFAs yields with 1/1 of water to rapeseed oil volumetric ratio.

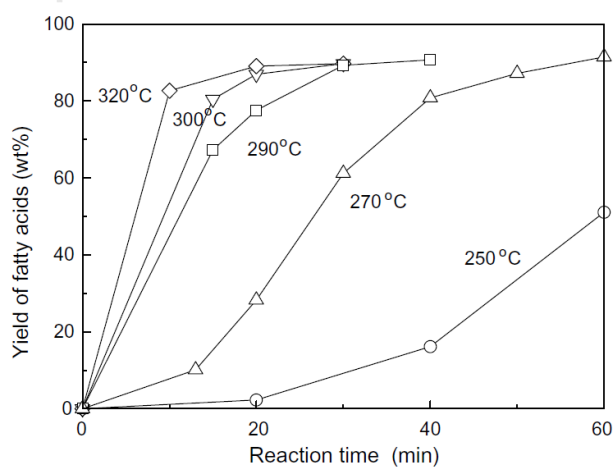


Figure 3.19 FFAs yields obtained from rapeseed oil in subcritical waters in various conditions⁴⁴.

Jenistova and co-workers⁴² also tested tall oil fatty acids (TOFA) as a raw material in the HDO reaction at 300 °C and 30 bar of total pressure in hydrogen. TOFA contains stearic acid (C18:0) in addition to unsaturated FFAs, including oleic acid (C18:1), linoleic acid (C18:2), and linolenic acid (C18:3).

Unsaturated FFAs are rapidly hydrogenated and provided stearic acid, which is evident from Figure 3.20. It shows that the concentration of stearic acid initially increases. In addition, 94% of conversion and 96% of selectivity of heptadecane were the final results.

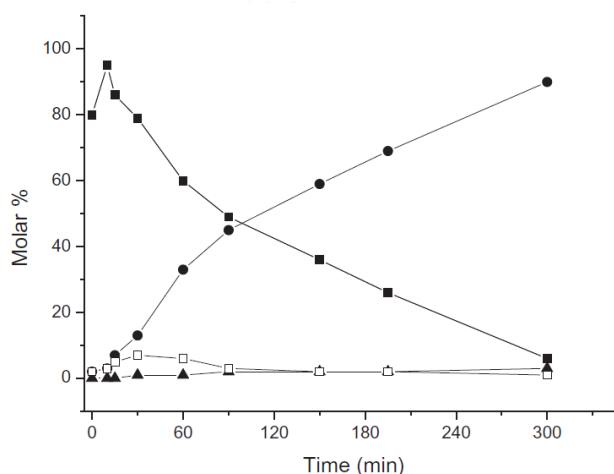


Figure 3.20 Molar (%) of stearic acid (■), heptadecane (●), stearylalcohol (□), and octadecane (Δ) in the HDO reaction of TOFA. Conditions of reaction: 300 °C of temperature and total pressure in hydrogen of 30 bar⁴².

Wang and co-workers⁴⁵ studied canola oil conversion to hydrocarbons, with the process shown in Figure 3.21. 99.7% conversion of hydrolysis was obtained from continuous thermal hydrolysis operated at 250 °C of temperature and 55 bar of pressure, with the water feed rate of 20 mL/min and the oil feed rate of 10 mL/min, and the volumetric ratio of 2:1. 90% of deoxygenation was obtained from using fed-batch thermo-catalytic decarboxylation, 5% Pd/C catalyst operated at 300 °C of temperature, 19 bar of pressure, with the feed rate of H₂ and He gas of 7.0 mL/min. The characteristics of DG appearing in Figure 3.22 show the step of the hydrolysis reaction that TG transformed into DG and converted to MG, respectively. Figure 3.23 shows that the concentrations of FFAs and glycerol (GLY) began to rise before 50 min and reached equilibrium at 180 min and 210 min, respectively. The

decarboxylation reaction was dominant with a higher CO_2 production rate than CO as shown in Figure 3.24.

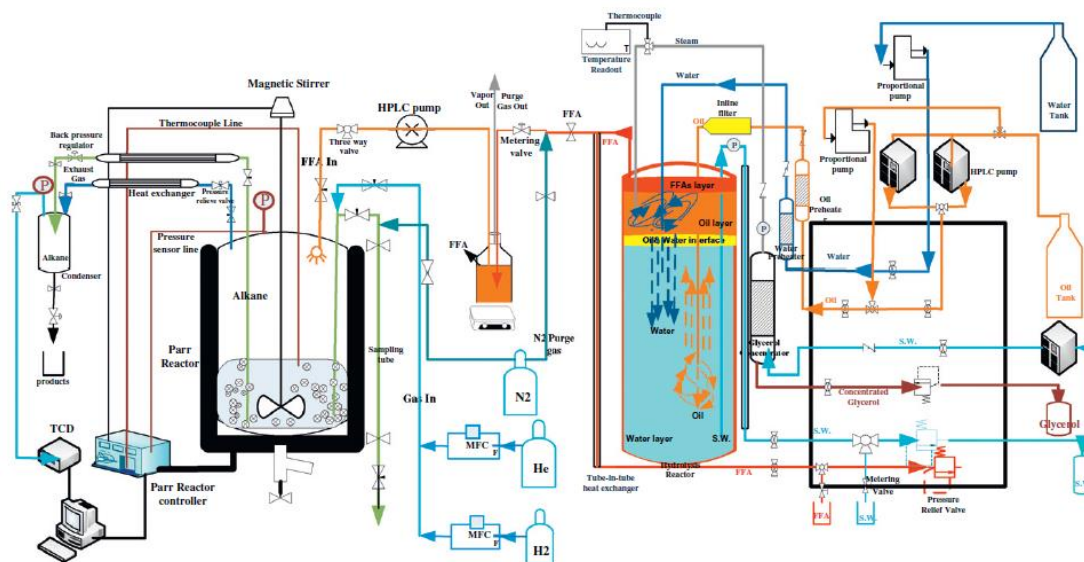


Figure 3.21 Continuous hydrolysis and fed-batch decarboxylation system⁴⁵.

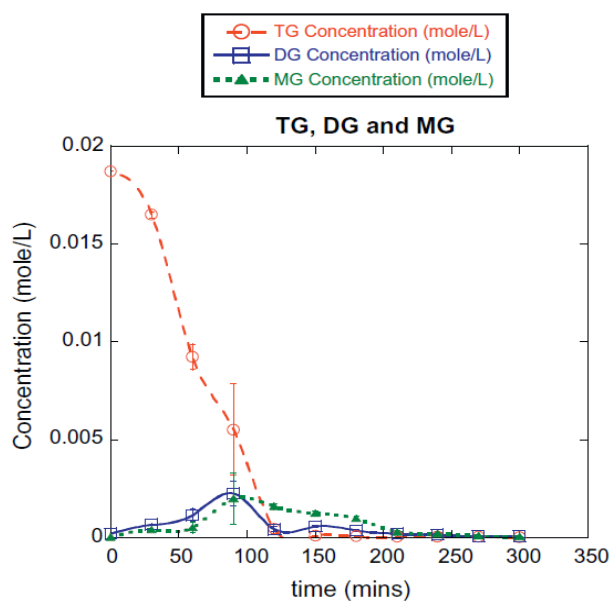


Figure 3.22 Concentrations of TG, DG, and MG with various times at 250 °C of temperature, water feed rate of 20 mL/min, and oil feed rate of 10 mL/min⁴⁵.

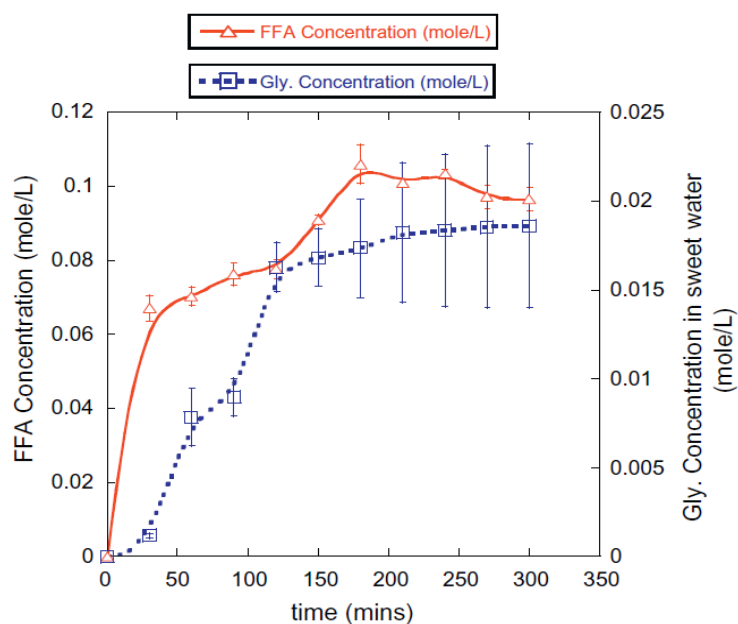


Figure 3.23 Concentrations of FFA and GLY with various times at 250 °C of temperature, water feed rate of 20 mL/min, and oil feed rate of 10 mL/min⁴⁵.

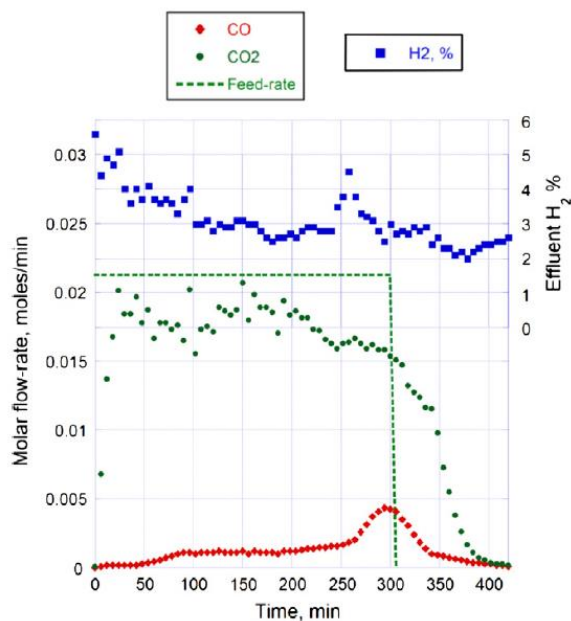


Figure 3.24 Molar flow rates of CO₂ and CO and mol (%) of effluent H₂ obtained from deoxygenation of canola oil derived FFA for fed-batch at 300 °C and 19 bar, using 5% Pd/C catalyst with dodecane solvent and 7.0 mL/min of feed rate⁴⁵.

Wang and co-worker⁴⁶ reported the hydrolysis reaction of canola oil at temperature of 250 °C and pressure of 55 bar with 20 ml of H₂O and 10 ml of oil,

which provide 85.87% of FFAs yield with time of 5 h and analyzed thermodynamic of the process, which reactor makeup heat of 6,840 kJ from the hydrolysis reaction of canola with a continuous reactor. However, the continuous process provided a higher degree of the hydrolysis reaction than the batch process because water-glycerol mixtures are replaced by the fresh water continuously, leading to the forward shift reaction.

Natelson and co-workers⁴⁷ studied jet fuel production with analysis of technoeconomic obtained from hydrolysis, DCO₂, and hydrogen generation from camelina oil. Operating conditions of 250 °C and 50 bar (5 MPa) resulted in 99.7% of yields for hydrolysis reaction. The optimal sweet-water flash condition was at temperature of 125 °C and 1 atm of pressure. The stream of FFAs oil is purified and it was sent to a decarboxylation reactor. A temperature of 200 °C and atmospheric pressure were optimal FFAs flash conditions. In the hydrotreating process, hydrogen saturates on the double bonds of FFAs with the catalytic reaction when operating at 280 °C of temperature and 20 bar (2 MPa) of pressure. A deoxygenation efficiency of 100% is assumed, with 95% to DCO₂ and 5% to HDCO. Aspen Plus was used for the simulation and the NRTL property method was thermodynamic model. For process energy, energy was obtained from glycerol by-product in the sweetwater by a boiler. The diagram of the hydrolysis, DCO₂, and isomerization/ hydrocracking process is shown in Figure 3.25.

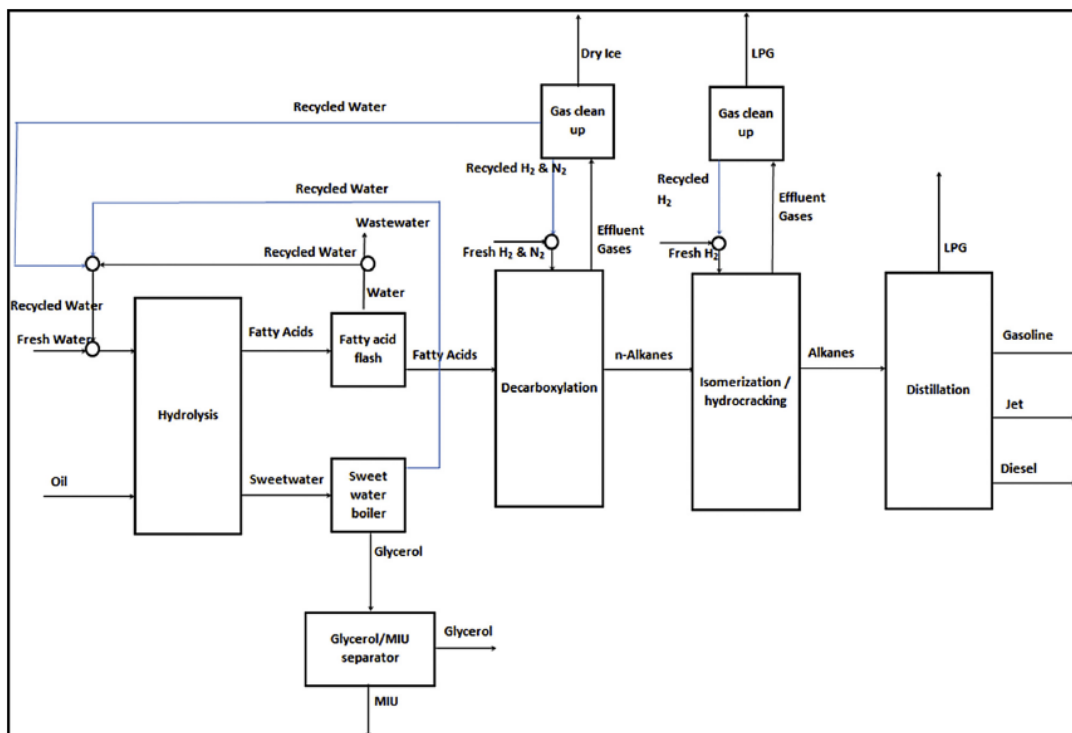


Figure 3.25 Diagram of the hydrolysis, DCO₂, and isomerization/hydrocracking process⁴⁷.

The literature review of modelling and design of plant for two-step: hydrolysis of TGs and deoxygenation of FFAs process for bio-hydrogenated diesel fuel production can be summarized in Table 3.4.

Table 3.4 Literature review of modelling and design of plant for two-step: hydrolysis of TGs and deoxygenation of FFAs process for bio-hydrogenated diesel fuel production.

Feedstock	Simulation model	Thermodynamic model	Reactor model	Reaction condition	Catalyst	Performance	Reference
Triolein	Aspen Plus	RK-ASPEN UNIFAC Kinetics model	Hydrolysis tubular reactor	T= 270 °C P=70 bar	-	Conversion 99.83%	Gomez-Castro and co-workers, 2013 ⁴³
Rape seed oil	Experimental	Kinetics model	Hydrolysis tubular reactor	T=270 °C P=200 bar	-	Yield FFA 90%	Minami and co-workers, 2006 ⁴⁴
Canola oil	Experimental	-	Continuous hydrolysis reactor Fed-batch deoxygenation reactor	T=250 ° P= 55 bar T=300 °C P=19 bar	- Pd/C	Conversion 99.7% Conversion 90%	Wang and co-workers, 2012 ⁴⁵
Canola oil	Experimental	-	Continuous hydrolysis reactor Batch reactor	T=250 ° P=55 bar	-	Yield FFA 85.8%	Wang and co-workers, 2012 ⁴⁶
Camelina oil	Aspen Plus	NRTL	Hydrolysis reactor Deoxygenation reactor	T=250 °C P= 50 bar T=280 °C P=20 bar	-	Yield 99.7% Conversion 100%	Natelson and co-workers, 2015 ⁴⁷

3.2 Hydrogen production

3.2.1 Propane steam reforming process

Wang and co-workers⁴⁸ studied thermodynamic of hydrogen production by PSR with the Gibbs free energy minimization method. Mole of hydrogen decreases with increasing pressure as shown in Figure 3.26.

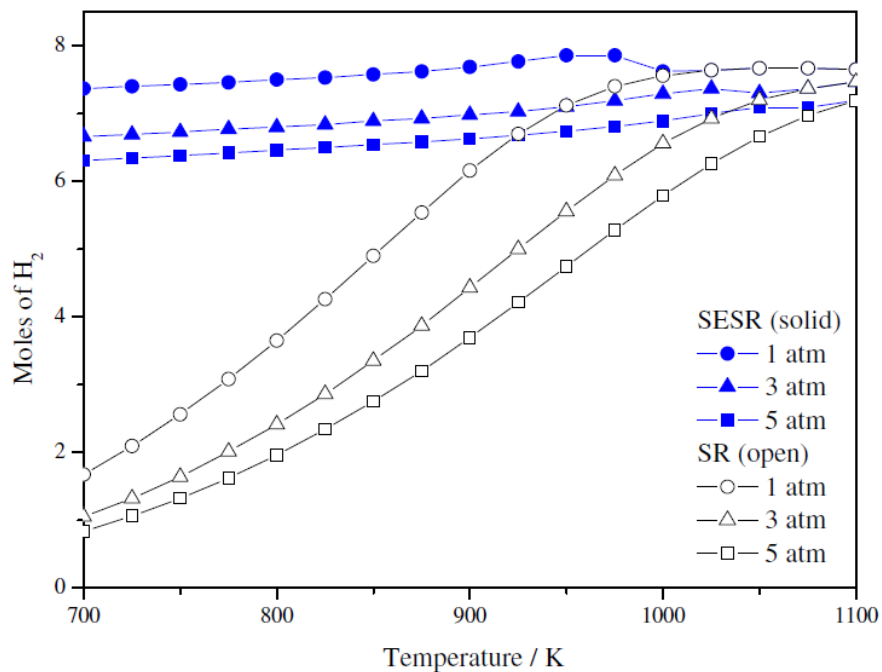


Figure 3.26 Moles of hydrogen generated per mole of propane (open symbol) and SESR (solid symbol) of propane with various pressures and 6 of WPMR⁴⁸.

Figure 3.27 indicates that the number of moles of hydrogen generated increases with the increase in temperature when water to propane molar ratio (WPMR) is less than 6 in steam reforming. For WPMR more than 6, hydrogen generation increases with increasing temperature, before reaching the maximum range of 652 - 700 °C (925 - 975 K), and then begins to decrease slightly at higher temperatures. The greatest quantity of hydrogen of 9.1 was obtained at 652 °C (925 K) of temperature, atmospheric pressure, and 18 of WPMR.

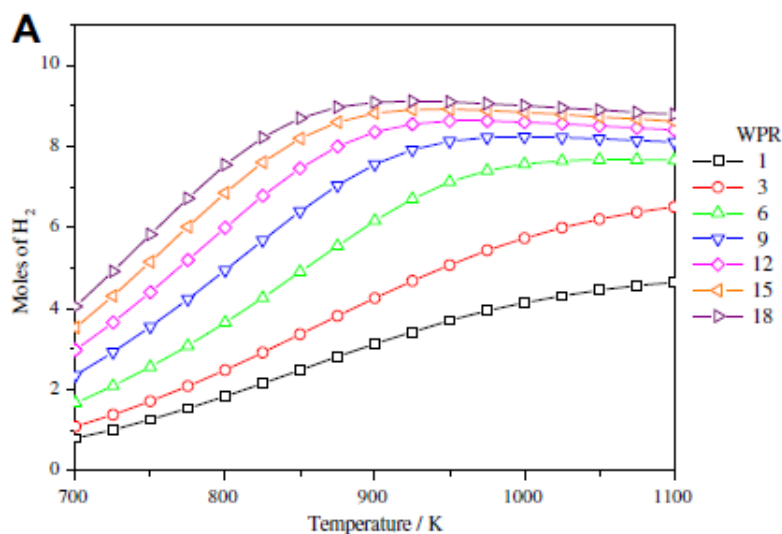


Figure 3.27 Moles of hydrogen generated per mole of propane with various WPMR and temperature at atmospheric pressure (A)⁴⁸.

Even though significant enhancement on reforming performance could be obtained with high WPMR, it required high volume of the reactor due to high steam volumetric flow and high heat duty of process from high vaporization energy. Figure 3.28 indicates that products composition with various temperatures at atmospheric pressure and 12 of WPMR yielded the highest hydrogen concentration of 74% in the product gas from PSR at 677 °C of temperature.

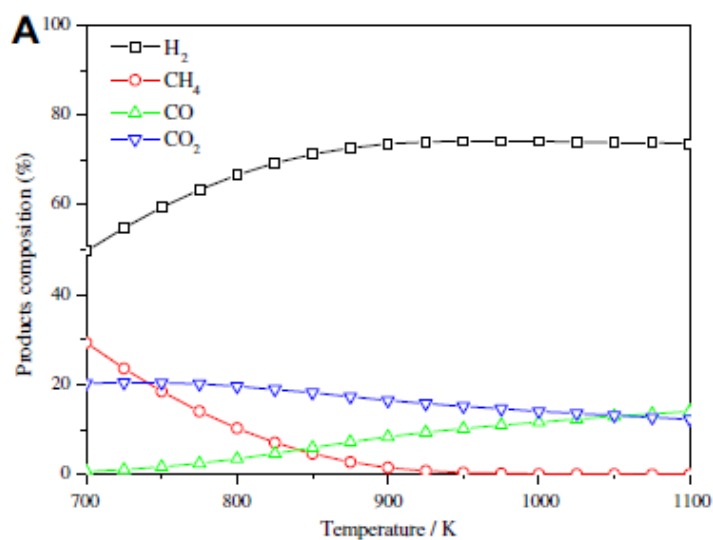


Figure 3.28 Products composition with various temperatures at atmospheric pressure and 12 of WPMR (A)⁴⁸.

Im and co-workers⁴⁹ studied the PSR performance with Ni/YSZ and 1.0% M/Ni/YSZ catalysts (M = Ru, Rh, Pd, and Ag) for effective hydrogen production. Outlet gas distribution and outlet gas selectivity of PSR with various catalysts at 650 °C of temperature consist of H₂, CH₄, CO, CO₂, and C₃H₈ as shown in Figure 3.29. The result of gas selectivity shows that using 1% Rh/Ni/YSZ catalyst for PSR was better than the other catalysts with 74.4% of H₂ gas selectivity.

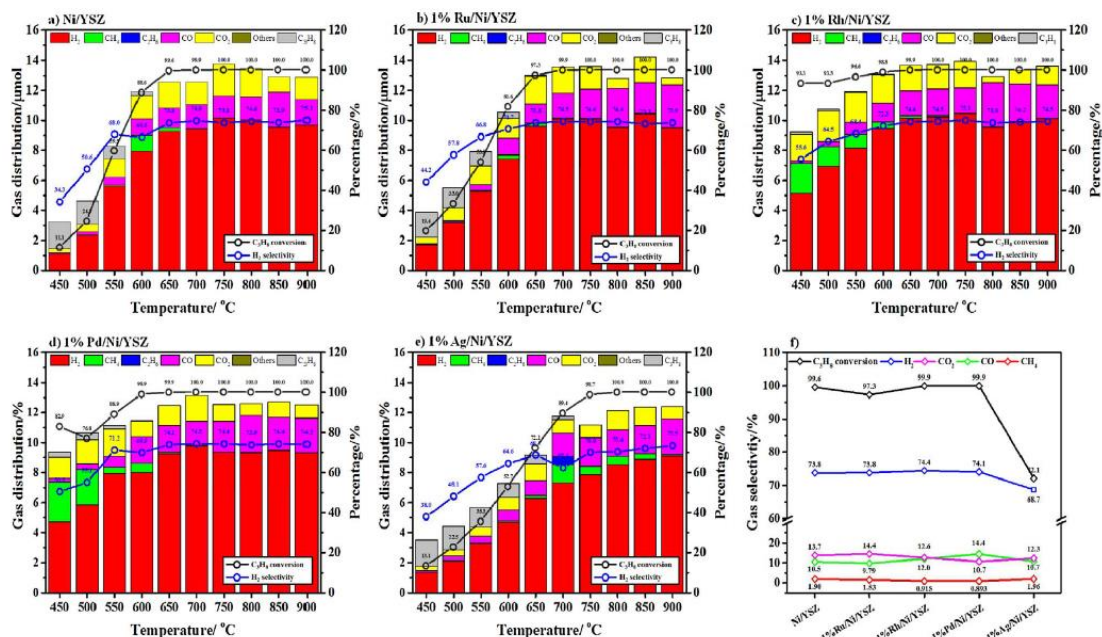


Figure 3.29 PSR performance on gas distribution from Ni/YSZ and 1.0% M/Ni/YSZ catalysts (M = Ru, Rh, Pd, and Ag), and selectivity of gas at 650 °C⁴⁹.

3.2.2 Glycerol steam reforming process

Profeti and co-worker⁵⁰ reported the performance of the Ni and the noble metal promoted catalysts for the GSR. The distribution of gaseous product obtained at 700 °C, especially on the amounts of CO, CO₂, and CH₄ produced, is very similar for all catalysts: 55 - 60% of H₂, 20% of CO₂, 15 - 25% of CO, and 2 - 5% of CH₄. Addition of noble metal with the Ni catalyst resulted in a markedly higher product yield and glycerol conversion.

As forecasted, the addition of the noble metal affected the yield of the product. Interestingly, catalytic activity of Ni affected the H₂ production, and a higher H₂ yield was achieved from the NiPt catalyst. The NiPt/CeO₂-Al₂O₃ catalyst for the GSR at

700 °C, 6 of water to glycerol molar ratio (WGMR), and atmospheric pressure can produce H₂ of 4.79 moles per mole of glycerol supplied.

Wang and co-workers¹⁰ studied H₂ generation from catalytic GSR using Ni-Mg-Al based catalysts, performing the evaluation in a fixed-bed reactor at 1 atm of pressure and 450 - 650 °C of temperature range. Three type of Ni-Mg-Al based catalysts with different Ni, Mg, and Al compositions as C1, C2, C3 catalysts were evaluated. The results of study showed that conversion of glycerol and selectivity of H₂ increased with increasing temperatures from 450 to 650 °C. CO and CH₄ formation in the GSR were almost negligible. Formation of carbon in GSR was of concern in the low temperature range. The C3 catalyst composing of 24.1 wt.% NiO, 26.1 wt.% MgO, and 49.8 wt.% Al₂O₃ was the significant catalyst yielding 78.5% of H₂ selectivity and up to 88% of glycerol conversion at 650 °C as shown in Figure 3.30 and Figure 3.31, respectively.

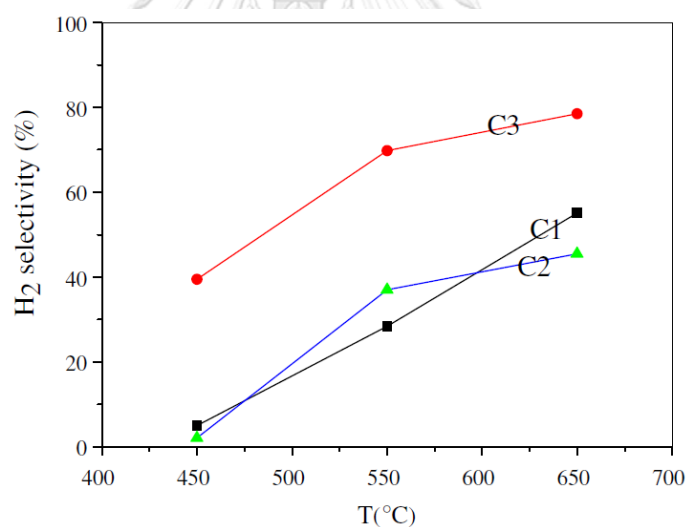


Figure 3.30 H₂ selectivity in GSR using three catalysts¹⁰.

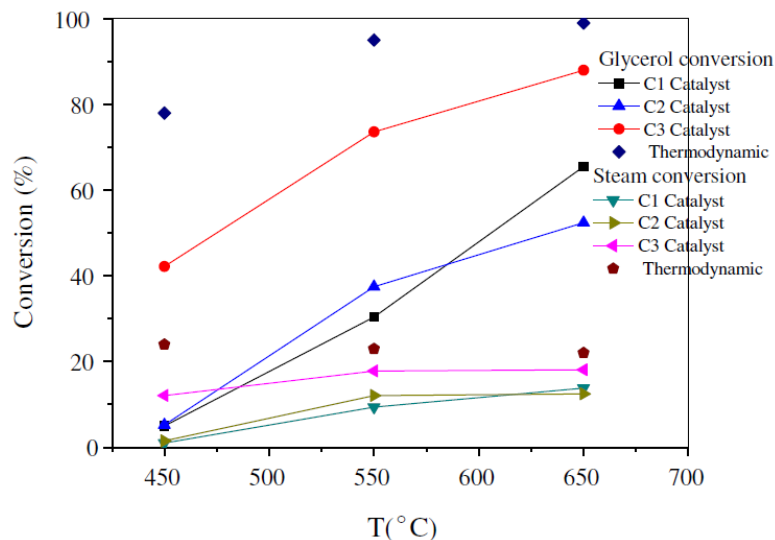


Figure 3.31 Conversions of glycerol and steam with various temperatures¹⁰.

Furthermore, based on thermodynamic of GSR, the number of mole of hydrogen increases with increasing temperature, and greater than 95% conversion at higher than 500 °C of temperature and the upper limit of 6 moles of hydrogen at 650 °C, atmospheric pressure, and 9 of WGMR was obtained as shown in Figure 3.32. Nonetheless, the theoretical mole number of hydrogen generation per unit mole of glycerol is 7.0, with the complete GSR.

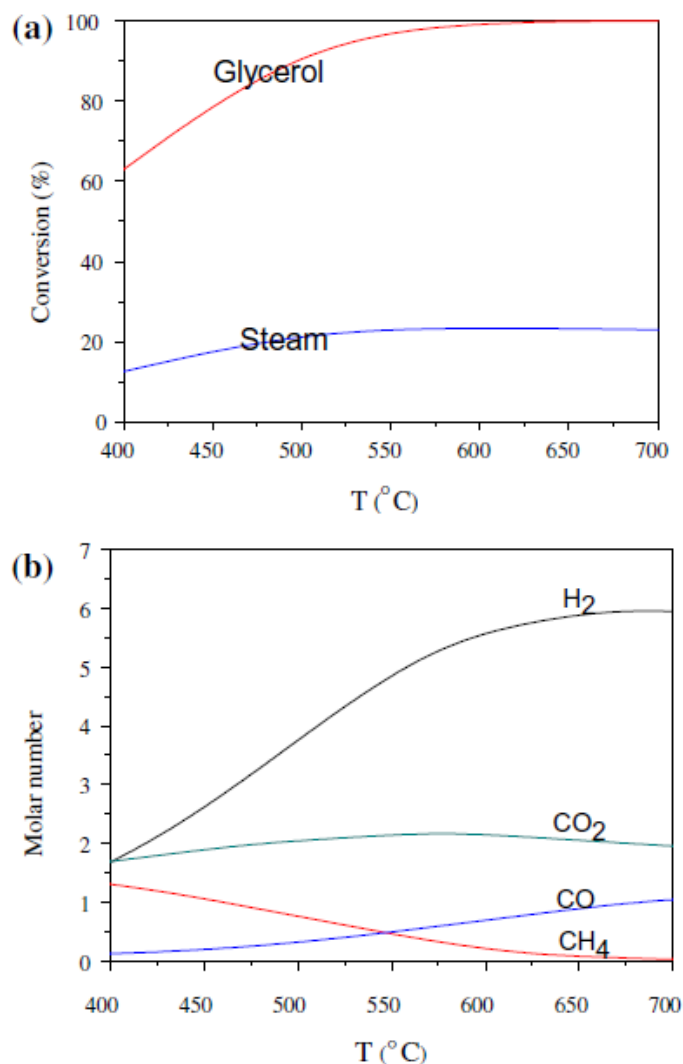


Figure 3.32 Molar number of thermodynamic equilibrium of GSR: (a) conversion and (b) gas products¹⁰.

Hajjaji and co-workers⁵¹ reported the result of thermodynamic and the optimal condition of GSR at 9 of WGMR, 677 °C of temperature, and atmospheric pressure based on the maximum H₂ production with the minimum CH₄ and CO contents and formation of coke. Under these conditions, approximately 6 moles of H₂ per unit mole of glycerol could be generated as shown in Figure 3.33 and the equilibrium synthesis gas yield is shown in Figure 3.34. The thermodynamic model was SRK using R-Gibbs model of the reactor.

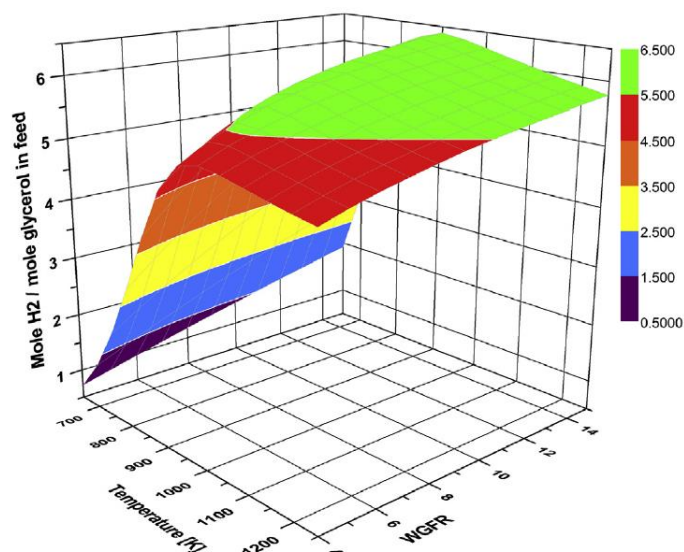


Figure 3.33 Hydrogen mole generated per glycerol mole unit in the GSR reactor with various WGMR and temperatures at atmospheric pressure⁵¹.

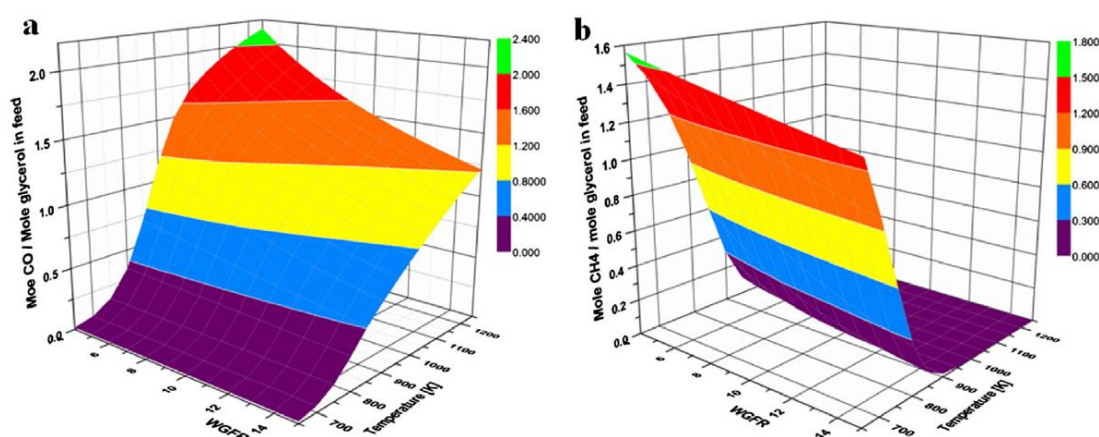


Figure 3.34 Yields of synthesis gas in the equilibrium GSR reactor with various temperatures and WGMR at atmospheric pressure: (a) CO, (b) CH₄⁵¹.

3.3 Integrated system of hydrotreating and hydrogen generation process

3.3.1 Multiple processes of integrated system of hydrotreating and hydrogen generation

McCall and co-workers from UOP LLC⁵² proposed production of aviation fuel from renewable feedstocks in a single reaction zone, using multifunctional catalysts (Pt, Pd, Ru, Rh, NiMoS₂, and NiWS₂) with 0.05 - 10 wt.%. The process was operated at 150 - 454 °C of temperature and 14 - 140 bar of pressure. Hydrogen is soluble in the liquid and the hydrocarbon was recycled. Hydrogen was produced from light

hydrocarbon products in the reforming zone using the Ni catalyst, which was operated at 700 - 950 °C of temperature and 40 bar of pressure. The diagram of aviation fuel production is shown in Figure 3.35.

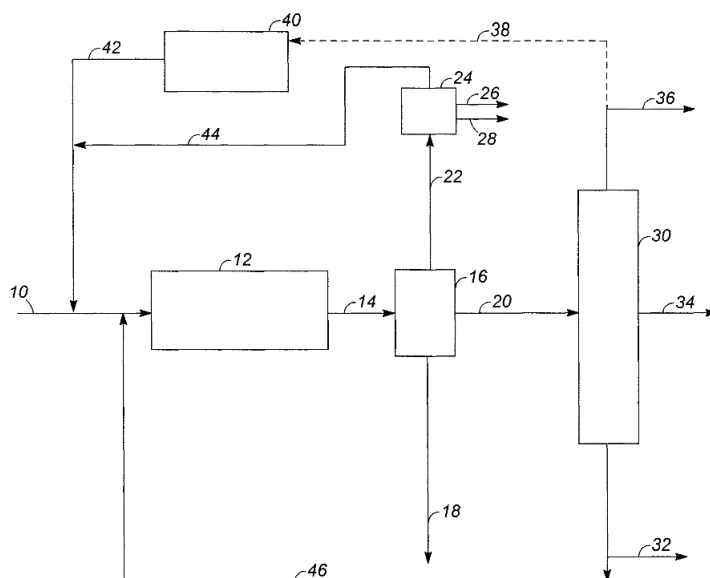


Figure 3.35 Diagram of aviation fuel production⁵².

Sungnoen and co-workers¹⁶ studied the simulation of combination process for biodiesel production, hydrogen generation via GSR, and green diesel production using soybean oil and stearic acid (SA) as raw materials. The process flow diagram for the base case condition of the combined process is shown in Figure 3.36. The operating condition for hydrogen generation via GSR was at 852 °C and 14.3 atm using the nickel catalyst. The process flow diagram for hydrogen generation via GSR is shown in Figure 3.37. The optimal operating condition was 290 °C of reaction temperature, 14.31 atm of pressure, and 1.5 of hydrogen to SA feed molar ratio for green diesel production. The process flow diagram for hydrotreating of stearic acid is shown in Figure 3.38. The simulation result shows that almost 100% of both SA and OCTDL were also converted to green diesel products. The suitable thermodynamic models were used in Aspen Plus in order to simulate the process. Soave-Redlich-Kwong (SRK) has been applied for glycerol reforming and Peng-Robinson equation of state (PENG-ROB) has been applied for green diesel production, which UNIFAC was used to forecast some parameters of binary interaction.

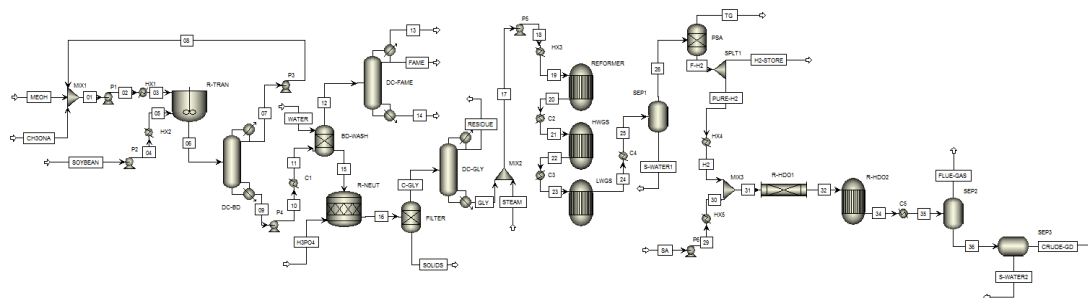


Figure 3.36 Process flow diagram for base case condition of combined process¹⁶.

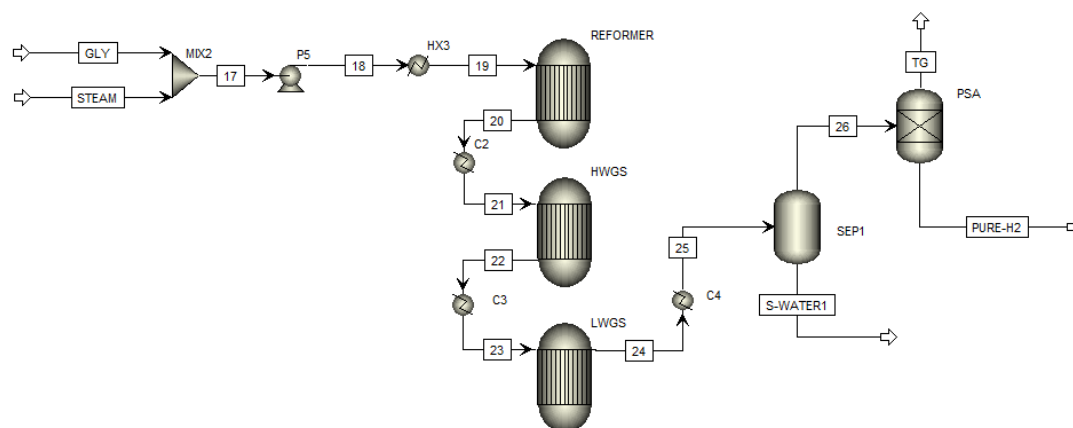


Figure 3.37 Process flow diagram for hydrogen generation via GSR¹⁶.

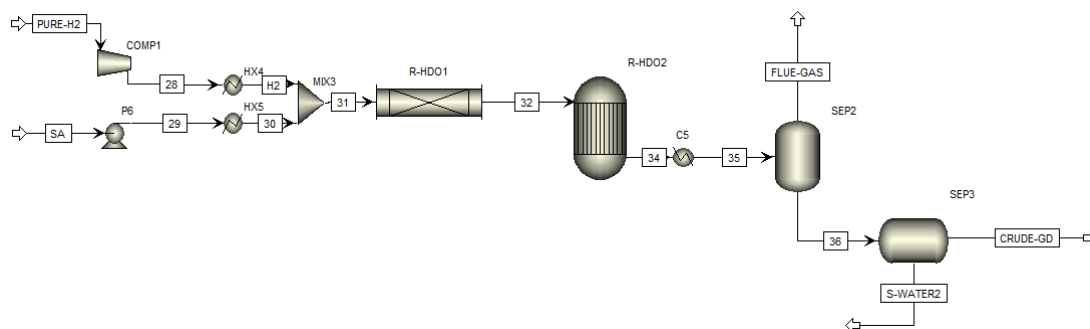


Figure 3.38 Process flow diagram for hydrotreating of stearic acid¹⁶.

Pujan and co-workers⁵³ studied algae oil conversion in order to obtain biokerosene by simulating the fluidized-bed catalytic cracking (FCC) process. The FCC unit and the ZSM-5 catalyst with RStoic and RYield model were used for the reactor. Methane was fed for steam reforming of hydrogen production with RStoic model for the reactor, which operated at 760 °C of temperature and 20 bar of pressure. For hydrotreatment using RStoic model of the reactor, the operating condition was 360 °C of temperature and 100 bar of pressure with PENG-ROB thermodynamic model. The result specified that 13.9 kg of diesel and 41.6 kg of biokerosene were

produced (55.5% product) and that methane consumption was 2 kg per 100 kg algae oil. The process structure of the simulation model is shown in Figure 3.39.

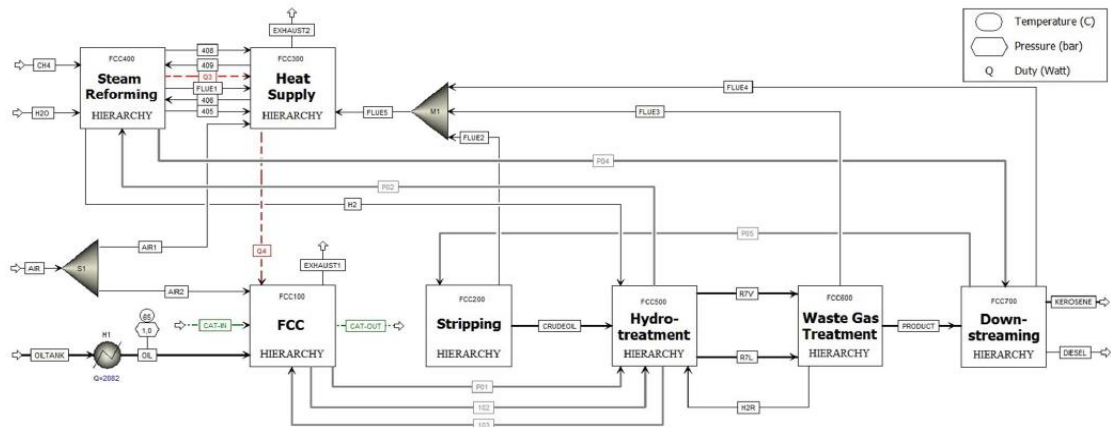


Figure 3.39 Process structure of the simulation model⁵³.

Atsonios and co-workers⁵⁴ studied hydroprocessing of vegetable oil as shown in Figure 3.40. REquil model is used for the equilibrium reactor in order to simulate the hydrotreating reactor at the operating condition of 360 °C of temperature, 40 bar of pressure, 100% of TGs decomposition rate, 20 molars of H₂/oil ratio, and the NiMo catalyst. The PSRK thermodynamic property method was used in Aspen Plus simulator. Light gases (by-products) and natural gas (feed) for the autothermal reformer reactor (ATR) was operated at 950 °C of temperature, 4.5 bar of pressure, and steam to carbon ratio of 2. The water gas shift (WGS) reactor was operated at 300 °C of temperature and 4.5 bar of pressure in order to improve the hydrogen yield. Chemical equilibrium was assumed for modeling of both ATR and WGS reactors.

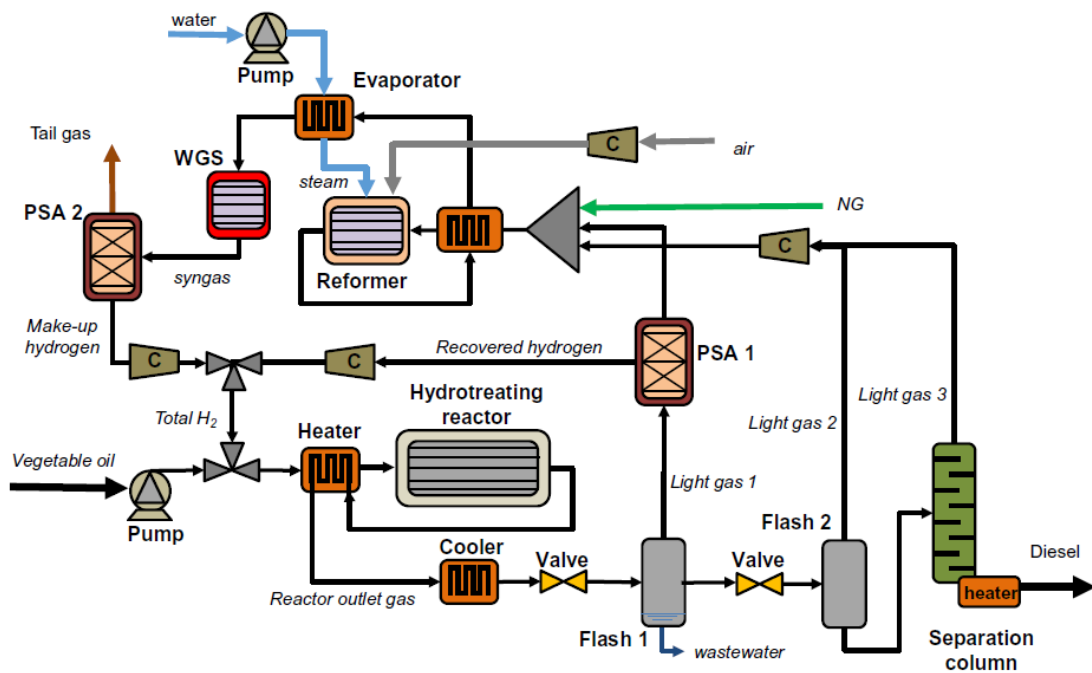


Figure 3.40 Vegetable oils hydroprocessing unit⁵⁴.

3.3.2 Single process of integrated system of hydrotreating and hydrogen generation

The single process which combined hydrotreating and hydrogen generated from sunflower oil was studied based on a catalytic fixed-bed reactor with the response of pressure. Dominguez-Barroso and co-workers⁵⁵ studied the overall process in one step containing the steps of hydrolysis, reforming of glycerol and hydrogenation in situ, and deoxygenation with the integration of Pt-Ni/Al₂O₃ and Pd/C catalysts under subcritical water condition ($T \leq 300$ °C) without external hydrogen support to yield 17 carbon atoms of alkane hydrocarbon. Figure 3.41 demonstrates the possible reaction of green diesel production from vegetable oil.

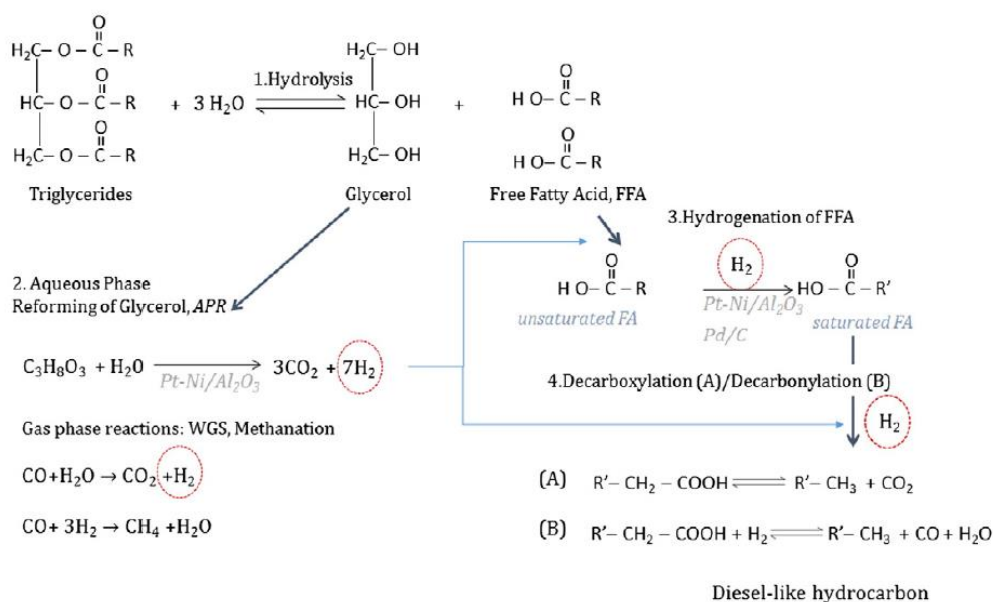


Figure 3.41 Possible reaction of green diesel production from vegetable oil using PtNi/Al₂O₃+Pd/C combined⁵⁵.

Mao and co-workers⁵⁶ studied the efficiency of TGs reaction (hydrothermal and hydrodeoxygenation) with hydrogen generation *in situ* for green diesel production. The result revealed that up to 71.91% yield of green diesel (C₁₇ + C₁₈ products) was achieved over the activated carbon supported palladium catalyst with decalin as solvent in the presence of water at 250 °C (523 K) with pressure of autogenous after 12 h of reaction time, which provided the hydrogen generated *in situ* from solvents.

The literature review of modelling and design of plant for combined hydrotreating and hydrogen generation for bio-hydrogenated diesel fuel production can be summarized in Table 3.5.

Table 3.5 Literature review of modelling and design of plant for integrated system of hydrotreating and hydrogen generation for bio-hydrogenated diesel fuel production.

Feedstock	Simulation model	Thermodynamic model	Reactor model	Reaction condition	Catalyst	Performance	Reference
Plant and animal oils	-	-	Single reaction zone Reforming zone	Hydro processing T=150-454 °C P=14-140 bar SR T=700-950 °C P=40 bar	Multifunctional catalyst Conventional catalyst	Aviation fuel Hydrogen	McCall and co-workers from UOP LLC, 2011 ⁵²
Soybean oil, Stearic acid	Aspen Plus	PENG-ROB UNIFAC SRK	RPlug, REquil REquil	DO T=290 °C P=14.31 atm GSR T=877 °C P=14.31 atm	Ni metal with support Ni	Conversion 100% Hydrogen	Sungnoen and co-workers, 2014 ¹⁶
Algae oil	Aspen Plus	NRTL(VLE) PENG-ROB(HT) SRK (Fractionation)	RStoic RYield RStoic RStoic	FCC Hydrotreatment T=360 °C P=100 bar SRM T=760 °C P= 20 bar	ZSM-5 N/A N/A	Crude oil Saturated products Conversion 99%	Pujan and co-workers, 2017 ⁵³

Table 3.5 Literature review of modelling and design of plant for integrated system of hydrotreating and hydrogen generation for bio-hydrogenated diesel fuel production. (*Continued*).

Feedstock	Simulation model	Thermodynamic model	Reactor model	Reaction condition	Catalyst	Performance	Reference
Vegetable oil, algal oil and bio-oil	Aspen Plus	NRTL PSRK	REquil ATR reactor WGS reactor	Hydrotreating T=360 °C P=40 bar T=950 °C P=4.5 bar T=300 °C P=4.5 bar	NiMo N/A N/A	Conversion 100% Hydrogen Hydrogen	Atsonios and co-workers, 2018 ⁵⁴
Sunflower oil	Experimental	-	Single process	Hydrolysis, APR, hydrogenation, DO, T=300 °C P=10 MPa (autogenic pressure)	Pt-Ni/Al ₂ O ₃ and Pd/C	Complete hydrogenation Partial DO	Dominguez-Barroso and co-workers, 2016 ⁵⁵
Triolein	Experimental	-	Batch reactor Single process	Hydrolysis, APR, hydrogenation, DO T=250 °C, autogenic pressure	Pd/C (decalin as solvent)	Complete conversion 71.91 % yield of GD	Mao and co-workers, 2017 ⁵⁶

3.4 Pressure swing adsorption technology

Technology of separation such as cryogenic, selective of membrane, absorption, and adsorption can present an optimal solution for each production process. Technology of pressure swing adsorption (PSA) is a technique used for recovery of H₂ and purification of H₂ from off-gases of refinery, including SRM, PSR and GSR of the hydrogen generation process. Principles of PSA are based on molecules of gas adsorbing to a material of a solid adsorbent. The material of the adsorbent can be integration of silica gel, activated carbon, zeolites, and carbon molecular sieves. The attractive forces between molecules of gas and the material of the adsorbent depend on the component of gas, the type of the adsorbent material, the partial pressure of component of gas and the operating temperature. Compounds, which are highly volatile with low polarity such as He or H₂, are typically not adsorbed compared to gas molecules such as CO, CO₂, N₂, and hydrocarbon. The relative attractive force between various gas molecules and a typical adsorbent material is shown in Figure 3.42⁵⁷.

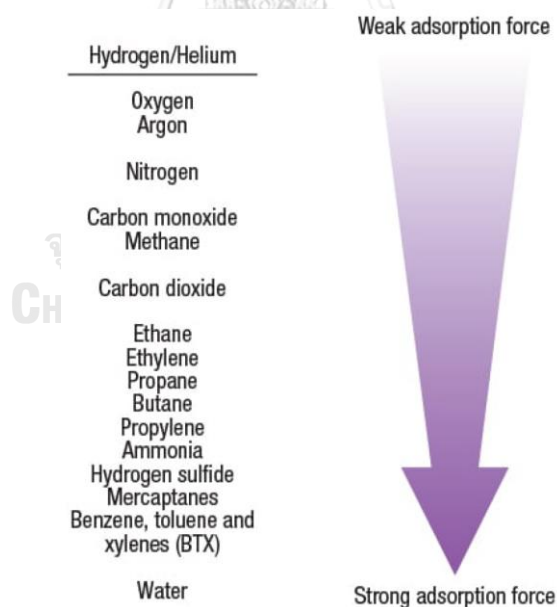


Figure 3.42 Range of adsorption force of compounds⁵⁷.

The PSA operates at constant temperature and is used between two pressure levels in order to affect adsorption loading and desorption loading. Impurities such as light hydrocarbons, heavy hydrocarbons, water, CO, CO₂, and N₂ are selectively adsorbed at high pressure in the typical range of 10 - 40 bar, from bottom to top of the

vessel and increases the impurities loading onto the material of the adsorbent. Desorption or regeneration of the adsorbent material is performed at low pressure to slightly above atmospheric pressure in order to reduce the residual impurities loading as much as possible. H_2 is recovered, which is high purity flow to product stream. Isotherm of adsorption showing the relationship between partial pressure of gas molecule and equilibrium of loading onto adsorbent material at each temperature is shown in Figure 3.43⁵⁷. The process diagram of the PSA system containing adsorption, desorption, and pressure equalization is shown in Figure 3.44⁵⁷. The literature review of PSA technology for hydrogen recovery and purification is summarized in Table 3.6.

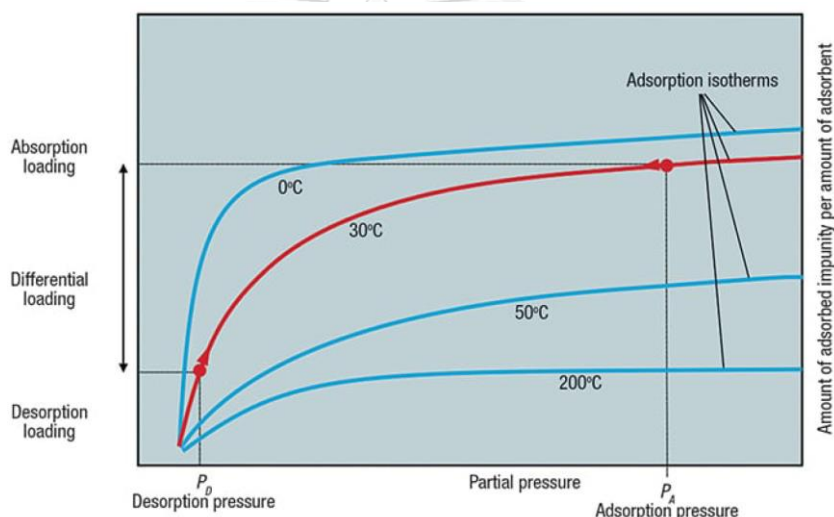


Figure 3.43 Isotherm of adsorption between partial pressure of molecule of gas and equilibrium of loading onto material of adsorbent⁵⁷.

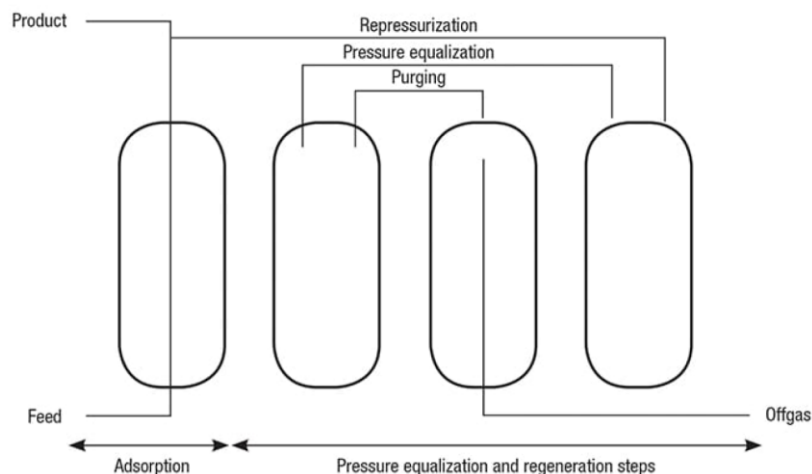


Figure 3.44 Process diagram of PSA system⁵⁷.

Table 3.6 Literature review of PSA technology for hydrogen recovery and purification.

Process	PSA-recycle H ₂	PSA-produce H ₂	Sep-2 phase (VL)	Sep-3 phase (VLL)	H ₂ recovery	H ₂ purity	Reference
PSA technology	10-40 bar (adsorption) Over 1 bar (desorption)		-	-	Up to 90%	99.9999%	Keller and co-workers, 2016 ⁵⁷
Hydrotreating, reforming	30 bar, 30 °C (adsorption) 1.0 bar (desorption)		30 bar, 30 °C	-	-	99% w/w	Pujan and co-workers, 2017 ⁵³
Hydrotreating, reforming	4.5 bar	4.5 bar, 300 °C	1.2 bar	4.5 bar	Total	100%	Atsonios and co-workers, 2018 ⁵⁴
Hydrotreating	35 bar, 150 °C	-	30 bar, 30 °C	35 bar, 160 °C	-	-	Hilbers and co-workers, 2015 ³⁹
Reforming	-	30 atm, 35 °C (adsorption) 1.1 atm (desorption)	30 atm, 35 °C	-	90%	99%	Ortiz and co-workers, 2013 ⁵⁸
Reforming	-	15 atm, 35 °C	15 atm, 35 °C	-	80%	99.999%	Ortiz and co-workers, 2013 ⁵⁹
Reforming	-	10.10 bar, 25 °C (adsorption) 1.01 bar, 25 °C (desorption)	10.10 bar, 25 °C	-	-	-	Song and co-workers, 2015 ⁶⁰

3.5 Catalysts for hydrotreating of triglycerides/ free fatty acids process

There are three catalyst types that have been widely used in hydrotreating of TGs/ FFAs: (1) noble metal catalysts, such as Pt, Pd, Ru, and Rh^{3-4, 26, 61-62}, (2) non-noble metal and non-sulfide catalysts, such as Ni, Co⁶³⁻⁶⁵, and bimetallic catalysts, such as NiMo supported on Al₂O₃⁶⁶, and (3) bimetallic sulfide catalysts, e.g., CoMoS₂, NiMoS₂ supported on Al₂O₃^{2, 61}. The favorable metal catalysts are HDCO and/or DCO₂, while the dominant bimetallic sulfide catalysts are HDO.

(1) Noble metal catalyst

Snare and co-workers²⁶ studied production of green diesel via heterogeneous stearic acid catalytic deoxygenation in a semi-batch reactor under 300 °C of temperature and 6 bar of pressure. When using 5% Pd/C, 100% conversion of deoxygenation and 95% selectivity to C₁₇ product were obtained. When using 5% Pt/C, 86% conversion of deoxygenation and 87% selectivity to C₁₇ product were obtained. Furthermore, the results of the CO₂/CO ratio with various sampling times using 5% Pd/C and 5% Pt/C catalysts are shown in Figure 3.45, which indicated that the palladium catalyst was dominating to decarboxylation, and that the platinum catalyst was dominating to hydrodecarbonylation. The noble metal catalysts supported on activated carbon in stearic acid deoxygenation was reviewed by Pattanaik and co-workers³, which showed that the Pd/C catalyst contributed to the DCO₂ dominating pathway and that the Pt/C catalyst contributed to the HDCO dominating pathway.

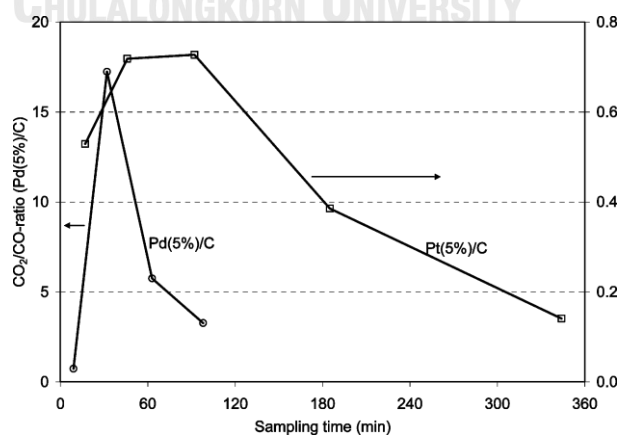


Figure 3.45 Results of CO₂/CO ratio with various sampling times using 5% Pd/C and 5% Pt/C catalysts, operating condition at 300 °C of temperature, 6 bar of pressure for stearic acid deoxygenation²⁶.

Kiatkittipong and co-workers⁴ studied green diesel production from hydrotreating of refined palm oil such as palm fatty acid distillate (PFAD) and crude palm oil (CPO). The Pd/C catalyst is proposed as a more suitable catalyst for the FFAs feedstock. The reaction temperature of 375 °C and 40 bar of pressure are the optimal condition to obtain the maximum diesel yield of 81%, while NiMoS₂/γ-Al₂O₃ is preferred for the TGs feedstock. The Ni/Al₂O₃ contributed decarboxylation while Mo/Al₂O₃ contributed mainly hydrodeoxygenation. The result of the deoxygenation reaction pathways was compared to the Pd/C catalyst, and the degree of HDO of NiMo/γ-Al₂O₃ was much higher.

Pongsiriyakul and co-workers⁶² studied hydrotreating under pure hydrogen and under synthesis atmosphere gas for green diesel production. The feedstock was PFAD and the Pd/C catalyst was used at 375 °C and 400 °C of reaction temperature and 40 bar of initial pressure. The conversion of PFAD and liquid fuel (diesel+gasoline) yields under the syngas atmosphere were lower than those under the pure H₂ atmosphere. Although gasoline and diesel yields increased with increasing temperature from 375 °C to 400 °C, the selectivity of diesel decreased. The DCO₂/HDCO reaction is the main reaction pathway of the deoxygenation reaction rather than HDO, and HDCO is the predominant pathway which is indicated by the lower CO₂ fraction in the gas product.

Liu and co-workers⁶¹ studied production of green diesel by hydrotreating of waste cooking oil using the ruthenium (Ru) catalyst supported on Al-polyoxocation-pillared montmorillonite (Al₁₃-Mont). The studied condition was 350 °C of reaction temperature, 20 bar (2 MPa) of H₂ pressure, 15.2 h⁻¹ of liquid hourly space velocity (LHSV), and 400 mL/mL of the H₂/oil ratio. The study achieved an initial C₅₊ hydrocarbon yield of 83.6% and did not show catalyst deactivation after 72 h on-stream when compared to the sulfide Ni-Mo/Al₁₃-Mont catalyst, which showed slow deactivation due to the loss of sulfur.

(2) Non-noble metal and non-sulfide catalyst

The non-noble metal and non-sulfide catalysts were studied with waste chicken fats through deoxygenation in order to obtain BHD using Ni/γ-Al₂O₃. Kaewmeesri and co-workers⁶³ reported that the main pathway of reaction was

hydrodecarbonylation/ decarboxylation (HDCO/DCO₂), whereas HDO was minor, which operated at 330 °C of temperature and pressure of 50 bar.

The catalytic behaviors of Ni/ γ -Al₂O₃ and Co/ γ -Al₂O₃ for hydrodeoxygenation of palm oil were studied by Srifa and co-workers⁶⁴, which operated at temperature of 300 °C and pressure of 50 bar. The Ni catalyst is favorable leading to combined hydrodecarbonylation (HDCO) and/or decarboxylation (DCO₂) reactions, which were dominant over the HDO reaction. Meanwhile, the Co catalyst contributed nearly comparably to HDCO/DCO₂ and HDO reactions.

Morgan and co-workers⁶⁵ studied catalytic deoxygenation of TGs to hydrocarbons using supported Ni-Al, Ni-Mg-Al, Mg-Al, and Ni/Al₂O₃ catalysts, with triolein and soybean oil as feedstocks. The use of unsaturated TGs favors cracking reactions, leading to the formation of lighter products and higher amount of coke deposits than using saturated TGs feeds, which were active and were operated at 350 °C of reaction temperature.

Orozco and co-workers⁶⁶ studied hydrotreating in a continuous fixed bed reactor from castor oil in order to produce green diesel, using the NiMo/Al₂O₃ catalyst, which was operated at temperature of 350 °C and 35 bar of pressure to achieve 100% conversion. The effect of the H₂/oil molar ratio was studied at 35:1, 70:1, and 105:1, which demonstrated that C₁₈H₃₈ increased while C₁₇H₃₆ decreased with increasing H₂/oil molar ratio. In addition, the gas fraction of CO and CO₂ decreased with increasing H₂/oil molar ratio and the low H₂/oil molar ratio provided the high CO₂ gas fraction. Thus, the increasing H₂/oil molar ratio affected DCO₂, HDCO, and HDO reactions.

(3) Bimetallic sulfide catalyst

Srifa and co-workers² studied production of BHD by catalytic hydrotreating of palm oil using the NiMoS₂/ γ -Al₂O₃ catalyst and reported that hydrodeoxygenation was dominant when operating at 270 - 420 °C of reaction temperature, 15 - 80 bar of H₂ pressure, 0.25 - 5 h⁻¹ of LHSV, and 250 - 2,000 N (cm³/cm³) of the H₂/oil ratio.

The maximum production yield was obtained at 1,000 to 1,500 N (cm³/cm³) of the H₂/oil ratio, which indicates that hydrogen should be about 3 - 5 times greater than

hydrogen consumption per oil. At the operating condition of 300 °C of temperature, 50 bar of pressure, and 1,000 N (cm³/cm³) of the H₂/oil ratio, 100% conversion, 89.8% product yield (C₁₅ - C₁₈), 72% contribution to HDO, and 16.8% contribution to HDCO/DCO₂ were achieved.

Furthermore, the performance of different catalysts with various deoxygenation pathways can be summarized in Table 3.7.

Table 3.7 Performance of different catalysts with various deoxygenation pathways.

Catalyst	Feedstock	Reaction condition	Major reaction	Conversion	Reference
Ni/ γ -Al ₂ O ₃	Palm oil	T=300 °C P=50 bar	HDCO/DCO ₂	100 %	Srifa and co-workers, 2015 ⁶⁴
Co/ γ -Al ₂ O ₃	Palm oil	T=300 °C P=50 bar	Comparable HDCO/DCO ₂ and HDO	100 %	Srifa and co-workers, 2015 ⁶⁴
NiMo/Al ₂ O ₃	Castor oil	T=350 °C P=35 bar, vary H ₂ /oil molar ratio	HDO>HDCO >DCO ₂	100 %	Orozco and co-worker, 2017 ⁶⁶
NiMoS ₂ / γ -Al ₂ O ₃	Palm oil	T=300 °C P=50 bar	HDO	100 %	Srifa and co-workers, 2014 ²
5% Pd/C	FFAs	T=300 °C P=19 bar	DCO ₂	90 %	Wang and co-work, 2012 ⁴⁵
5% Pd/C	Stearic acid	T=300 °C P=6 bar	DCO ₂	100%	Snare and co-workers, 2016 ²⁶
5% Pt/C	Stearic acid	T=300 °C P=6 bar	HDCO	86 %	Snare and co-workers, 2016 ²⁶

3.6 Thermodynamic of hydrotreating

Burgess and co-workers⁶⁷ and Smejkal and co-workers⁴⁰ reported heat of formation of TGs at standard temperature and pressure (STP). Heat of hydrogenation reaction of TGs and FFAs was exothermic reaction, which was reported by Burgess and co-workers⁶⁷. Heat of hydrogenolysis reaction of TGs at STP was exothermic reaction, which was reported by Valencia and co-workers⁶⁸. Snare and co-workers²⁶ reported heat of reaction of DCO₂, HDCO, and HDO at 300 °C as endothermic,

endothermic, and exothermic reaction, respectively. However, Valencia and co-workers⁶⁸ reported heat of reaction of DCO₂, HDCO, and HDO at STP as exothermic, endothermic, and exothermic reaction, respectively. The literature review of thermodynamic of hydrotreating can be summarized in Table 3.8.

Table 3.8 Literature review of thermodynamic of hydrotreating.

Reference	Burgess ⁶⁷	Smejkal ⁴⁰	Yenumala ⁶⁹	Snare ²⁶	Valencia ⁶⁸
Condition	STP	STP	STP	300 °C	STP
Component	Heat of formation (kJ/mol)				
Tripalmitin			-2,050		
Tristearin		-2,176.9	-2,180		
Triolein	-2,193.7		-1,840		
Trilinolein	-1,880.1				
Component	Reaction	Heat of reaction (kJ/mol)			
Triolein	Hydrogenation	-378			
Trilinolein	Hydrogenation	-757			
Trilinolenin	Hydrogenation	-1,132			
Oleic acid	Hydrogenation	-123.6			
Linoleic acid	Hydrogenation	-254.4			
Linolenic acid	Hydrogenation	-380.2			
Trimyristin	Hydrogenolysis				-286
Tripalmitin	Hydrogenolysis				-284.4
Tristearin	Hydrogenolysis				-286
Myristic acid	DCO ₂				-25
Palmitic acid	DCO ₂				-28.6
Stearic acid	DCO ₂			9.2	-25.3
Myristic acid	HDCO				28.8
Palmitic acid	HDCO				45.2
Stearic acid	HDCO			48.1	48.5
Myristic acid	HDO				-122.8
Palmitic acid	HDO				-123.2
Stearic acid	HDO			-115	-122.5

CHAPTER IV PROCESS SIMULATION

The integrated system of hydrotreating and hydrogen generation for bio-hydrogenated diesel fuel production from palm oil was designed and proposed in this chapter. This is used to evaluate the performance of the process. Tripalmitin and triolein, the main components of palm oil, were used as model compounds for this simulation. The basis of feedstock for BHD production was 1.0 kmol/h of tripalmitin or triolein. In addition, 3.0 times of the theoretical requirement of the H₂/oil molar ratio was fed initially, which was presented by the calculation in APPENDIX B. In the case of tripalmitin with the DCO₂ pathway, although H₂ is not required theoretically both in hydrogenation and deoxygenation, the H₂ to tripalmitin ratio of 1.35 is fed initially to prevent catalyst decomposition and in order to obtain alkane hydrocarbon products with reducing intermediate alkene hydrocarbon as mentioned earlier^{45, 47, 62, 70}.

4.1 Thermodynamic property methods

All processes in the present work were simulated using the Aspen Plus simulation model. The thermodynamic model applied to the hydrotreating process was PSRK^{33, 54}, which was an appropriate thermodynamic model with an estimation method for equilibrium phase of chemical components mixtures at high pressures (>10 bar)⁷¹. The SRK method model was applied to the hydrogen generation process, and the model provided a satisfying result for the vapor-liquid equilibrium phase of systems formed by hydrocarbons^{16, 51}. For introduction of oil to hydrotreating and hydrolysis homogeneous liquid process, the NRTL property method has been applied, which is appropriate for liquid phase^{47, 54}. The thermodynamic property method model in Aspen Plus was simulated in order to select the appropriate thermodynamic property method, which was reported in APPENDIX A.

4.2 Bio-hydrogenated diesel fuel production

4.2.1 Single-step of hydrogenolysis of triglycerides/ deoxygenation of free fatty acids process

4.2.1.1 Modelling validation of hydrogenolysis of triglycerides/ deoxygenation of free fatty acids

The reaction temperature affects conversion of stearic acid, which can be shown by experiment and simulation of the kinetic model of Kumar and co-workers⁴¹ in Figure 4.1 by using the nickel supported catalyst with 0.18 kmol/m³ of concentration of stearic acid and 8 bar of initial hydrogen pressure. The values of kinetic parameters are given in Table 4.1 by following the Equations 3.1 - 3.6.

Table 4.1 Formation rates of different components with different temperatures, pre-exponential factor (A_0), and activation energy (E)⁴¹.

Temperature (K)	Rate constants (s ⁻¹)				
	k_1	k_2	k_3	k_4	k_5
533	4.20×10^{-05}	3.55×10^{-04}	8.44×10^{-06}	6.03×10^{-06}	1.30×10^{-05}
543	6.43×10^{-05}	1.52×10^{-03}	2.43×10^{-05}	1.96×10^{-05}	4.57×10^{-05}
553	1.59×10^{-04}	3.68×10^{-03}	6.70×10^{-05}	1.58×10^{-04}	3.37×10^{-04}
563	3.24×10^{-04}	7.39×10^{-03}	7.59×10^{-05}	5.33×10^{-04}	1.03×10^{-03}
E (kJ/mol)	175.4	250.0	190.9	387.7	377.2
A_0 (s ⁻¹)	5.57×10^{12}	1.34×10^{21}	4.77×10^{13}	5.08×10^{32}	1.08×10^{32}

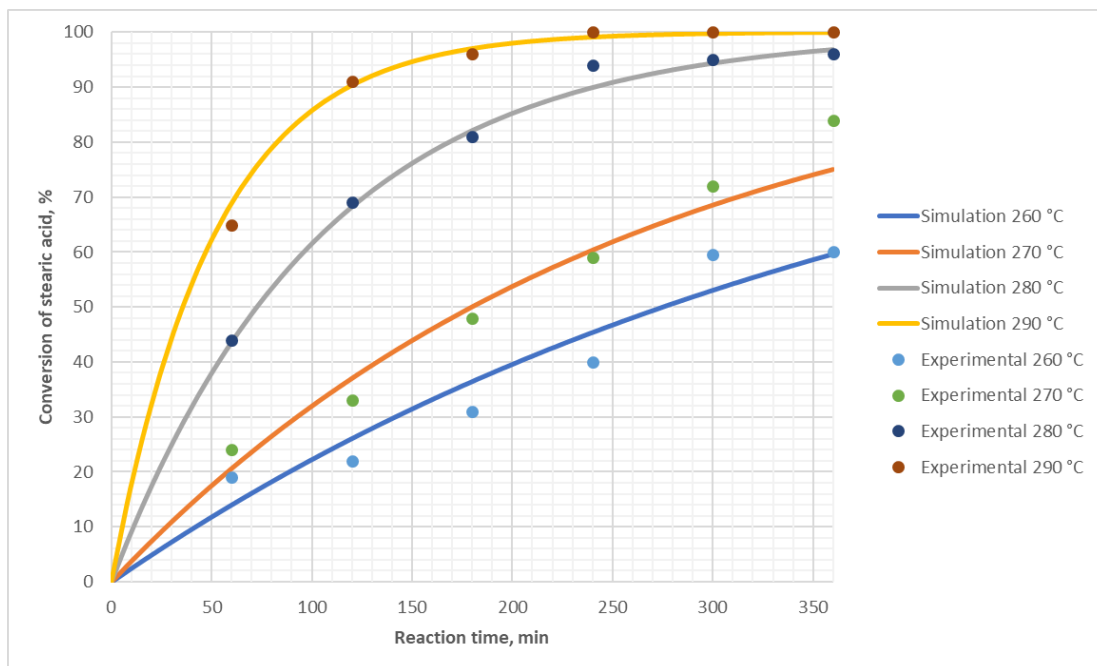


Figure 4.1 Reaction temperature effect on conversion of stearic acid using nickel supported catalyst, 0.18 kmol/m^3 of concentration of stearic acid and 8 bar of initial hydrogen pressure between experiment and simulation from kinetic model of Kumar and co-workers⁴¹.

The comparison on product selectivity between experiment and simulation from the kinetic model of Kumar and co-workers⁴¹ is shown in Figure 4.2. The result showed that product selectivity at $290 \text{ }^\circ\text{C}$ of reaction temperature was acceptable.

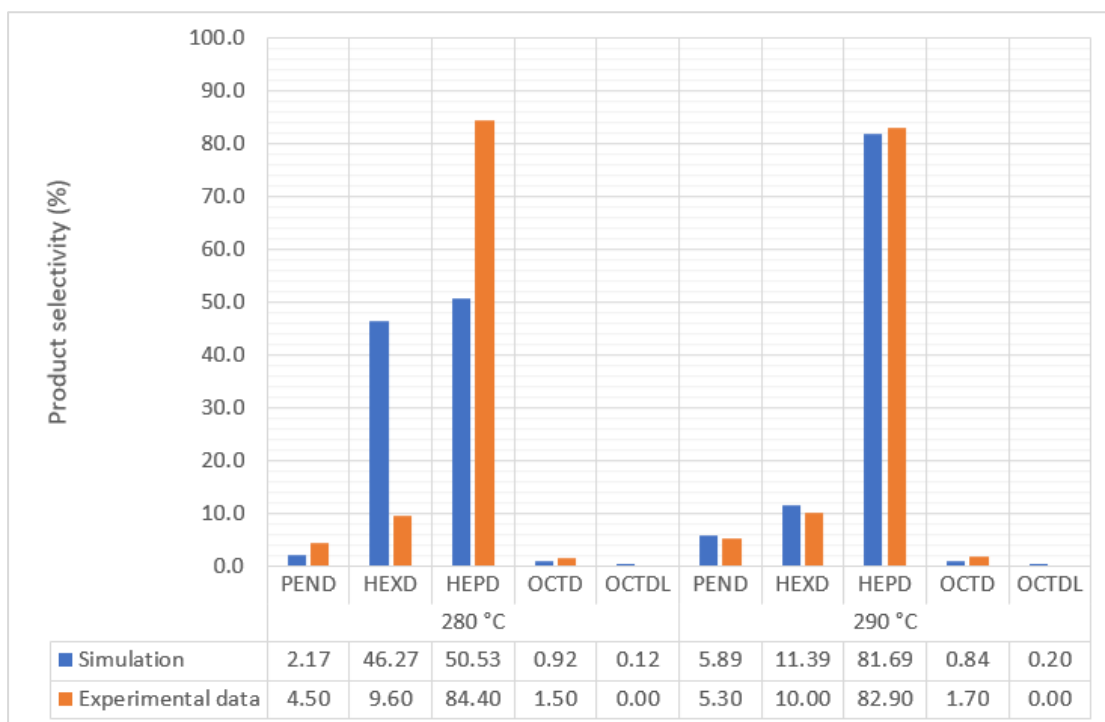


Figure 4.2 Product selectivity of hydrotreating of stearic acid using nickel supported catalyst at 95% conversion of stearic acid, 0.18 kmol/m^3 of concentration of stearic acid, $280 \text{ }^\circ\text{C}$ and $290 \text{ }^\circ\text{C}$ of reaction temperature and 8 bar of initial hydrogen pressure between experiment and simulation from kinetic model of Kumar and co-workers⁴¹.

Figure 4.3 shows product selectivity of hydrotreating of stearic acid using the nickel supported catalyst at 95% and 99.91% conversion of stearic acid with 154 and 360 min of reaction time, respectively, 0.18 kmol/m^3 of concentration of stearic acid, $290 \text{ }^\circ\text{C}$ of reaction temperature, and 8 bar of hydrogen pressure for simulation from the kinetic model of Kumar and co-workers⁴¹. The results at 99.91% conversion present lower OCTDL than those obtained from 95% conversion with slight difference of the results.

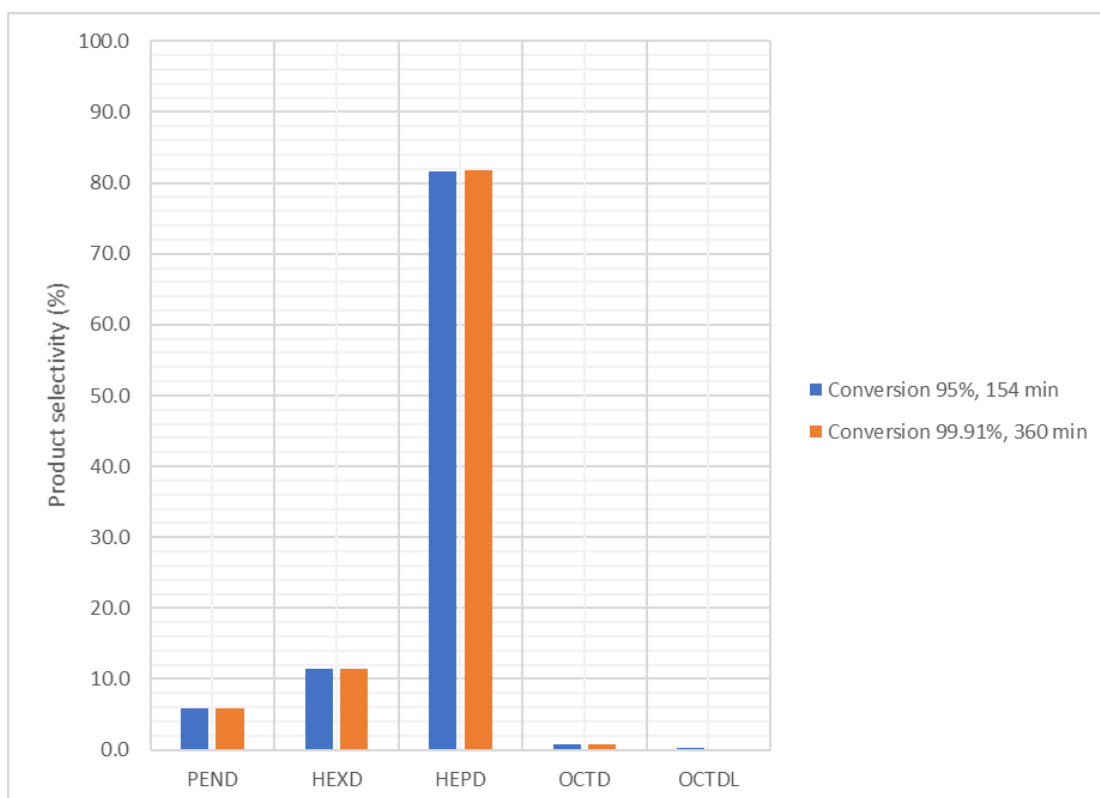


Figure 4.3 Product selectivity of hydrotreating of stearic acid using nickel supported catalyst at 95% and 99.91% conversion of stearic acid with 154 and 360 min of reaction time, respectively, 0.18 kmol/m^3 of concentration of stearic acid, $290 \text{ }^\circ\text{C}$ of reaction temperature, and 8 bar of hydrogen pressure for simulation from kinetic model of Kumar and co-workers⁴¹.

The comparison on product selectivity between experiment and simulation from the kinetic model of Jenistova and co-workers⁴² is shown in Figure 4.4. The conditions are validated at 360 min of reaction time which obtained 99% of stearic acid conversion using 5% Ni- γ -Al₂O₃, 0.035 M (mol/L) of concentration of stearic acid, $300 \text{ }^\circ\text{C}$ of reaction temperature, and 30 bar of hydrogen pressure. The values of kinetic parameters are given in Table 4.2. by following the Equations 3.7 - 3.13.

Table 4.2 Estimated rate constant for HDO of stearic acid using 5 wt.% Ni- γ -Al₂O₃ catalyst at temperature of $300 \text{ }^\circ\text{C}$ with various total pressures⁴².

$k_1 \text{ min}^{-1} \text{ bar}^{-1}$	Rel. St. error (%)	$k_2 \text{ min}^{-1}$	Rel. St. error (%)	$k_3 \text{ min}^{-1} \text{ bar}^{-1}$	Rel. St. error (%)	$K_A [-]$	Rel. St. error (%)	$k_H \text{ bar}^{-1}$	Rel. St. error (%)
1.56×10^{-3}	18.5	4.31×10^{-1}	21.8	7.83×10^{-4}	23.5	1.36×10^2	23.2	1.58×10^{-2}	13.2

* Relative standard error.

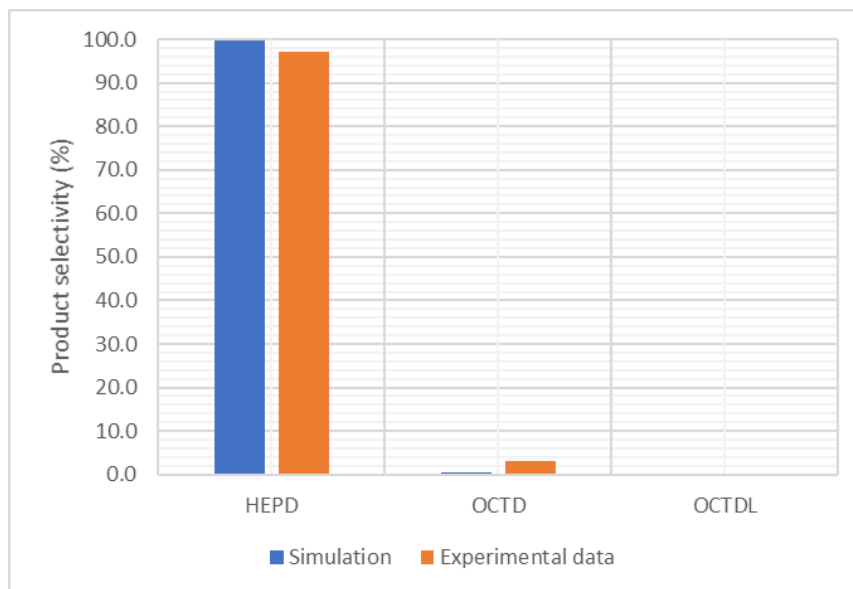


Figure 4.4 Product selectivity of hydrotreating of stearic acid over 5% Ni- γ -Al₂O₃ at 360 min of reaction time, 99% of stearic acid conversion, 0.035 M (mole/L) of concentration of stearic acid, 300 °C of reaction temperature, 30 bar of hydrogen pressure between experiment and simulation from kinetic model of Jenistova and co-workers⁴².

The product selectivity of hydrotreating of stearic acid at 360 min of reaction time was compared between the kinetic model of Kumar and co-workers⁴¹ using the nickel supported catalyst, 0.18 kmol/m³ of concentration of stearic acid, 290 °C of reaction temperature, and 8 bar of hydrogen pressure which obtained 99.91% conversion, the kinetic model of Jenistova and co-workers⁴² using 5% Ni- γ -Al₂O₃, 0.035 M (mol/L) of concentration of stearic acid, 300 °C of reaction temperature, and 30 bar of hydrogen pressure which obtained 99% conversion. Both of the results of the kinetic model of Kumar and co-workers⁴¹ and Jenistova and co-workers⁴² provided n-heptadecane (HEPD) was the main product selectivity and n-octadecane (OCTD) was slight, but the kinetic model of Jenistova and co-workers⁴² also provided n-pentadecane (PEND) and n-hexadecane (HEXD).

However, model validation was discussed in order to show kinetic model⁴¹⁻⁴² can approach at high temperature around 300 °C.

4.2.1.2 Process and operating condition selection of single-step of hydrotreating

BHD production requires a bifunctional solid catalyst (acid/metal) operating at temperature around 300 °C and hydrogen pressure around 50 bar in a continuous flow process.¹⁴

Thus, the operating condition for this work was selected at reaction temperature of 300 °C, pressure of 50 bar and amount of hydrogen of 300% of the theoretical requirement². The basis calculation is based on 1.0 kmol/h of palm oil as tripalmitin and triolein as a feedstock for section of hydrotreating via hydrogenation, hydrogenolysis, and various deoxygenation reaction pathways and the simulation was assumed with complete hydrotreating as shown by the literature review in Table 3.7.

4.2.1.3 Process description of single-step of hydrotreating

Figure 4.5 illustrates the hydrotreating via the hydrogenolysis of TGs process. Palm oil (OIL-1) and high purity H₂ (H2-1) were heated to a temperature of 300 °C and pressurized to 50 bar before mixing and entering the reactor (R-101). Multiple reactions such as hydrogenation, hydrogenolysis, and deoxygenation reaction pathways can occur simultaneously over the catalyst bed in the hydrotreating reactor (R-101) using RSTOIC reactor⁵¹. The R-STOIC was chosen as a model reactor since the pathway of deoxygenation can be specified. In addition, R-101 represented the reaction zone of TGs converting to various products with different reaction pathways.

The products (PD-1) of hydrotreating of TGs mainly consist of n-heptadecane (C₁₇H₃₆) and n-octadecane (C₁₈H₃₈) hydrocarbons for the triolein feedstock, and n-pentadecane (C₁₅H₃₂) and n-hexadecane (C₁₆H₃₄) hydrocarbon for the tripalmitin feedstock, which could be separated from one another as a stream BHD-1. The pressure of the stream product (PD-1) was reduced to 30 bar for the PSA unit (PSA-1). In order to obtain the highest carbon recovery ratio, the temperature of the stream S8 was decreased by a cooler (CL-2) to 117 °C for tripalmitin and 126 °C for triolein for separation of residue of hydrogen including propane, carbon dioxide, carbon monoxide, and the rest of H₂O by a three-phase separator (SEP-1), and in order to reduce the volume of the PSA unit by separation of H₂O for recycling (R-H2O-1). The suitable temperature of CL-2 was obtained from the sensitivity result

curve, which was reported in APPENDIX D with Figure D.1 and Figure D.3 from tripalmitin and triolein, respectively.

The temperature of the gaseous portion from SEP-1 (stream S10) was decreased to 30 °C by a cooler (CL-3) in order to obtain higher H₂ recovery and purity (R-H2-1) from the PSA unit (PSA-1), while other gases such as propane, carbon dioxide, carbon monoxide, and the rest of H₂O were adsorbed at 30 bar and desorbed at 1.1 bar by a valve (V-3) and were released at atmospheric pressure by a valve (V-4) to obtain the stream (BP-1) to be sent to the hydrogen generation process.

Stream description and equipment description of single-step of hydrotreating is demonstrated in Figure 4.5 and is shown in Table 4.3 and Table 4.4, respectively.



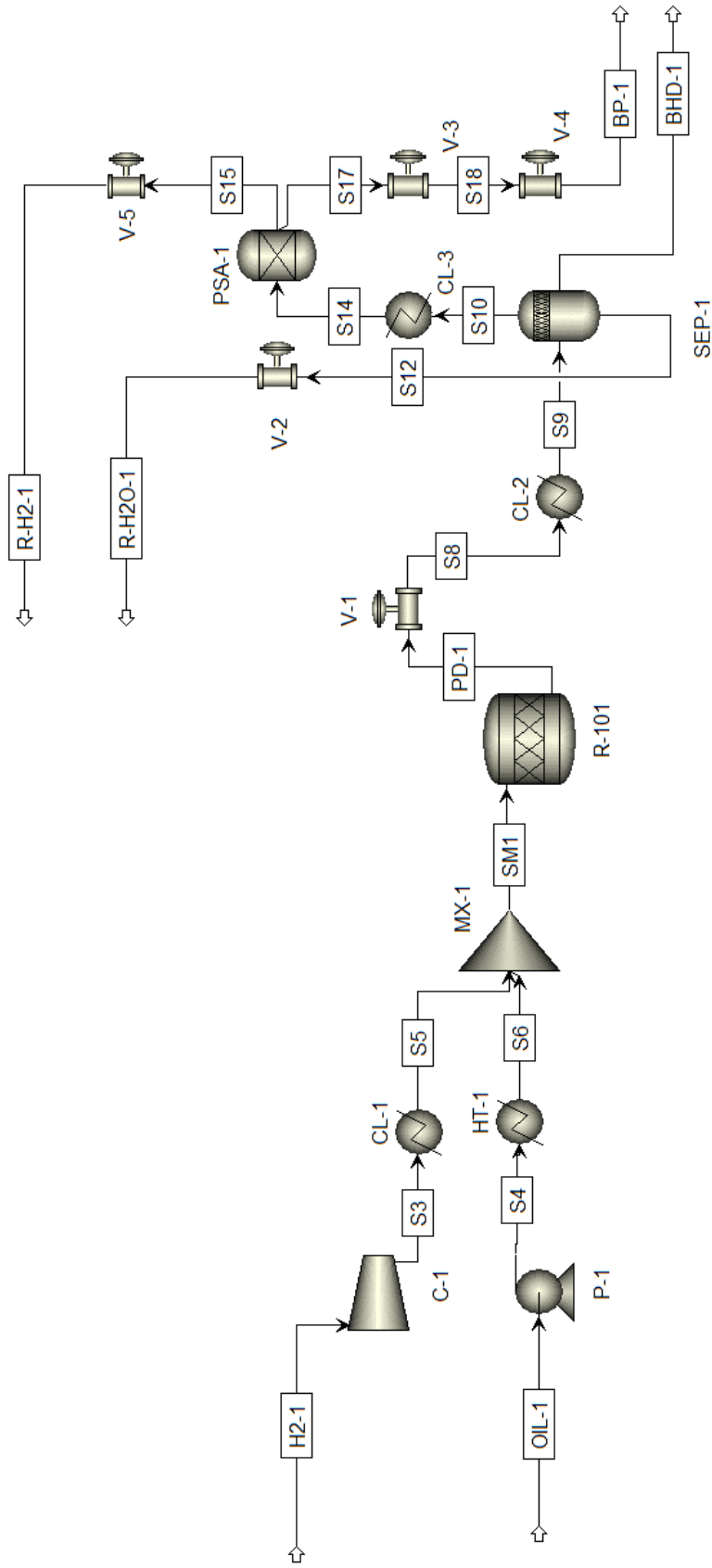


Figure 4.5 Process flow diagram of single-step of hydrotreating.

Table 4.3 Stream description of single-step of hydrotreating demonstrated in Figure 4.5.

Stream name	From	To	Stream description
H2-1		C-1	The high purity H ₂ was a raw material for hydrotreating of palm oil
OIL-1		P-1	Palm oil was a raw material for hydrotreating of TGs as triolein and tripalmitin
S3	C-1	CL-1	The high purity H ₂ was cooled to the temperature
S4	P-1	HT-1	Palm oil was sent to be heated by a pump
S5	CL-1	MX-1	The high purity H ₂ after temperature reduction was sent to the mixer
S6	HT-1	MX-1	Palm oil after being heated was sent to the mixer
SM1	MX-1	R-101	The mixer stream was sent to the multiple-bed hydrotreating reactor
PD-1	R-101	V-1	The pressure of the product mixture was reduced
S8	V-1	CL-2	The temperature of the product mixture was decreased
S9	CL-2	SEP-1	The product mixture was sent to be separated by a three-phase separator
S10	SEP-1	CL-3	The temperature of the gaseous portion was decreased
BHD-1	SEP-1		Bio-hydrogenated diesel
S12	SEP-1	V-2	The pressure of H ₂ O was released at atmospheric pressure
R-H2O-1	V-2		H ₂ O for recycling
S14	CL-3	PSA-1	The gaseous portion was sent to the H ₂ purification unit to adsorb impurity
S15	PSA-1	V-5	90% of H ₂ was recovered with high purity via pressure swing adsorption
R-H2-1	V-5		H ₂ for recycling
S17	PSA-1	V-3	The other gases were desorbed at 1.1 bar

Table 4.3 Stream description of single-step of hydrotreating demonstrated in Figure 4.5. (*Continued*).

Stream name	From	To	Stream description
S18	V-3	V-4	The other gases were released at atmospheric pressure
BP-1	V-4		Fuel gas containing mainly C ₃ H ₈ , CO ₂ , CO, and H ₂ O



Table 4.4 Equipment description of single-step of hydrotreating demonstrated in Figure 4.5.

Name	Model	Equipment description
C-1	COMPR	Adjusts H ₂ pressure before heating
P-1	PUMP	Pumps palm oil to the destination pressure
CL-1	HEATER	Cools H ₂ to the reaction temperature
HT-1	HEATER	Heats palm oil to the reaction temperature
MX-1	MIXER	Mixes the stream of the high purity H ₂ and palm oil
R-101	RSTOIC	Simulates palm oil conversion to various products with the different reaction pathways
V-1	VALVE	Reduces pressure for the PSA unit
CL-2	HEATER	Decreases temperature of the product mixture for separation
SEP-1	FLASH3	Separates the vapor-liquid-liquid phase products consisting of gas, oil, and water
V-2	VALVE	Releases pressure of H ₂ O to atmospheric pressure
CL-3	HEATER	Decreases temperature for the PSA unit
PSA-1	SEP	Recovers and purifies H ₂ with the adsorption of gaseous impurity
V-3	VALVE	Reduces pressure to 1.1 bar for the desorption of gaseous impurity
V-4	VALVE	Releases pressure of the other gases to atmospheric pressure
V-5	VALVE	Releases pressure of H ₂ to atmospheric pressure

4.2.2 Two-step: hydrolysis of triglycerides and deoxygenation of free fatty acids process

4.2.2.1 Modelling validation of hydrolysis of triglycerides and deoxygenation of free fatty acids

The hydrolysis of triolein model is simulated from the kinetic model of Minami and co-worker⁴⁴ with condition of Gomez-Castro and co-worker⁴³. The results shown in Figure 4.6 demonstrate conversion of triolein and the moles number of liquid products per unit mole of triolein at temperature of 270 °C and pressure of 70 bar and 1.0 of water per triolein volumetric ratio. Thus, this result indicates that the predictions from the kinetic model provides complete conversion of the hydrolysis reaction and liquid products from hydrolysis of triolein following stoichiometry.

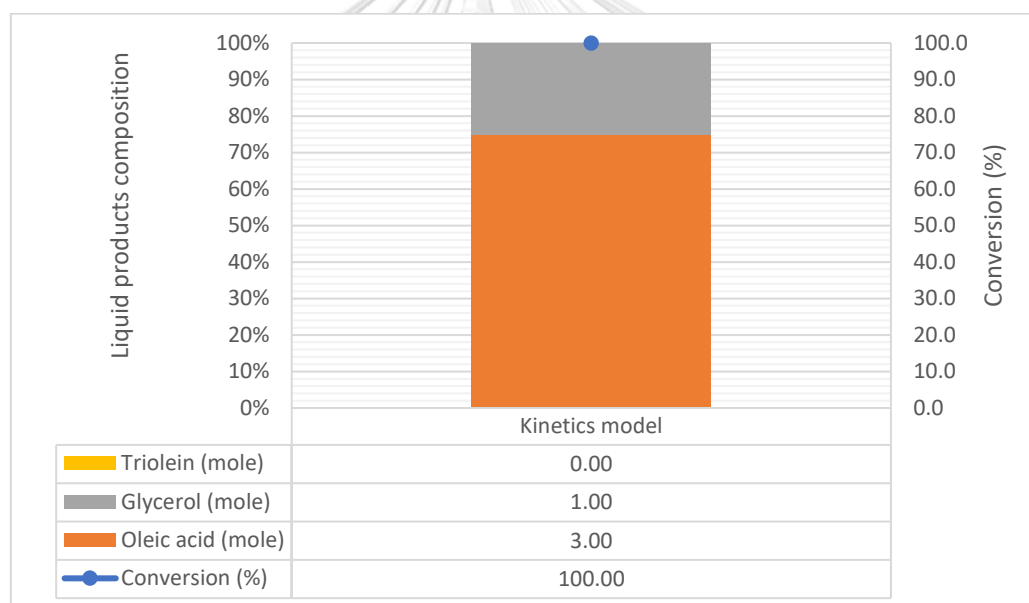


Figure 4.6 Conversion of triolein and the moles number of liquid products per unit mole of triolein for hydrolysis reaction at temperature of 270 °C and pressure of 70 bar, 1.0 of water per triolein volumetric ratio from kinetic model of Minami⁴⁴ with condition of Gomez-Castro⁴³.

4.2.2.2 Process and operating condition selection of two-step of hydrotreating

The operating condition for the hydrolysis reaction was selected at 250 °C of reaction temperature, 50 bar of pressure⁴⁷, and the water to oil molar ratio of 54.0 (18

times of the stoichiometric requirement)⁴³, which was presented by the calculation in APPENDIX C. The basis is based on 1.0 kmol/h of palm oil as tripalmitin and triolein as a feedstock. For hydrotreating via hydrogenation and various deoxygenation reaction pathways, the operating condition was selected at reaction temperature of 300 °C, pressure of 50 bar and 3.0 times of the theoretical requirement of the H₂/FFAs molar ratio. In the case of tripalmitin with the DCO₂ pathway, the H₂ to tripalmitin ratio of 1.35 is fed initially to prevent catalyst deactivation. In this simulation, the effect of the reverse reaction was assumed to be negligible with a complete hydrolysis reaction^{43, 45, 47} and complete hydrotreating according to the literature review shown in Table 3.7.

4.2.2.3 Process description of two-step of hydrotreating

Figure 4.7 illustrates the hydrotreating via hydrolysis of TGs process. Palm oil (OIL-2) and water (H₂O-1) were heated to a temperature of 250 °C and pressurized to 50 bar before mixing and entering the reactor (R-102). In addition, R-102 represents the hydrolysis reaction zone of TGs converting to FFAs and glycerol with complete conversion.

The stream (PD-2) left the reactor and entered a decanter (SEP-2) where the phase of oil (S30) is separated from the aqueous phase. The glycerol aqueous phase (S31) leaving the decanter contains excess water and glycerol. It was released at atmospheric pressure and heated up by a heater (HT-5) to vaporize to obtain the excess water (R-H₂O-2). It was then separated to obtain 9.0 of WGMR for the glycerol aqueous phase (BP-2) from a second phase separator (SEP-3). The glycerol aqueous phase (BP-2) was prepared for the hydrogen generation process such as GSR. The oil phase (S30) and high purity H₂ (H₂-2) were heated to a temperature of 300 °C and pressurized to 50 bar before mixing and entering the reactor (R-103). The multiple reactions such as hydrogenation and deoxygenation can occur simultaneously in the hydrotreating packed bed reactor (R-103). In addition, R-103 represents the reaction zone of FFAs converting to various products with various deoxygenation reaction pathways.

The products (PD-3) of hydrotreating of FFAs mainly consist of n-heptadecane (C₁₇H₃₆) and n-octadecane (C₁₈H₃₈) hydrocarbons for the triolein

feedstock, and n-pentadecane ($C_{15}H_{32}$) and n-hexadecane ($C_{16}H_{34}$) hydrocarbon for the tripalmitin feedstock, which could be separated from one another as a stream BHD-2.

The pressure of the stream product (PD-3) was reduced to 30 bar for the PSA unit (PSA-2). The temperature of the stream S38 was decreased to 40 °C by a cooler (CL-5) for separation of residue of hydrogen including carbon dioxide, carbon monoxide, and the rest of H_2O by a three-phase separator (SEP-4), and in order to reduce the volume of the PSA unit by separation of H_2O for recycling (R-H2O-3). Temperature of CL-5 was obtained from the sensitivity result curve, which was reported in APPENDIX D with Figure D.5 and Figure D.7 from tripalmitin and triolein, respectively. Figure D.5 and Figure D.7 demonstrated that at temperature is higher than 180 °C and 170 °C, from tripalmitin and triolein, respectively, the process could not separate H_2O and at higher temperature, the process could separate lower H_2O and lower purity of H_2O . But at low temperature, the process need high cooling utility. Thus, Figure D.5 was selected temperature of 40 °C, which provided high recovery and purity of H_2O .

The temperature of the gaseous portion from SEP-4 (stream S43) was decreased to 30 °C by a cooler (CL-6) in order to obtain higher H_2 recovery and purity (R-H2-2) from the PSA unit (PSA-2), while other gases such as carbon dioxide, carbon monoxide, and the rest of H_2O were adsorbed at 30 bar and desorbed at 1.1 bar by a valve (V-10) and were released as the outlet off-gas stream (OG-1).

Stream description and equipment description of two-step of hydrotreating is demonstrated in Figure 4.7 and is shown in Table 4.5 and Table 4.6, respectively.

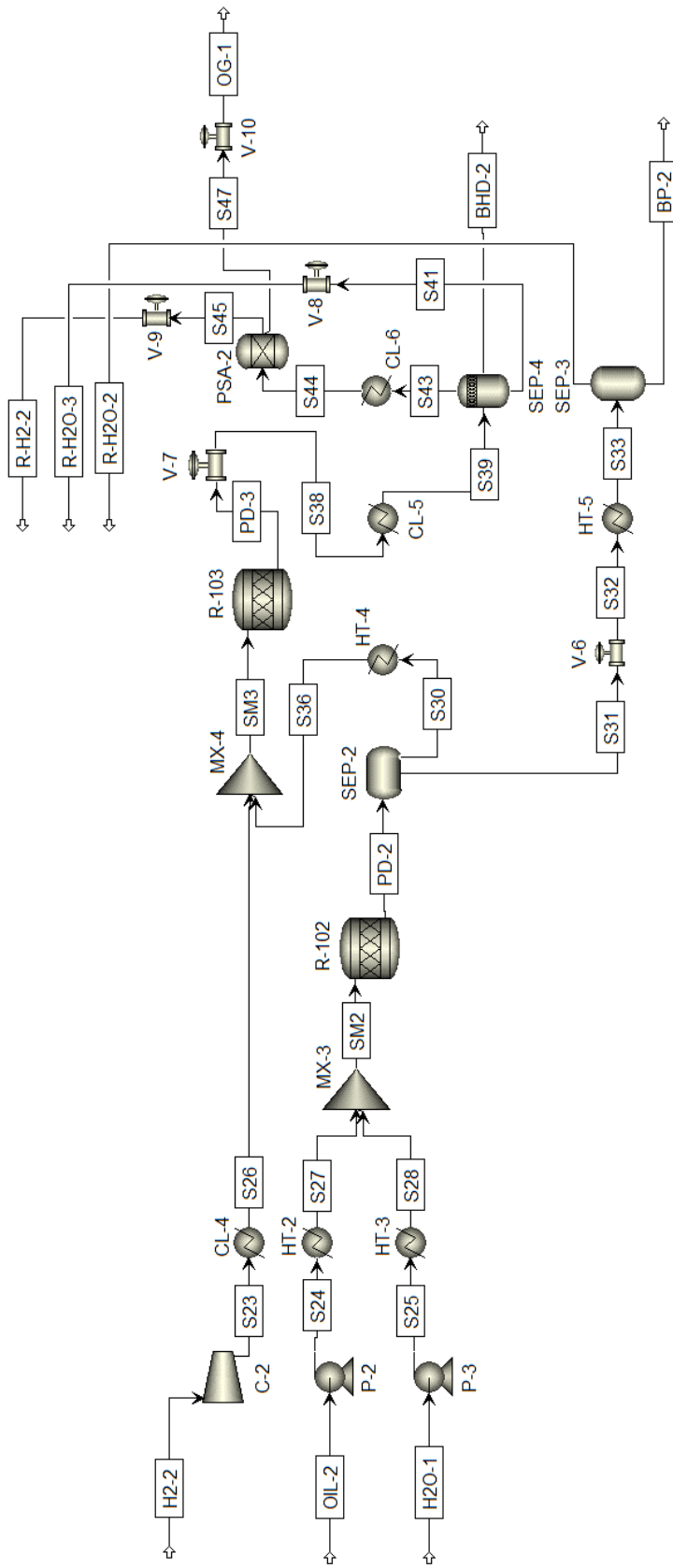


Figure 4.7 Process flow diagram for two-step of hydrotreating.

Table 4.5 Stream description of two-step of hydrotreating demonstrated in Figure 4.7.

Stream name	From	To	Stream description
H2-2		C-2	The high purity H ₂ was a raw material for hydrotreating of FFAs
OIL-2		P-2	Palm oil was a raw material for hydrolysis of TGs as triolein and tripalmitin
H2O-1		P-3	Water was a raw material for hydrolysis of TGs
S23	C-2	CL-4	The high purity H ₂ was cooled to the temperature
S24	P-2	HT-2	Palm oil was sent to be heated by a pump
S25	P-3	HT-3	Water was sent to be heated by a pump
S26	CL-4	MX-4	The high purity H ₂ after temperature reduction was sent to the mixer
S27	HT-2	MX-3	Palm oil after being heated was sent to the mixer
S28	HT-3	MX-3	Water after being heated was sent to the mixer
SM-2	MX-3	R-102	The mixer stream was sent to the hydrolysis reactor
PD-2	R-102	SEP-2	The liquid product was sent to be separated by a decanter
S30	SEP-2	HT-4	The oil phase was sent to be heated
S31	SEP-2	V-6	The glycerol aqueous phase was released at atmospheric pressure
S32	V-6	HT-5	The glycerol aqueous phase was heated up
S33	HT-5	SEP-3	H ₂ O was vaporized to obtain the excess water and the glycerol aqueous phase was separated to obtain 9.0 of WGMR
R-H2O-2	SEP-3		Vapor of the excess water for recycling
BP-2	SEP-3		The glycerol aqueous phase was prepared for the hydrogen generation process
S36	HT-4	MX-4	The oil phase for hydrotreating was sent to the mixer

Table 4.5 Stream description of two-step of hydrotreating demonstrated in Figure 4.7. (*Continued*).

Stream name	From	To	Stream description
SM3	MX-4	R-103	The mixer stream was sent to the multiple-bed hydrotreating reactor
PD-3	R-103	V-7	The pressure of the product mixture was reduced
S38	V-7	CL-5	The temperature of the product mixture was decreased
S39	CL-5	SEP-4	The product mixture was sent to be separated by a three-phase separator
BHD-2	SEP-4		Bio-hydrogenated diesel
S41	SEP-4	V-8	The pressure of H ₂ O was released at atmospheric pressure
R-H2O-3	V-8		H ₂ O for recycling
S43	SEP-4	CL-6	The temperature of the gaseous portion was decreased
S44	CL-6	PSA-2	The gaseous portion was sent to the H ₂ purification unit to adsorb impurity
S45	PSA-2	V-9	90% of H ₂ was recovered with high purity via pressure swing adsorption
R-H2-2	V-9		H ₂ for recycling
S47	PSA-2	V-10	The other gases were desorbed at 1.1 bar
OG-1	V-10		The outlet off-gas containing mainly CO ₂ , CO, and H ₂ O

Table 4.6 Equipment description of two-step of hydrotreating demonstrated in Figure 4.7.

Name	Model	Equipment description
C-2	COMPR	Adjusts H ₂ pressure before heating
P-2	PUMP	Pumps palm oil to the destination pressure
P-3	PUMP	Pumps water to the destination pressure
CL-4	HEATER	Cools H ₂ to the reaction temperature
HT-2	HEATER	Heats palm oil to the reaction temperature
HT-3	HEATER	Heats water to the reaction temperature
MX-3	MIXER	Mixes the stream of palm oil and water
R-102	RSTOIC	Simulates palm oil conversion to FFAs and glycerol
SEP-2	DECANTER	Separates the liquid-liquid phase products consisting of glycerol aqueous phase and oil
V-6	VALVE	Releases pressure of glycerol aqueous phase to atmospheric pressure
HT-5	HEATER	Heats the glycerol aqueous phase
SEP-3	FLASH2	Separates the vapor-liquid phase with the vaporization of H ₂ O from the glycerol aqueous phase
HT-4	HEATER	Heats the oil phase to the reaction temperature
MX-4	MIXER	Mixes the stream of the high purity H ₂ and the oil phase
R-103	RSTOIC	Simulates FFAs conversion to various products with the different reaction pathways
V-7	VALVE	Reduces pressure for the PSA unit
CL-5	HEATER	Decreases temperature of the product mixture for separation
SEP-4	FLASH3	Separates the vapor-liquid-liquid phase products consisting of gas, oil, and water

Table 4.6 Equipment description of two-step of hydrotreating demonstrated in Figure 4.7. (Continued).

Name	Model	Equipment description
V-8	VALVE	Releases pressure of H ₂ O to atmospheric pressure
CL-6	HEATER	Decreases temperature for the PSA unit
PSA-2	SEP	Recovers and purifies H ₂ with the adsorption of gaseous impurity
V-9	VALVE	Releases pressure of H ₂ to atmospheric pressure
V-10	VALVE	Reduces pressure to 1.1 bar for the desorption of gaseous impurity



4.3 Hydrogen production

4.3.1 Propane steam reforming process

4.3.1.1 Modelling validation of propane steam reforming

The PSR model is validated by comparison with the result of the thermodynamic model reported by Wang and co-workers⁴⁸. The results shown in Figure 4.8 demonstrate the product gas composition with dry basis for an equilibrium reactor with the reformer operating condition of 12 of WPMR, 677 °C of temperature, and atmospheric pressure. The mole number of H₂ from the simulation is 8.65 moles per unit mole of propane, which is consistent with the report by Wang and co-workers of 8.64 moles of the mole number of hydrogen produced. This result indicated that the model prediction and thermodynamic data of the product gas composition obtained from the propane steam reformers are in good agreement.

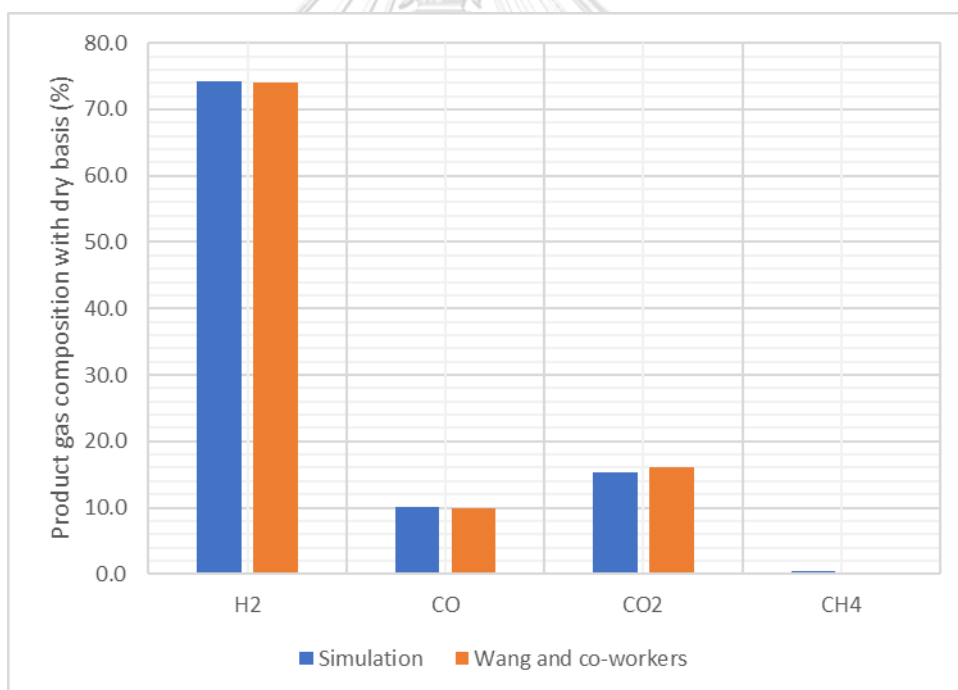


Figure 4.8 Product gas composition with dry basis for equilibrium reactor of PSR, 12 of WPMR, 677 °C of temperature and atmospheric pressure between thermodynamic data of Wang and co-workers⁴⁸ and equilibrium simulation.

The PSR model is validated by comparison with the experimental data reported by Im and co-workers⁴⁹. The results shown in Figure 4.9 demonstrate the product gas composition with dry basis and the conversion of propane for the

equilibrium reactor of the PSR performance using Ni/YSZ and 1.0% M/Ni/YSZ catalysts (M = Ru, Rh and Pd) with the reformer operating at 9 of WPMR, 650 °C of temperature, and atmospheric pressure. The mole number of H₂ from simulation is 7.93 moles per unit mole of propane, while the experimental data shows the mole number of hydrogen for Ni/YSZ, 1% Ru/Ni/YSZ, 1% Rh/Ni/YSZ, and 1% Pd/Ni/YSZ of 4.48, 4.71, 9.09, and 8.36, respectively, as shown in Figure 4.10. Moreover, this result indicated that the experimental data using 1% Rh/Ni/YSZ and 1% Pd/Ni/YSZ of the product gas composition obtained from the propane steam reformers are thermodynamically approach equilibrium calculation, and therefore the results are in good agreement.

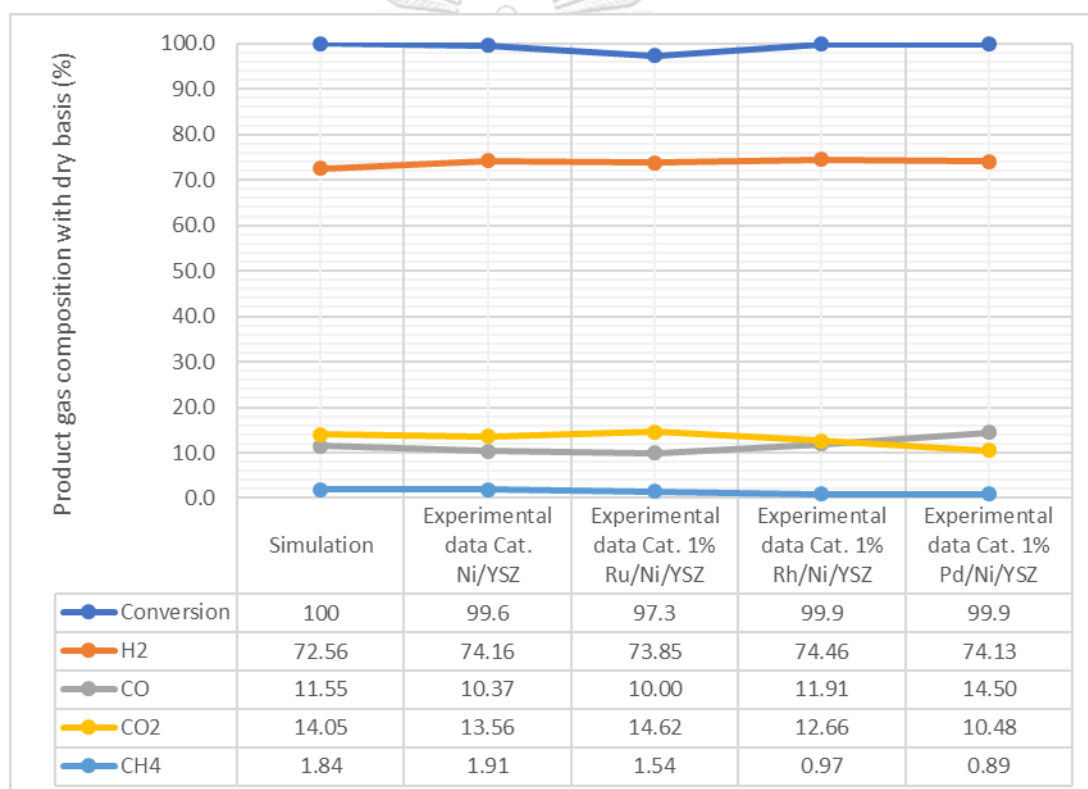


Figure 4.9 Product gas composition with dry basis and conversion of propane for equilibrium reactor of PSR performance using various catalysts of Ni/YSZ, 1% Ru/Ni/YSZ, 1% Rh/Ni/YSZ, and 1% Pd/Ni/YSZ, 9 of WPMR, 650 °C of temperature and atmospheric pressure between experiment of Im and co-workers⁴⁹ and equilibrium simulation.

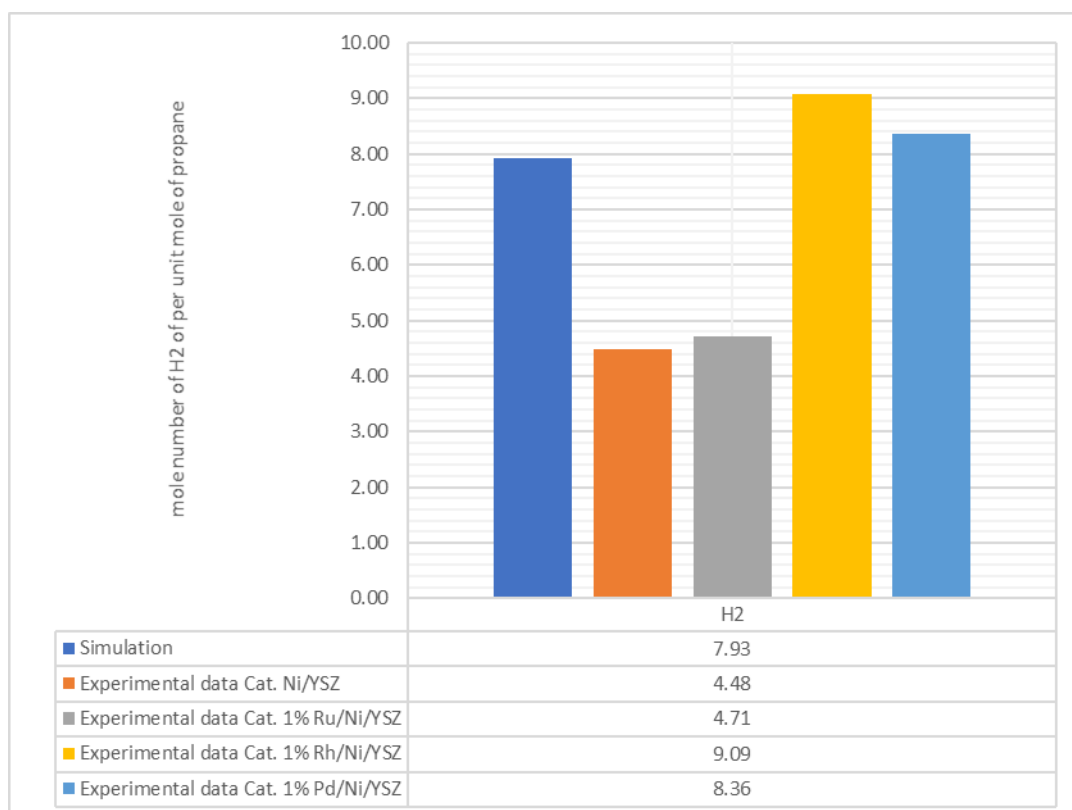


Figure 4.10 Mole number of H₂ per unit mole of propane using various catalysts of Ni/YSZ, 1% Ru/Ni/YSZ, 1% Rh/Ni/YSZ, and 1% Pd/Ni/YSZ, 9 of WPMR, 650 °C of temperature and atmospheric pressure between experiment of Im and co-workers⁴⁹ and equilibrium simulation.

4.3.1.2 Process and operating condition selection of propane steam reforming

The operating condition at atmospheric pressure was selected for the optimum condition of PSR for hydrogen generation because the reaction favors low pressure⁴⁸.

The result of PSR simulation revealed that the higher efficiency of H₂ generation in mole number of H₂ per unit mole of propane can be obtained at atmospheric pressure, 12 of WPMR, and 667 °C of temperature than at atmospheric pressure, 9 of WPMR, and 650 °C of temperature, due to higher WPMR and higher temperature.

Thus, the operating condition for this work was selected at 667 °C of temperature, 12 of WPMR, and atmospheric pressure for section of the PSR process⁴⁸.

4.3.1.3 Process description of propane steam reforming

Figure 4.11 illustrates the PSR section. The mixture of propane-water was heated to a temperature of 677 °C, atmospheric pressure, and 12.0 of WPMR before entering the reactor (R-104), using REQUIL reactor. The temperature of the stream product (PD-4) was decreased to 40 °C by a cooler (CL-7) for separation of residue of H₂O by the two-phase separator (SEP-5), and in order to reduce the volume of the PSA unit by separation of H₂O for recycling (R-H₂O-4). Temperature of CL-7 was obtained from the sensitivity result curve, which was reported in APPENDIX D with Figure D.2 and Figure D.4 from tripalmitin and triolein, respectively. The main gas products (S58) consist of H₂, CO₂, and CO. The pressure of the gas products was increased to 30 bar by a compressor (C-3) and was decreased to 30 °C by a cooler (CL-8) in order to obtain higher H₂ recovery and purity (R-H₂-3) from the PSA unit (PSA-3), while other gases such as carbon dioxide, carbon monoxide, and the rest of H₂O were adsorbed at 30 bar and desorbed at 1.1 bar by a valve (V-11) to obtain the outlet off-gas stream (OG-2).

Stream description and equipment description of PSR is demonstrated in Figure 4.11 and is shown in Table 4.7 and Table 4.8, respectively.

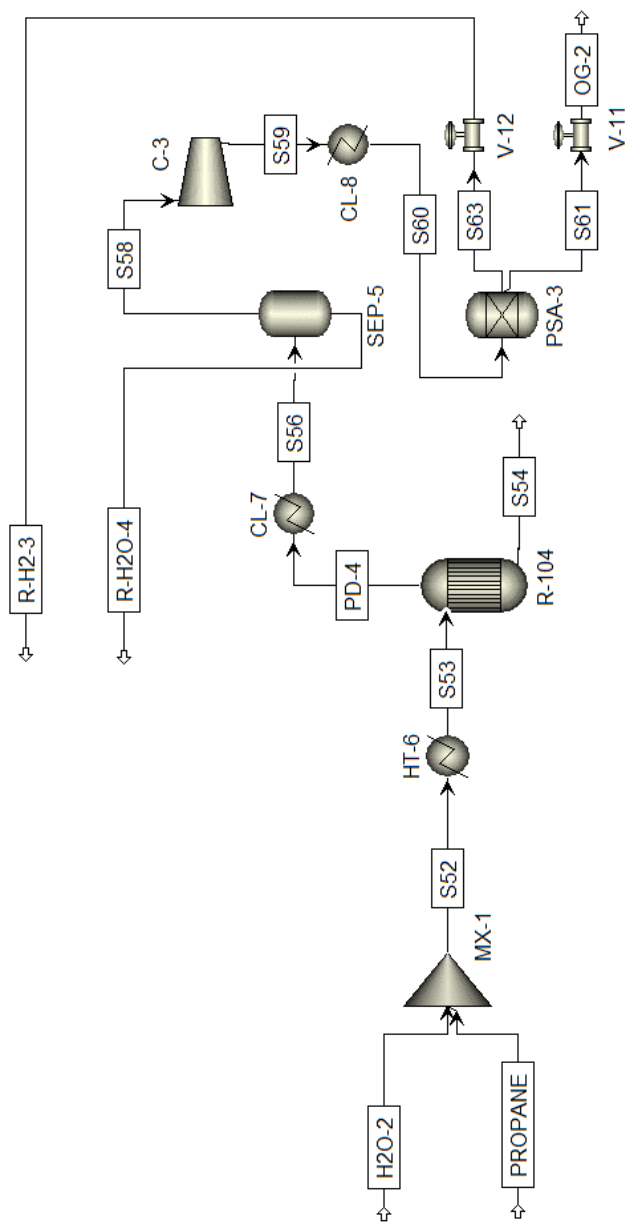


Figure 4.11 Process flow diagram of propane steam reforming.

Table 4.7 Stream description of PSR demonstrated in Figure 4.11.

Stream name	From	To	Stream description
H2O-2		MX-1	Water was a raw material for the PSR process
PROPANE		MX-1	Propane was a raw material for the PSR process
S52	MIX-1	HT-6	Propane-water mixture was sent to be heated
S53	HT-6	R-104	Propane-water mixture after being heated was sent to the reformer
PD-4	R-104	CL-7	The temperature of the stream gas product was decreased
S54	R-104		The stream liquid product (no product)
S56	CL-7	SEP-5	The stream product was sent to be separated by a two-phase separator
R-H2O-4	SEP-5		Residue of H ₂ O for recycling
S58	SEP-5	C-3	The pressure of the gas products was increased
S59	C-3	CL-8	The temperature of the gas products was decreased
S60	CL-8	PSA-3	The gas products were sent to the H ₂ purification unit to adsorb impurity
S61	PSA-3	V-11	The other gases were desorbed at 1.1 bar
OG-2	V-11		The outlet off-gas containing mainly CO ₂ , CO, H ₂ , and H ₂ O
S63	PSA-3	V-12	90% of H ₂ was recovered with high purity via pressure swing adsorption
R-H2-3	V-12		H ₂ was generated for recycling

Table 4.8 Equipment description of PSR demonstrated in Figure 4.11.

Name	Model	Equipment description
MX-1	MIXER	Mixes propane and water from storage
HT-6	HEATER	Heats reactant to reaction temperature
R-104	REQUIL	Simulates hydrogen generation via PSR (677 °C, 1.0 bar)
CL-7	HEATER	Decreases temperature of the stream gas product for separation
SEP-5	FLASH2	Separates the vapor-liquid phase with the condensation of H ₂ O
C-3	COMPR	Increases pressure of the gas products for the PSA unit
CL-8	HEATER	Decreases temperature of the gas products for the PSA unit
PSA-3	SEP	Recovers and purifies H ₂ with the adsorption of gaseous impurity
V-11	VALVE	Reduces pressure to 1.1 bar for the desorption of gaseous impurity
V-12	VALVE	Releases pressure of H ₂ to atmospheric pressure

4.3.2 Glycerol steam reforming process

4.3.2.1 Modelling validation of glycerol steam reforming

The GSR model is validated by comparison with the experimental data reported by Profeti and co-workers⁵⁰. The results shown in Figure 4.12 demonstrate the product gas composition with dry basis for the equilibrium reactor of GSR using metal un-promoted and metal promoted Ni catalysts, 6 of WGMR, 700 °C of temperature, and atmospheric pressure between experiment and equilibrium simulation. This result demonstrates that the modelling and experimental data of the product gas components derived from the GSR have been well accepted. Furthermore, at this operating condition, the mole number of H₂ per unit mole of glycerol from the simulation was 5.59 moles.

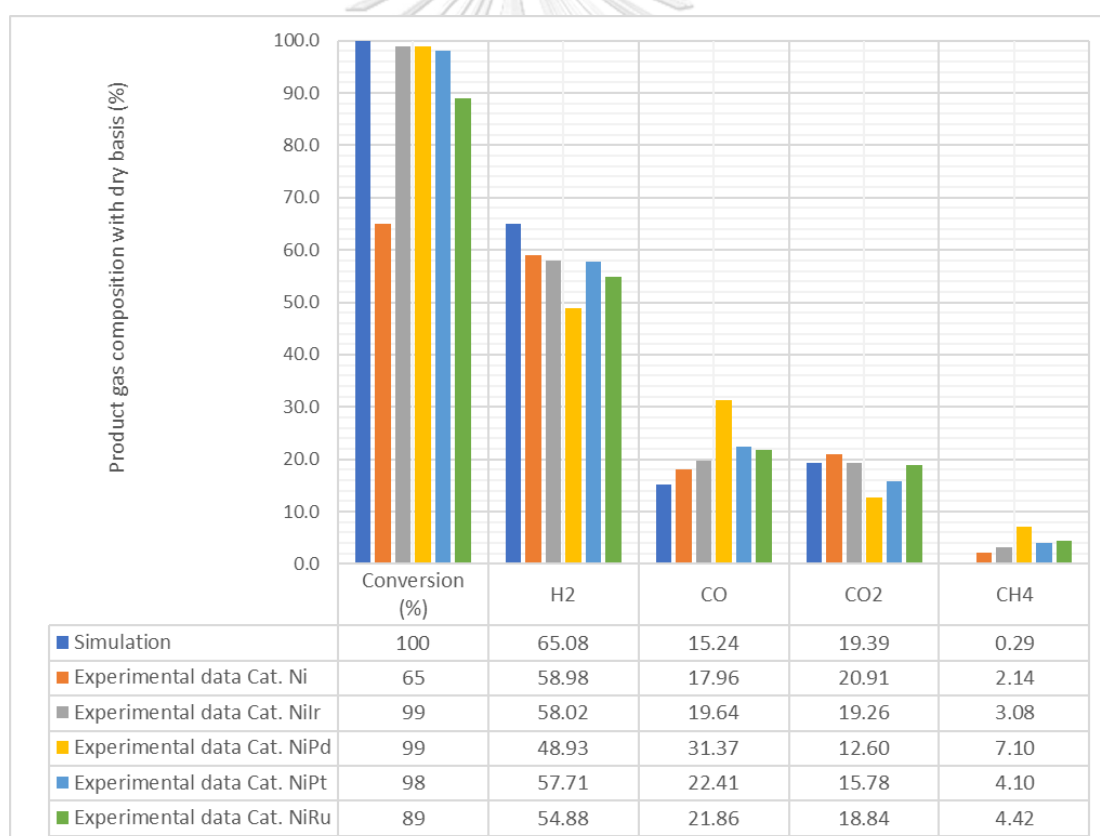


Figure 4.12 Product gas composition with dry basis for equilibrium reactor of GSR using un-promoted and promoted Ni catalysts, 6 of WGMR, 700 °C of temperature, and atmospheric pressure between experiment of Profeti and co-workers⁵⁰ and equilibrium simulation.

The GSR model is validated by comparison with the experimental data reported by Wang and co-workers¹⁰ when using the Ni-Mg-Al based catalyst. The conversion of glycerol and the mole number of H₂ per unit mole of glycerol for the equilibrium reactor, using catalyst C3 with the following composition: NiO (24.1 wt.%), MgO (26.1 wt.%), and Al₂O₃ (49.8 wt.%), 9 of WGMR, 450, 550, and 650 °C of temperature, and atmospheric pressure between experiment and equilibrium simulation are shown in Figure 4.13. Based on the simulation results, conversion of glycerol was complete under all conditions and the mole number of H₂ per unit mole of glycerol increased with increasing temperature, which is consistent with the experimental data of Wang and co-workers¹⁰. For the operating condition at 650 °C of temperature, the mole number of H₂ per unit mole of glycerol from simulation was 5.97 moles, while the experimental data gave 5.57 moles.

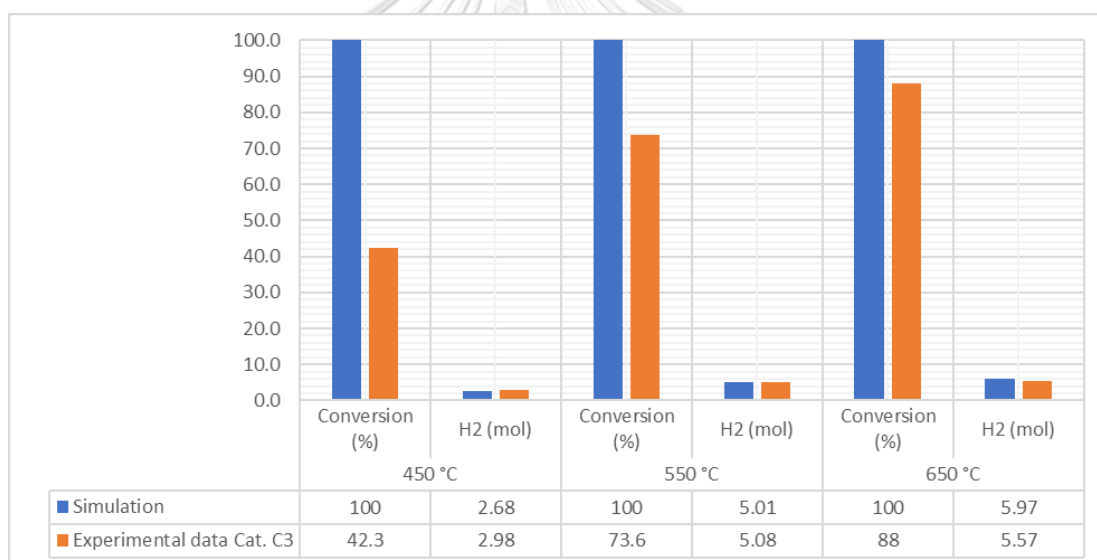


Figure 4.13 Conversion of glycerol and the mole number of H₂ per unit mole of glycerol, using catalyst C3, 9 of WGMR, 450, 550, and 650 °C of temperature, and atmospheric pressure between experiment of Wang and co-workers¹⁰ and equilibrium simulation.

The H₂ selectivity for the equilibrium reactor of GSR, 9 of WGMR, 450, 550 and, 650 °C of temperature, and atmospheric pressure between experiment and equilibrium simulation is shown in Figure 4.14. According to the simulation result, H₂ selectivity increased with increasing temperature, which is consistent with the experimental data of Wang and co-workers¹⁰ under all conditions with the C3

catalyst. The higher operating temperature, the result of experimental data approach the thermodynamic data.

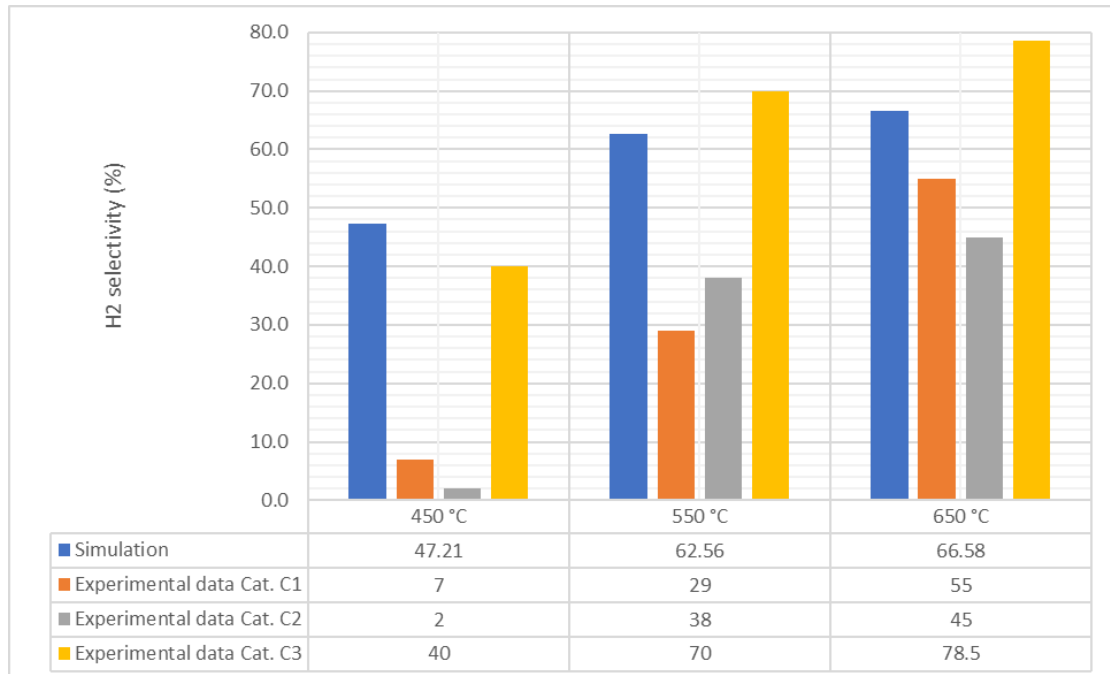


Figure 4.14 Comparing H₂ selectivity of GSR, 9 of WGMR, 450, 550, and 650 °C of temperature, and atmospheric pressure between experiment of Wang and co-workers¹⁰ and equilibrium simulation.

4.3.2.2 Process and operating condition selection of glycerol steam reforming

The result of GSR simulation revealed that the efficiency of H₂ generation that the higher efficiency of H₂ generation in mole number of H₂ per unit mole of glycerol can be obtained at atmospheric pressure, 9 of WGMR, and 650 °C of temperature than at atmospheric pressure, 6 of WGMR, and 700 °C of temperature. Even though the mole number of H₂ per unit mole of glycerol increased with increasing temperature, WGMR also affected the efficiency of GSR.

Thus, the operating condition for this work was selected at 650 °C of temperature, 9 of WGMR, and atmospheric pressure for the section of the GSR process¹⁰.

4.3.2.3 Process description of glycerol steam reforming

Figure 4.15 illustrates the GSR section. The mixture of glycerol-water was heated to a temperature of 650 °C under atmospheric pressure and 9.0 of WGMR before entering the reactor (R-105), using REQUIL reactor. The temperature of the stream product (PD-5) was decreased to 40 °C by a cooler (CL-9) for separation of the residue of H₂O by the two-phase separator (SEP-6), and in order to reduce the volume of the PSA unit by separation of H₂O for recycling (R-H₂O-5). Temperature of CL-9 was obtained from the sensitivity result curve, which was reported in APPENDIX D with Figure D.6 and Figure D.8 from tripalmitin and triolein, respectively.

The main gas products (S72) consist of H₂, CO₂, and CO. The pressure of gas products was increased to 30 bar by a compressor (C-4) and was decreased to 30 °C by a cooler (CL-10) in order to obtain higher H₂ recovery and purity (R-H₂-4) from the PSA unit (PSA-4), while other gases such as carbon dioxide, carbon monoxide, and the rest of H₂O were adsorbed at 30 bar and desorbed at 1.1 bar by a valve (V-13) to obtain the outlet off-gas stream (OG-3).

Stream description and equipment description of GSR is demonstrated in Figure 4.15 and is shown in Table 4.9 and Table 4.10, respectively.

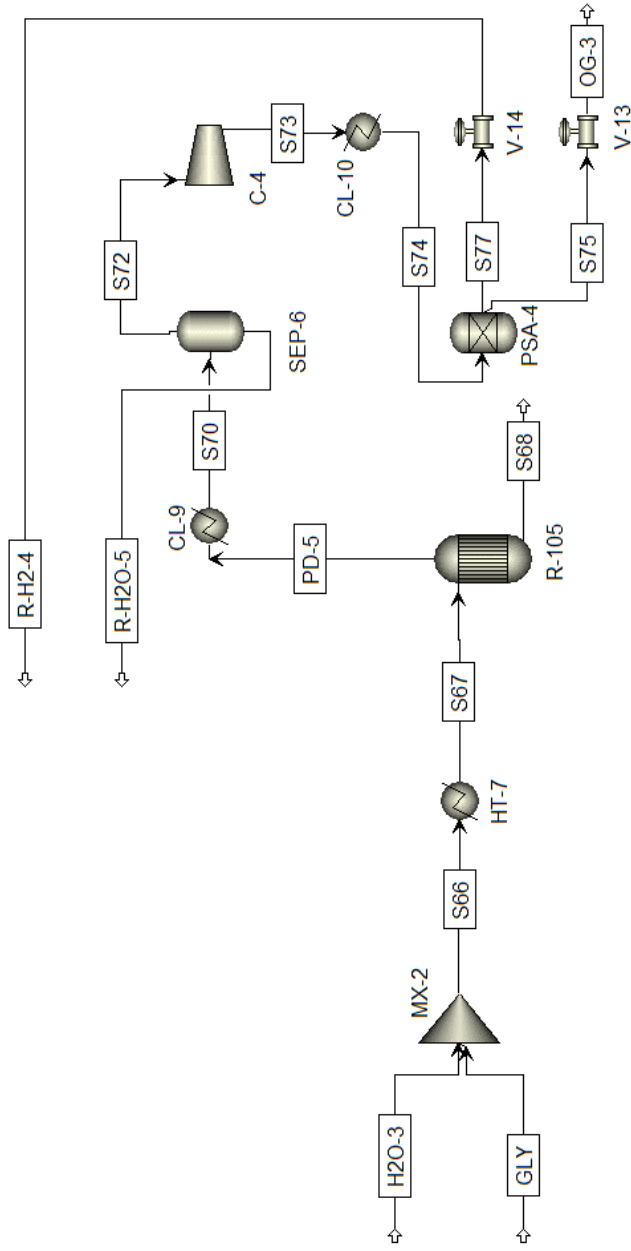


Figure 4.15 Process flow diagram of glycerol steam reforming.

Table 4.9 Stream description of GSR demonstrated in Figure 4.15.

Stream name	From	To	Stream description
H2O-3		MX-2	Water was a raw material for the GSR process
GLY		MX-2	Glycerol was a raw material for the GSR process
S66	MIX-2	HT-7	Glycerol-water mixture was sent to be heated
S67	HT-7	R-105	Glycerol-water mixture after being heated was sent to the reformer
PD-5	R-105	CL-9	The temperature of the stream gas product was decreased
S68	R-105		The stream liquid product (no product)
S70	CL-9	SEP-6	The stream product was sent to be separated by a two-phase separator
R-H2O-5	SEP-6		Residue of H ₂ O for recycling
S72	SEP-6	C-4	The pressure of the gas products was increased
S73	C-4	CL-10	The temperature of the gas products was decreased
S74	CL-10	PSA-4	The gas products were sent to the H ₂ purification unit to adsorb impurity
S75	PSA-4	V-13	The other gases were desorbed at 1.1 bar
OG-3	V-13		The outlet off-gas containing mainly CO ₂ , CO, H ₂ , and H ₂ O
S77	PSA-4	V-14	90% of H ₂ was recovered with high purity via pressure swing adsorption
R-H2-4	V-14		H ₂ was generated for recycling

Table 4.10 Equipment description of GSR demonstrated in Figure 4.15.

Name	Model	Equipment description
MX-2	MIXER	Mixes propane and water from storage
HT-7	HEATER	Heats reactant to reaction temperature
R-105	REQUIL	Simulates hydrogen generation via GSR (650 °C, 1.0 bar)
CL-9	HEATER	Decreases temperature of the stream gas product for separation
SEP-6	FLASH2	Separates the vapor-liquid phase with the condensation of H ₂ O
C-4	COMPR	Increases pressure of the gas products for the PSA unit
CL-10	HEATER	Decreases temperature of the gas products for the PSA unit
PSA-4	SEP	Recovers and purifies H ₂ with the adsorption of gaseous impurity
V-13	VALVE	Reduces pressure to 1.1 bar for the desorption of gaseous impurity
V-14	VALVE	Releases pressure of H ₂ to atmospheric pressure

4.4 Integrated system of hydrotreating and hydrogen generation

The integrated system of hydrotreating and hydrogen generation was proposed in this section, which is used to evaluate the performance of the process.

4.4.1 Integrated system of single-step of hydrotreating and propane steam reforming

4.4.1.1 Base case condition of integrated system

The base case process design, including bio-hydrogenated diesel fuel production via single-step of hydrogenolysis of TGs/ deoxygenation of FFAs process (Section 4.2.1.2), and hydrogen generation via PSR (Section 4.3.1.2), was simulated and the process flow diagram without recycle is shown in Figure 4.16.

4.4.1.2 Material balance condition of integrated system

The suitable operating condition of hydrotreating at 300 °C of temperature, 50 bar of pressure, and 3.0 times of the H₂ stoichiometric requirement was applied in order to provide the complete conversion reaction. The basis calculation is based on 1.0 kmol/h of tripalmitin or triolein as a feedstock. The operating condition of hydrogen generation via PSR was set at 677 °C of temperature, atmospheric pressure, and 12.0 of WPMR. Fuel gas (BP-1) was fed to the reformer.

In order to recycle excess hydrogen and excess H₂O and in order to recover energy, the material balance of the process is needed to specify a reactant to be added or to drain the product from the process, in which a stream splitter was used. The amount of the H₂ initial feed (H2-1) varied with the selectivity of deoxygenation reaction pathways. For the PSR process, the amount of the H₂O initial feed (H2O-2) depending on the amount of H₂O as a by-product produced from the deoxygenation reaction of hydrotreating.

The processes flow diagram of the integrated system of single-step of hydrotreating and the PSR process with recycle are shown in Figure 4.17 and Figure 4.18, respectively. Since, a pair of M-H2-1 and H2-1 streams, and a pair of M-H2O-1 and H2O-2 streams in Figure 4.17 are equal, they can be connected as summarized in Figure 4.18. The unit specification is shown in Table 4.11.

The splitter (SP-1) was used to split the flow rate of the mixed H₂O stream (M-H₂O-1) as initial feed H₂O (H₂O-2) in order to determine WPMR and split excess H₂O (S-H₂O-1). The mixed H₂O stream (M-H₂O-1) composed of the H₂O by-product of hydrotreating (R-H₂O-1), excess unreacted H₂O (R-H₂O-4), and feed H₂O (H₂O-4) for the insufficient H₂O case. The H₂O (H₂O-4) feed was equal to the H₂O consumption.

The splitter (SP-2) was used to split the flow rate of the mixed H₂ gas stream (M-H₂-1) as an initial feed (H₂-1) in order to determine the H₂/ oil molar ratio and in order to split excess H₂ (S-H₂-1). The mixed H₂ gas stream (M-H₂-1) composed of excess H₂ gas from unreacted (R-H₂-1), H₂ gas product (R-H₂-3), and H₂ make up (H₂-3) for the insufficient H₂ case. If hydrogen generation is sufficient for H₂ consumption, H₂ feed is not required.

Calculator specification of flow rate calculation was reported in APPENDIX E with Table E.1, Table E.2, and Table E.3 for M-H₂O-1, H₂O-4 and, H₂-3 stream, respectively.

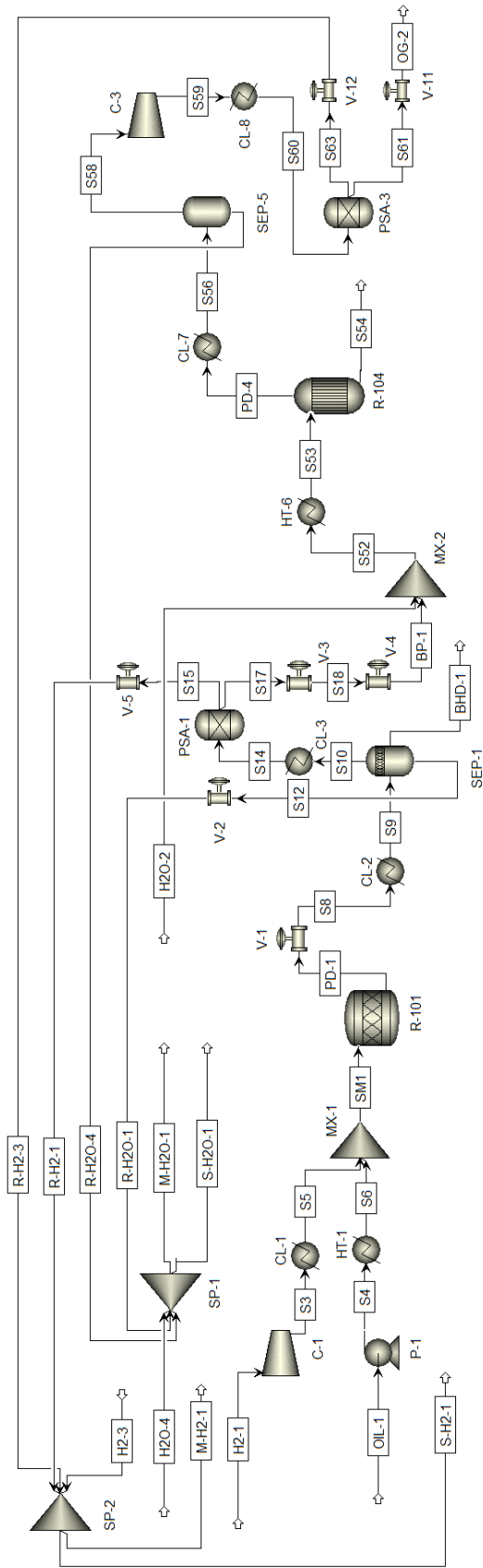


Figure 4.17 Process flow diagram of integrated system of hydrotreating and propane steam reforming with recycle consideration.

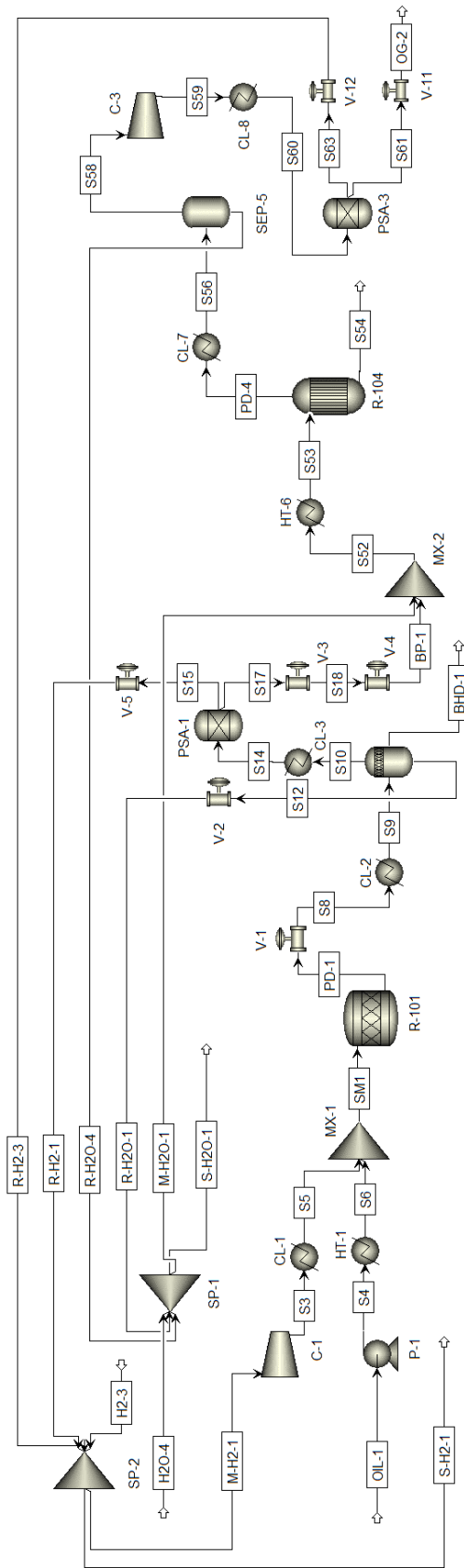


Figure 4.18 Complete process flow diagram of integrated system of hydrotreating and propane steam reforming.



Table 4.11 Unit specification of integrated system of hydrotreating and PSR demonstrated in Figure 4.18.

Name	Model	Equipment	Design specification
C-1	COMPR	Compressor	Isentropic compressor Discharge pressure: 50 bar Efficiency: 0.72
P-1	PUMP	Pump	Discharge pressure: 50 bar Pump efficiency: 0.75
CL-1	HEATER	Cooler	Pressure drop: 0.0 bar Outlet temperature: 300 °C
HT-1	HEATER	Heater	Pressure drop: 0.0 bar Outlet temperature: 300 °C
MX-1	MIXER	Mixer	Pressure drop: 0.0 bar
R-101	RSTOIC	Hydrotreating reactor	Stoichiometry reactor Reaction: Hydrogenation of triolein to tristearin $C_{57}H_{104}O_6 + 3H_2 \rightarrow C_{57}H_{110}O_6$ (2.1) Hydrogenolysis of tripalmitin to palmitic acid $C_{51}H_{98}O_6 + 3H_2 \rightarrow 3C_{15}H_{31}COOH + C_3H_8$ (2.8) Hydrogenolysis of tristearin to stearic acid $C_{57}H_{110}O_6 + 3H_2 \rightarrow 3C_{17}H_{35}COOH + C_3H_8$ (2.9) Decarboxylation of palmitic acid $C_{15}H_{31}COOH \rightarrow C_{15}H_{32} + CO_2$ (2.21)

Table 4.11 Unit specification of integrated system of hydrotreating and PSR demonstrated in Figure 4.18. (Continued).

Name	Model	Equipment	Design specification
R-101 (Continued)	RSTOIC	Hydrotreating reactor	<p>Decarboxylation of stearic acid $C_{17}H_{35}COOH \rightarrow C_{17}H_{36} + CO_2$ (2.22)</p> <p>Hydrodecarbonylation of palmitic acid $C_{15}H_{31}COOH + H_2 \rightarrow C_{15}H_{32} + CO + H_2O$ (2.25)</p> <p>Hydrodecarbonylation of stearic acid $C_{17}H_{35}COOH + H_2 \rightarrow C_{17}H_{36} + CO + H_2O$ (2.26)</p> <p>Hydrodeoxygenation of palmitic acid $C_{15}H_{31}COOH + 3H_2 \rightarrow C_{16}H_{34} + 2H_2O$ (2.32)</p> <p>Hydrodeoxygenation of stearic acid $C_{17}H_{35}COOH + 3H_2 \rightarrow C_{18}H_{38} + 2H_2O$ (2.33)</p> <p>Operating pressure: 50 bar Operating temperature: 300 °C</p>
V-1	VALVE	Valve	Outlet pressure: 30.0 bar
CL-2	HEATER	Cooler	Pressure drop: 0.0 bar Outlet temperature: 117 °C (Tripalmitin feedstock) Outlet temperature: 126 °C (Triolein feedstock)
SEP-1	FLASH3	Separator	Vapor-liquid-liquid phase Pressure drop: 0.0 bar Heat duty: 0.0 MJ/h
V-2	VALVE	Valve	Outlet pressure: 1.0 bar

Table 4.11 Unit specification of integrated system of single-step of hydrotreating and PSR demonstrated in Figure 4.18. (Continued).

Name	Model	Equipment	Design specification
CL-3	HEATER	Cooler	Pressure drop: 0.0 bar Outlet temperature: 30 °C
PSA-1	SEP	Pressure swing adsorption unit	H ₂ split: 90.00% Pressure drop: 0.0 bar
V-3	VALVE	Valve	Outlet pressure: 1.1 bar
V-4	VALVE	Valve	Outlet pressure: 1.0 bar
V-5	VALVE	Valve	Outlet pressure: 1.0 bar
MIX-2	MIXER	Stream mixer	Pressure drop: 0.0 bar
HT-6	HEATER	Heater	Pressure drop: 0.0 bar Outlet temperature: 677 °C
R-104	REQUIL	Propane reformer	Equilibrium reactor Reaction: PSR $C_3H_8 + 3H_2O \rightleftharpoons 3CO + 7H_2$ (2.61)
			Water-gas shift $CO + H_2O \rightleftharpoons CO_2 + H_2$ (2.18)
			Methanation $CO + 3H_2 \rightleftharpoons CH_4 + H_2O$ (2.34)
			$CO_2 + 4H_2 \rightleftharpoons CH_4 + 2H_2O$ (2.35)
			Operating pressure: 1.0 bar

Table 4.11 Unit specification of integrated system of single-step of hydrotreating and PSR demonstrated in Figure 4.18. (Continued).

Name	Model	Equipment	Design specification
R-104 (Continued)	REQUIL	Propane reformer	Operating temperature: 677 °C
CL-5	HEATER	Cooler	Pressure drop: 0.0 bar Outlet temperature: 40 °C
SEP-5	FLASH2	Separator	Vapor-liquid phase Pressure drop: 0.0 bar Heat duty: 0.0 MJ/h
C-3	COMPR	Compressor	Isentropic compressor Discharge pressure: 30 bar Efficiency: 0.72
CL-8	HEATER	Cooler	Pressure drop: 0.0 bar Outlet temperature: 30 °C
PSA-3	SEP	Pressure swing adsorption unit	H ₂ split: 90.0% Pressure drop: 0.0 bar
V-11	VALVE	Valve	Outlet pressure: 1.1 bar
V-12	VALVE	Valve	Outlet pressure: 1.0 bar
SP-1	FSPLIT	Stream splitter	Pressure drop: 0.0 bar Flow split: Flow of H ₂ O requirement
SP-2	FSPLIT	Stream splitter	Pressure drop: 0.0 bar Flow split: Flow of H ₂ requirement

4.4.2 Integrated system of two-step of hydrotreating and glycerol steam reforming

4.4.4.1 Base case condition of integrated system

The base case process design, including bio-hydrogenated diesel fuel production via two-step: hydrolysis of TGs and deoxygenation of FFAs process (Section 4.2.2.2), and hydrogen generation via GSR (Section 4.3.2.2), was simulated. The process flow diagram without recycle is shown in Figure 4.19.

4.4.2.2 Material balance condition of integrated system

The suitable operating condition for two-step is hydrolysis of palm oil at 250 °C of temperature, 50 bar of pressure, and 54.0 of H₂O/oil molar ratio of initial feed water (H₂O-1). The basis is based on 1.0 kmol/h of tripalmitin or triolein as a feedstock. For hydrogenation, deoxygenation of FFAs at 300 °C of temperature, 50 bar of pressure, and 3.0 times of the H₂ stoichiometric requirement was applied in order to provide the complete conversion reaction. For the tripalmitin feedstock and selectivity to decarboxylation of the deoxygenation reaction, the H₂ to tripalmitin ratio of 1.35 is fed initially to prevent catalyst deactivation. For the operating condition of hydrogen generation via GSR at 650 °C of temperature and atmospheric pressure, the glycerol aqueous phase (BP-2) was fed to the reformer with 9.0 of WGMR.

In order to recycle excess hydrogen and excess H₂O and in order to recover energy, the material balance of the process is needed to specify a reactant to be added or to drain the product from the process, in which a stream splitter and a mixer were used. The amount of the H₂ initial feed (H₂-2) varied with the selectivity of deoxygenation reaction pathways.

The processes flow diagram of the integrated system of two-step of hydrotreating and the GSR with recycle are shown in Figure 4.20 and Figure 4.21, respectively. Since, a pair of M-H₂-2 and H₂-2 streams, and a pair of M-H₂O-2 and H₂O-1 streams in Figure 4.20 are equal, they can be connected as summarized in Figure 4.21. The unit specification is shown in Table 4.12.

The splitter (SP-3) was used to split the flow rate of the mixed H₂O stream (S84) as initial feed H₂O (H2O-1) in order to determine the H₂O/oil molar ratio and split excess H₂O (S-H2O-2). The mixed H₂O stream (S84) composed of excess H₂O from unreacted (R-H2O-2), the H₂O by-product of hydrotreating (R-H2O-3), excess H₂O from unreacted (R-H2O-5), and feed H₂O (H2O-5) for the insufficient H₂O case. The H₂O (H2O-5) feed was equal to the H₂O consumption. A cooler (CL-11) was used for condensation of the vapor stream to liquid in order to prepare for recycle of the H₂O stream (M-H2O-2).

The splitter (SP-4) was used to split the flow rate of the mixed H₂ gas stream (M-H2-2) as an initial feed (H2-2) in order to determine the H₂/ oil molar and in order to split excess H₂ (S-H2-2). The mixed H₂ gas stream (M-H2-2) composed of excess H₂ gas from unreacted (R-H2-2), H₂ gas product (R-H2-4), and H₂ make up (H2-4) for the insufficient H₂ case. If hydrogen generation is sufficient for H₂ consumption, H₂ feed is not required.

Design specification with various temperatures and calculator specification of flow rate calculation was reported in APPENDIX E with Table E.4 for HT-5 equipment and Table E.5 and Table E.6 for H2O-5 and H2-4 stream, respectively.

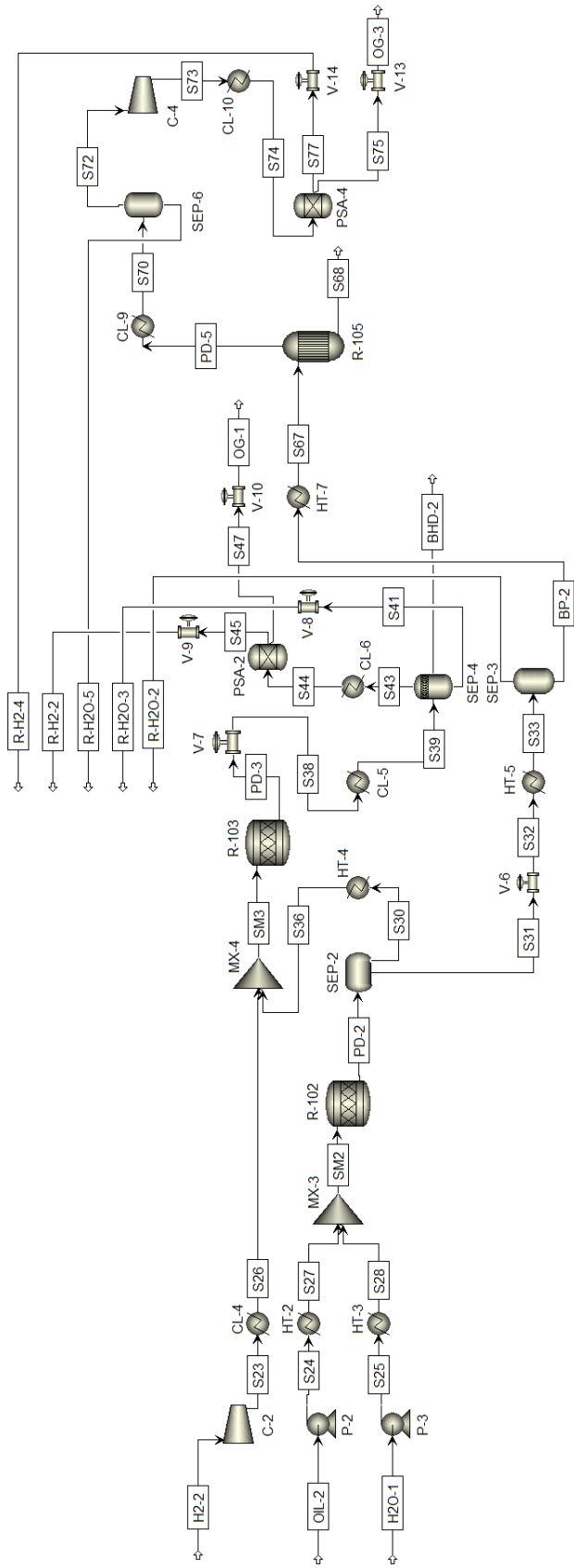


Figure 4.19 Process flow diagram of two-step of hydrotreating and glycerol steam reforming without recycle.

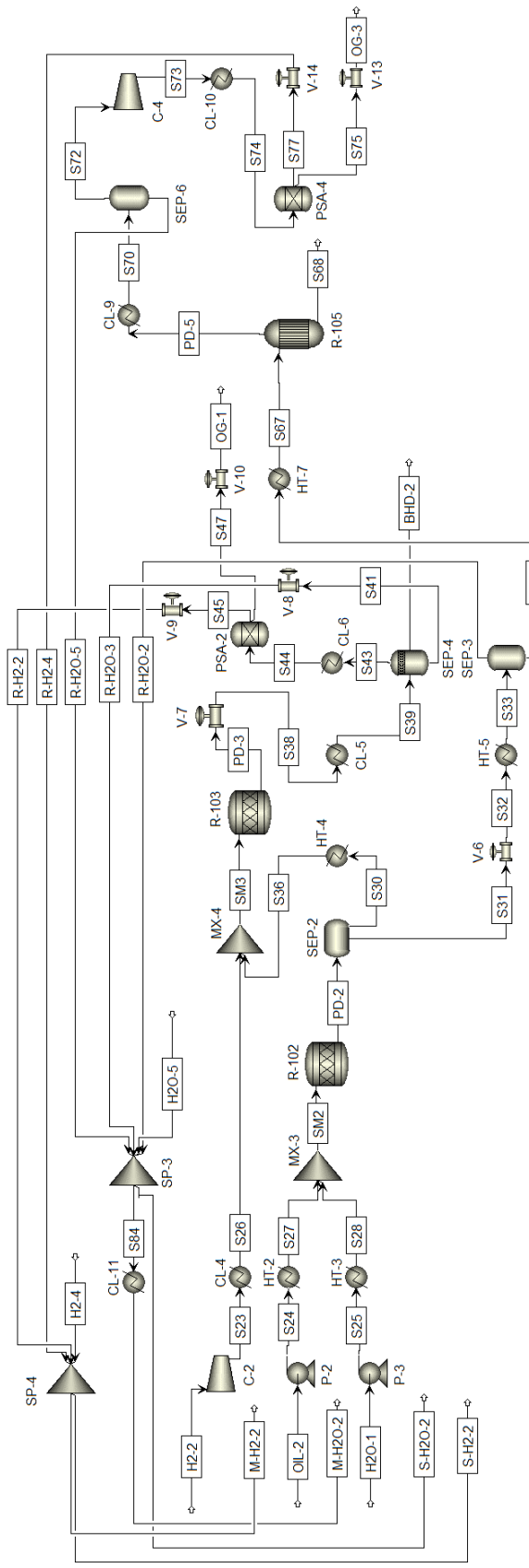


Figure 4.20 Process flow diagram of integrated system of hydrotreating and glycerol steam reforming with recycle consideration.

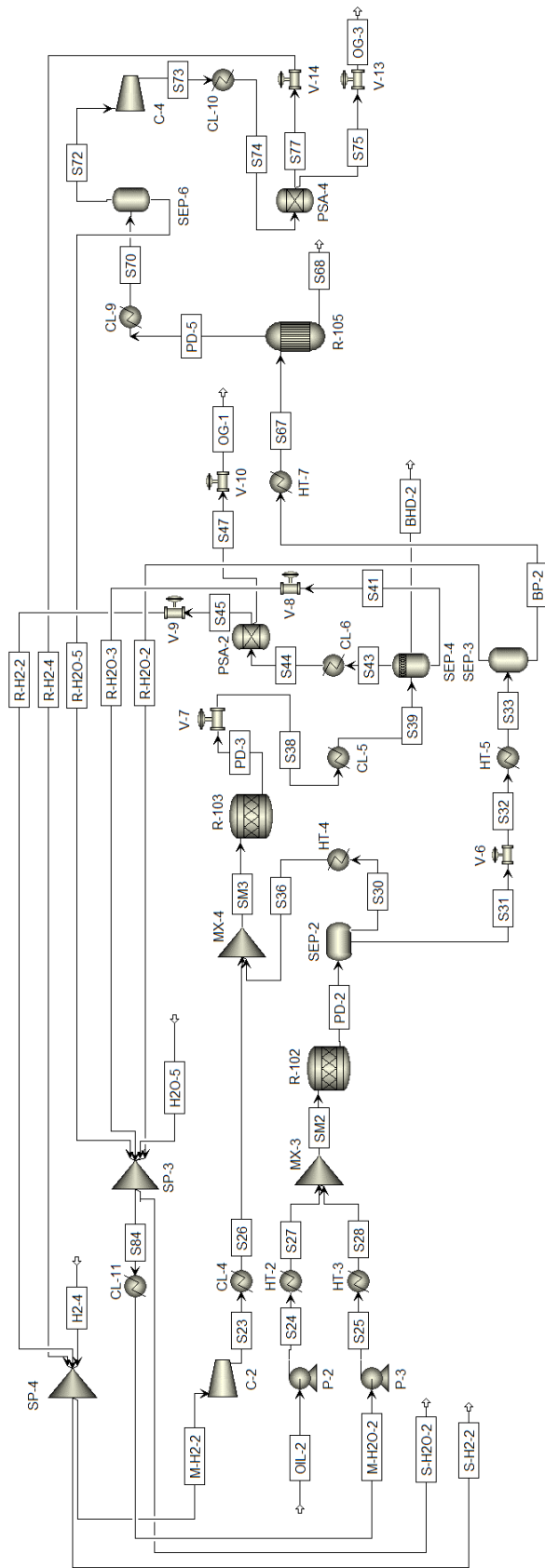


Figure 4.21 Complete process flow diagram of integrated system of hydrotreating and glycerol steam reforming.

Table 4.12 Unit specification of integrated system of two-step of hydrotreating and GSR demonstrated in Figure 4.21.

Name	Model	Equipment	Design specification
C-2	COMPR	Compressor	Isentropic compressor Discharge pressure: 50 bar Efficiency: 0.72
P-2	PUMP	Pump	Discharge pressure: 50 bar Pump efficiency: 0.75
P-3	PUMP	Pump	Discharge pressure: 50 bar Pump efficiency: 0.75
CL-4	HEATER	Cooler	Pressure drop: 0.0 bar Outlet temperature: 300 °C
HT-2	HEATER	Heater	Pressure drop: 0.0 bar Outlet temperature: 250 °C
HT-3	HEATER	Heater	Pressure drop: 0.0 bar Outlet temperature: 250 °C
MX-3	MIXER	Mixer	Pressure drop: 0.0 bar
R-102	RSTOIC	Hydrolysis reactor	Stoichiometry reactor Reaction: Hydrolysis of tripalmitin to palmitic acid $C_{51}H_{98}O_6 + 3H_2O \rightleftharpoons 3C_{15}H_{31}COOH + C_3H_8O_3$ (2.11) Hydrolysis of triolein to oleic acid $C_{57}H_{104}O_6 + 3H_2O \rightleftharpoons 3C_{17}H_{33}COOH + C_3H_8O_3$ (2.13) Operating pressure: 50 bar Operating temperature: 250 °C

Table 4.12 Unit specification of integrated system of two-step of hydrotreating and GSR demonstrated in Figure 4.21. (Continued).

Name	Model	Equipment	Design specification
SEP-2	DECANTER	Separator	Liquid-liquid phase Pressure drop: 0.0 bar Heat duty: 0.0 MJ/h 2 nd liquid phase: Glycerol and water
V-6	VALVE	Valve	Outlet pressure: 1.0 bar
HT-5	HEATER	Heater	Pressure drop: 0.0 bar Outlet temperature: 102.1374 - 102.3615 °C
SEP-3	FLASH2	Separator	Vapor-liquid phase Pressure drop: 0.0 bar Heat duty: 0.0 MJ/h
HT-4	HEATER	Heater	Pressure drop: 0.0 bar Outlet temperature: 300 °C
MX-4	MIXER	Mixer	Pressure drop: 0.0 bar
R-103	RSTOIC	Hydrotreating reactor	Stoichiometry reactor Reaction: Hydrogenation of oleic acid to stearic acid $C_{17}H_{33}COOH + H_2 \rightarrow C_{17}H_{35}COOH$ (2.4) Decarboxylation of palmitic acid $C_{15}H_{31}COOH \rightarrow C_{15}H_{32} + CO_2$ (2.21) Decarboxylation of stearic acid $C_{17}H_{35}COOH \rightarrow C_{17}H_{36} + CO_2$ (2.22)

Table 4.12 Unit specification of integrated system of two-step of hydrotreating and GSR demonstrated in Figure 4.21. (Continued).

Name	Model	Equipment	Design specification
R-103 (Continued)	RSTOIC	Hydrotreating reactor	Hydrodecarbonylation of palmitic acid $C_{15}H_{31}COOH + H_2 \rightarrow C_{15}H_{32} + CO + H_2O$ (2.25)
			Hydrodecarbonylation of stearic acid $C_{17}H_{35}COOH + H_2 \rightarrow C_{17}H_{36} + CO + H_2O$ (2.26)
			Hydrodeoxygenation of palmitic acid $C_{15}H_{31}COOH + 3H_2 \rightarrow C_{16}H_{34} + 2H_2O$ (2.32)
			Hydrodeoxygenation of stearic acid $C_{17}H_{35}COOH + 3H_2 \rightarrow C_{18}H_{38} + 2H_2O$ Operating pressure: 50 bar Operating temperature: 300 °C (2.33)
V-7	VALVE	Valve	Outlet pressure: 30.0 bar
CL-5	HEATER	Cooler	Pressure drop: 0.0 bar Outlet temperature: 40 °C
SEP-4	FLASH3	Separator	Vapor-liquid-liquid phase Pressure drop: 0.0 bar Heat duty: 0.0 MJ/h
V-8	VALVE	Valve	Outlet pressure: 1.0 bar
CL-6	HEATER	Cooler	Pressure drop: 0.0 bar Outlet temperature: 30 °C
PSA-2	SEP	Pressure swing adsorption unit	H ₂ split: 90.00 % Pressure drop: 0.0 bar

Table 4.12 Unit specification of integrated system of two-step of hydrotreating and GSR demonstrated in Figure 4.21. (Continued).

Name	Model	Equipment	Design specification
V-9	VALVE	Valve	Outlet pressure: 1.0 bar
V-10	VALVE	Valve	Outlet pressure: 1.1 bar
HT-7	HEATER	Heater	Pressure drop: 0.0 bar Outlet temperature: 650 °C
R-105	REQUIL	Propane reformer	Equilibrium reactor
			Reaction:
			Glycerol decomposition $C_3H_8O_3 \rightleftharpoons 3CO + 4H_2$ (2.63)
			Water-gas shift $CO + H_2O \rightleftharpoons CO_2 + H_2$ (2.18)
CL-9	HEATER	Cooler	Methanation $CO + 3H_2 \rightleftharpoons CH_4 + H_2O$ (2.34)
			$CO_2 + 4H_2 \rightleftharpoons CH_4 + 2H_2O$ (2.35) Operating pressure: 1.0 bar Operating temperature: 650 °C Pressure drop: 0.0 bar Outlet temperature: 40 °C
SEP-6	FLASH2	Separator	Vapor-liquid phase Pressure drop: 0.0 bar Heat duty: 0.0 MJ/h

Table 4.12 Unit specification of integrated system of two-step of hydrotreating and GSR demonstrated in Figure 4.21. (Continued).

Name	Model	Equipment	Design specification
C-4	COMPR	Compressor	Isentropic compressor Discharge pressure: 30 bar Efficiency: 0.72
CL-10	HEATER	Cooler	Pressure drop: 0.0 bar Outlet temperature: 30 °C
PSA-4	SEP	Pressure swing adsorption unit	H ₂ split: 90.00% Pressure drop: 0.0 bar
V-13	VALVE	Valve	Outlet pressure: 1.0 bar
V-14	VALVE	Valve	Outlet pressure: 1.1 bar
SP-3	FSPLIT	Stream splitter	Pressure drop: 0.0 bar Flow split: Flow of H ₂ O requirement
SP-4	FSPLIT	Stream splitter	Pressure drop: 0.0 bar Flow split: Flow of H ₂ requirement Liquid phase
CL-11	HEATER	Cooler	Pressure drop: 0.0 bar Outlet temperature: 95.5 °C

CHAPTER V RESULTS AND DISCUSSION

The integrated system of hydrotreating and hydrogen generation for bio-hydrogenated diesel fuel production from palm oil with various selectivity of deoxygenation reaction pathways was evaluated on the process performance. The result in terms of net H_2 , energy requirement, electricity requirement, minimum energy requirement, and thermal efficiency were reported. The key performance parameters are considered total minimum energy requirement and total efficiency. However, the integrated system of hydrotreating and hydrogen generation required high energy. Thus, an energy analysis for heat integration is needed for this process.

5.1 Performance evaluation of integrated system of hydrotreating and hydrogen generation

The evaluation result of the integrated system was reported in APPENDIX F. The results of the integrated system of single-step of hydrotreating and PSR with various selectivity of deoxygenation reaction pathways from tripalmitin and triolein are shown in Table F.1 and Table F.2, respectively. The results of the integrated system of two-step of hydrotreating and GSR with various selectivity of deoxygenation reaction pathways from tripalmitin and triolein are shown in Table F.3 and Table F.4, respectively. The performance of the integrated system of hydrotreating and hydrogen generation with deoxygenation reaction pathways from tripalmitin and triolein and the comparative performance of the integrated system among the different deoxygenation reaction pathways using tripalmitin and triolein as feedstock is demonstrated in Table 5.1. The comparative performance of the integrated system among the different deoxygenation reaction pathways using tripalmitin and triolein as feedstock is demonstrated in Table 5.2.

Table 5.1 Performance of integrated system of hydrotreating and hydrogen generation with deoxygenation reaction pathways from tripalmitin and triolein.

Process	Result/ Performance	Integrated system of hydrotreating and hydrogen generation														
		DO selectivity				Integrated system of single-step of hydrotreating and PSR				Integrated system of two-step of hydrotreating and GSR						
		Feedstock		Tripalmitin		Triolein		Tripalmitin		Triolein		Triolein				
		1	0	0	1	0	0	1	0	0	0	1	0	1	0	0
	DCO ₂	0	1	0	0	1	0	0	1	0	0	1	0	0	1	0
	HDCO	0	0	1	0	0	1	0	0	1	0	0	1	0	0	1
	HDO	0	0	1	0	0	1	0	0	1	0	0	1	0	0	1
Hydrotreating	Heating (MJ/h)	510	510	510	323	323	323	323	323	323	323	2,254	2,379	2,228	2,278	2,279
	Cooling (MJ/h)	1,086	1,339	2,418	1,350	1,622	2,711	2,372	2,709	3,589	3,589	2,709	2,830	3,066	4,143	4,143
	Utility (MJ/h)	1,596	1,849	2,929	1,673	1,945	3,033	4,626	5,088	5,817	5,817	4,626	5,109	5,344	6,421	6,421
	Electricity (kW)	70	150	292	136	227	370	14	72	199	199	72	72	136	262	262
Reforming	Heating (MJ/h)	1,248	1,197	1,262	1,369	1,251	1,292	958	958	958	958	958	924	924	924	924
	Cooling (MJ/h)	948	977	980	1,050	1,036	1,023	851	851	851	851	851	830	830	830	830
	Utility (MJ/h)	2,197	2,174	2,242	2,419	2,287	2,315	1,809	1,809	1,809	1,809	1,809	1,754	1,754	1,754	1,754
	Electricity (kW)	68	88	76	76	94	80	50	50	50	50	50	51	51	51	51
Integrated system	(1) Net H ₂ products (kmol/h)	2.31	1.37	-5.39	-0.28	-1.49	-8.35	5.22	1.82	-5.26	1.74	-1.85	-9.04			
	Total heating (MJ/h)	1,759	1,708	1,773	1,692	1,573	1,614	3,212	3,337	3,186	3,203	3,203	3,203	3,203	3,203	3,203
	Total cooling (MJ/h)	2,034	2,316	3,399	2,400	2,658	3,733	3,224	3,560	4,440	3,660	3,660	3,895	4,972	4,972	4,972
	(2) Energy requirement (MJ/h)	3,793	4,024	5,171	4,092	4,232	5,348	6,436	6,897	7,627	6,863	7,098	8,175			
	(3) Electricity requirement (kW)	138	238	368	212	321	450	64	121	248	124	187	313			
	Heating of MER (MJ/h)	361	165	66	335	63	0	1,774	1,632	690	1,328	1,166	186			
	Cooling of MER (MJ/h)	636	773	1,692	1,044	1,147	2,119	1,786	1,856	1,944	1,786	1,857	1,956			
	(4) MER (MJ/h)	997	937	1,758	1,379	1,210	2,119	3,560	3,488	2,634	3,114	3,023	2,142			
	Thermal for Electricity (MJ/h)	1,241	2,143	3,308	1,911	2,886	4,050	575	1,092	2,234	1,112	1,686	2,819			
	Thermal of net H ₂ (MJ/h)	-549	-326	1,281	66	353	1,984	-1,240	-432	1,249	-414	439	2,148			
(5) Total MER (MJ/h)	1,690	2,754	6,347	3,356	4,449	8,153	2,895	4,148	6,117	3,811	5,148	7,108				
(6) Thermal efficiency (%)	96.15	95.36	96.20	95.47	94.62	95.39	96.12	93.37	93.87	96.70	94.16	94.70				
(7) Total efficiency (%)	89.31	86.27	82.51	86.73	84.16	80.95	84.21	80.73	80.95	85.60	82.41	82.86				

Table 5.2 Comparative performance of integrated system among different deoxygenation reaction pathways using tripalmitin and triolein as feedstock.

Process	Result/ Performance	Integrated system of hydrotreating and hydrogen generation					
		Integrated system of single-step of hydrotreating and PSR		Integrated system of two-step of hydrotreating and GSR		Integrated system of two-step of hydrotreating and GSR	
	Feedstock	Tripalmitin	Triolein	Tripalmitin	Triolein	Tripalmitin	Triolein
Integrated system	H ₂ requirement (kmol/h)	HDO>HDCO>DCO ₂	HDO>HDCO>DCO ₂	HDO>HDCO>DCO ₂	HDO>HDCO>DCO ₂	HDO>HDCO>DCO ₂	HDO>HDCO>DCO ₂
	H ₂ generation (kmol/h)	HDCO>HDO>DCO ₂	HDCO>HDO>DCO ₂	HDCO>HDCO>DCO ₂	HDCO>HDCO>DCO ₂	HDO=HDCO=DCO ₂	HDO=HDCO=DCO ₂
	(1) Net H ₂ products (kmol/h)	DCO ₂ >HDCO>HDO	DCO ₂ >HDCO>HDO	DCO ₂ >HDCO>HDO	DCO ₂ >HDCO>HDO	DCO ₂ >HDCO>HDO	DCO ₂ >HDCO>HDO
	HT-6 (MJ/h)	HDCO>DCO ₂ >HDO	HDCO>DCO ₂ >HDO	HDCO>DCO ₂ >HDO	HDCO>DCO ₂ >HDO	-	-
	R-104 (MJ/h)	HDO>DCO ₂ >HDCO	HDO>DCO ₂ >HDCO	HDO>DCO ₂ >HDCO	HDO>DCO ₂ >HDCO	-	-
	R-103 (MJ/h)	-	-	HDCO>DCO ₂	HDCO>DCO ₂	-	-
	Heating utility (MJ/h)	HDO>DCO ₂ >HDCO	HDO>DCO ₂ >HDCO	DCO ₂ >HDO>HDCO	DCO ₂ >HDO>HDCO	HDCO=DCO ₂ =HDO	HDCO=DCO ₂ =HDO
	CL-1 (MJ/h)	HDO>HDCO>DCO ₂	HDO>HDCO>DCO ₂	HDO>HDCO>DCO ₂	HDO>HDCO>DCO ₂	-	-
	R-101 (MJ/h)	HDO>DCO ₂ >HDCO	HDO>DCO ₂ >HDCO	HDO>DCO ₂ >HDCO	HDO>DCO ₂ >HDCO	-	-
	CL-4 (MJ/h)	-	-	-	HDO>HDCO>DCO ₂	HDO>HDCO>DCO ₂	HDO>HDCO>DCO ₂
	R-103 (MJ/h)	-	-	-	HDO	HDO	HDO>DCO ₂ >HDCO
	Cooling utility (MJ/h)	HDO>HDCO>DCO ₂	HDO>HDCO>DCO ₂	HDO>HDCO>DCO ₂	HDO>HDCO>DCO ₂	HDO>HDCO>DCO ₂	HDO>HDCO>DCO ₂
	(2) Energy requirement (MJ/h)	HDO>HDCO>DCO ₂	HDO>HDCO>DCO ₂	HDO>HDCO>DCO ₂	HDO>HDCO>DCO ₂	HDO>HDCO>DCO ₂	HDO>HDCO>DCO ₂
	(3) Electricity requirement (kW)	HDO>HDCO>DCO ₂	HDO>HDCO>DCO ₂	HDO>HDCO>DCO ₂	HDO>HDCO>DCO ₂	HDO>HDCO>DCO ₂	HDO>HDCO>DCO ₂
	Heating of MER (MJ/h)	DCO ₂ >HDCO>HDO	DCO ₂ >HDCO>HDO	DCO ₂ >HDCO>HDO	DCO ₂ >HDCO>HDO	DCO ₂ >HDCO>HDO	DCO ₂ >HDCO>HDO
	Cooling of MER (MJ/h)	HDO>HDCO>DCO ₂	HDO>HDCO>DCO ₂	HDO>HDCO>DCO ₂	HDO>HDCO>DCO ₂	HDO>HDCO>DCO ₂	HDO>HDCO>DCO ₂
	(4) MER (MJ/h)	HDO>DCO ₂ >HDCO	HDO>DCO ₂ >HDCO	HDO>DCO ₂ >HDCO	HDO>DCO ₂ >HDCO	DCO ₂ >HDCO>HDO	DCO ₂ >HDCO>HDO
(5) Total MER (MJ/h)	HDO>HDCO>DCO ₂	HDO>HDCO>DCO ₂	HDO>HDCO>DCO ₂	HDO>HDCO>DCO ₂	HDO>HDCO>DCO ₂	HDO>HDCO>DCO ₂	
(6) Thermal efficiency (%)	HDO>DCO ₂ >HDCO	HDO>DCO ₂ >HDCO	DCO ₂ >HDO>HDCO	DCO ₂ >HDO>HDCO	DCO ₂ >HDO>HDCO	DCO ₂ >HDO>HDCO	
(7) Total efficiency (%)	DCO ₂ >HDCO>HDO	DCO ₂ >HDCO>HDO	DCO ₂ >HDCO>HDO	DCO ₂ >HDCO>HDO	DCO ₂ >HDCO>HDCO	DCO ₂ >HDCO>HDCO	

5.1.1 Net H₂ of integrated system

Studies of H₂ consumption and H₂ generation were performed in order to obtain net H₂ of the integrated system. Various selectivity of deoxygenation reaction pathways provided different amount of H₂ consumption, gas products, C₁₅ and C₁₆ or C₁₇ and C₁₈. However, the performance of the integrated system was considered from sufficient hydrogen generation for H₂ consumption as the integrated system is considered sustaining without an external support of H₂ which included performance hydrocarbon products generation. Net H₂ was calculated from Equations 5.1 and 5.2.

$$\text{Net H}_2 \text{ (kmol/h)} = \text{H}_2 \text{ generation} - \text{H}_2 \text{ consumption} \quad (5.1)$$

$$\text{Net H}_2 \text{ (kmol/h)} = \text{H}_2 \text{ generation} - (\text{Initial feed H}_2 - \text{Excess H}_2) \quad (5.2)$$

Values of net H₂ of the integrated system of single-step of hydrotreating and PSR with various selectivity of deoxygenation reaction pathways (DCO₂: HDCO: HDO) from tripalmitin and triolein are presented in Figure 5.1 (a) and (b), respectively, and the values for two-step of hydrotreating and GSR from tripalmitin and triolein are presented in Figure 5.1 (c) and (d), respectively. The result of net H₂ is more than or equal to zero kmol/h, indicating the performance of the integrated system which hydrogen generation being sufficient for H₂ consumption.

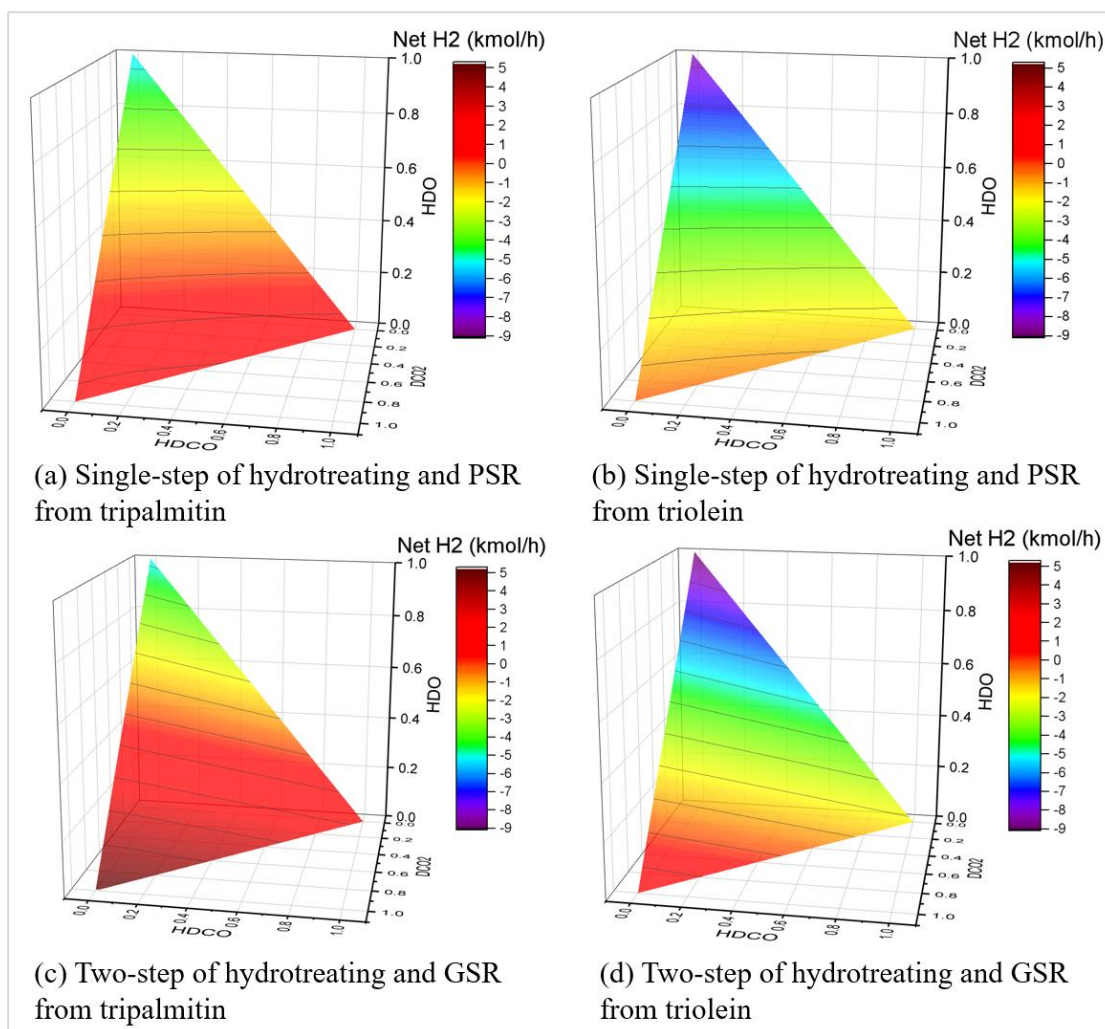


Figure 5.1 Net H_2 of integrated system with various selectivity of deoxygenation reaction pathways. Single-step of hydrotreating and PSR from (a) tripalmitin and (b) triolein. Two-step of hydrotreating and GSR from (c) tripalmitin and (d) triolein.

5.1.1.1 Net H_2 of integrated system of single-step of hydrotreating and propane steam reforming

H_2 consumption of tripalmitin consisted of hydrogenolysis 3.0 kmol/h and deoxygenation reaction: HDCO 1.0 kmol/h and HDO 3.0 kmol/h of palmitic acid. But H_2 consumption of triolein consisted of hydrogenation 3.0 kmol/h, hydrogenolysis of tristearin 3.0 kmol/h and deoxygenation reaction: HDCO 1.0 kmol/h and HDO 3.0 kmol/h of stearic acid per the stoichiometric requirement of each reaction.

When the Deoxygenation is via DCO_2 a 100% (selectivity of $DCO_2 = 1$), there is no H_2 consumption of DO, but 3.0 kmol/h of H_2 was consumed for hydrogenolysis

of tripalmitin and 6.0 kmol/h of H_2 was consumed for hydrogenation and hydrogenolysis of triolein.

For HDCO selectivity of DO equal 1, 6.0 kmol/h of H_2 was consumed for tripalmitin and 9.0 kmol/h was consumed for triolein, which increased from the DCO_2 pathway. Furthermore, the amount of H_2 consumption increased with increasing HDO selectivity of deoxygenation reaction pathways, and the highest amount of H_2 consumption was when HDO selectivity of DO equaled 1 with 12.0 kmol/h for tripalmitin and 15.0 kmol/h for triolein.

A complete hydrogenolysis reaction produced 1.0 kmol/h of propane as a by-product. Since, various deoxygenation reaction pathways provided different gas product composition. Only H_2 was separated from the gas product and recycle to hydrotreating process, while the rest of gas product including propane, CO, CO_2 and small content of H_2O and H_2 . The rest of gas product was fed to reformer (R-104), therefore the composition of gas product affects to the reaction in the reformer (R-104). For hydrogen generation of various deoxygenation reaction pathways from the propane reformer (R-104), DCO_2 selectivity of DO equal 1 generated the lowest amount of H_2 because the by-product of the DCO_2 pathway was CO_2 , which high CO_2 content leads to the reverse water gas shift reaction, causing H_2 consumption in the reformer (R-104).

The HDCO selectivity of DO equal 1 generated the highest amount of H_2 because the by-product of the HDCO pathway was CO and H_2O , which leads to the water gas shift reaction, causing H_2 generation.

For HDO selectivity of DO equal 1, the generated amount of H_2 was more than the DCO_2 pathway, but the generated amount of H_2 was lower than the HDCO pathway, because the by-product of the HDO pathway was only H_2O , no CO_2 , which was caused H_2 consumption, and no CO, which was caused H_2 generation.

For the tripalmitin feedstock shown in Figure 5.1 (a), the highest of net H_2 equals 2.31 kmol/h for DCO_2 , the lowest of net H_2 equals -5.39 kmol/h for HDO, and for HDCO, net H_2 equals 1.37 kmol/h with H_2 generation of 7.53, 8.37, and 9.54 moles per unit mole of propane, respectively.

For triolein feedstock shown in Figure 5.1 (b), the highest of net H_2 equals -0.28 kmol/h for DCO_2 , the lowest of net H_2 equals -8.35 kmol/h for HDO, and for HDCO, net H_2 equals -1.49 kmol/h with H_2 generation of 7.49, 8.31 and 9.41 moles per unit mole of propane, respectively. Thus, there is no case for H_2 sufficient, and H_2 feeding is required for this integrated system. Furthermore, the amount of net H_2 decreased from tripalmitin to triolein, due to required H_2 for hydrogenation of the triolein feedstock.

By the most likely HDO reaction pathway that makes hydrogen generation sufficient for H_2 consumption to provide BHD, most of C_{16} hydrocarbon products from tripalmitin and C_{18} hydrocarbon products from triolein, in which hydrocarbon contains more carbon, will provide more heating value of products, but the value is slightly different. BHD (BHD-1) obtained from tripalmitin contains $C_{15}H_{32}$ and $C_{16}H_{34}$ of approximately 3.00 kmol/h and 97.48 - 99.37 wt.% of product purity. BHD (BHD-1) obtained from triolein contains $C_{17}H_{36}$ and $C_{18}H_{38}$ of approximately 3.00 kmol/h and 98.62 - 99.54 wt.% of product purity. The off-gas (OG-2) such as CO_2 and CO are combusted by a flare. Excess hydrogen and excess H_2O were recycled into the process.

5.1.1.2 Net H_2 of integrated system of two-step of hydrotreating and glycerol steam reforming

H_2O is consumed for hydrolysis of tripalmitin and triolein to palmitic acid and oleic acid, respectively. H_2 consumption of palmitic acid consists of deoxygenation reaction: HDCO 1.0 kmol/h and HDO 3.0 kmol/h. But H_2 consumption of oleic acid consists of hydrogenation 1.0 kmol/h and deoxygenation reaction: HDCO 1.0 kmol/h and HDO 3.0 kmol/h of stearic acid per the stoichiometric requirement of each reaction.

For DCO_2 selectivity of DO equals 1, there is no H_2 consumption of DO from both tripalmitin and triolein. But 3.0 kmol/h of H_2 was consumed for hydrogenation of the triolein feedstock.

For HDCO selectivity of DO equals 1, H_2 consumption for tripalmitin was 3.0 kmol/h and 6.0 kmol/h for triolein, which increased from DCO_2 pathway.

Furthermore, the amount of H_2 consumption increased with increasing HDO selectivity of deoxygenation reaction pathways and the highest amount of H_2 consumption was when HDO selectivity of DO equaled 1 with 9.0 kmol/h for the tripalmitin feedstock and 12.0 kmol/h for the triolein feedstock.

The glycerol by-product was produced from hydrolysis reaction of 1.0 kmol/h with complete conversion. For hydrogen generation (R-H2-4) of various deoxygenation reaction pathways from the glycerol reformer, 5.38 kmol/h (H_2 generation of 5.98 moles per unit mole of glycerol) can be achieved for both tripalmitin and triolein feedstocks.

For the tripalmitin feedstock shown in Figure 5.1 (c), the highest of net H_2 equals 5.22 kmol/h for DCO_2 , the lowest of net H_2 equals -5.26 kmol/h for HDO and HDCO, and net H_2 equals 1.82 kmol/h.

For the triolein feedstock shown in Figure 5.1 (d), the highest of net H_2 equals 1.74 kmol/h for DCO_2 , the lowest of net H_2 equals -9.04 kmol/h for HDO and HDCO, and net H_2 equals -1.85 kmol/h. Furthermore, the amount of net H_2 decreases from tripalmitin to triolein, due to required H_2 for hydrogenation of oleic acid.

BHD (BHD-2) obtained from tripalmitin contains $C_{15}H_{32}$ and $C_{16}H_{34}$ of approximately 2.92 kmol/h and 95.04 - 99.97 wt.% of product purity. BHD (BHD-2) obtained from triolein contains $C_{17}H_{36}$ and $C_{18}H_{38}$ of approximately 2.99 kmol/h and 97.82 - 99.97 wt.% of product purity. The off-gas (OG-1 and OG-3) such as CO_2 and CO are combusted by a flare. Excess hydrogen and excess H_2O were recycled into the process.

The H_2 flow rates for each of net H_2 of the integrated system of single-step of hydrotreating and PSR with selectivity of deoxygenation reaction pathways from tripalmitin and triolein are presented in Figure 5.2 (a) and (b), respectively. The H_2 flow rates for two-step of hydrotreating and GSR from tripalmitin and triolein are presented in Figure 5.2 (c) and (d), respectively.

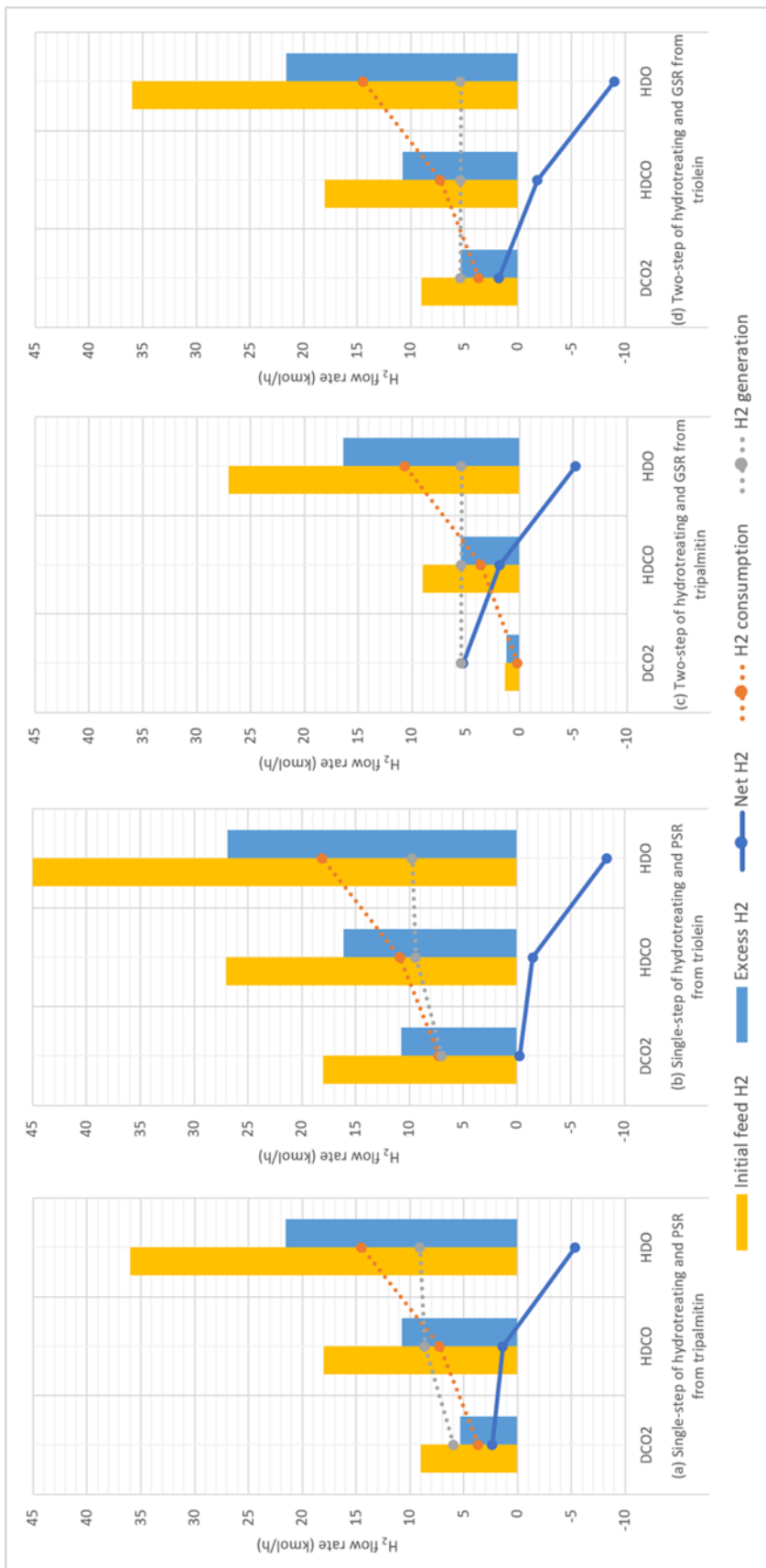


Figure 5.2 H₂ flow rate for each of net H₂ of integrated system with selectivity of deoxygenation reaction pathways. Single-step of hydrotreating and PSR from (a) tripalmitin and (b) triolein. Two-step of hydrotreating and GSR from (c) tripalmitin and (d) triolein.

5.1.2 Energy requirement of integrated system

Heating utility and cooling utility are considered for energy requirement of the integrated system. The energy requirements of the integrated system of single-step of hydrotreating and PSR with various selectivity of deoxygenation reaction pathways (DCO₂: HDCO: HDO) from tripalmitin and triolein are presented in Figure 5.3 (a) and (b), respectively, and for two-step of hydrotreating and GSR from tripalmitin and triolein the energy requirements are presented in Figure 5.3 (c) and (d), respectively.

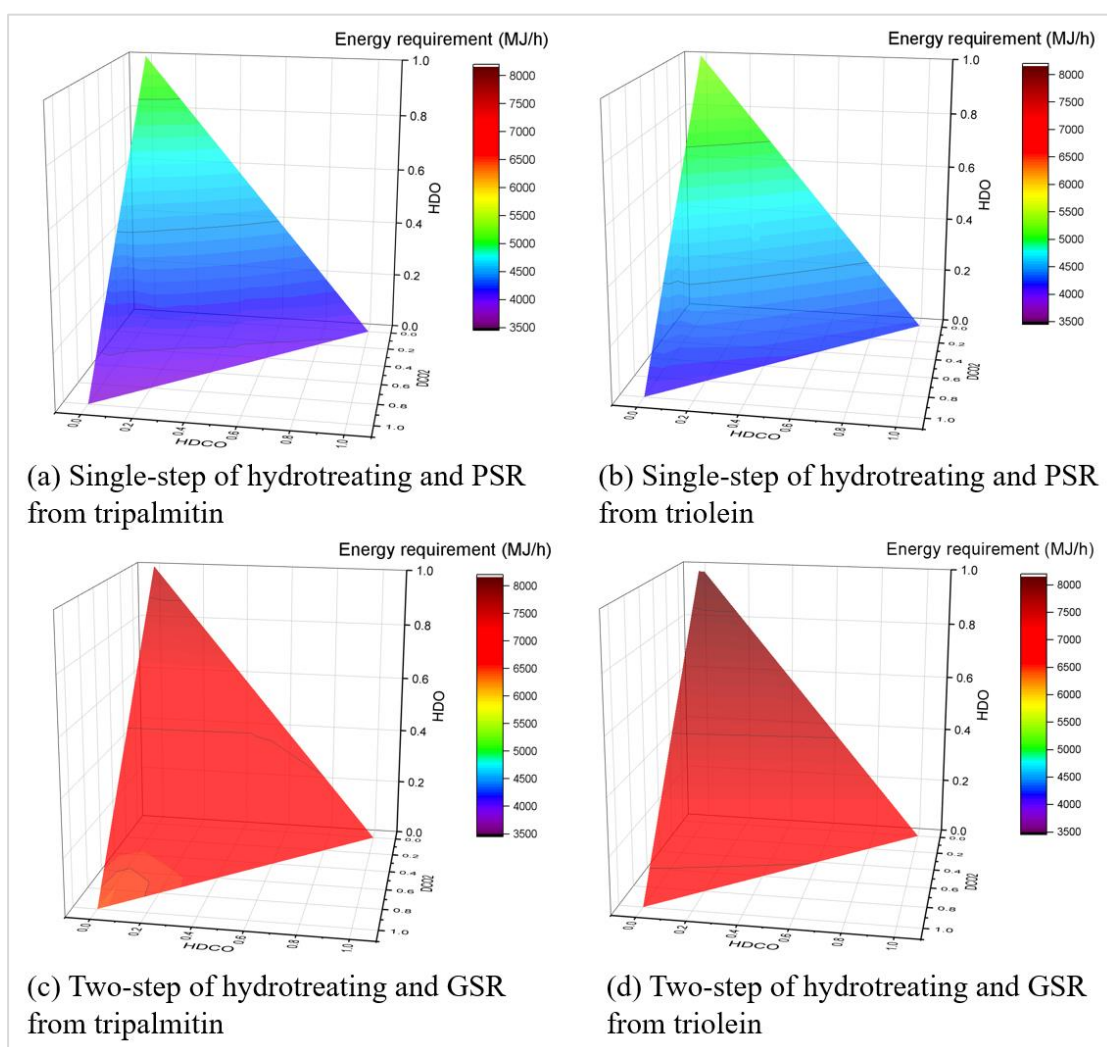


Figure 5.3 Energy requirement of integrated system with various selectivity of deoxygenation reaction pathways. Single-step of hydrotreating and PSR from (a) tripalmitin and (b) triolein. Two-step of hydrotreating and GSR from (c) tripalmitin and (d) triolein.

5.1.2.1 Energy requirement of integrated system of single-step of hydrotreating and propane steam reforming

The energy requirement for each equipment of the integrated system of single-step of hydrotreating and PSR with selectivity of deoxygenation reaction pathways from tripalmitin and triolein is shown in Figure 5.4.

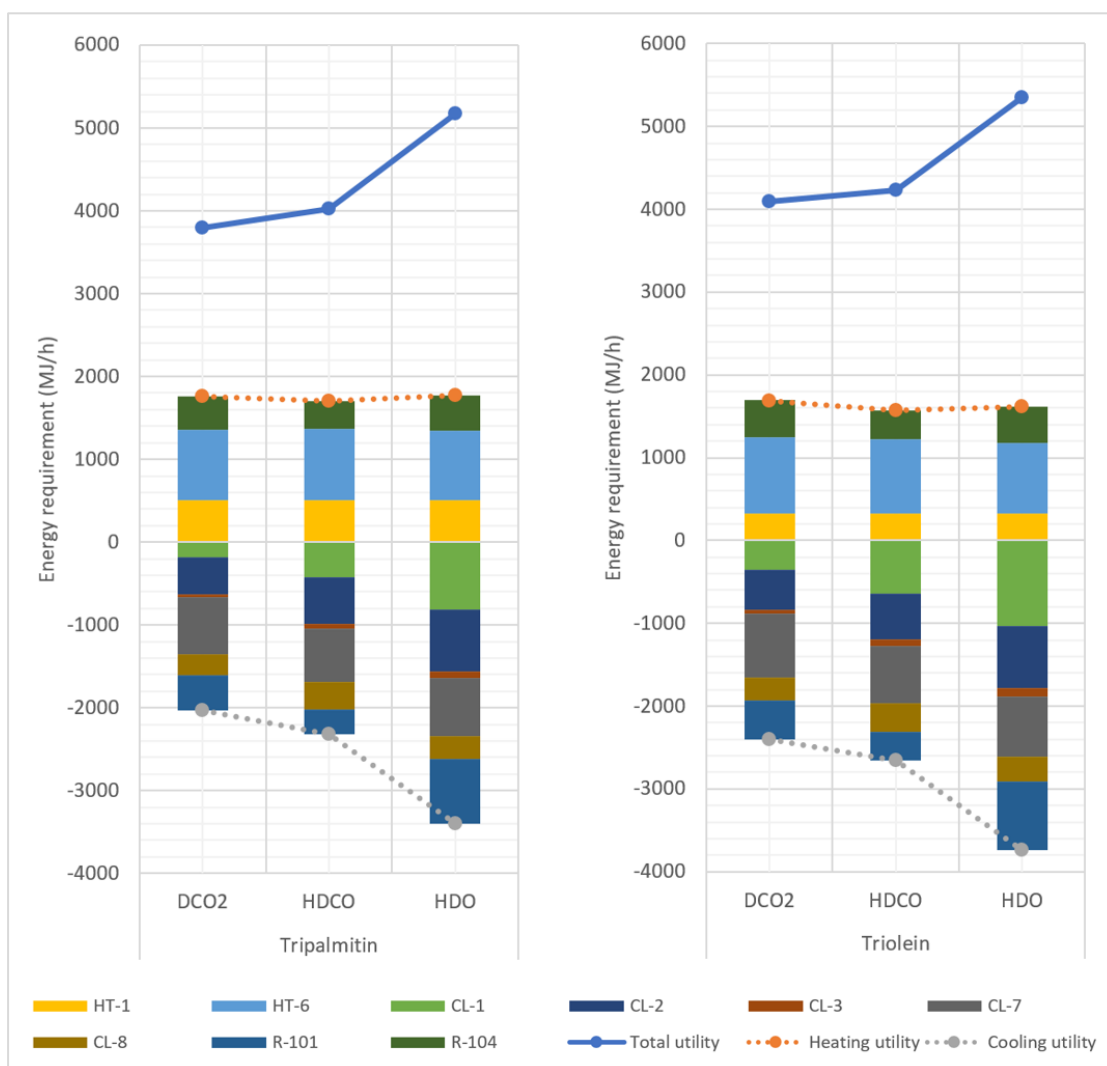


Figure 5.4 Energy requirement for each equipment of integrated system of single-step of hydrotreating and PSR with selectivity of deoxygenation reaction pathways from tripalmitin and triolein.

Heating utility was supported to heat palm oil to reaction temperature (HT-1), to heat the reactant to reaction temperature (HT-6), and to the reformer (R-104).

For the triolein feedstock, the highest heating utility was used for DCO₂, HDO, and HDCO, respectively. Because PSR is an endothermic reaction, water gas shift is an exothermic reaction, and methanation is an exothermic reaction. As a result, the HDCO pathway can generate the highest H₂ equal to 9.54 and 9.41 moles of H₂ per unit mole of propane from tripalmitin and triolein, respectively. The HDCO pathway produces H₂O and CO by-products in the hydrotreating reactor (R-101), and the CO by-product reacted to water gas shift of PSR in the reformer (R-104). Then, the reformer (R-104) of the HDCO pathway required the lowest heat duty. The DCO₂ pathway required the highest heat duty because the CO₂ by-product from hydrotreating process reacted to reverse water gas shift, which is an endothermic reaction. Also, methane (CH₄) was produced from methanation with the lowest from DCO₂, HDO, and HDCO pathways, respectively. The amount of H₂O (H₂O-4) of the integrated system affects the heater (HT-6), with DCO₂ pathway requiring more heat duty than HDCO and HDO, respectively because both HDO and HDCO pathways produced the H₂O by-product, but the HDO pathway produced more H₂O.

For the tripalmitin feedstock, the highest heating utility was used for HDO, DCO₂, and HDCO, respectively. Following the analysis results above, the HDCO pathway required the lowest heat duty, but because 0.80 kmol/h of the lowest of the propane by-product (propane was produced at 1 kmol/h) with the DCO₂ pathway was fed into the reformer (R-104), this affects PSR to require lower heat duty than the HDO pathway with 0.92 kmol/h of the propane by-product.

Cooling utility was supported to cool H₂ to reaction temperature (CL-1), to cool the product mixture from the hydrotreating reactor before being fed to phase separation (CL-2), to cool mixture gas before being fed to the PSA unit (CL-3) and (CL-8), to cool the mixture gas products from the reformer before being fed to the phase separation unit (CL-7), and to palm oil conversion to various products in the multiple bed reactor (R-101). The main contributions of cooling utility are CL-1 and R-101. For R-101, the highest cooling utility was used for HDO, HDCO, and DCO₂, respectively, because hydrogenolysis is an exothermic reaction, HDO is an exothermic reaction, HDCO is an endothermic reaction, and DCO₂ is slightly endothermic reaction. Then, the hydrotreating reactor (R-101) of the HDO pathway

required the highest cooling duty and the DCO₂ pathway required more cooling duty than the HDCO pathway. For CL-1, the cooling utility depending on the amount of H₂ required for the reaction. The HDCO pathway required more H₂ than the DCO₂ pathway, the HDO pathway required the highest H₂ which affects the cooling duty of the cooler (CL-1). Thus, the cooling utility for the HDCO pathway is more than that of the DCO₂ pathway and the HDO pathway requires the highest cooling utility. Thus CL-1 of HDO > HDCO > DCO₂.

For the tripalmitin feedstock shown in Figure 5.3 (a), the highest energy requirement equals 5,171 MJ/h for HDO; the lowest energy requirement equals 3,793 MJ/h for DCO₂; and for HDCO, the energy requirement equals 4,024 MJ/h.

For the triolein feedstock shown in Figure 5.3 (b), the highest energy requirement equals 5,348 MJ/h for HDO; the lowest energy requirement equals 4,092 MJ/h for DCO₂; and for HDCO, the energy requirement equals 4,232 MJ/h.

5.1.2.2 Energy requirement of integrated system of two-step of hydrotreating and glycerol steam reforming

The energy requirement for each equipment of the integrated system of two-step of hydrotreating and GSR with selectivity of deoxygenation reaction pathways from tripalmitin and triolein is shown in Figure 5.5.

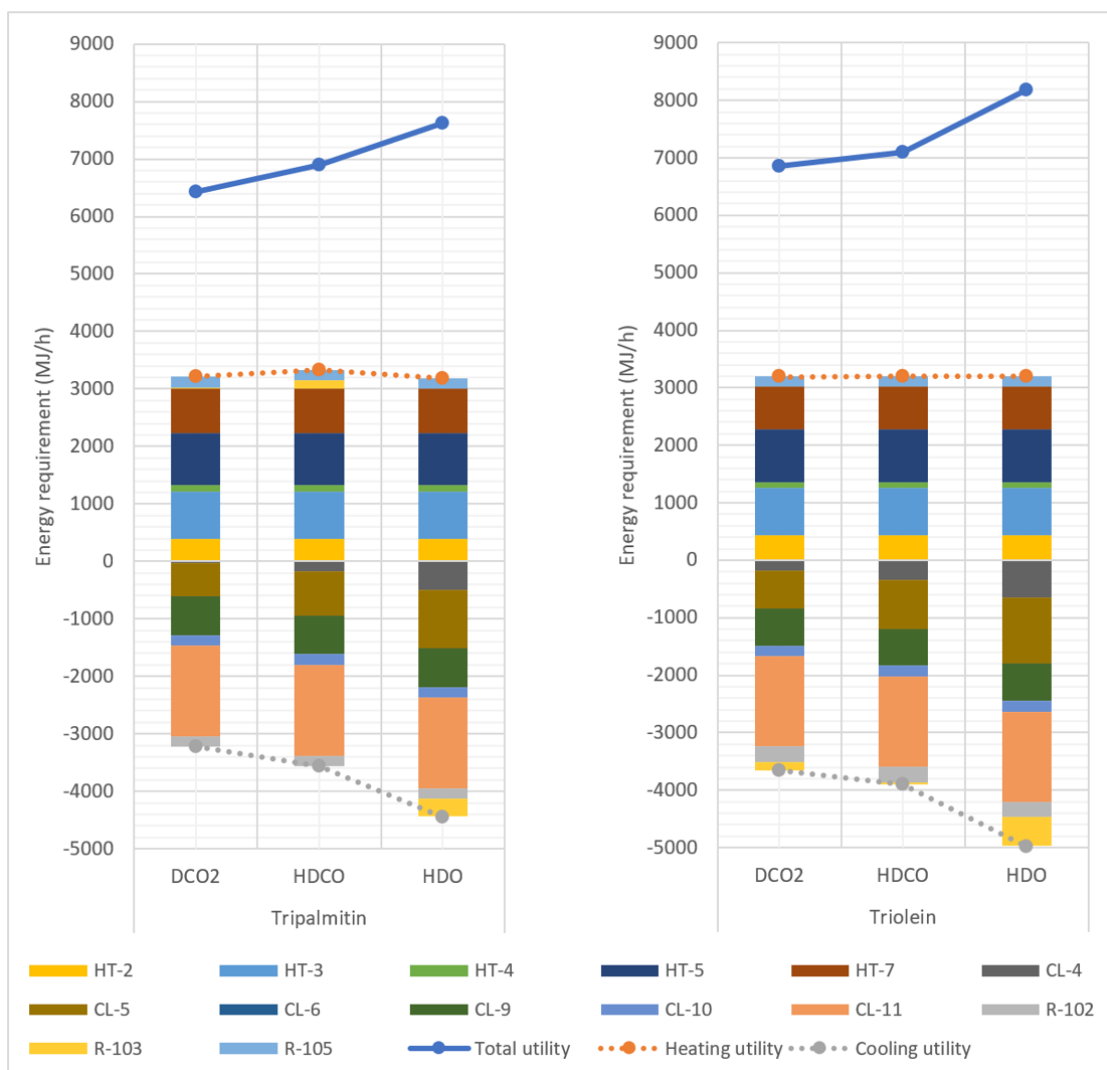


Figure 5.5 Energy requirement for each equipment of integrated system of two-step of hydrotreating and GSR with selectivity of deoxygenation reaction pathways from tripalmitin and triolein.

Heating utility was supported to heat palm oil to reaction temperature (HT-2), to heat water to reaction temperature (HT-3), to heat oil phase to reaction temperature (HT-4), to vaporize the glycerol aqueous phase from decanter before being fed to the phase separation unit (HT-5), to heat reactant to reaction temperature (HT-7), and to the reformer (R-105).

For tripalmitin, the highest heating utility was used for HDCO, DCO₂, and HDO, respectively. Because inside the hydrotreating reactor (R-103), only the deoxygenation reaction of palmitic acid occurred and the pathway of DO consists of HDO, which is an exothermic reaction, HDCO, which is an endothermic reaction, and

DCO₂, which is slightly endothermic reaction, then, the HDCO pathway of palmitic acid converting to various products in the multiple bed reactor (R-103) required more heat duty than the DCO₂ pathway, and for the HDO pathway, cooling duty is required.

For triolein, heating utility was used equally for each of the reaction pathway. Because hydrogenation of oleic acid occurred in the hydrotreating reactor (R-103), which is a highly exothermic reaction and deoxygenation reaction of stearic acid, then, the hydrotreating reactor (R-103) required cooling duty.

Cooling utility was supported to cool H₂ to reaction temperature (CL-4), to cool the product mixture from the hydrotreating reactor before being fed to phase separation (CL-5), to cool mixture gas before being fed to the PSA unit (CL-6) and (CL-10), to cool the mixture gas products from the reformer before being fed to the phase separation unit (CL-9), to condense partial steam to liquid water before being fed to the pump (CL-11), and to convert palm oil to FFAs and glycerol. For both feedstocks, the highest cooling utility was used for HDO, HDCO, and DCO₂, respectively. The HDO reaction is highly exothermic reaction. However, the HDCO pathway required more H₂ than the DCO₂ pathway, which affects the cooling duty of the cooler (CL-4). Then, cooling utility for the HDCO pathway is more than that of the DCO₂ pathway.

For the tripalmitin feedstock shown in Figure 5.3 (c), the highest energy requirement equals 7,627 MJ/h for HDO; the lowest energy requirement equals 6,436 MJ/h for DCO₂; and for HDCO, the energy requirement equals 6,897 MJ/h.

For the triolein feedstock shown in Figure 5.3 (d), the highest energy requirement equals 8,175 MJ/h for HDO; the lowest energy requirement equals 6,863 MJ/h for DCO₂; and for HDCO, the energy requirement equals 7,098 MJ/h.

Thus, triolein required more energy requirement than tripalmitin for both of the integrated systems.

5.1.3 Electricity requirement of integrated system

The electricity requirement of the integrated system of single-step of hydrotreating and PSR with various selectivity of deoxygenation reaction pathways

(DCO₂: HDCO: HDO) from tripalmitin and triolein is presented in Figure 5.6 (a) and (b), respectively, and the electricity requirement for two-step of hydrotreating and GSR from tripalmitin and triolein is presented in Figure 5.6 (c) and (d), respectively.

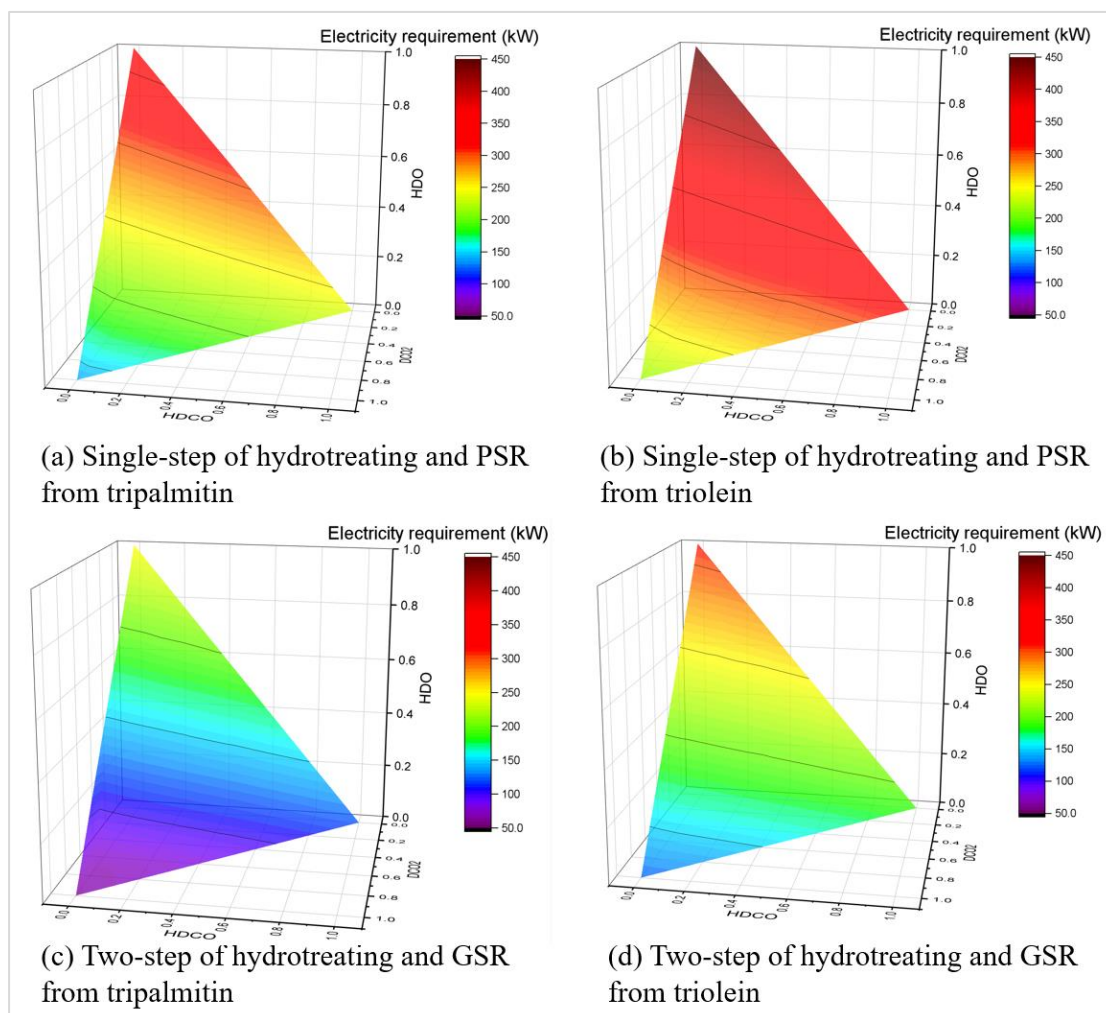


Figure 5.6 Electricity requirement of integrated system with various selectivity of deoxygenation reaction pathways. Single-step of hydrotreating and PSR from (a) tripalmitin and (b) triolein. Two-step of hydrotreating and GSR from (c) tripalmitin and (d) triolein.

5.1.3.1 Electricity requirement of integrated system of single-step of hydrotreating and propane steam reforming

The electricity requirement for each equipment of the integrated system of single-step of hydrotreating and PSR with selectivity of deoxygenation reaction pathways from tripalmitin and triolein is shown in Figure 5.7.

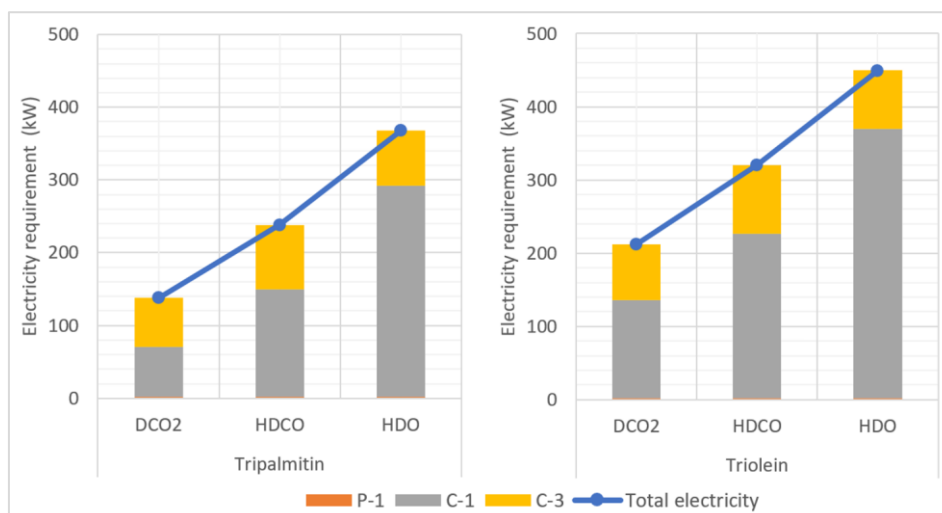


Figure 5.7 Electricity requirement for each equipment of integrated system of single-step of hydrotreating and PSR with selectivity of deoxygenation reaction pathways from tripalmitin and triolein.

Electricity was supported to pump palm oil to destination pressure (P-1), to adjust H₂ pressure before heating (C-1), and to adjust gas pressure before being fed to the PSA unit (C-3). The highest electricity requirement was for HDO, HDCO, and DCO₂, respectively, for both tripalmitin and triolein feedstocks, because the process needs to compress H₂ to reaction pressure, because the HDO pathway required the highest H₂, and because the HDCO pathway required more H₂ than the DCO₂ pathway.

For the tripalmitin feedstock shown in Figure 5.6 (a), the highest electricity requirement equals 368 MW for HDO; the lowest electricity requirement equals 138 MW for DCO₂; and for HDCO, the electricity requirement equals 238 MW.

For the triolein feedstock shown in Figure 5.6 (b), the highest electricity requirement equals 450 MW for HDO, the lowest electricity requirement equals 212 MW for DCO₂; and for HDCO, the electricity requirement equals 321 MJ/h.

5.1.3.2 Electricity requirement of integrated system of two-step of hydrotreating and glycerol steam reforming

The electricity requirement for each equipment of the integrated system of two-step of hydrotreating and GSR with selectivity of deoxygenation reaction pathways from tripalmitin and triolein is shown in Figure 5.8.

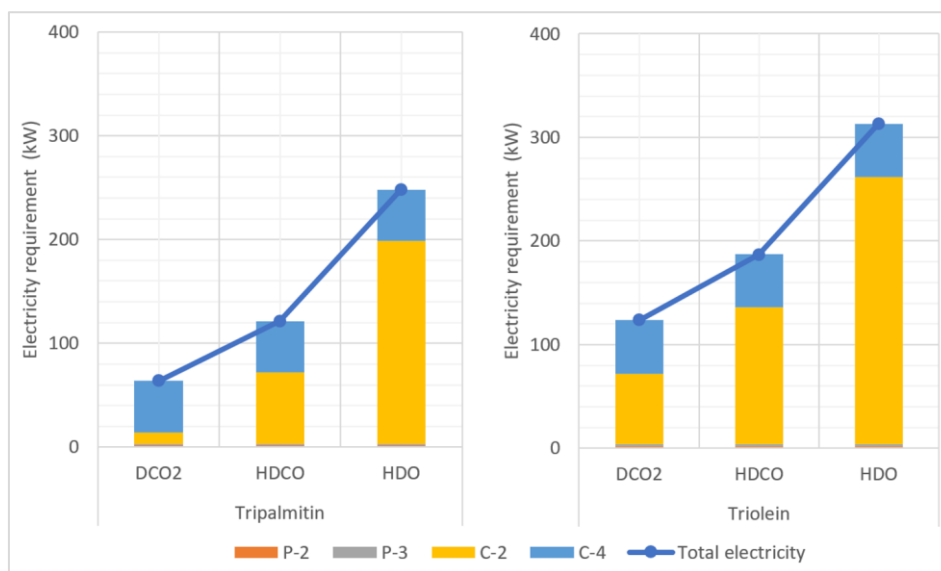


Figure 5.8 Electricity requirement for each equipment of integrated system of two-step of hydrotreating and GSR with selectivity of deoxygenation reaction pathways from tripalmitin and triolein.

Electricity was supported to pump palm oil to destination pressure (P-2), to pump water to destination pressure (P-3), to adjust H₂ pressure before heating (C-2), and to adjust gas pressure before being fed to the PSA unit (C-4). The highest electricity requirement was for HDO, HDCO, and DCO₂, respectively, for both tripalmitin and triolein feedstocks, following Section 5.1.3.1.

For the tripalmitin feedstock shown in Figure 5.6 (c), the highest electricity requirement equals 248 MW for HDO, the lowest electricity requirement equals 64 MW for DCO₂; and for HDCO, the electricity requirement equals 121 MW.

For the triolein feedstock shown in Figure 5.6 (d), the highest electricity requirement equals 313 MW for HDO, the lowest electricity requirement equals 124 MW for DCO₂; and for HDCO, the electricity requirement equals 187 MJ/h.

Similar to single-step, the electricity requirement for two-step of HDO > HDCO > DCO₂, corresponding to the requirement of pressurized H₂. Moreover, two-step of hydrotreating required less H₂ than single-step of hydrotreating.

The electricity requirement for the triolein feedstock is more than that of the tripalmitin feedstock for both integrated systems because the triolein feedstock required more H₂ than tripalmitin.

5.1.4 Minimum energy requirement of integrated system

Aspen Energy Analyzer was used to determine the minimum heating utility requirement and the minimum cooling utility requirement with pinch analysis to obtain the cold and hot composite curve of the integrated system with 30 °C of ΔT_{\min} , which was studied for the gas-oil hydrotreater unit and the hydrogen production unit⁷¹. For the pinch analysis, on the left side represent the hot composite curve. And then, on the right side away from hot composite curve represent the cold composite curve by fixing the temperature and enthalpy change of the curves. The maximum heat can be exchanged within the process is represented by the overlap of cold and hot composite curve. The minimum heating utility requirement is represented by the excess point from the top of the cold composite curve for heating the cold streams and the minimum cooling utility requirement is represented by the the excess point from the bottom of the hot composite for cooling the hot streams⁷²⁻⁷³. Then, both of the minimum heating utility and the minimum cooling utility requirement provided the minimum energy requirement (MER) of the integrated system.

Although the lowest of the minimum heating utility requirement was used for HDO, HDCO, and DCO₂, respectively, the lowest of the minimum cooling utility requirement was used for DCO₂, HDCO, and HDO, respectively, for both integrated systems and feedstock. Thus, the optimum MER of the integrated system of hydrotreating and hydrogen generation with various selectivity of deoxygenation reaction pathways from tripalmitin and triolein was defined as the lowest of MER.

However, for the composite curves of optimum MER of the integrated system of single-step of hydrotreating and PSR with the HDCO pathway, pinch temperature is 647.0 and 677.0 °C from tripalmitin and triolein, as presented in Figure 5.9 (a) and (b), respectively. For two-step of hydrotreating and GSR with the HDO pathway, pinch temperature is 127.8 and 97.8 °C from tripalmitin and pinch temperature is 128.2 and 98.2 °C from triolein as presented in Figure 5.9 (c) and (d), respectively.

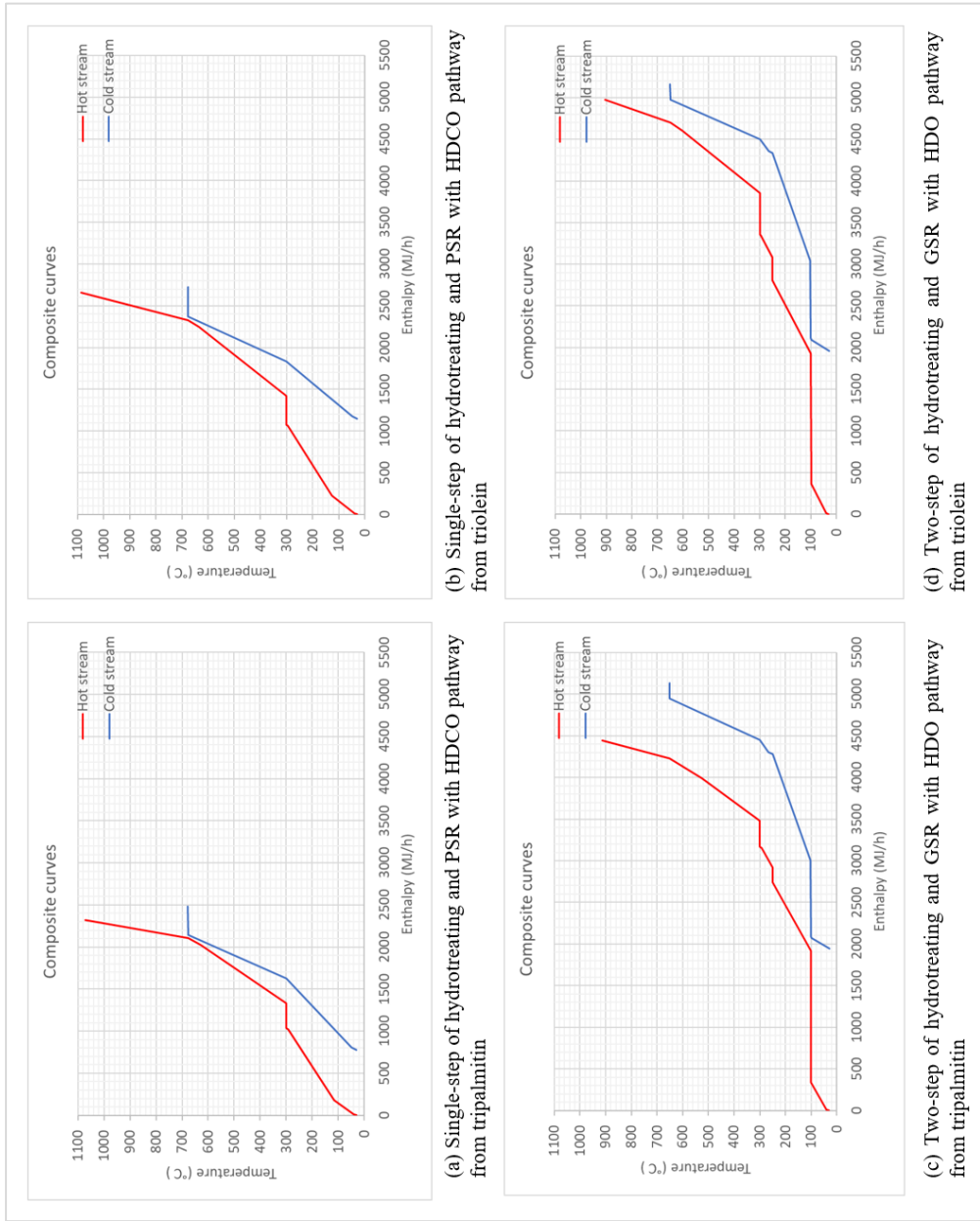


Figure 5.9 Composite curves of optimum MER of integrated system. Single-step of hydrotreating and PSR with HDGO pathway from (a) tripalmitin and (b) triolein. Two-step of hydrotreating and GSR with HDO pathway from (c) tripalmitin and (d) triolein.

MER of the integrated system of single-step of hydrotreating and PSR with various selectivity of deoxygenation reaction pathways (DCO₂: HDCO: HDO) from tripalmitin and triolein is presented in Figure 5.10 (a) and (b), respectively, and MER for two-step of hydrotreating and GSR from tripalmitin and triolein is presented in Figure 5.10 (c) and (d), respectively.

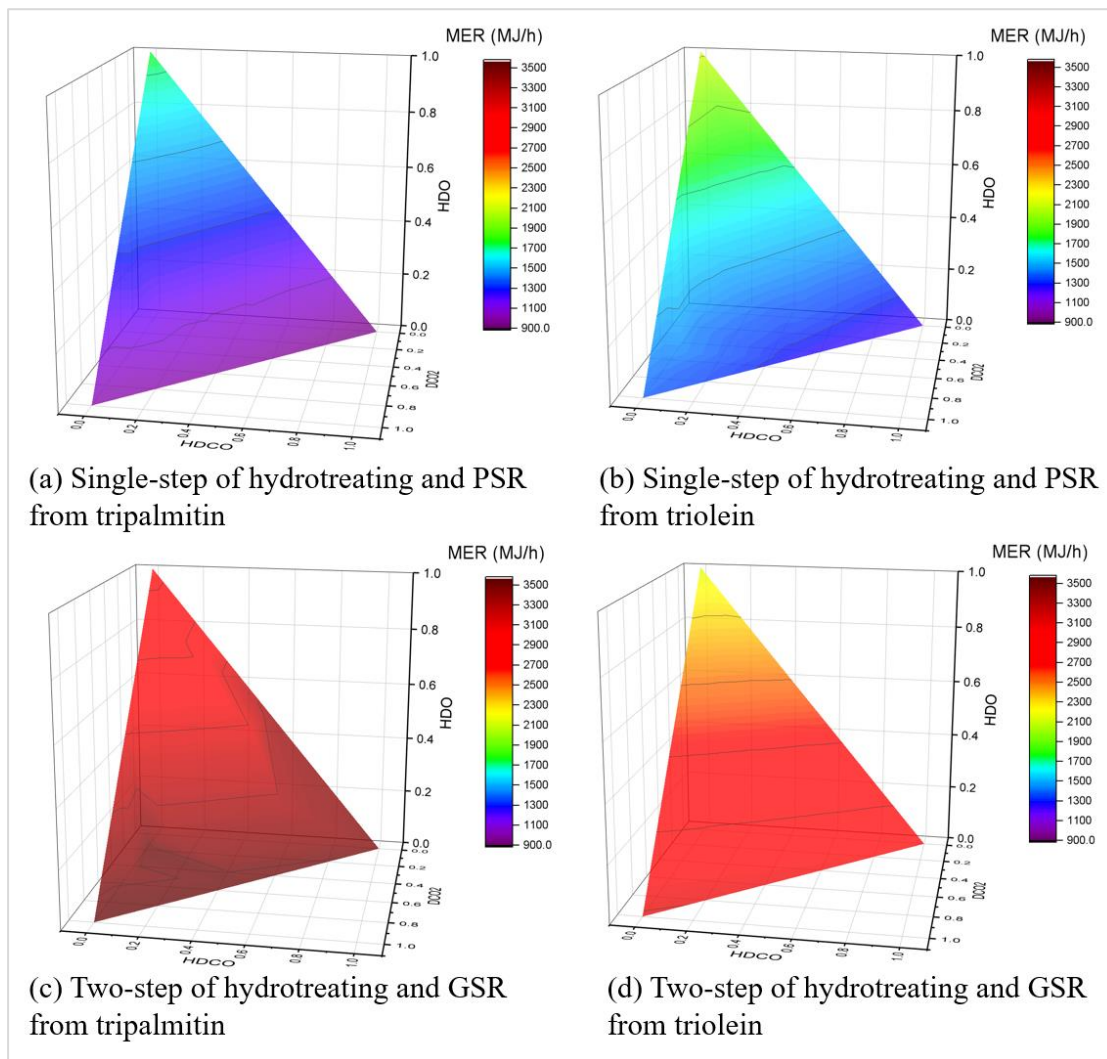


Figure 5.10 MER of integrated system with various selectivity of deoxygenation reaction pathways. Single-step of hydrotreating and PSR from (a) tripalmitin and (b) triolein. Two-step of hydrotreating and GSR from (c) tripalmitin and (d) triolein.

5.1.4.1 Minimum energy requirement of integrated system of single-step of hydrotreating and propane steam reforming

For the tripalmitin feedstock shown in **Error! Reference source not found.** (a), the highest MER equals 1,758 MJ/h for HDO; the lowest MER equals 937 MJ/h for HDCO; and for DCO₂, MER equals 997 MJ/h.

For the triolein feedstock shown in **Error! Reference source not found.** (b), the highest MER equals 2,119 MJ/h for HDO; the lowest MER equals 1,210 MJ/h for HDCO; and for DCO₂, MER equals 1,379 MJ/h.

5.1.4.2 Minimum energy requirement of integrated system of two-step of hydrotreating and glycerol steam reforming

For the tripalmitin feedstock shown in **Error! Reference source not found.** (c), the highest MER equals 3,560 MJ/h for DCO₂; the lowest MER equals 2,634 MJ/h for HDO; and for HDCO, MER equals 3,488 MJ/h.

For the triolein feedstock shown in **Error! Reference source not found.** (d), the highest MER equals 3,114 MJ/h for DCO₂; the lowest MER equals 2,142 MJ/h for HDO; and for HDCO, MER equals 3,023 MJ/h.

5.1.5 Total minimum energy requirement of integrated system

The integrated system required electricity for BHD production. Then, thermal for electricity production was considered with 40% net efficiency, which is described in Equation 5.3⁷⁴, including thermal of net H₂ of the integrated system with lower heating value, which was reported in APPENDIX G, in order to evaluate the performance of the integrated system of hydrotreating and hydrogen generation. Total MER was calculated in Equation 5.4, with thermal for electricity (Q_{Elec}) and thermal of net H₂ being calculated in Equations 5.5 and 5.6, respectively.

$$\text{Electricity (W)} = \text{Thermal for electricity (J/s)} \times 40\% \quad (5.3)$$

$$\begin{aligned} \text{Total MER (MJ/h)} = & (\text{Thermal for electricity} + \text{Thermal of net H}_2 + \text{MER})_{\text{Heating}} \\ & + (\text{MER})_{\text{Cooling}} \end{aligned} \quad (5.4)$$

$$\text{Thermal for electricity (Q}_{\text{Elec}}\text{) (MJ/h)} = \text{Electricity (kW)} \times 9 \text{ of thermal} \left(\frac{\text{MJ / h}}{\text{kW}} \right) \quad (5.5)$$

$$\text{Thermal of net H}_2 \text{ (MJ/h)} = \text{Net H}_2 \text{ (kmol/h)} \times \{-\text{LHV}_{\text{H}_2} \text{ (MJ/kmol)}\} \quad (5.6)$$

Total MER of the integrated system of single-step of hydrotreating and PSR with various selectivity of deoxygenation reaction pathways (DCO₂: HDCO: HDO) from tripalmitin and triolein is presented in Figure 5.11 (a) and (b), respectively, and total MER for two-step of hydrotreating and GSR from tripalmitin and triolein is presented in Figure 5.11 (c) and (d), respectively.

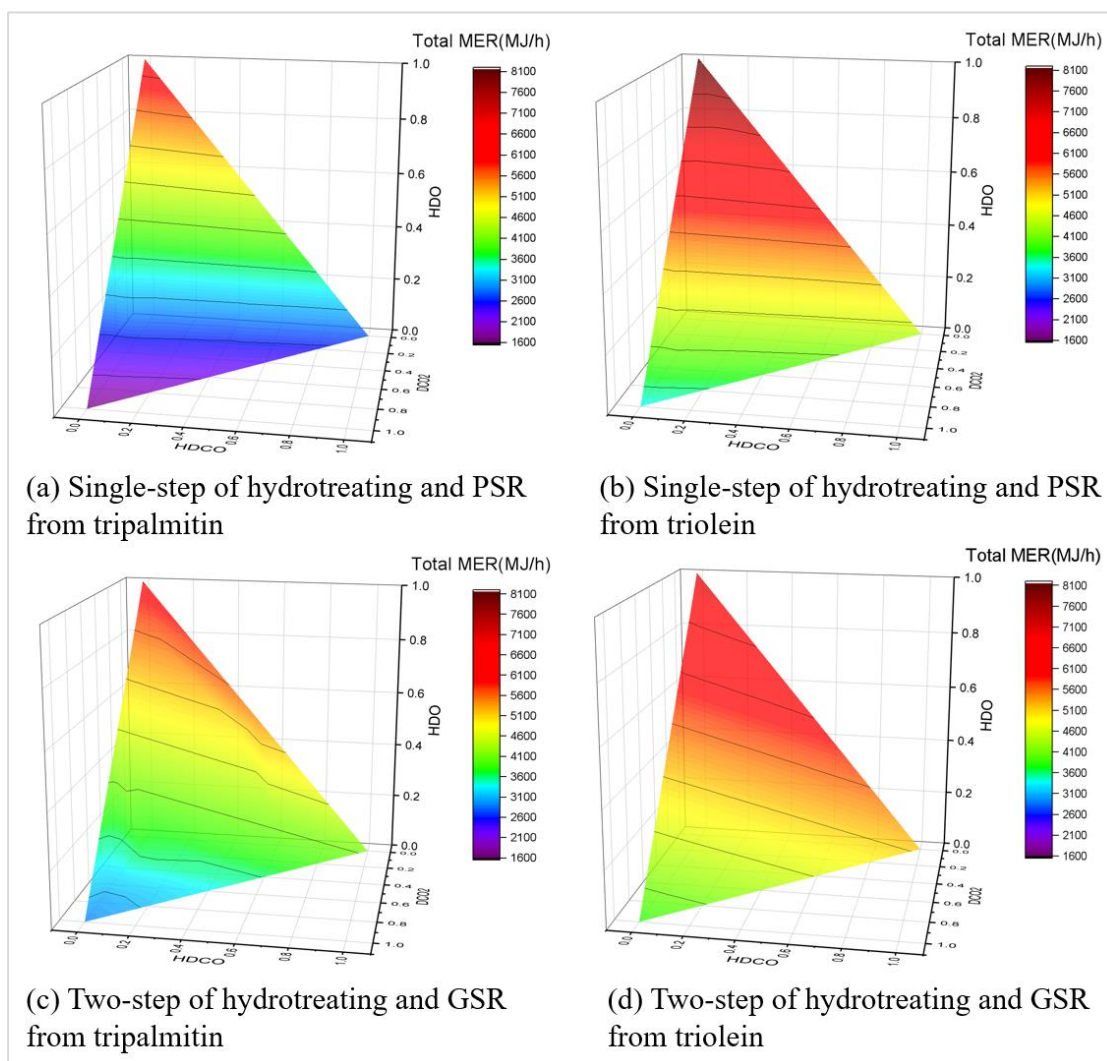


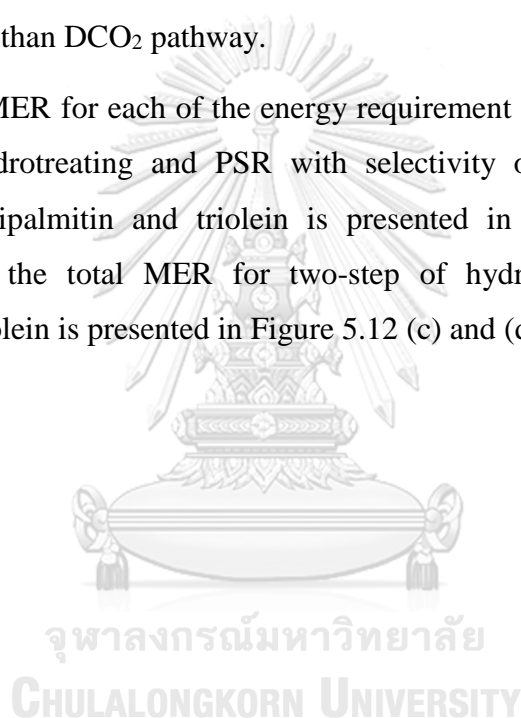
Figure 5.11 Total MER of integrated system with various selectivity of deoxygenation reaction pathways. Single-step of hydrotreating and PSR from (a) tripalmitin and (b) triolein. Two-step of hydrotreating and GSR from (c) tripalmitin and (d) triolein.

For the tripalmitin feedstock, the integrated system of single-step of hydrotreating and PSR with the DCO₂ pathway provides the lowest of total MER equal to 1,690 MJ/h.

For the triolein feedstock, the integrated system of single-step of hydrotreating and PSR with the DCO₂ pathway provides the lowest of total MER equal to 3,356 MJ/h.

As a result, the effect of the electricity requirement and the net H₂ on the performance of the integrated system is strong, with HDCO and HDO pathways requiring more H₂ than DCO₂ pathway.

The total MER for each of the energy requirement of the integrated system of single-step of hydrotreating and PSR with selectivity of deoxygenation reaction pathways from tripalmitin and triolein is presented in Figure 5.12 (a) and (b), respectively, and the total MER for two-step of hydrotreating and GSR from tripalmitin and triolein is presented in Figure 5.12 (c) and (d), respectively.



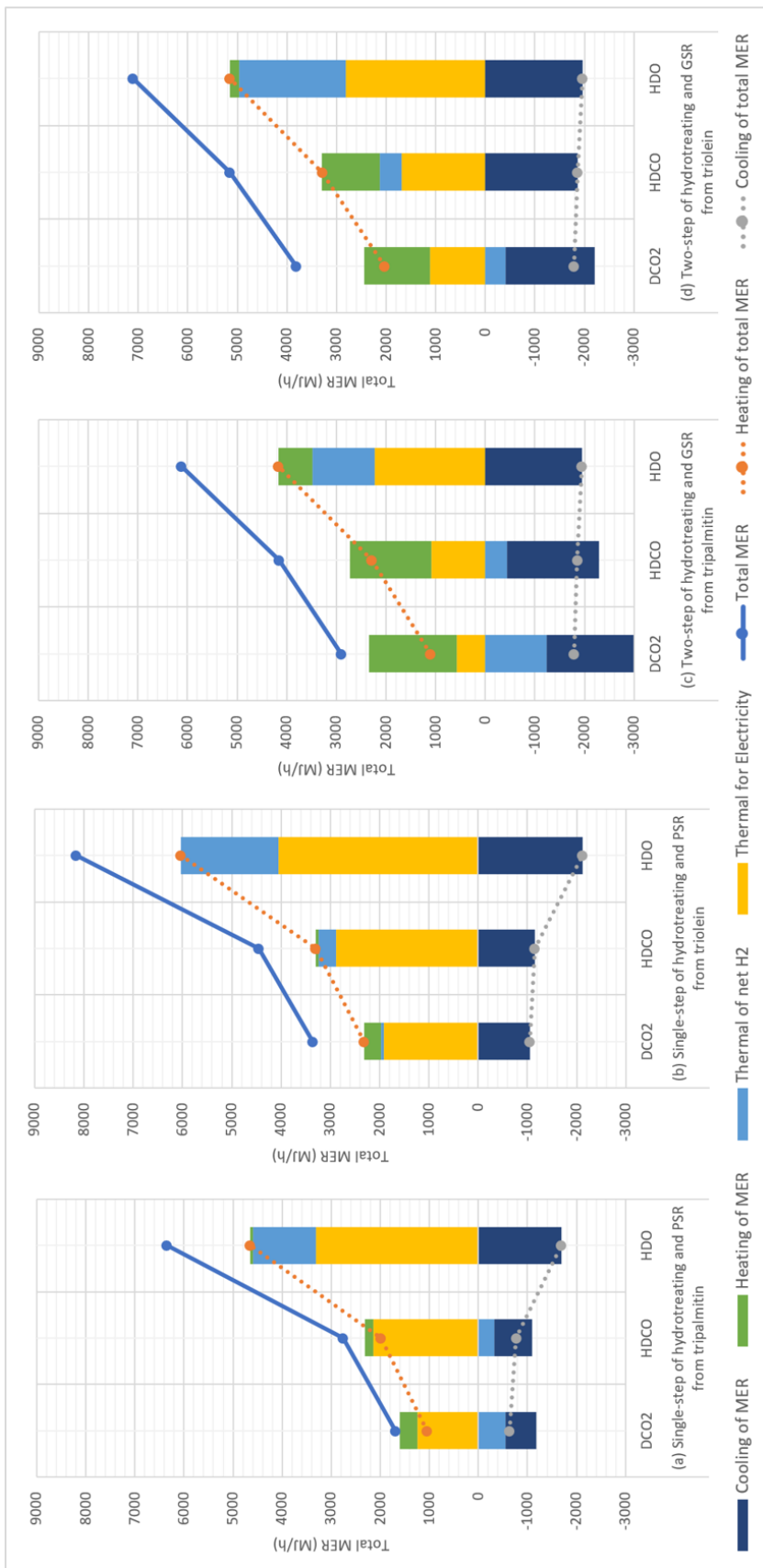


Figure 5.12 Total MER for each of energy requirement of integrated system with selectivity of deoxygenation reaction pathways. Single-step of hydrotreating and PSR from (a) tripalmitin and (b) triolein. Two-step of hydrotreating and GSR from (c) tripalmitin and (d) triolein.

5.1.6 Thermal efficiency of integrated system

The deoxygenation reaction provides BHD with different hydrocarbon products. N-pentadecane (C₁₅H₃₂) and n-hexadecane (C₁₆H₃₄) are obtained from the tripalmitin feedstock, while n-heptadecane (C₁₇H₃₆) and n-octadecane (C₁₈H₃₈) are obtained from the triolein feedstock. The heating value of feedstocks and products including H₂ are needed for performance evaluation of the integrated system⁵⁴. Thermal efficiency (η_{Thermal}) was described in Equation 5.7 and was calculated in Equation 5.8, with thermal of each component with lower heating value ($Q_{\text{LHVComponent}}$) calculated in Equation 5.9 and lower heating value of each component ($\text{LHV}_{\text{Component}}$) was reported in APPENDIX G.

$$\eta_{\text{Thermal}} \left(\frac{\text{MJ} / \text{h}}{\text{MJ} / \text{h}} \right) = \frac{\left(Q_{\text{LHV}_{\text{BHD}}} + Q_{\text{LHV}_{\text{H}_2}} \right)_{\text{product}}}{\left(Q_{\text{LHV}_{\text{palmoil}}} + Q_{\text{LHV}_{\text{H}_2}} \right)_{\text{feedstock}}} \times 100\% \quad (5.7)$$

$$\eta_{\text{Thermal}} = \frac{\left(Q_{\text{LHV}_{\text{C}_{15}\text{H}_{32}}} + Q_{\text{LHV}_{\text{C}_{16}\text{H}_{34}}} + Q_{\text{LHV}_{\text{C}_{17}\text{H}_{36}}} + Q_{\text{LHV}_{\text{C}_{18}\text{H}_{38}}} + Q_{\text{LHV}_{\text{H}_2}} \right)_{\text{Product}}}{\left(Q_{\text{LHV}_{\text{Tripalmitin}}} + Q_{\text{LHV}_{\text{Triolein}}} + Q_{\text{LHV}_{\text{H}_2}} \right)_{\text{Feedstock}}} \times 100\% \quad (5.8)$$

$$Q_{\text{LHV}_{\text{Component}}} \text{ (MJ/h)} = \text{Flow rate}_{\text{Component}} \text{ (kmol/h)} \times \text{LHV}_{\text{Component}} \text{ (MJ/kmol)} \quad (5.9)$$

Thermal efficiency of the integrated system of single-step of hydrotreating and PSR with various selectivity of deoxygenation reaction pathways (DCO₂: HDCO: HDO) from tripalmitin and triolein is presented in Figure 5.13 (a) and (b), respectively, and thermal efficiency for two-step of hydrotreating and GSR from tripalmitin and triolein is presented in Figure 5.13 (c) and (d), respectively.

For the tripalmitin feedstock, the integrated system of single-step of hydrotreating and PSR with the HDO pathway provides the highest thermal efficiency of 96.20%. Although DCO₂ and HDCO pathways can produce sufficient H₂ for BHD production with remaining H₂ as fuel to provide heating, C₁₆H₃₄ provided more heating value than C₁₅H₃₂. Thus, the composition of BHD products is important for performance evaluation.

For the triolein feedstock, the integrated system of two-step of hydrotreating and GSR with the DCO₂ pathway provides the highest thermal efficiency of 96.70%. However, this integrated system can produce sufficient H₂ for BHD production with

remaining H_2 as fuel to provide heating, in another process, H_2 was supported from an external source.

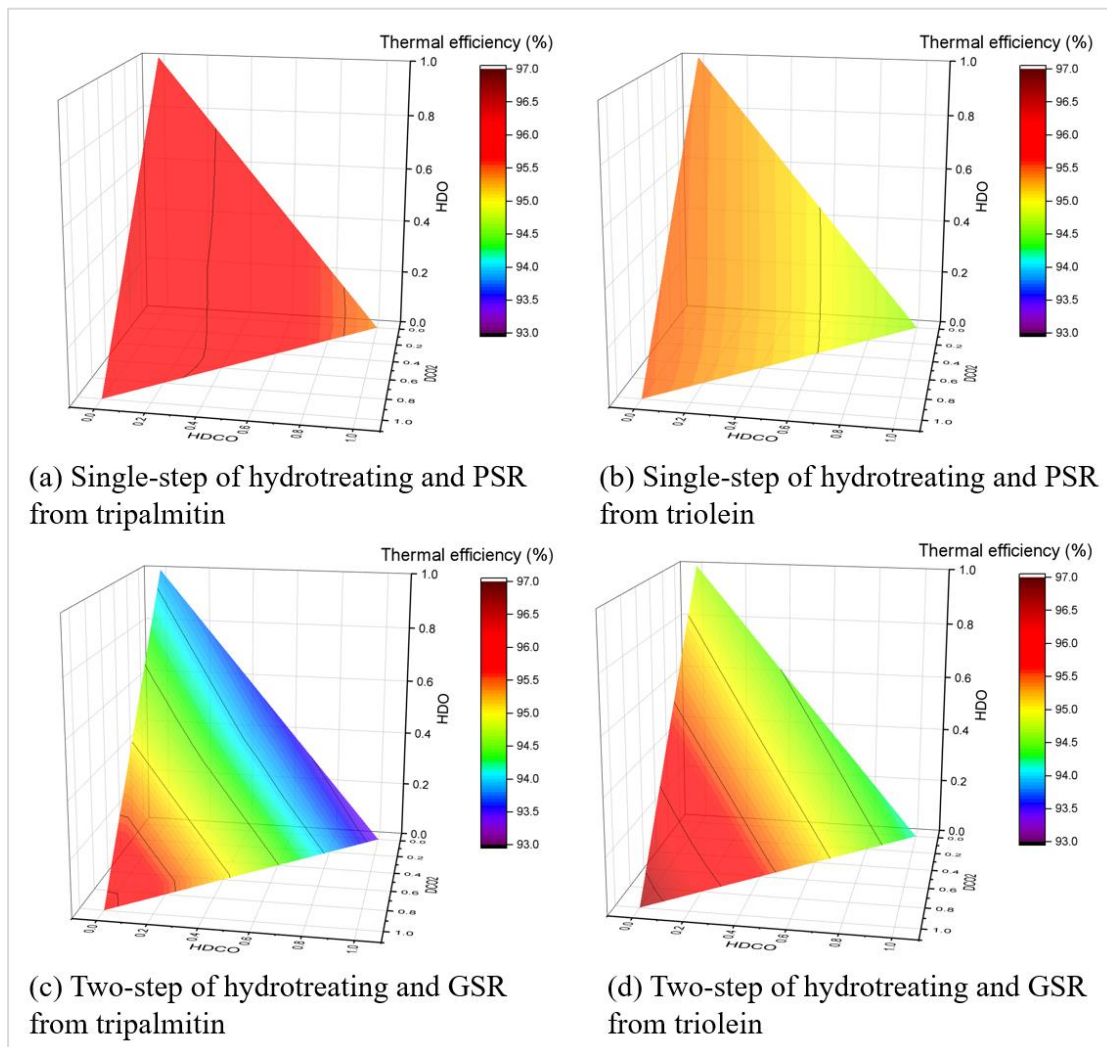


Figure 5.13 Thermal efficiency of integrated system with various selectivity of deoxygenation reaction pathways. Single-step of hydrotreating and PSR from (a) tripalmitin and (b) triolein. Two-step of hydrotreating and GSR from (c) tripalmitin and (d) triolein.

5.1.7 Total efficiency of integrated system

The overall efficiency of the integrated system was considered from MER, thermal for electricity (Q_{Elec}), thermal of each component with lower heating value ($Q_{LHVComponent}$), for both feedstock and product including H_2 . Total efficiency (η_{Total}) was described in Equation 5.10 and was calculated in Equation 5.11.

$$\eta_{Total} \left(\frac{MJ/h}{MJ/h} \right) = \frac{\left(Q_{LHV_{BHD}} + Q_{LHV_{H_2}} \right)_{Product}}{\left(Q_{LHV_{PalmOil}} + Q_{LHV_{H_2}} \right)_{Feedstock} + Q_{MER} + Q_{Elec}} \times 100\% \quad (5.10)$$

$$\eta_{Total} = \frac{\left(Q_{LHV_{C_{15}H_{32}}} + Q_{LHV_{C_{16}H_{34}}} + Q_{LHV_{C_{17}H_{36}}} + Q_{LHV_{C_{18}H_{38}}} + Q_{LHV_{H_2}} \right)_{Product}}{\left(Q_{LHV_{Tripalmitin}} + Q_{LHV_{Triolein}} + Q_{LHV_{H_2}} \right)_{Feedstock} + Q_{MER} + Q_{Elec}} \times 100\% \quad (5.11)$$

Total efficiency of the integrated system of single-step of hydrotreating and PSR with various selectivity of deoxygenation reaction pathways (DCO₂: HDCO: HDO) from tripalmitin and triolein is presented in Figure 5.14 (a) and (b), respectively, and total efficiency for two-step of hydrotreating and GSR from tripalmitin and triolein is presented in Figure 5.14 (c) and (d), respectively.



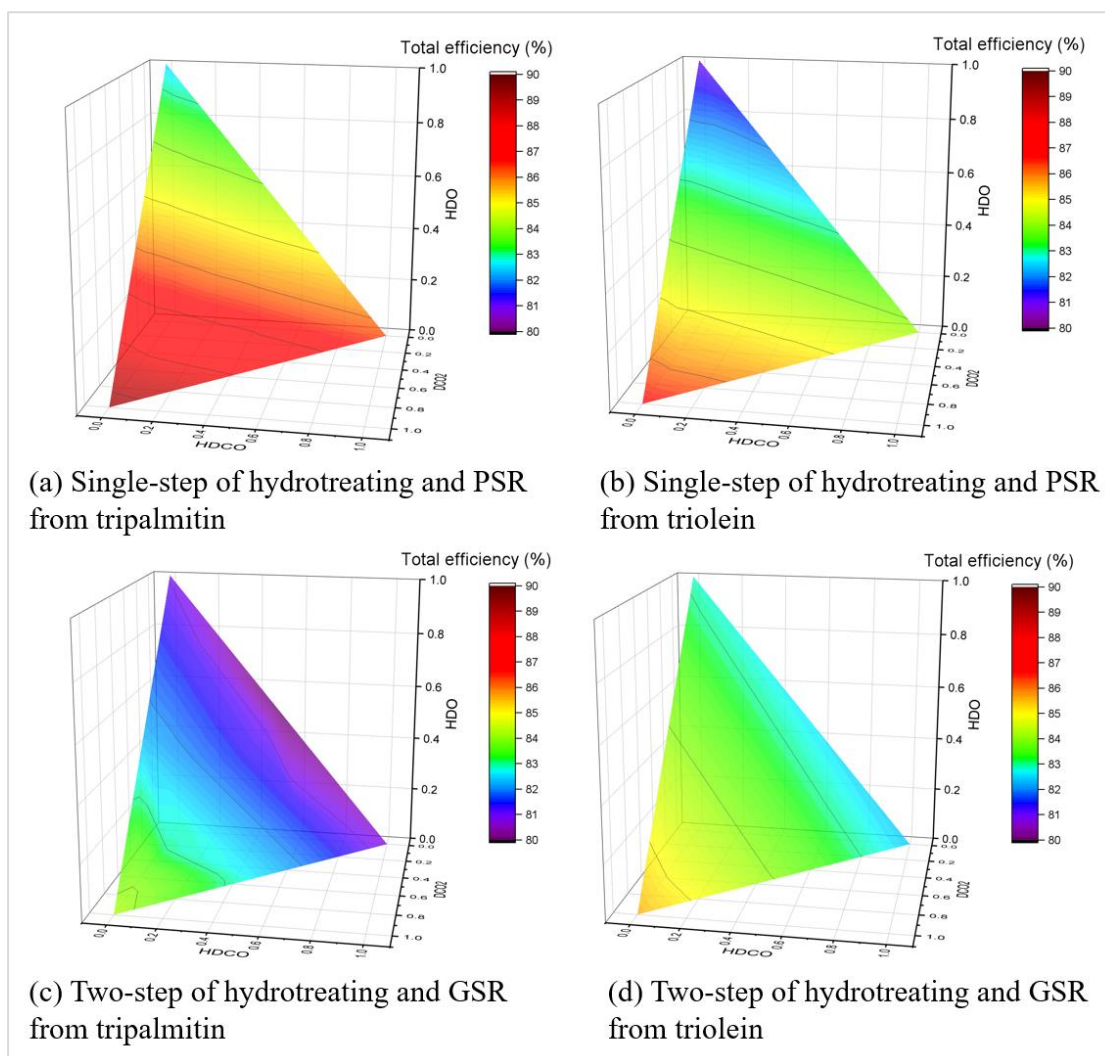


Figure 5.14 Total efficiency of integrated system with various selectivity of deoxygenation reaction pathways. Single-step of hydrotreating and PSR from (a) tripalmitin and (b) triolein. Two-step of hydrotreating and GSR from (c) tripalmitin and (d) triolein.

For the tripalmitin feedstock, the integrated system of single-step of hydrotreating and PSR with the DCO_2 pathway provides the highest total efficiency of 89.31%. Although this integrated system with the DCO_2 pathway required more electricity with less remaining net H_2 , it required less MER than the other integrated system.

For the triolein feedstock, the integrated system of single-step of hydrotreating and PSR with the DCO_2 pathway provides the highest total efficiency of 86.73%. Although this integrated system with the DCO_2 pathway required H_2 support from an

external source and required more electricity, it required less MER than the other integrated system. Thus, heat integration is needed for process improvement.

However, the integrated system of two-step of hydrotreating and GSR with the DCO₂ pathway from triolein provided total efficiency of 85.60%, which is not very different from the last one. Then, the number of equipment unit for each the integrated system was compared, which is shown in Table 5.3. It was found that the integrated system of single-step of hydrotreating and PSR required fewer number of pumps, coolers, heaters, reactors, and separators than the other integrated system. Thus, this integrated system presents less process complication and, therefore, it is the optimum integrated system.

Table 5.3 Number of equipment unit of each integrated system.

Equipment unit	The integrated system of single-step of hydrotreating and PSR	The integrated system of two-step of hydrotreating and GSR
Pump	1	2
Compressor	2	2
Cooler	5	6
Heater	2	5
Reactor	2	3
Separator	2	4
PSA unit	2	2
Stream mixer	1	1
Stream splitter	2	2
Valve	7	7
Total equipment unit	26	34

5.2 Comparison of the results of integrated system of hydrotreating and hydrogen generation

Hydrotreating of vegetable oil required H_2 for hydrogenolysis of converted TGs to FFAs and propane by-products, and for deoxygenation of converted FFAs to alkane hydrocarbon range diesel fuel. The literatures in Table 5.4 reported H_2 /oil molar ratio depending on the type of vegetable oil following unsaturated TGs and deoxygenation reaction pathway.

Firstly, H_2 was not produced in the process, and the single-step of hydrotreating process required H_2 support from external sources as reported in the literatures of Plazas-Gonzalez³², Kantama⁶, Cheah³⁴, and Glisic³⁸. This value of H_2 feed/oil molar ratio for PFAD reported by Kantama⁶ is lower than that for TGs because PFAD is FFAs, which does not require H_2 for hydrogenolysis.

Secondly, H_2 was produced in the process without an external support of H_2 and was reported in the literatures^{16, 39, 53-56}. For this work, the integrated system of single-step of hydrotreating and PSR with the decarboxylation reaction pathway from tripalmitin produced H_2 sufficiently in the process but required H_2 support from external sources for the integrated system from triolein.

From literatures, fuel from an external source such as CH_4 was fed to produce H_2 via SRM, which was reported by Pujan⁵³ and Atsonios⁵⁴ with multiple processes of the integrated system. Atsonios⁵⁴ reported 84.63% of BHD/ oil mass ratio from palm oil which demonstrated the performance of BHD production, which is more than the performance of the present work which obtained 80.89% and 82.85% of BHD/ oil mass ratio from tripalmitin and triolein, respectively. Pujan⁵³ reported a low BHD/ oil mass ratio because BHD production provided main kerosene.

For the process without an external support of fuel, Hilbers³⁹ did not design the integrated system, but reported that H_2 was produced from PSR sufficiently in single-step of hydrotreating. Sungnoen¹⁶ designed a process to produce H_2 from glycerol by-products via GSR for hydrotreating of stearic acid with multiple processes of the integrated system, which stearic acid requiring less H_2 than TGs according to the above discussion. Dominguez-Barroso⁵⁵ and Mao⁵⁶ reported BHD production in a

single process, with H₂ generation via aqueous phase reforming of glycerol by-products from hydrolysis. However, these processes provided lower yield and resulted in residual oxygen content in the product as Mao⁵⁶ and Dominguez-Barroso⁵⁵ reported, respectively.

Energy requirement and electricity requirement per ton of oil of the present work were compared to the literatures^{6, 34, 54}. The energy requirement of the present work was lower than those reported by Kantama⁶, Cheah³⁴, and Atsonios⁵⁴. BHD production of Kantana⁶ was improved with heat integration, but BHD production of Cheah³⁴ and Atsonios⁵⁴ was not improved with heat integration. The electricity requirement of the present work was lower than what Cheah³⁴ reported, but higher than what Kantama⁶ and Atsonios⁵⁴ reported. However, Kantama⁶ did not report electricity requirement of the compressor and Atsonios⁵⁴ operated at lower pressure than the present work for both hydrotreating and the PSA unit.

Thus, the present integrated system from both tripalmitin and triolein provided superior performance for BHD production with the use of the Ni/ γ -Al₂O₃ catalyst for hydrotreating process, which it is favorable leading to the DCO₂ reaction pathway⁶⁴ and the Ni with support catalyst for PSR process, which it is widely used for hydrogen generation^{9, 49}.

Comparison of the results of the integrated system of hydrotreating and hydrogen generation to the literature review for bio-hydrogenated diesel fuel production can be summarized in Table 5.4.

Table 5.4 Summarization of the comparative results of integrated system of hydrotreating and hydrogen generation to the literature review for bio-hydrogenated diesel fuel production.

Feedstock	Integrated system	H ₂ / oil molar ratio	H ₂ feed/ oil molar ratio	CH ₄ feed/ oil mass ratio	BHD/ oil (wt.%)	BHD purity (wt.%)	HT catalyst	Energy (MJ/ ton oil)	Elec. (kWh/ ton oil)	Reference
Tripalmitin	Multiple processes	9.0	-	-	80.89	97.48	Ni/γ-Al ₂ O ₃	1,340	171	This work
Triolein	Multiple processes	18.0	0.28	-	82.85	98.62	Ni/γ-Al ₂ O ₃	1,589	240	This work
Palm oil	Single-step of hydrotreating	20.0	N/A	-	N/A	97	NiMo/γ-Al ₂ O ₃	N/A	N/A	Plazas-Gonzalez, 2018 ³²
PFAD	Single-step of hydrotreating	1.82	1.82	-	59.58	99.7	Pd/C	1,610	5.84	Kantama, 2015 ⁶
Rubber seed oil (Triolein, FFAs)	Single-step of hydrotreating	N/A	9.22	-	76.26	98.7	Pd/C	3,328	1,313	Cheah, 2017 ³⁴
WVO (Triolein)	Single-step of hydrotreating	46	7.33 (Reacted)	-	66.39 (Yield)	N/A	CoMo/Al ₂ O ₃	N/A	N/A	Glisic, 2016 ³⁸
Palm oil	Single-step of hydrotreating	N/A	-	-	41.61	N/A	NiMo/γ-Al ₂ O ₃	N/A	N/A	Hilbers, 2015 ³⁹

Table 5.4 Summarization of the comparative results of integrated system of hydrotreating and hydrogen generation to the literature review for bio-hydrogenated diesel fuel production. (*Continued*).

Feedstock	Integrated system	H ₂ / oil molar ratio	H ₂ feed/ oil molar ratio	CH ₄ feed/ oil mass ratio	BHD/ oil (wt.%)	BHD purity (wt.%)	HT catalyst	Energy (MJ/ ton oil)	Elec. (kWh/ ton oil)	Reference
Soybean oil, Stearic acid	Multiple processes	1.5	-	-	N/A	99.28	Ni with support	N/A	N/A	Sungnoen, 2014 ¹⁶
Algae oil	Multiple processes	1000 cm ³ /cm ³	-	0.0195	13.93	99.94	N/A	N/A	N/A	Pujan, 2017 ⁵³
Palm oil	Multiple processes	20	-	0.051	84.63	N/A	NiMo	2,374	105	Atsonios, 2018 ⁵⁴
Jatropha oil	Multiple processes	20	-	0.059	85.36	N/A	NiMo	1,921	106	Atsonios, 2018 ⁵⁴
Olive oil	Multiple processes	20	-	0.054	85.26	N/A	NiMo	2,382	104	Atsonios, 2018 ⁵⁴
Sunflower oil	Single process	N/A	-	-	N/A	N/A	Pt- Ni/Al ₂ O ₃ and Pd/C	N/A	N/A	Domingue z-Barroso, 2016 ⁵⁵
Triolein	Single process	N/A	-	-	71.91 (yield)	N/A	Pd/C (decalin solvent)	N/A	N/A	Mao, 2017 ⁵⁶

CHAPTER VI CONCLUSION AND RECOMMENDATIONS

6.1 Conclusion

In this work, the integrated system comprising of the bio-hydrogenated diesel production via single-step and two-step of hydrotreating, and hydrogen production via PSR and GSR using tripalmitin and triolein as a palm oil feedstock, was simulated and the performance was evaluated. According to the results of the performance evaluation of the integrated system of hydrotreating and hydrogen generation with various selectivity of DO reaction pathways (DCO_2 : HDCO : HDO) from tripalmitin and triolein, it was found that the DCO_2 pathway with the use of the $\text{Ni}/\gamma\text{-Al}_2\text{O}_3$ catalyst for hydrotreating process⁶⁴ and the Ni with support catalyst for hydrogen generation^{9-10, 49} exhibited the highest performance of each integrated system for both tripalmitin and triolein feedstocks. However, the integrated system of single-step of hydrotreating and PSR with DCO_2 pathway provided higher performance with lower total MER and higher total efficiency than the other integrated system for both tripalmitin and triolein feedstocks. The process of this integrated system was also less complicated; therefore, it is the optimum integrated system. The following conclusions can be made.

6.1.1 Integrated system of single-step of hydrotreating and propane steam reforming

1) This integrated system was simulated for single-step of BHD production at 300 °C, 50 bar, and 3 times of H_2 stoichiometric requirement with complete conversion and hydrogen production via PSR at 677 °C, atmospheric pressure, and 12.0 of WPMR with equilibrium reactor.

2) For tripalmitin with DCO_2 pathway, the initial feed of H_2 equals 9.0 kmol/h. Net H_2 equals 2.31 kmol/h, with H_2 production of 7.53 moles per unit mole of propane. The system required H_2O of 3.63 kmol/h. Mole flow rate of BHD equals 3.43 kmol/h, which contains $\text{C}_{15}\text{H}_{32}$ of approximately 2.997 kmol/h and 97.48 wt.% of product purity. This integrated system required energy, electricity, MER, total MER, thermal efficiency, and total efficiency of 3,793 MJ/h, 138 MW, 997 MJ/h,

1,690 MJ/h, 96.15%, 90.90%, respectively. Heat integration can recover heat equal to 1,355.7 MJ/h, which presented a 71% saving and the remaining required utility was reduced to 1,081.7 MJ/h as shown in APPENDIX H.1.

3) For triolein with DCO₂ pathway, the initial feed of H₂ equals 18.0 kmol/h. Net H₂ equals -0.28 kmol/h, with H₂ production of 7.49 moles per unit mole of propane. Thus, H₂ is insufficient for this case and H₂ feeding is required for this integrated system, which triolein requiring more H₂ than tripalmitin. The system required H₂O equal to 3.97 kmol/h. Mole flow rate of BHD equals 3.30 kmol/h, which contains C₁₇H₃₆ of approximately 2.998 kmol/h and 98.62 wt.% of product purity. This integrated system required energy, electricity, MER, total MER, thermal efficiency, and total efficiency of 4,092 MJ/h, 212 MW, 1,379 MJ/h, 3,356 MJ/h, 95.47%, 86.73%, and 157.15 kg/h, respectively. Heat integration can recover heat equal to 1,342.5 MJ/h, which presented a 66% saving and the remaining required utility was reduced to 1,407.2 MJ/h as shown in APPENDIX H.2.

6.1.2 Integrated system of two-step of hydrotreating and glycerol steam reforming

1) This integrated system was simulated for two-step: hydrolysis of palm oil at 250 °C, 50 bar, and 54.0 of H₂O/oil molar ratio and hydrotreating at 300 °C, 50 bar, and 3 times of H₂ stoichiometric requirement of BHD production with complete conversion. And hydrogen production via GSR at 650 °C, atmospheric pressure, and 9.0 of WGMR with equilibrium reactor.

2) For tripalmitin with DCO₂ pathway, the initial feed of H₂ equals 1.35 kmol/h. Net H₂ equal 5.22 kmol/h, with H₂ production of 5.98 moles per unit mole of glycerol. The system required H₂O of 5.63 kmol/h. Mole flow rate of BHD equals 3.69 kmol/h, which contains C₁₅H₃₂ of approximately 2.921 kmol/h and 95.04 wt.% of product purity. This integrated system required energy, electricity, MER, total MER, thermal efficiency, and total efficiency of 6,436 MJ/h, 64 MW, 3,560 MJ/h, 3,580 MJ/h, 96.12%, and 85.64%, respectively.

3) For triolein with DCO₂ pathway, the initial feed of H₂ equals 9.0 kmol/h. Net H₂ equals 1.74 kmol/h, with H₂ production of 5.98 moles per unit mole of

glycerol. The system required H_2O of 5.64 kmol/h. Mole flow rate of BHD equals 3.41 kmol/h, which contains $\text{C}_{17}\text{H}_{36}$ of approximately 2.99 kmol/h and 97.82 wt.% of product purity. This integrated system required energy, electricity, MER, total MER, thermal efficiency, and total efficiency, of 6,863 MJ/h, 124 MW, 3,114 MJ/h, 3,452 MJ/h, 96.70%, and 87.44%, respectively.

However, comparison of the two integrated systems of hydrotreating and hydrogen generation revealed the lower total MER and the higher total efficiency of single-step of hydrotreating and PSR than the other integrated system with the DCO_2 pathway.

6.2 Recommendations

1) Composition of palm oil contains many kinds of TGs, which is not pure tripalmitin or triolein, but tripalmitin and triolein are the main component of palm oil. Then, the ratio of tripalmitin and triolein for the feedstock as palm oil are attractive should be further investigated.

2) For the integrated system of single-step of hydrotreating and PSR with DCO_2 reaction pathway from tripalmitin, the propane by-product was separated in the three-phase separator (SEP-1) with 80% of propane produced. The temperature of the separation process with the cooler (CL-2) should be decreased in order to obtain a higher propane from the separation process.

3) Heat integration of the integrated system of single-step of hydrotreating and PSR with DCO_2 reaction pathway provided a higher energy requirement than MER of the integrated system. This work did not investigate heat integration of the integrated system of two-step of hydrotreating and GSR, thus, it should be further analyzed.

4) This work did not consider several components of the total cost such as the operating cost and the capital cost of the integrated system to decide the operation. However, comparison of the total cost and the cost of total utility should be strongly discussed in the future.

5) Electricity requirement of pumps and compressors was considered from assumption of the single stage of each unit. But this work was operated at high pressure drop, thus, multistage pumps and compressors should be further investigated.

REFERENCES

1. Chu, P. L.; Vanderghem, C.; MacLean, H. L.; Saville, B. A., Process modeling of hydrodeoxygenation to produce renewable jet fuel and other hydrocarbon fuels. *Fuel* **2017**, *196*, 298-305.
2. Srifa, A.; Faungnawakij, K.; Itthibenchapong, V.; Viriya-Empikul, N.; Charinpanitkul, T.; Assabumrungrat, S., Production of bio-hydrogenated diesel by catalytic hydrotreating of palm oil over NiMoS 2/ γ -Al₂O₃ catalyst. *Bioresource technology* **2014**, *158*, 81-90.
3. Pattanaik, B. P.; Misra, R. D., Effect of reaction pathway and operating parameters on the deoxygenation of vegetable oils to produce diesel range hydrocarbon fuels: A review. *Renewable and Sustainable Energy Reviews* **2017**, *73*, 545-557.
4. Kiatkittipong, W.; Phimsen, S.; Kiatkittipong, K.; Wongsakulphasatch, S.; Laosiripojana, N.; Assabumrungrat, S., Diesel-like hydrocarbon production from hydroprocessing of relevant refining palm oil. *Fuel processing technology* **2013**, *116*, 16-26.
5. Hari, T. K.; Yaakob, Z.; Binitha, N. N., Aviation biofuel from renewable resources: routes, opportunities and challenges. *Renewable and Sustainable Energy Reviews* **2015**, *42*, 1234-1244.
6. Kantama, A.; Narataruksa, P.; Hunpinyo, P.; Prapainainar, C., Techno-economic assessment of a heat-integrated process for hydrogenated renewable diesel production from palm fatty acid distillate. *Biomass and Bioenergy* **2015**, *83*, 448-459.
7. Veriansyah, B.; Han, J. Y.; Kim, S. K.; Hong, S.-A.; Kim, Y. J.; Lim, J. S.; Shu, Y.-W.; Oh, S.-G.; Kim, J., Production of renewable diesel by hydroprocessing of soybean oil: Effect of catalysts. *Fuel* **2012**, *94*, 578-585.
8. Wang, W.-C.; Tao, L., Bio-jet fuel conversion technologies. *Renewable and Sustainable Energy Reviews* **2016**, *53*, 801-822.

9. Rakib, M. A.; Grace, J. R.; Lim, C. J.; Elnashaie, S. S.; Ghiasi, B., Steam reforming of propane in a fluidized bed membrane reactor for hydrogen production. *International journal of hydrogen energy* **2010**, *35* (12), 6276-6290.
10. Wang, C.; Dou, B.; Chen, H.; Song, Y.; Xu, Y.; Du, X.; Luo, T.; Tan, C., Hydrogen production from steam reforming of glycerol by Ni–Mg–Al based catalysts in a fixed-bed reactor. *Chemical engineering journal* **2013**, *220*, 133-142.
11. Svennerholm, L., The nomenclature of lipids. IUPAC-IUB Commission on Biochemical Nomenclature (CBN). *Eur. J. Biochem* **1977**, *79*, 11-21.
12. Nelson, D. L.; Lehninger, A. L.; Cox, M. M., *Lehninger principles of biochemistry*. Macmillan: 2008.
13. Thomas, A., Fats and fatty oils. *Ullmann's Encyclopedia of Industrial Chemistry* **2000**.
14. Sotelo-Boyás, R.; Trejo-Zárraga, F.; de Jesús Hernández-Loyo, F., Hydroconversion of triglycerides into green liquid fuels. In *Hydrogenation*, InTech: 2012.
15. Daels, E.; Foubert, I.; Goderis, B., The effect of adding a commercial phytosterol ester mixture on the phase behavior of palm oil. *Food Research International* **2017**, *100*, 841-849.
16. Sungnoen, B. DESIGN AND SIMULATION OF COMBINED BIODIESEL PRODUCTION, GLYCEROL REFORMING AND GREEN DIESEL PRODUCTION. Chulalongkorn University, Bangkok, 2014.
17. UOP, H. Honeywell Green Diesel™. <https://www.uop.com/processing-solutions/renewables/green-diesel/#ecofining>.
18. Water, C., Green diesel production by hydrotreating renewable feedstocks. **2008**.
19. Egeberg, R.; Knudsen, K.; Nyström, S.; GRENNFELT, E. L.; Efraimsson, K., Industrial-scale production of renewable diesel. *Petroleum technology quarterly* **2011**, *16* (4).

20. Oil, N. NExBTL Renewable Synthetic Diesel.
https://web.archive.org/web/20100418133813/http://www.climatechange.ca.gov/events/2006-06-27+28_symposium/presentations/CalHodge_handout_NESTE_OIL.PDF.
21. Gandarias, I.; Arias, P. L., Hydrotreating catalytic processes for oxygen removal in the upgrading of bio-oils and bio-chemicals. In *Liquid, Gaseous and Solid Biofuels-Conversion Techniques*, InTech: 2013.
22. Hudlicky, M., *Reductions in organic chemistry*. American Chemical Society: 1996.
23. Sanfilippo, D.; Rylander, P. N., Hydrogenation and dehydrogenation. *Ullmann's Encyclopedia of Industrial Chemistry* **2000**.
24. Freeman, I. P., Margarines and shortenings. *Ullmann's Encyclopedia of Industrial Chemistry* **2000**.
25. Connor, R.; Adkins, H., Hydrogenolysis of oxygenated organic compounds. *Journal of the American Chemical Society* **1932**, *54* (12), 4678-4690.
26. Snåre, M.; Kubic'kova, I.; Mäki-Arvela, P.; Eränen, K.; Murzin, D. Y., Heterogeneous catalytic deoxygenation of stearic acid for production of biodiesel. *Industrial & engineering chemistry research* **2006**, *45* (16), 5708-5715.
27. Hermida, L.; Abdullah, A. Z.; Mohamed, A. R., Deoxygenation of fatty acid to produce diesel-like hydrocarbons: a review of process conditions, reaction kinetics and mechanism. *Renewable and Sustainable Energy Reviews* **2015**, *42*, 1223-1233.
28. IUPAC, M. A.; Wilkinson, A., *IUPAC Compendium of Chemical Terminology: the Gold Book*. Oxford: Blackwell: 1997.
29. Schädel, B. T.; Duisberg, M.; Deutschmann, O., Steam reforming of methane, ethane, propane, butane, and natural gas over a rhodium-based catalyst. *Catalysis today* **2009**, *142* (1-2), 42-51.

30. Silva, J. M.; Soria, M.; Madeira, L. M., Challenges and strategies for optimization of glycerol steam reforming process. *Renewable and Sustainable Energy Reviews* **2015**, *42*, 1187-1213.
31. Cheng, C. K.; Foo, S. Y.; Adesina, A. A., H₂-rich synthesis gas production over Co/Al₂O₃ catalyst via glycerol steam reforming. *Catalysis Communications* **2010**, *12* (4), 292-298.
32. Plazas-González, M.; Guerrero-Fajardo, C. A.; Sodr , J. R., Modelling and simulation of hydrotreating of palm oil components to obtain green diesel. *Journal of Cleaner Production* **2018**, *184*, 301-308.
33. Guzman, A.; Torres, J. E.; Prada, L. P.; Nunez, M. L., Hydroprocessing of crude palm oil at pilot plant scale. *Catalysis Today* **2010**, *156* (1-2), 38-43.
34. Cheah, K. W.; Yusup, S.; Singh, H. K. G.; Uemura, Y.; Lam, H. L., Process simulation and techno economic analysis of renewable diesel production via catalytic decarboxylation of rubber seed oil—A case study in Malaysia. *Journal of environmental management* **2017**, *203*, 950-961.
35. Miller, P.; Kumar, A., Techno-economic assessment of hydrogenation-derived renewable diesel production from canola and camelina. *Sustainable Energy Technologies and Assessments* **2014**, *6*, 105-115.
36. Azizan, M. T.; Jais, K. A.; Sa'aid, M. H.; Ameen, M.; Shahudin, A. F.; Yasir, M.; Yusup, S.; Ramli, A., Thermodynamic Equilibrium Analysis of Triolein Hydrodeoxygenation for Green Diesel Production. *Procedia engineering* **2016**, *148*, 1369-1376.
37. Perez-Cisneros, E. S.; Sales-Cruz, M.; Lobo-Oehmichen, R.; Viveros-García, T., A reactive distillation process for co-hydrotreating of non-edible vegetable oils and petro-diesel blends to produce green diesel fuel. *Computers & Chemical Engineering* **2017**, *105*, 105-122.
38. Glisic, S. B.; Pajnik, J. M.; Orlović, A. M., Process and techno-economic analysis of green diesel production from waste vegetable oil and the comparison with ester type biodiesel

- production. *Applied Energy* **2016**, *170*, 176-185.
39. Hilbers, T. J.; Sprakel, L. M.; van den Enk, L. B.; Zaalberg, B.; van den Berg, H.; van der Ham, L. G., Green diesel from hydrotreated vegetable oil process design study. *Chemical Engineering & Technology* **2015**, *38* (4), 651-657.
40. Smejkal, Q.; Smejkalová, L.; Kubička, D., Thermodynamic balance in reaction system of total vegetable oil hydrogenation. *Chemical Engineering Journal* **2009**, *146* (1), 155-160.
41. Kumar, P.; Yenumala, S. R.; Maity, S. K.; Shee, D., Kinetics of hydrodeoxygenation of stearic acid using supported nickel catalysts: Effects of supports. *Applied Catalysis A: General* **2014**, *471*, 28-38.
42. Jenišťová, K.; Hachemi, I.; Mäki-Arvela, P.; Kumar, N.; Peurla, M.; Čapek, L.; Wärnå, J.; Murzin, D. Y., Hydrodeoxygenation of stearic acid and tall oil fatty acids over Ni-alumina catalysts: Influence of reaction parameters and kinetic modelling. *Chemical Engineering Journal* **2017**, *316*, 401-409.
43. Gomez-Castro, F. I.; Rico-Ramirez, V.; Segovia-Hernandez, J. G.; Hernandez-Castro, S.; El-Halwagi, M. M., Simulation study on biodiesel production by reactive distillation with methanol at high pressure and temperature: Impact on costs and pollutant emissions. *Computers & Chemical Engineering* **2013**, *52*, 204-215.
44. Minami, E.; Saka, S., Kinetics of hydrolysis and methyl esterification for biodiesel production in two-step supercritical methanol process. *Fuel* **2006**, *85* (17-18), 2479-2483.
45. Wang, W.-C.; Thapaliya, N.; Campos, A.; Stikeleather, L. F.; Roberts, W. L., Hydrocarbon fuels from vegetable oils via hydrolysis and thermo-catalytic decarboxylation. *Fuel* **2012**, *95*, 622-629.
46. Wang, W.-C.; Turner, T. L.; Stikeleather, L. F.; Roberts, W. L., Exploration of process parameters for continuous hydrolysis of canola oil, camelina oil and algal oil. *Chemical Engineering and Processing: Process Intensification* **2012**, *57*, 51-58.

47. Natelson, R. H.; Wang, W.-C.; Roberts, W. L.; Zering, K. D., Technoeconomic analysis of jet fuel production from hydrolysis, decarboxylation, and reforming of camelina oil. *Biomass and Bioenergy* **2015**, *75*, 23-34.
48. Wang, X.; Wang, N.; Wang, L., Hydrogen production by sorption enhanced steam reforming of propane: a thermodynamic investigation. *International Journal of Hydrogen Energy* **2011**, *36* (1), 466-472.
49. Im, Y.; Lee, J. H.; Kwak, B. S.; Do, J. Y.; Kang, M., Effective hydrogen production from propane steam reforming using M/NiO/YSZ catalysts (M= Ru, Rh, Pd, and Ag). *Catalysis Today* **2017**.
50. Profeti, L. P.; Ticianelli, E. A.; Assaf, E. M., Production of hydrogen via steam reforming of biofuels on Ni/CeO₂-Al₂O₃ catalysts promoted by noble metals. *International Journal of Hydrogen Energy* **2009**, *34* (12), 5049-5060.
51. Hajjaji, N.; Chahbani, A.; Khila, Z.; Pons, M.-N., A comprehensive energy-exergy-based assessment and parametric study of a hydrogen production process using steam glycerol reforming. *Energy* **2014**, *64*, 473-483.
52. McCall, M. J.; Kocal, J. A.; Bhattacharyya, A.; Kalnes, T. N.; Brandvold, T. A., Production of aviation fuel from renewable feedstocks. Google Patents: 2011.
53. Pujan, R.; Hauschild, S.; Gröngröft, A., Process simulation of a fluidized-bed catalytic cracking process for the conversion of algae oil to biokerosene. *Fuel Processing Technology* **2017**, *167*, 582-607.
54. Atsonios, K.; Panopoulos, K. D.; Nikolopoulos, N.; Lappas, A. A.; Kakaras, E., Integration of hydroprocessing modeling of bio-liquids into flowsheeting design tools for biofuels production. *Fuel Processing Technology* **2018**, *171*, 148-161.
55. Domínguez-Barroso, M.; Herrera, C.; Larrubia, M.; Alemany, L., Diesel oil-like hydrocarbon production from vegetable oil in a single process over Pt-Ni/Al₂O₃ and

Pd/C combined catalysts. *Fuel Processing Technology* **2016**, *148*, 110-116.

56. Mao, J.; Jiang, D.; Fang, Z.; Wu, X.; Ni, J.; Li, X., Efficient hydrothermal hydrodeoxygenation of triglycerides with in situ generated hydrogen for production of diesel-like hydrocarbons. *Catalysis Communications* **2017**, *90*, 47-50.
57. Keller, T.; Shahani, G., PSA technology: beyond hydrogen purification. *Chemical Engineering* **2016**, *123* (1), 50.
58. Ortiz, F. G.; Serrera, A.; Galera, S.; Ollero, P., Methanol synthesis from syngas obtained by supercritical water reforming of glycerol. *Fuel* **2013**, *105*, 739-751.
59. Ortiz, F. J. G.; Ollero, P.; Serrera, A.; Galera, S., Optimization of power and hydrogen production from glycerol by supercritical water reforming. *Chemical engineering journal* **2013**, *218*, 309-318.
60. Song, C.; Liu, Q.; Ji, N.; Kansha, Y.; Tsutsumi, A., Optimization of steam methane reforming coupled with pressure swing adsorption hydrogen production process by heat integration. *Applied energy* **2015**, *154*, 392-401.
61. Liu, Y.; Sotelo-Boyás, R.; Murata, K.; Minowa, T.; Sakanishi, K., Production of bio-hydrogenated diesel by hydrotreatment of high-acid-value waste cooking oil over ruthenium catalyst supported on Al-polyoxocation-pillared montmorillonite. *Catalysts* **2012**, *2* (1), 171-190.
62. Pongsiriyakul, K.; Kiatkittipong, W.; Kiatkittipong, K.; Laosiripojana, N.; Faungnawakij, K.; Adhikari, S.; Assabumrungrat, S., Alternative Hydrocarbon Biofuel Production via Hydrotreating under a Synthesis Gas Atmosphere. *Energy & Fuels* **2017**, *31* (11), 12256-12262.
63. Kaewmeesri, R.; Srifa, A.; Itthibenchapong, V.; Faungnawakij, K., Deoxygenation of waste chicken fats to green diesel over Ni/Al₂O₃: effect of water and free fatty acid content. *Energy & Fuels* **2015**, *29* (2), 833-840.

64. Srifa, A.; Viriya-empikul, N.; Assabumrungrat, S.; Faungnawakij, K., Catalytic behaviors of Ni/ γ -Al₂O₃ and Co/ γ -Al₂O₃ during the hydrodeoxygenation of palm oil. *Catalysis Science & Technology* **2015**, 5 (7), 3693-3705.
65. Morgan, T.; Santillan-Jimenez, E.; Harman-Ware, A. E.; Ji, Y.; Grubb, D.; Crocker, M., Catalytic deoxygenation of triglycerides to hydrocarbons over supported nickel catalysts. *Chemical Engineering Journal* **2012**, 189, 346-355.
66. Orozco, L. M.; Echeverri, D. A.; Sánchez, L.; Rios, L. A., Second-generation green diesel from castor oil: Development of a new and efficient continuous-production process. *Chemical Engineering Journal* **2017**, 322, 149-156.
67. D.R. Burgess, E. P. J. L. a. W. G. M. Thermochemical Data in NIST Chemistry WebBook, NIST Standard Reference Database Number 69. <https://webbook.nist.gov/chemistry/>.
68. Valencia, D.; García-Cruz, I.; Uc, V. H.; Ramírez-Verduzco, L. F.; Amezcua-Allieri, M. A.; Aburto, J., Unravelling the chemical reactions of fatty acids and triacylglycerides under hydrodeoxygenation conditions based on a comprehensive thermodynamic analysis. *Biomass and Bioenergy* **2018**, 112, 37-44.
69. Yenumala, S. R.; Maity, S. K., Reforming of vegetable oil for production of hydrogen: a thermodynamic analysis. *International Journal of Hydrogen Energy* **2011**, 36 (18), 11666-11675.
70. Immer, J. G.; Kelly, M. J.; Lamb, H. H., Catalytic reaction pathways in liquid-phase deoxygenation of C18 free fatty acids. *Applied Catalysis A: General* **2010**, 375 (1), 134-139.
71. Al-Malah, K. I., *Aspen Plus: Chemical Engineering Applications*. John Wiley & Sons: 2017.
72. Linnhoff, B.; Hindmarsh, E., The pinch design method for heat exchanger networks. *Chemical Engineering Science* **1983**, 38 (5), 745-763.

73. Kemp, I. C., *Pinch analysis and process integration: a user guide on process integration for the efficient use of energy*. Elsevier: 2011.
74. Goto, K.; Yogo, K.; Higashii, T., A review of efficiency penalty in a coal-fired power plant with post-combustion CO₂ capture. *Applied Energy* **2013**, *111*, 710-720.
75. Gutierrez, J. P.; Benítez, L. A.; Martínez, J.; Ale Ruiz, L.; Erdmann, E., Thermodynamic Properties for the Simulation of Crude Oil Primary Refining. **2014**.
76. Guerra, M. J. Aspen HYSYS Property Packages.
<http://sites.poli.usp.br/d/pqi2408/BestPracticesOptimumSimulationsHYSYSPropertyPackages.pdf>.
77. Bandyopadhyay, R.; Upadhyayula, S., Thermodynamic analysis of diesel hydrotreating reactions. *Fuel* **2018**, *214*, 314-321.
78. Boonrod, B.; Prapainainar, C.; Narataruksa, P.; Kantama, A.; Saibautrong, W.; Sudsakorn, K.; Mungcharoen, T.; Prapainainar, P., Evaluating the environmental impacts of bio-hydrogenated diesel production from palm oil and fatty acid methyl ester through life cycle assessment. *Journal of Cleaner Production* **2017**, *142*, 1210-1221.
79. De Almeida, S. C.; Belchior, C. R.; Nascimento, M. V.; dos SR Vieira, L.; Fleury, G., Performance of a diesel generator fuelled with palm oil. *Fuel* **2002**, *81* (16), 2097-2102.

APPENDIX



จุฬาลงกรณ์มหาวิทยาลัย
CHULALONGKORN UNIVERSITY

APPENDIX A

Thermodynamic property methods

Principle selection of thermodynamic property methods is based on categories of difference, such as polar vs. non-polar, ideal liquid vs. non-ideal liquid, and high pressure vs. low pressure, including type of process. For operating condition at high pressure (>10 bar), an equation of state method such as SRK and PSRK⁷¹ is used. Furthermore, literature review provided the thermodynamic property method for hydrotreating operating condition at high pressure and high temperature, such as NRTL-RK^{6, 39}, NRTL^{1, 34, 47}, PENG-ROB^{1, 16, 32, 36, 40, 53}, BK10³⁵, PC-SAFT³⁷, RK-ASPEN^{32, 38, 43}, PSRK^{33, 54}, CHAO-SEA⁷⁵⁻⁷⁶, GRAYSON⁷⁶, and SRK⁷⁷.

The thermodynamic property method model in Aspen Plus was simulated in order to select the appropriate thermodynamic property method for the hydrotreating process, which was considered and was compared with thermodynamic models from literature reviews^{26, 40, 67-68} such as enthalpy of TGs, heat of reaction, including density of triolein and tripalmitin compared to NIST ThermoData Engine⁷¹.

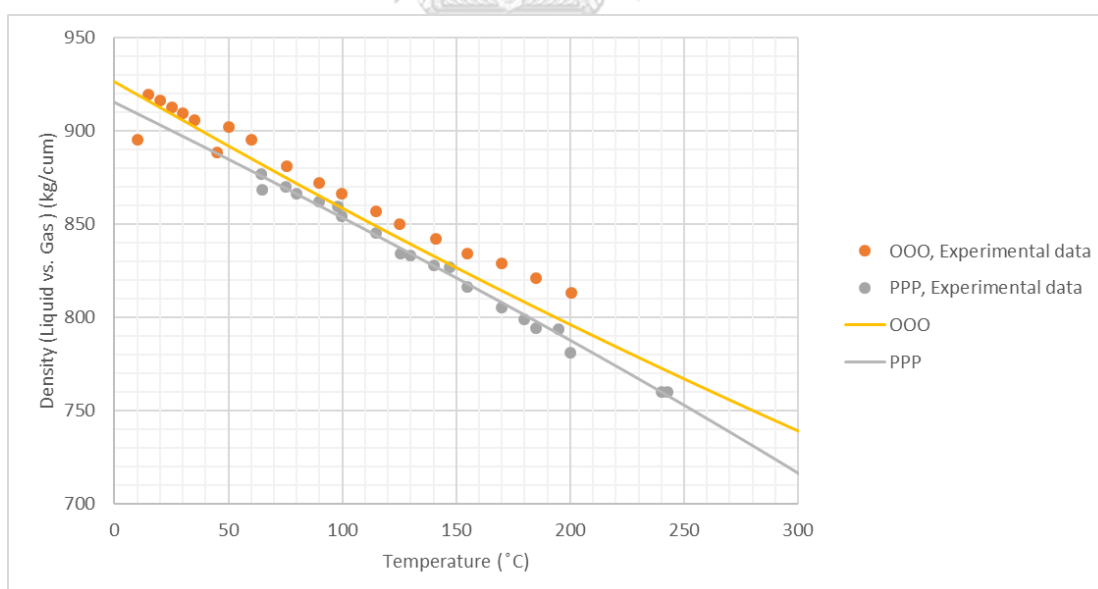


Figure A.1 Density of tripalmitin and triolein with various temperatures at pressure 1.0 bar.

The density of tripalmitin and triolein at various temperatures at pressure of 1.0 bar is shown in Figure A.1 The results of density from the NRTL model estimation are close to the experimental data⁷¹.

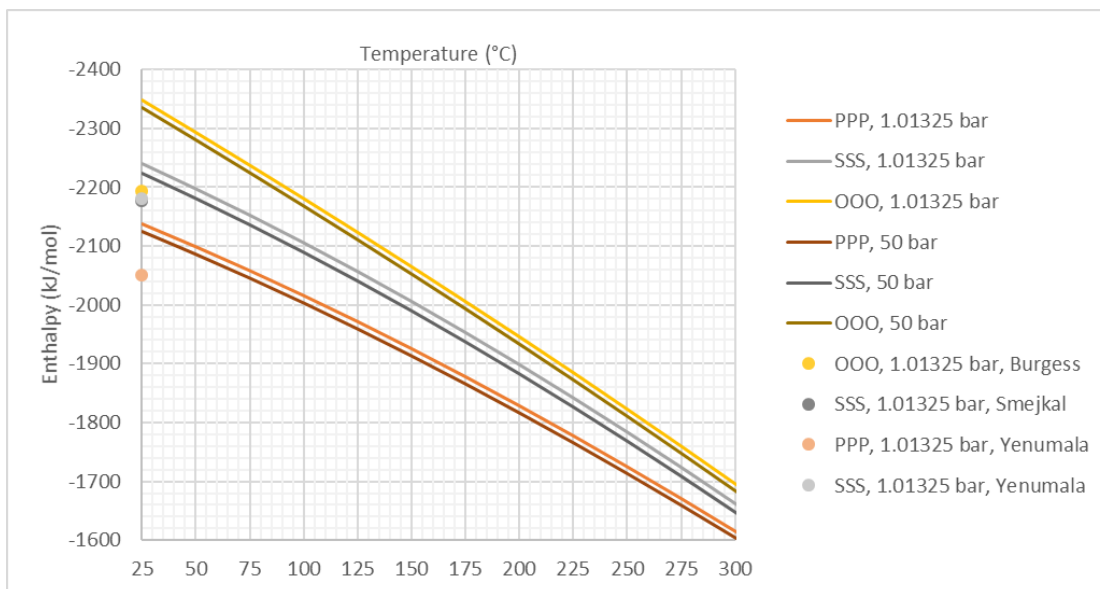


Figure A.2 Enthalpy of tripalmitin, tristearin and triolein with various temperatures at pressure 1.0 bar and 50 bar.

The enthalpy of TGs at various temperatures at pressure of 1.0 and 50 bar is shown in Figure A.2. The enthalpy values at the two pressures are very close to one another, thus, pressure slightly affects enthalpy of TGs. Moreover, at 25 °C, enthalpy of tristearin obtained from the PSRK thermodynamic model is similar to the result of Smejkal⁴⁰ and Yenumala⁶⁹, but enthalpy of tripalmitin and triolein obtained from the PSRK thermodynamic model had an error of 4.31% and 7.02% compared to the result of Yenumala⁶⁹ and Burgess⁶⁷, respectively. However, the present work was operated at temperature of 300 °C and pressure of 50 bar for the hydrotreating process.

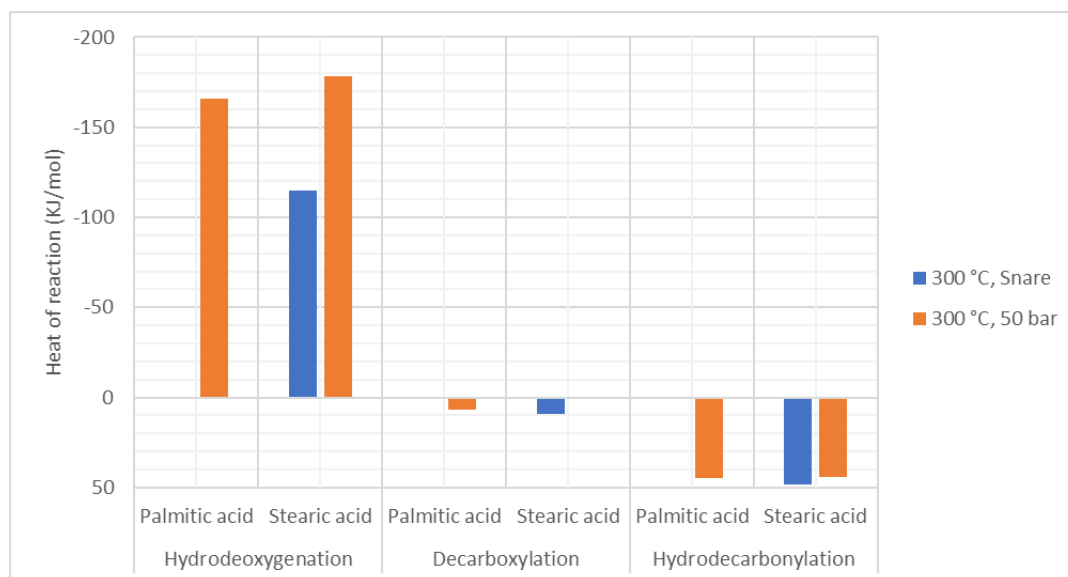


Figure A.3 Heat of deoxygenation reaction of palmitic acid and stearic acid at temperature of 300 °C and pressure of 50 bar.

Figure A.3 shows the heat of deoxygenation reaction at temperature of 300 °C and pressure of 50 bar obtained from the PSRK thermodynamic model, which is consistent with the report by Snare and co-workers²⁶ at 300 °C for exothermic of the hydrodeoxygenation reaction, endothermic of the hydrodecarbonylation reaction, and slightly endothermic of the decarboxylation reaction.

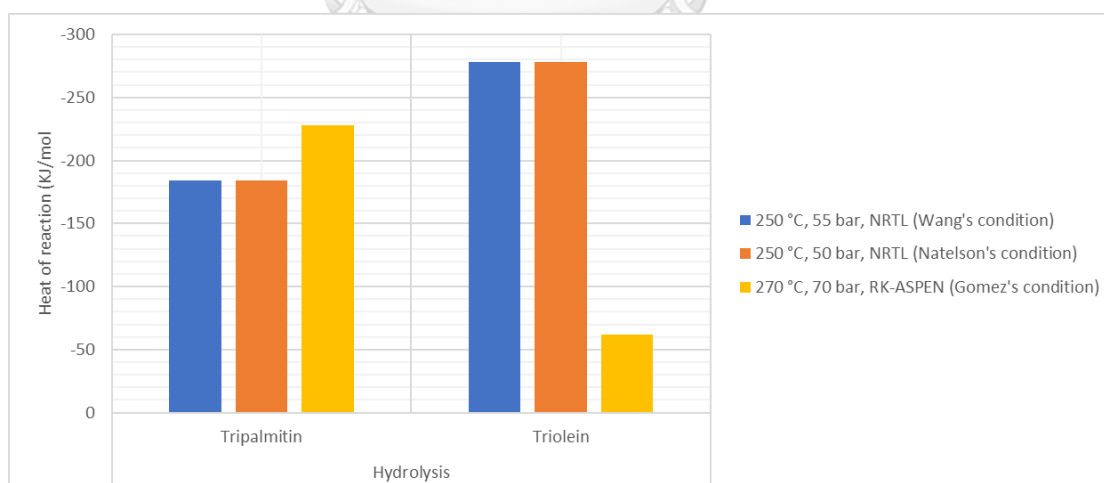


Figure A.4 Heat of hydrolysis reaction of triglycerides at high temperature and high pressure.

Figure A.4 shows the heat of hydrolysis reaction at temperature of 250 °C between pressure of 55 (Wang's condition⁴⁵) and 50 bar (Natelson's condition⁴⁷)

obtained from the NRTL thermodynamic model, and at temperature of 270 °C and pressure of 70 bar (Gomez's condition⁴³) obtained from the RK-ASPEN thermodynamic model. At high temperature and high pressure, the hydrolysis reaction is an exothermic reaction.



APPENDIX B

Hydrogen to oil molar ratio

Srifa and co-workers² reported H₂/oil ratio should be higher than 3-5 times of theoretical requirement of hydroprocessing via hydrogenation and hydrodeoxygenation.

Palm oil consisting of 50% of tripalmitin and 50% of triolein, 1 mole of palm oil will consume 13.5 moles of H₂ (6 moles for tripalmitin, 7.5 moles for triolein)

1 mole of palm oil consume 13.5 moles of H₂
 Density of palm oil 0.903 g/mL
 Molecular weight of palm oil 838 g/mol

1 mole of H₂ occupied 22.4 L at standard temperature and pressure
 Molecular weight of H₂ 2 g/mol

Solution

$$1 \text{ mol of palm oil} = 1 \text{ mol} \times 838 \frac{\text{g}}{\text{mol}} = 838 \text{g}$$

$$= 838 \text{ g} \times \frac{1 \text{ mL}}{0.903 \text{ g}} = 928.02 \text{ ml}$$

$$1 \text{ mol of H}_2 = 22.4 \text{ L}$$

$$2 \text{ g of H}_2 = 22.4 \text{ L}$$

$$\text{Density of H}_2 = \frac{2 \text{ g}}{22.4 \text{ L}} = 0.089 \text{ g/L}$$

$$= 0.089 \frac{\text{g}}{\text{L}} \times \frac{1 \text{ L}}{1000 \text{ mL}} = 8.95 \times 10^{-5} \frac{\text{g}}{\text{mL}}$$

$$13.5 \text{ mol of H}_2 = 13.5 \text{ mol} \times \frac{2 \text{ g}}{1 \text{ mol}} = 27 \text{g}$$

$$= 27 \text{g} \times \frac{1 \text{ mL}}{8.92 \times 10^{-5} \text{ g}} = 302,690.583 \text{ mL}$$

928.02 mL of palm oil consume 302,690.583 mL of H₂

$$1 \text{ mL of palm oil consume } \frac{302,690.583}{928.02} = 326.17 \text{ mL of H}_2$$

(Srifa and co-worker² determined that 1 mL of palm oil will consume about 325 mL of hydrogen)

The highest production yield 1000 N (cm³/cm³) of H₂ to palm oil ratio

or 1 mL of palm oil feed 1,000 mL of H₂

$$\begin{aligned} \text{Suggesting the hydrogen feed} &= \frac{1000 \text{ mL of H}_2 \text{ feed}}{326.17 \text{ mL of H}_2 \text{ required}} \\ &= 3.07 \text{ times as the ratio consume H}_2 \text{ to oil} \end{aligned}$$

$$\text{Or 1 mL of palm oil} = 1 \text{ mL} \times \frac{1 \text{ mol}}{928.02 \text{ mL}} = 1.0776 \times 10^{-3} \text{ mol}$$

$$\text{Feed H}_2 \text{ 1000 mL} = 1000 \text{ mL} \times \frac{1 \text{ L}}{1000 \text{ mL}} \times \frac{1 \text{ mol}}{22.4 \text{ L}} = 0.0447 \text{ mol}$$

$$1 \text{ mol of palm oil feed} \frac{0.0447}{1.0776 \times 10^{-3}} = 41.48 \text{ mol of H}_2$$

$$\begin{aligned} \text{Suggesting the hydrogen feed} &= \frac{41.48 \text{ mol of H}_2 \text{ feed}}{13.5 \text{ mol of H}_2 \text{ required}} \\ &= 3.07 \text{ times as the ratio consume H}_2 \text{ to oil} \end{aligned}$$

Thus, 3.0 times of the theoretical requirement of the H₂/oil molar ratio is an initial feed for this work.

APPENDIX C

Water to oil molar ratio

Gomez-Castro and co-workers⁴³ reported simulation of hydrolysis reactor with feed rate 2,476.45 kmol/h of water and 45.89 kmol/h of triolein, water to oil volumetric ratio of 1:1.

Feed rate	2476.45 kmol/h
Feed rate	45.89 kmol/h of triolein
Density of triolein at STP	909.2 kg/m ³ , 0.9092 g/cm ³
Density of water at STP	998.2071 kg/m ³ , 0.9982 g/cm ³
Molecular weight of triolein	885.44 g/mol
Molecular weight of water	18 g/mol

Solution

$$\text{Feed water to oil molar ratio} = \frac{2476.45 \text{ kmol/h}}{45.89 \text{ kmol/h}} = 53.96 \approx 54$$

$$\text{Or the water feed} = \frac{54 \text{ mol of H}_2\text{O feed per triolein}}{3 \text{ mol of H}_2\text{O required per triolein}} = 18 \text{ times}$$

as the ratio consumed H₂O to oil

Calculation volumetric ratio of water to triolein

$$\begin{aligned} \text{Triolein} = 45.89 \text{ kmol} &= 45.89 \text{ kmol} \times \frac{885.44 \text{ kg}}{1 \text{ kmol}} = 40,632 \text{ kg} \\ &= 40,632 \text{ kg} \times \frac{1 \text{ m}^3}{909.2 \text{ kg}} = 44.69 \text{ m}^3 \end{aligned}$$

$$\begin{aligned} \text{Water} = 2,476.45 \text{ kmol} &= 2,476.45 \text{ kmol} \times \frac{18 \text{ kg}}{1 \text{ kmol}} = 44,576.1 \text{ kg} \\ &= 44,576.1 \text{ kg} \times \frac{1 \text{ m}^3}{998.2071 \text{ kg}} = 44.66 \text{ m}^3 \end{aligned}$$

$$\text{Volumetric ratio of water to triolein} = \frac{44.66 \text{ m}^3}{44.69 \text{ m}^3} = 0.99924 \approx 1$$

Thus, 54.0 of the water to oil molar ratio is an initial feed for this work.

APPENDIX D

Sensitivity result curve

Sensitivity to temperature of cooler was simulated in order to define optimum temperature for integrated system of hydrotreating and hydrogen generation with HDO reaction pathway in order to reduce volume of PSA unit by separation H₂O.

The integrated system of single-step of hydrotreating and PSR with HDO reaction pathway was sensitivity to temperature of CL-2 and temperature of CL-7 as shown in Figure D.1 and Figure D.2 from tripalmitin and Figure D.3 and Figure D.4 from triolein, respectively.

Figure D.1 and Figure D.3 demonstrated that at temperature is higher than 152 °C and 146 °C from tripalmitin and triolein, respectively, the process could not separate H₂O and at low temperature, C₃H₈ could not become total vapor. However, Figure D.1, at higher temperature, the process provided higher purity of C₁₆H₃₄, but composition of C₁₆H₃₄ was decreased. Highest of carbon recovery ratio was considered for selected temperature of 117 °C, which provided recovery ratio of C₁₆H₃₄ and C₃H₈ equal 99.82% and 91.80%, respectively and H₂O was separated equal 4.12 kmol/h (H₂O was produced 6 kmol/h). Figure D.3 at higher temperature, the process provided higher purity of C₁₈H₃₈, but composition of C₁₈H₃₈ was decreased. Temperature was selected at 126 °C, which provided recovery ratio of C₁₈H₃₈ and C₃H₈ equal 99.93% and 93.87%, respectively and H₂O was separated equal 2.87 kmol/h (H₂O was produced 6 kmol/h).

Figure D.2 and Figure D.4 demonstrated that at higher temperature, the process could separate lower H₂O. But at low temperature, the process need high cooling utility. Thus, Figure D.2 was selected temperature of 40 °C, which provided 6.07 kmol/h of flow rate of H₂O and Figure D.4 was selected temperature of 40 °C, which provided 6.22 kmol/h of flow rate of H₂O.

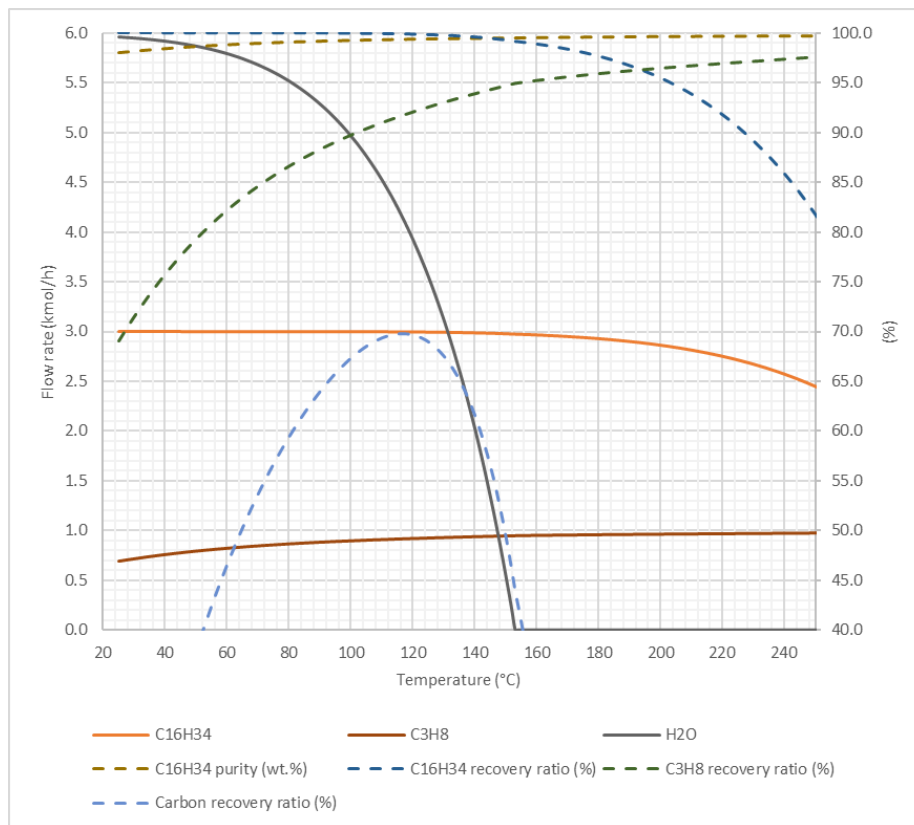


Figure D.1 Sensitivity composition of separation with various temperatures of CL-2 from tripalmitin.

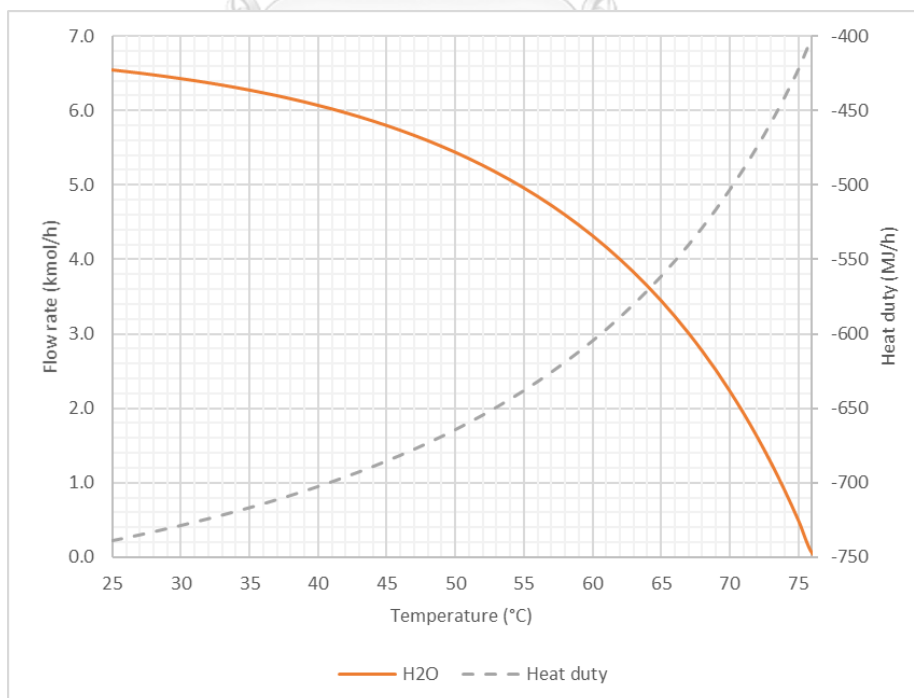


Figure D.2 Sensitivity composition of separation with various temperatures of CL-7 from tripalmitin.

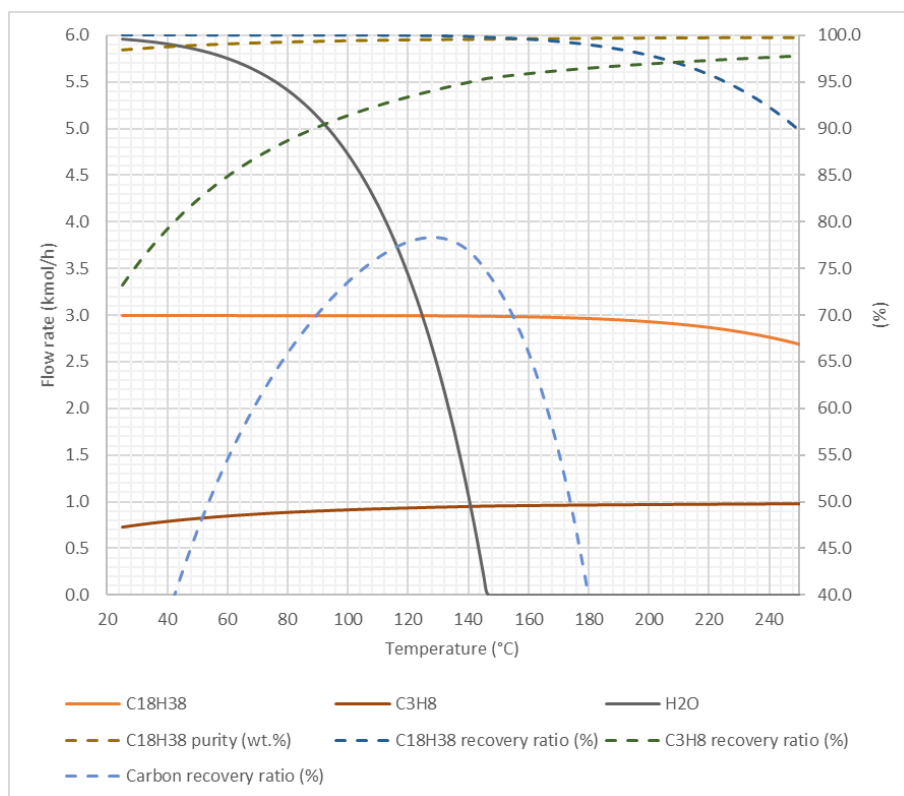


Figure D.3 Sensitivity composition of separation with various temperatures of CL-2 from triolein.

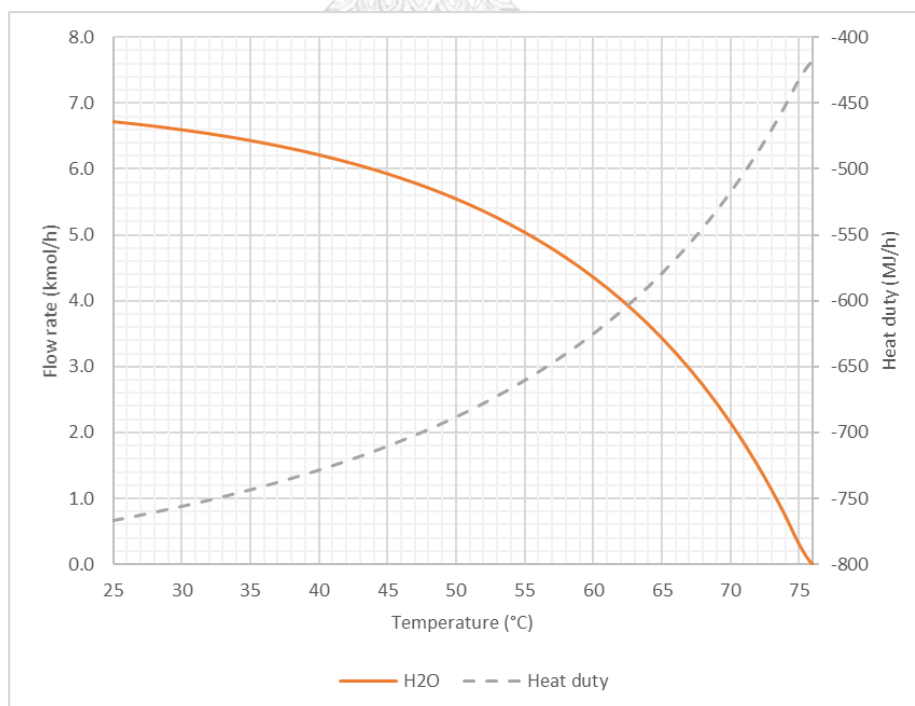


Figure D.4 Sensitivity composition of separation with various temperatures of CL-7 from triolein.

The integrated system of two-step of hydrotreating and GSR with HDO reaction pathway was sensitivity to temperature of CL-5 and temperature of CL-9 as shown in Figure D.5 and Figure D.6 from tripalmitin and Figure D.7 and Figure D.8 from triolein, respectively.

Figure D.5 and Figure D.7 demonstrated that at temperature is higher than 180 °C and 170 °C, from tripalmitin and triolein, respectively, the process could not separate H₂O and at higher temperature, the process could separate lower H₂O and lower purity of H₂O. But at low temperature, the process need high cooling utility. Thus, Figure D.5 was selected temperature of 40 °C, which provided recovery ratio of C₁₆H₃₄ equal 97.16%, 7.23 kmol/h of flow rate of H₂O and purity of C₁₆H₃₄ and H₂O equal 99.97% and 99.12%, respectively. Figure D.7 was selected temperature of 40 °C, which provided recovery ratio of C₁₈H₃₈ equal 98.75%, 7.44 kmol/h of flow rate of H₂O and purity of C₁₈H₃₈ and H₂O equal 99.97% and 99.21%, respectively.

Figure D.6 and Figure D.8 demonstrated that at higher temperature, the process could separate lower H₂O. But at low temperature, the process need high cooling utility. Thus, Figure D.6 was selected temperature of 40 °C, which provided 6.30 kmol/h of flow rate of H₂O and Figure D.8 was selected temperature of 40 °C, which provided 6.31 kmol/h of flow rate of H₂O.

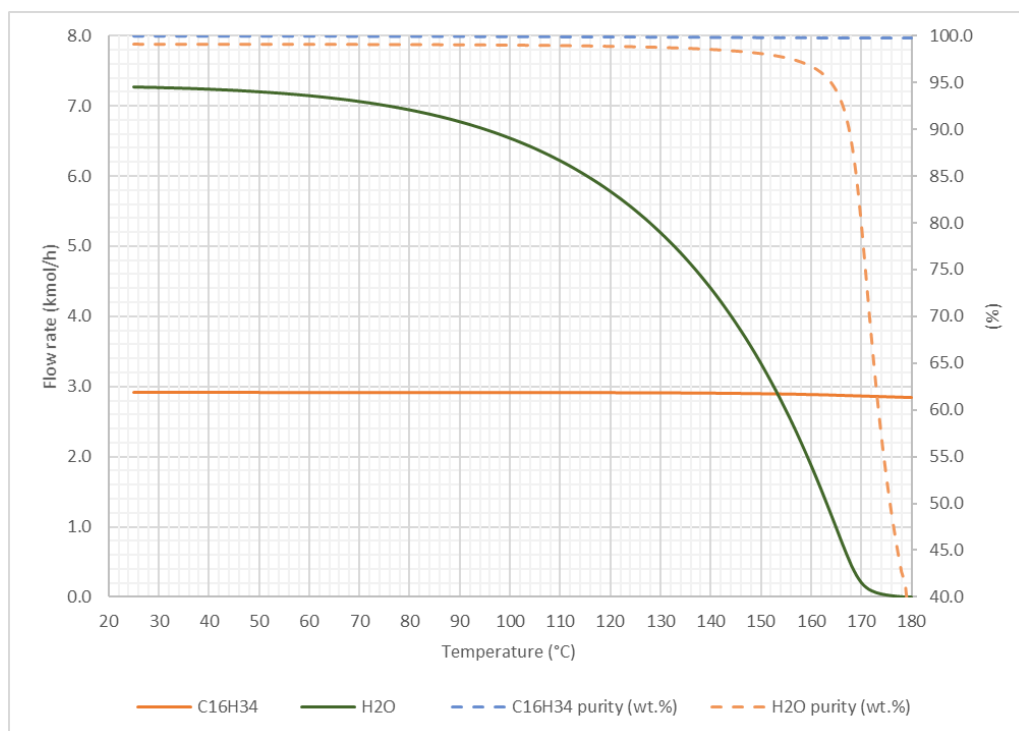


Figure D.5 Sensitivity composition of separation with various temperatures of CL-5 from tripalmitin.

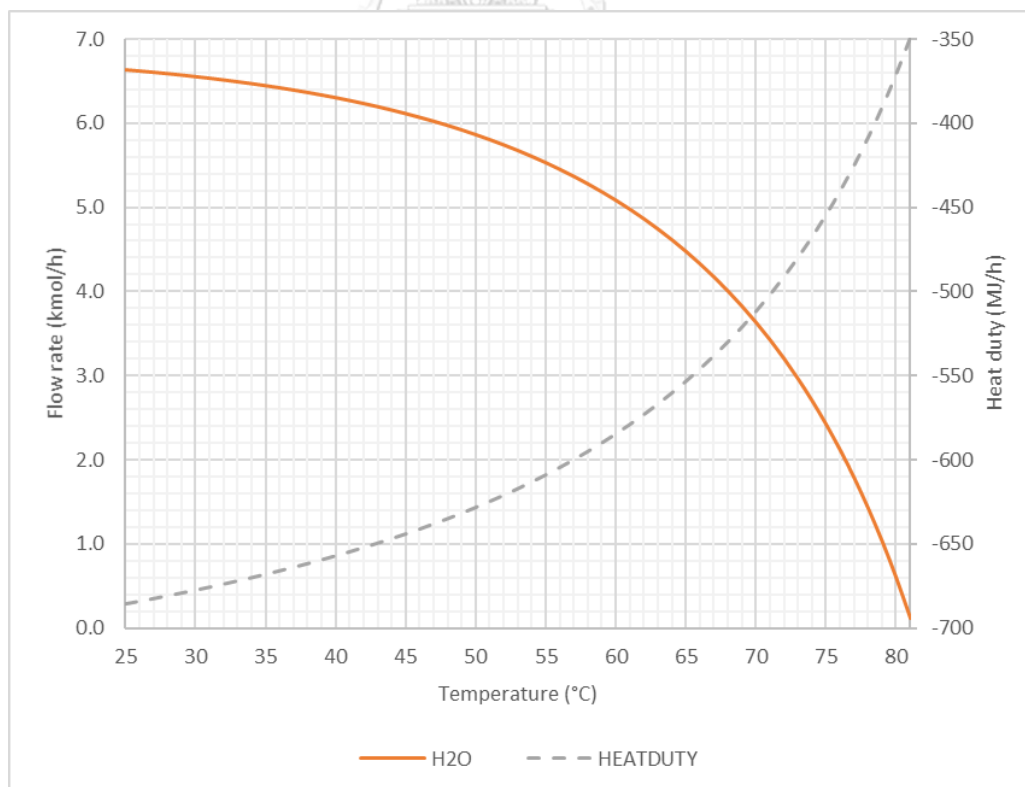


Figure D.6 Sensitivity composition of separation with various temperatures of CL-9 from tripalmitin.

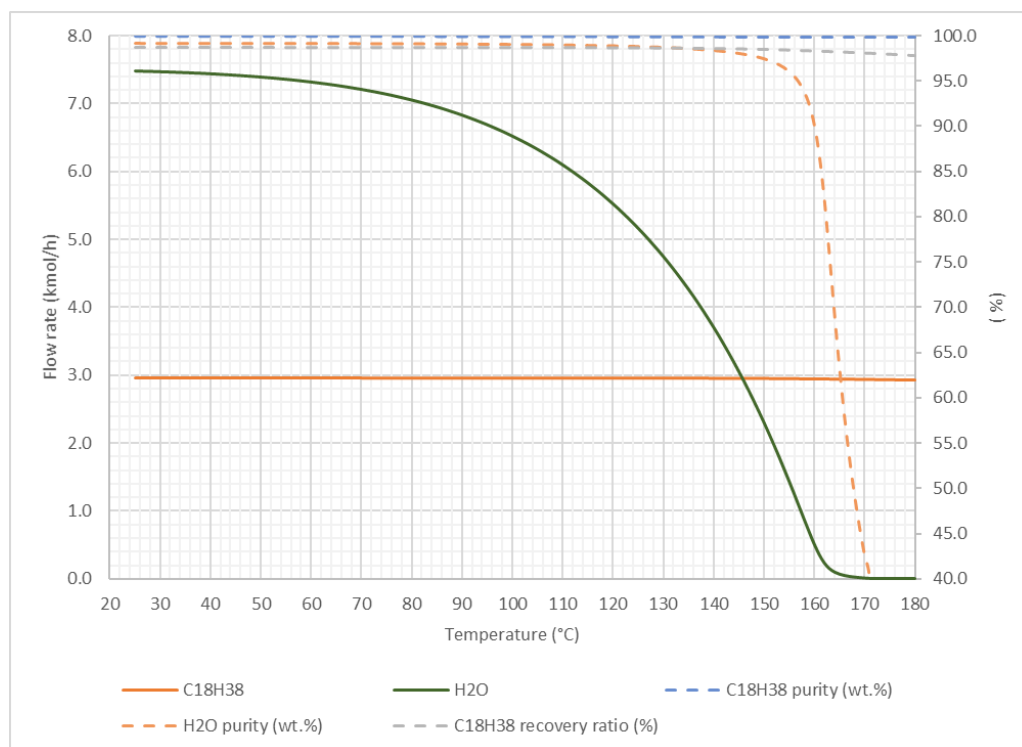


Figure D.7 Sensitivity composition of separation with various temperatures of CL-5 from triolein.

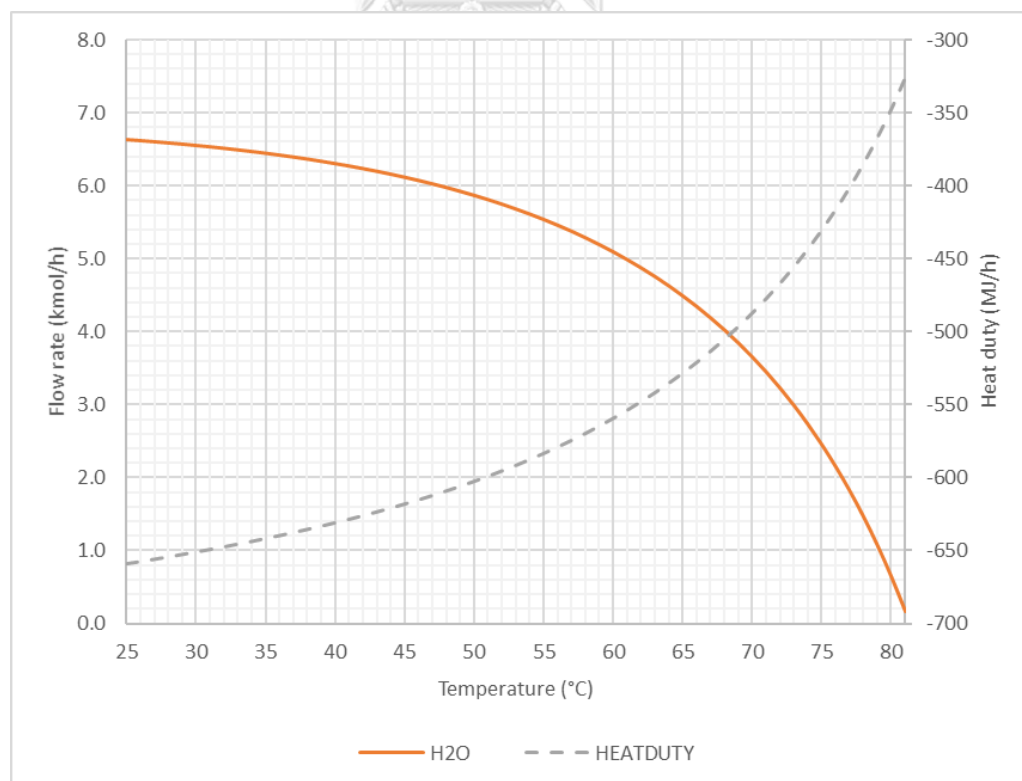


Figure D.8 Sensitivity composition of separation with various temperatures of CL-9 from triolein.

APPENDIX E

Calculator and design specs function of integrated system

Table E.1 Calculator specification of flow rate calculation of M-H2O-1 stream.

Define	Variable	Category	Type	Stream	Component	Units
	C3H8P	Streams	Mole-Flow	BP-1	C ₃ H ₈	kmol/h
	H2OP	Streams	Mole-Flow	BP-1	H ₂ O	kmol/h
	H2O2F	Streams	Mole-Flow	M-H2O-1	H ₂ O	kmol/h
	C3H8R	Streams	Mole-Flow	M-H2O-1	C ₃ H ₈	kmol/h
Calculate	Calculation method		Fortran			
	Executable Fortran statements		H2O2F=(12*(C3H8P+C3H8R))-H2OP			
Sequence	Execute		Before			
	Block type		Unit operation			
	Block name		MX-2			

Table E.2 Calculator specification of flow rate calculation of H₂O-4 stream.

Define	Variable	Category	Type	Stream/ Block	Variable	ID1	Units
	SP1	Blocks	Block-Var	SP-1	FLOW/FRAC	M-H2O-1	kmol/h
	RH2O1	Streams	Stream-Var	R-H2O-1	MOLE-FLOW	-	kmol/h
	RH2O4	Streams	Stream-Var	R-H2O-4	MOLE-FLOW	-	kmol/h
	H2O4F	Streams	Stream-Var	H2O-4	MOLE-FLOW	-	kmol/h
	H2O2	Streams	Stream-Var	M-H2O-1	MOLE-FLOW	-	kmol/h
Calculate	Calculation method		Fortran				
	Executable Fortran statements		SP1=H2O2 H2O4F=SP1-RH2O1-RH2O4				
Sequence	Execute		Before				
	Block type		Unit operation				
	Block name		SP-1				

Table E.3 Calculator specification of flow rate calculation of H2-3 stream.

Define	Variable	Category	Type	Stream/ Block	Variable	ID1	Units
	SP2	Blocks	Block-Var	SP-2	FLOW/FRAC	M-H2-1	kmol/h
	RH21	Streams	Stream-Var	R-H2-1	MOLE-FLOW	-	kmol/h
	RH23	Streams	Stream-Var	R-H2-3	MOLE-FLOW	-	kmol/h
	H23F	Streams	Stream-Var	H2-3	MOLE-FLOW	-	kmol/h
	H21	Streams	Stream-Var	M-H2-1	MOLE-FLOW	-	kmol/h
Calculate	Calculation method		Fortran				
	Executable Fortran statements		SP2=H21 H23F=SP2-RH21-RH23				
Sequence	Execute		Before				
	Block type		Unit operation				
	Block name		SP-2				

Table E.4 Design specification with various temperatures of HT-5 equipment.

Define	Variable	Category	Type	Stream	Component	Units
	H2OL	Streams	Mole-Flow	BP-2	H ₂ O	kmol/h
	GLYL	Streams	Mole-Flow	BP-2	Glycerol	kmol/h
Spec	Spec			H2OL		
	Target			9*GLYL		
	Tolerance			0.0001		
Vary	Type			Block-Var		
	Block			HT-5		
	Variable			TEMP		
	Units			°C		
	Manipulated variable limits		Lower	100		
			Upper	110		

Table E.5 Calculator specification of flow rate calculation of H2O-5 stream.

Define	Variable	Category	Type	Stream/ Block	Variable	ID1	Units
	SP3	Blocks	Block-Var	SP-3	FLOW/FAC	S84	kmol/h
	RH2O2	Streams	Stream-Var	R-H2O-2	MOLE-FLOW	-	kmol/h
	RH2O3	Streams	Stream-Var	R-H2O-3	MOLE-FLOW	-	kmol/h
	RH2O5	Streams	Stream-Var	R-H2O-5	MOLE-FLOW	-	kmol/h
	H2O5F	Streams	Stream-Var	H2O-5	MOLE-FLOW	-	kmol/h
	H2O1	Streams	Stream-Var	M-H2O-2	MOLE-FLOW	-	kmol/h
Calculate	Calculation method		Fortran				
	Executable Fortran statements		SP3=H2O1 H2O5F=SP3-RH2O2-RH2O3-RH2O5				
Sequence	Execute		Before				
	Block type		Unit operation				
	Block name		SP-3				

Table E.6 Calculator specification of flow rate calculation of H2-4 stream.

Define	Variable	Category	Type	Stream/ Block	Variable	ID1	Units
	SP4	Blocks	Block-Var	SP-4	FLOW/FRAC	M-H2-2	kmol/h
	RH22	Streams	Stream-Var	R-H2-2	MOLE-FLOW	-	kmol/h
	RH24	Streams	Stream-Var	R-H2-4	MOLE-FLOW	-	kmol/h
	H24F	Streams	Stream-Var	H2-4	MOLE-FLOW	-	kmol/h
	H22	Streams	Stream-Var	M-H2-2	MOLE-FLOW	-	kmol/h
Calculate	Calculation method	Fortran					
	Executable Fortran statements	SP4=H22 H24F=SP4-RH22-RH24					
Sequence	Execute	Before					
	Block type	Unit operation					
	Block name	SP-4					

APPENDIX F

The results of integrated system of hydrotreating and hydrogen generation



Table F.1 The results of integrated system of single-step of hydrotreating and PSR with various selectivity of DO reaction pathways from tripalmitin.

Selectivity of DO		Initial Feed				C ₁₅ H ₃₂ in BHD		C ₁₆ H ₃₄ in BHD		BHD	BHD purity (mol%)	BHD purity (wt.%)	Off-gas (kmol/h)
DCO ₂	HDCO	HDO	H ₂ (kmol/h)	Net H ₂ O (kmol/h)	Net H ₂ (kmol/h)	(kmol/h)	(kmol/h)	(kmol/h)	(kmol/h)	(kmol/h)	(mol%)	(wt.%)	(kmol/h)
1	0	0	9.00	-3.63	2.31	2.997	0.000	3.43	87.41	97.48	6.62		
0	1	0	18.00	-3.17	1.37	2.996	0.000	3.23	92.70	98.96	7.50		
0	0	1	36.00	1.02	-5.39	0.000	2.996	3.18	94.09	99.37	4.55		
0.5	0.5	0	13.50	-3.50	1.99	2.996	0.000	3.31	90.52	98.42	7.16		
0.5	0	0.5	22.50	-1.39	-1.40	1.497	1.499	3.26	92.01	98.85	5.74		
0	0.5	0.5	27.00	-1.13	-1.94	1.497	1.499	3.20	93.54	99.21	6.06		
0.45	0.45	0.1	15.75	-3.07	1.28	2.696	0.300	3.29	91.13	98.59	6.92		
0.4	0.4	0.2	18.00	-2.63	0.55	2.396	0.600	3.27	91.65	98.73	6.68		
0.35	0.35	0.3	20.25	-2.18	-0.18	2.097	0.899	3.25	92.10	98.85	6.43		
0.3	0.3	0.4	22.50	-1.73	-0.91	1.797	1.199	3.24	92.49	98.96	6.17		
0.25	0.25	0.5	24.75	-1.27	-1.66	1.497	1.499	3.23	92.84	99.05	5.91		
0.2	0.2	0.6	27.00	-0.81	-2.40	1.198	1.798	3.22	93.14	99.13	5.64		
0.15	0.15	0.7	29.25	-0.36	-3.15	0.898	2.098	3.21	93.42	99.20	5.37		
0.1	0.1	0.8	31.50	0.10	-3.89	0.599	2.397	3.20	93.67	99.26	5.10		
0.05	0.05	0.9	33.75	0.56	-4.64	0.299	2.697	3.19	93.89	99.32	4.83		
0.45	0.1	0.45	22.05	-1.59	-1.10	1.647	1.349	3.25	92.08	98.86	5.92		
0.4	0.2	0.4	21.60	-1.78	-0.81	1.797	1.199	3.25	92.14	98.87	6.10		
0.35	0.3	0.35	21.15	-1.97	-0.52	1.947	1.049	3.25	92.21	98.88	6.28		
0.3	0.4	0.3	20.70	-2.15	-0.23	2.097	0.899	3.25	92.28	98.89	6.46		
0.25	0.5	0.25	20.25	-2.33	0.05	2.247	0.749	3.24	92.35	98.91	6.64		
0.2	0.6	0.2	19.80	-2.50	0.32	2.396	0.600	3.24	92.42	98.92	6.81		
0.15	0.7	0.15	19.35	-2.68	0.59	2.546	0.450	3.24	92.48	98.93	6.99		
0.1	0.8	0.1	18.90	-2.84	0.86	2.696	0.300	3.24	92.56	98.94	7.16		
0.05	0.9	0.05	18.45	-3.01	1.12	2.846	0.150	3.23	92.63	98.95	7.33		
0.1	0.45	0.45	25.20	-1.40	-1.48	1.647	1.349	3.21	93.20	99.13	6.15		
0.2	0.4	0.4	23.40	-1.67	-1.03	1.797	1.199	3.23	92.81	99.03	6.23		
0.3	0.35	0.35	21.60	-1.94	-0.57	1.947	1.049	3.24	92.39	98.93	6.31		
0.4	0.3	0.3	19.80	-2.21	-0.12	2.097	0.899	3.26	91.91	98.80	6.39		
0.5	0.25	0.25	18.00	-2.47	0.32	2.247	0.749	3.28	91.37	98.67	6.47		
0.6	0.2	0.2	16.20	-2.73	0.76	2.396	0.600	3.30	90.75	98.51	6.53		
0.7	0.15	0.15	14.40	-2.99	1.19	2.546	0.450	3.33	90.05	98.32	6.59		
0.8	0.1	0.1	12.60	-3.24	1.61	2.696	0.300	3.36	89.23	98.10	6.64		
0.9	0.05	0.05	10.80	-3.45	1.98	2.846	0.150	3.39	88.44	97.83	6.64		

Table F.1 The results of integrated system of single-step of hydrotreating and PSR with various selectivity of DO reaction pathways from tripalmitin. (*Continued*).

Selectivity of DO		Heating	Cooling	Utility	Electricity	MER	Total MER	Thermal efficiency	Total efficiency
DCO ₂	HDCO	HDO	(MJ/h)	(MJ/h)	(kW)	(MJ/h)	(MJ/h)	(%)	(%)
1	0	0	1,759	2,034	138	997	1,690	96.15	96.15
0	1	0	1,708	2,316	238	937	2,754	95.36	95.36
0	0	1	1,773	3,399	368	1,758	6,347	96.20	96.20
0.5	0.5	0	1,724	2,188	192	989	2,242	95.87	95.87
0.5	0	0.5	1,797	2,752	258	1,377	4,035	96.23	96.23
0	0.5	0.5	1,743	2,865	304	1,347	4,547	95.81	95.81
0.45	0.45	0.1	1,758	2,317	210	1,043	2,632	95.90	95.90
0.4	0.4	0.2	1,764	2,445	229	1,121	3,048	95.93	95.93
0.35	0.35	0.3	1,768	2,570	247	1,200	3,464	95.96	95.96
0.3	0.3	0.4	1,770	2,692	264	1,282	3,877	96.00	96.00
0.25	0.25	0.5	1,772	2,810	281	1,362	4,289	96.03	96.03
0.2	0.2	0.6	1,772	2,929	299	1,444	4,702	96.07	96.07
0.15	0.15	0.7	1,772	3,047	316	1,523	5,115	96.10	96.10
0.1	0.1	0.8	1,772	3,164	333	1,603	5,527	96.14	96.14
0.05	0.05	0.9	1,772	3,282	350	1,681	5,937	96.17	96.17
0.45	0.1	0.45	1,789	2,710	257	1,332	3,903	96.16	96.16
0.4	0.2	0.4	1,780	2,667	255	1,287	3,774	96.08	96.08
0.35	0.3	0.35	1,772	2,624	253	1,242	3,644	96.00	96.00
0.3	0.4	0.3	1,763	2,581	251	1,197	3,516	95.91	95.91
0.25	0.5	0.25	1,754	2,538	250	1,153	3,388	95.82	95.82
0.2	0.6	0.2	1,745	2,494	247	1,110	3,260	95.74	95.74
0.15	0.7	0.15	1,736	2,449	245	1,067	3,132	95.65	95.65
0.1	0.8	0.1	1,727	2,405	243	1,024	3,006	95.56	95.56
0.05	0.9	0.05	1,717	2,360	240	981	2,879	95.46	95.46
0.1	0.45	0.45	1,752	2,789	289	1,312	4,264	95.86	95.86
0.2	0.4	0.4	1,760	2,713	273	1,276	3,980	95.91	95.91
0.3	0.35	0.35	1,767	2,636	258	1,239	3,696	95.96	95.96
0.4	0.3	0.3	1,772	2,558	242	1,203	3,412	96.00	96.00
0.5	0.25	0.25	1,777	2,477	226	1,167	3,126	96.05	96.05
0.6	0.2	0.2	1,779	2,394	210	1,130	2,839	96.10	96.10
0.7	0.15	0.15	1,752	2,310	194	1,119	2,578	96.14	96.14
0.8	0.1	0.1	1,753	2,223	177	1,078	2,288	96.18	96.18
0.9	0.05	0.05	1,771	2,132	158	1,028	1,977	96.18	96.18

Table F.2 The results of integrated system of single-step of hydrotreating and PSR with various selectivity of DO reaction pathways from triolein.

Selectivity of DO		Initial Feed		Net H ₂ O	Net H ₂	C ₁₇ H ₃₆ in BHD	C ₁₈ H ₃₈ in BHD	BHD (kmol/h)	BHD purity (mol%)	BHD purity (wt.%)	Off-gas (kmol/h)
DCO ₂	HDCO	HDO	H ₂								
1	0	0	18.00	-3.97	-0.28	2.998	0.000	3.30	90.93	98.62	7.12
0	1	0	27.00	-3.34	-1.49	2.997	0.000	3.20	93.61	99.32	7.76
0	0	1	45.00	0.92	-8.35	0.000	2.998	3.17	94.46	99.54	4.73
0.5	0.5	0	22.50	-3.72	-0.79	2.997	0.000	3.24	92.42	99.04	7.48
0.5	0	0.5	31.50	-1.54	-4.28	1.498	1.499	3.22	93.07	99.24	5.99
0	0.5	0.5	36.00	-1.26	-4.88	1.498	1.499	3.19	94.10	99.45	6.26
0.45	0.45	0.1	24.75	-3.27	-1.53	2.697	0.300	3.24	92.65	99.11	7.22
0.4	0.4	0.2	27.00	-2.81	-2.29	2.398	0.600	3.23	92.91	99.18	6.96
0.35	0.35	0.3	29.25	-2.34	-3.04	2.098	0.900	3.22	93.17	99.24	6.68
0.3	0.3	0.4	31.50	-1.88	-3.80	1.798	1.199	3.21	93.41	99.30	6.41
0.25	0.25	0.5	33.75	-1.41	-4.56	1.498	1.499	3.20	93.62	99.35	6.13
0.2	0.2	0.6	36.00	-0.94	-5.32	1.199	2.799	3.19	93.82	99.40	5.85
0.15	0.15	0.7	38.25	-0.48	-6.08	0.899	4.099	3.19	94.00	99.44	5.57
0.1	0.1	0.8	40.50	-0.01	-6.84	0.599	5.398	3.18	94.16	99.48	5.29
0.05	0.05	0.9	42.75	0.46	-7.60	0.300	6.698	3.18	94.32	99.51	5.01
0.45	0.1	0.45	31.05	-1.74	-3.98	1.648	1.349	3.22	93.13	99.25	6.17
0.4	0.2	0.4	30.60	-1.93	-3.68	1.798	1.199	3.22	93.18	99.25	6.35
0.35	0.3	0.35	30.15	-2.12	-3.39	1.948	1.049	3.21	93.23	99.26	6.53
0.3	0.4	0.3	29.70	-2.31	-3.11	2.098	0.900	3.21	93.29	99.27	6.71
0.25	0.5	0.25	29.25	-2.49	-2.83	2.248	0.750	3.21	93.34	99.28	6.89
0.2	0.6	0.2	28.80	-2.67	-2.55	2.398	0.600	3.21	93.39	99.28	7.06
0.15	0.7	0.15	28.35	-2.84	-2.28	2.547	0.450	3.21	93.45	99.29	7.24
0.1	0.8	0.1	27.90	-3.01	-2.01	2.697	0.300	3.21	93.50	99.30	7.41
0.05	0.9	0.05	27.45	-3.18	-1.75	2.847	0.150	3.20	93.56	99.31	7.59
0.1	0.45	0.45	34.20	-1.53	-4.40	1.648	1.349	3.19	93.87	99.40	6.36
0.2	0.4	0.4	32.40	-1.81	-3.93	1.798	1.199	3.20	93.62	99.35	6.46
0.3	0.35	0.35	30.60	-2.09	-3.45	1.948	1.049	3.21	93.35	99.29	6.56
0.4	0.3	0.3	28.80	-2.37	-2.98	2.098	0.900	3.22	93.05	99.22	6.66
0.5	0.25	0.25	27.00	-2.65	-2.51	2.248	0.750	3.23	92.72	99.15	6.75
0.6	0.2	0.2	25.20	-2.93	-2.05	2.398	0.600	3.24	92.44	99.07	6.84
0.7	0.15	0.15	23.40	-3.19	-1.60	2.548	0.450	3.25	92.14	98.98	6.92
0.8	0.1	0.1	21.60	-3.46	-1.15	2.698	0.300	3.27	91.80	98.88	6.99
0.9	0.05	0.05	19.80	-3.71	-0.71	2.848	0.150	3.28	91.40	98.76	7.06

Table F.2 The results of integrated system of single-step of hydrotreating and PSR with various selectivity of DO reaction pathways from triolein. (*Continued*).

Selectivity of DO			Heating	Cooling	Utility	Electricity	MER	Total MER	Thermal efficiency	Total efficiency
DCO ₂	HDCO	HDO	(MJ/h)	(MJ/h)	(MJ/h)	(kW)	(MJ/h)	(MJ/h)	(%)	(%)
1	0	0	1,692	2,400	4,092	212	1,379	3,356	95.47	86.73
0	1	0	1,573	2,658	4,232	321	1,210	4,449	94.62	84.16
0	0	1	1,614	3,733	5,348	450	2,119	8,153	95.39	80.95
0.5	0.5	0	1,639	2,547	4,186	272	1,271	3,910	95.10	85.41
0.5	0	0.5	1,661	3,092	4,753	340	1,660	5,733	95.44	83.70
0	0.5	0.5	1,594	3,197	4,791	386	1,617	6,246	95.04	82.59
0.45	0.45	0.1	1,637	2,669	4,306	292	1,333	4,327	95.14	84.93
0.4	0.4	0.2	1,635	2,789	4,424	310	1,406	4,743	95.17	84.46
0.35	0.35	0.3	1,633	2,908	4,542	328	1,485	5,159	95.20	84.01
0.3	0.3	0.4	1,631	3,059	4,690	345	1,562	5,574	95.22	83.57
0.25	0.25	0.5	1,629	3,145	4,774	363	1,640	5,988	95.25	83.14
0.2	0.2	0.6	1,625	3,263	4,889	380	1,718	6,404	95.28	82.72
0.15	0.15	0.7	1,622	3,381	5,003	398	1,795	6,818	95.31	82.31
0.1	0.1	0.8	1,619	3,499	5,117	415	1,880	7,240	95.33	81.89
0.05	0.05	0.9	1,616	3,616	5,233	433	2,000	7,697	95.36	81.41
0.45	0.1	0.45	1,652	3,049	4,701	338	1,615	5,601	95.38	83.75
0.4	0.2	0.4	1,644	3,006	4,650	336	1,571	5,470	95.30	83.80
0.35	0.3	0.35	1,636	2,962	4,598	334	1,525	5,340	95.23	83.85
0.3	0.4	0.3	1,627	2,919	4,546	332	1,480	5,210	95.15	83.90
0.25	0.5	0.25	1,618	2,875	4,494	331	1,435	5,082	95.07	83.94
0.2	0.6	0.2	1,610	2,832	4,442	329	1,390	4,953	94.99	83.99
0.15	0.7	0.15	1,601	2,789	4,389	327	1,346	4,827	94.90	84.03
0.1	0.8	0.1	1,592	2,745	4,337	325	1,300	4,700	94.81	84.08
0.05	0.9	0.05	1,583	2,702	4,284	323	1,255	4,574	94.72	84.12
0.1	0.45	0.45	1,606	3,123	4,729	370	1,586	5,962	95.09	82.96
0.2	0.4	0.4	1,618	3,048	4,666	354	1,554	5,677	95.14	83.35
0.3	0.35	0.35	1,629	2,973	4,602	339	1,521	5,391	95.19	83.73
0.4	0.3	0.3	1,640	2,897	4,537	323	1,488	5,106	95.24	84.13
0.5	0.25	0.25	1,650	2,821	4,471	308	1,454	4,820	95.29	84.53
0.6	0.2	0.2	1,660	2,744	4,404	290	1,434	4,533	95.33	84.94
0.7	0.15	0.15	1,670	2,664	4,334	272	1,418	4,243	95.37	85.37
0.8	0.1	0.1	1,652	2,581	4,233	253	1,429	3,977	95.41	85.75
0.9	0.05	0.05	1,686	2,493	4,179	233	1,391	3,655	95.44	86.26

Table F.3 The results of integrated system of two-step of hydrotreating and GSR with various selectivity of DO reaction pathways from tripalmitin.

Selectivity of DO		Initial Feed			Net H ₂ O	Net H ₂	C ₁₅ H ₃₂ in BHD	C ₁₆ H ₃₄ in BHD	BHD	BHD purity (mol%)	BHD purity (wt.%)	Off-gas (kmol/h)
DCO ₂	HDCO	HDO	H ₂									
1	0	0	1.35	-5.63	5.22	2.921	0.000	3.69	79.17	95.04	6.57	
0	1	0	9.00	-2.72	1.82	2.921	0.000	3.00	97.31	99.81	7.75	
0	0	1	27.00	0.18	-5.26	0.000	2.921	2.98	97.89	99.97	6.10	
0.5	0.5	0	4.50	-4.17	3.59	2.921	0.000	3.21	90.91	98.29	7.22	
0.5	0	0.5	13.50	-2.72	0.04	1.460	1.460	3.11	93.97	99.09	6.50	
0	0.5	0.5	18.00	-1.27	-1.72	1.460	1.460	2.99	97.70	99.91	6.93	
0.45	0.45	0.1	6.75	-3.74	2.70	2.629	0.292	3.15	92.60	98.72	7.14	
0.4	0.4	0.2	9.00	-3.30	1.81	2.337	0.584	3.11	93.81	99.02	7.05	
0.35	0.35	0.3	11.25	-2.87	0.93	2.045	0.876	3.08	94.74	99.25	6.95	
0.3	0.3	0.4	13.50	-2.43	0.04	1.752	1.168	3.06	95.47	99.42	6.84	
0.25	0.25	0.5	15.75	-2.00	-0.84	1.460	1.460	3.04	96.06	99.56	6.72	
0.2	0.2	0.6	18.00	-1.56	-1.73	1.168	1.753	3.03	96.55	99.67	6.60	
0.15	0.15	0.7	20.25	-1.13	-2.61	0.876	2.045	3.01	96.96	99.76	6.48	
0.1	0.1	0.8	22.50	-0.69	-3.49	0.584	2.337	3.00	97.32	99.84	6.35	
0.05	0.05	0.9	24.75	-0.26	-4.37	0.292	2.629	2.99	97.62	99.91	6.23	
0.45	0.1	0.45	13.05	-2.72	0.22	1.606	1.314	3.10	94.27	99.15	6.62	
0.4	0.2	0.4	12.60	-2.72	0.40	1.752	1.168	3.09	94.58	99.22	6.75	
0.35	0.3	0.35	12.15	-2.72	0.57	1.899	1.022	3.08	94.90	99.29	6.87	
0.3	0.4	0.3	11.70	-2.72	0.75	2.045	0.876	3.07	95.22	99.35	7.00	
0.25	0.5	0.25	11.25	-2.72	0.93	2.191	0.730	3.06	95.54	99.42	7.12	
0.2	0.6	0.2	10.80	-2.72	1.11	2.337	0.584	3.05	95.88	99.50	7.25	
0.15	0.7	0.15	10.35	-2.72	1.28	2.483	0.438	3.04	96.22	99.57	7.37	
0.1	0.8	0.1	9.90	-2.72	1.46	2.629	0.292	3.02	96.58	99.65	7.50	
0.05	0.9	0.05	9.45	-2.72	1.64	2.775	0.146	3.01	96.94	99.72	7.62	
0.1	0.45	0.45	16.20	-1.71	-1.02	1.607	1.314	3.01	97.04	99.77	6.93	
0.2	0.4	0.4	14.40	-2.14	-0.31	1.753	1.168	3.03	96.27	99.60	6.93	
0.3	0.35	0.35	12.60	-2.58	0.40	1.899	1.022	3.06	95.35	99.39	6.92	
0.4	0.3	0.3	10.80	-3.01	1.10	2.045	0.876	3.10	94.23	99.13	6.90	
0.5	0.25	0.25	9.00	-3.45	1.81	2.191	0.730	3.15	92.85	98.80	6.88	
0.6	0.2	0.2	7.20	-3.88	2.52	2.337	0.584	3.21	91.09	98.37	6.83	
0.7	0.15	0.15	5.40	-4.32	3.23	2.483	0.438	3.29	88.73	97.77	6.77	
0.8	0.1	0.1	3.60	-4.75	3.94	2.629	0.292	3.42	85.38	96.87	6.66	
0.9	0.05	0.05	1.80	-5.19	4.65	2.774	0.146	3.65	80.00	95.31	6.44	

Table F.3 The results of integrated system of two-step of hydrotreating and GSR with various selectivity of DO reaction pathways from tripalmitin. (*Continued*).

Selectivity of DO		Heating	Cooling	Utility	Electricity	MER	Total MER	Thermal efficiency	Total efficiency
DCO ₂	HDCO	HDO	(MJ/h)	(MJ/h)	(kW)	(MJ/h)	(MJ/h)	(%)	(%)
1	0	0	3,212	3,224	64	3,560	2,895	96.12	84.21
0	1	0	3,337	3,560	121	3,488	4,148	93.37	80.73
0	0	1	3,186	4,440	248	2,634	6,117	93.87	80.95
0.5	0.5	0	3,274	3,375	88	3,535	3,476	94.80	82.58
0.5	0	0.5	3,186	3,814	154	3,104	4,479	94.91	82.28
0	0.5	0.5	3,186	3,932	185	3,354	5,433	93.58	80.02
0.45	0.45	0.1	3,235	3,455	105	3,444	3,747	94.68	82.32
0.4	0.4	0.2	3,196	3,533	121	3,353	4,014	94.56	82.08
0.35	0.35	0.3	3,186	3,642	138	3,261	4,281	94.44	81.84
0.3	0.3	0.4	3,186	3,759	154	3,171	4,548	94.32	81.60
0.25	0.25	0.5	3,186	3,874	170	3,082	4,810	94.24	81.48
0.2	0.2	0.6	3,186	3,988	185	2,994	5,073	94.16	81.37
0.15	0.15	0.7	3,186	4,103	201	2,906	5,336	94.09	81.26
0.1	0.1	0.8	3,186	4,215	216	2,820	5,597	94.02	81.15
0.05	0.05	0.9	3,186	4,332	233	2,729	5,861	93.94	81.04
0.45	0.1	0.45	3,186	3,775	151	3,141	4,447	94.76	82.12
0.4	0.2	0.4	3,186	3,735	148	3,179	4,413	94.60	81.97
0.35	0.3	0.35	3,186	3,694	144	3,218	4,381	94.45	81.81
0.3	0.4	0.3	3,186	3,654	141	3,256	4,347	94.29	81.66
0.25	0.5	0.25	3,191	3,617	138	3,296	4,314	94.14	81.50
0.2	0.6	0.2	3,220	3,607	135	3,333	4,281	93.99	81.35
0.15	0.7	0.15	3,249	3,595	131	3,372	4,249	93.83	81.19
0.1	0.8	0.1	3,278	3,584	128	3,410	4,215	93.68	81.03
0.05	0.9	0.05	3,307	3,572	125	3,449	4,182	93.52	80.88
0.1	0.45	0.45	3,186	3,855	173	3,113	4,908	93.81	80.99
0.2	0.4	0.4	3,186	3,782	160	3,162	4,679	94.05	81.28
0.3	0.35	0.35	3,186	3,707	148	3,214	4,448	94.31	81.63
0.4	0.3	0.3	3,186	3,630	135	3,265	4,214	94.58	82.02
0.5	0.25	0.25	3,186	3,553	121	3,318	3,981	94.85	82.42
0.6	0.2	0.2	3,186	3,475	108	3,371	3,747	95.13	82.82
0.7	0.15	0.15	3,186	3,397	95	3,535	3,622	95.40	82.95
0.8	0.1	0.1	3,190	3,323	81	3,477	3,273	95.68	83.64
0.9	0.05	0.05	3,199	3,253	67	3,531	3,034	95.95	84.06

Table F.4 The results of integrated system of two-step of hydrotreating and GSR with various selectivity of DO reaction pathways from triolein.

Selectivity of DO		Initial Feed		Net H ₂ O	Net H ₂	C ₁₇ H ₃₆ in		C ₁₈ H ₃₈ in		BHD	BHD purity (mol%)	BHD purity (wt.%)	Off-gas (kmol/h)
DCO ₂	HDCO	HDO	H ₂			BHD	BHD	BHD	BHD				
1	0	0	9.00	-5.64	1.74	2.990	0.000	0.000	3.41	87.80	97.82	7.41	
0	1	0	18.00	-2.66	-1.85	2.990	0.000	0.000	3.07	97.36	99.87	8.36	
0	0	1	36.00	0.31	-9.04	0.000	2.990	0.000	3.06	97.85	99.97	6.62	
0.5	0.5	0	13.50	-4.15	-0.05	2.990	0.000	0.000	3.19	93.74	99.14	7.94	
0.5	0	0.5	22.50	-2.67	-3.65	1.495	1.495	1.495	3.15	95.02	99.42	7.10	
0	0.5	0.5	27.00	-1.18	-5.45	1.495	1.495	1.495	3.06	97.65	99.93	7.50	
0.45	0.45	0.1	15.75	-3.70	-0.95	2.691	0.299	0.299	3.17	94.47	99.29	7.82	
0.4	0.4	0.2	18.00	-3.26	-1.85	2.392	0.598	0.598	3.14	95.08	99.42	7.69	
0.35	0.35	0.3	20.25	-2.81	-2.75	2.093	0.897	0.897	3.13	95.60	99.53	7.57	
0.3	0.3	0.4	22.50	-2.37	-3.65	1.794	1.196	1.196	3.11	96.06	99.62	7.44	
0.25	0.25	0.5	24.75	-1.92	-4.55	1.495	1.495	1.495	3.10	96.45	99.70	7.30	
0.2	0.2	0.6	27.00	-1.48	-5.45	1.196	1.794	1.794	3.09	96.80	99.77	7.17	
0.15	0.15	0.7	29.25	-1.03	-6.34	0.897	2.093	2.093	3.08	97.10	99.83	7.03	
0.1	0.1	0.8	31.50	-0.59	-7.24	0.598	2.392	2.392	3.07	97.38	99.88	6.90	
0.05	0.05	0.9	33.75	-0.14	-8.14	0.299	2.691	2.691	3.06	97.63	99.93	6.76	
0.45	0.1	0.45	22.05	-2.67	-3.47	1.645	1.346	1.346	3.14	95.24	99.46	7.23	
0.4	0.2	0.4	21.60	-2.67	-3.29	1.794	1.196	1.196	3.13	95.46	99.50	7.35	
0.35	0.3	0.35	21.15	-2.67	-3.11	1.944	1.047	1.047	3.13	95.69	99.55	7.48	
0.3	0.4	0.3	20.70	-2.66	-2.93	2.093	0.897	0.897	3.12	95.91	99.59	7.61	
0.25	0.5	0.25	20.25	-2.66	-2.75	2.243	0.748	0.748	3.11	96.14	99.64	7.73	
0.2	0.6	0.2	19.80	-2.66	-2.57	2.392	0.598	0.598	3.10	96.38	99.68	7.86	
0.15	0.7	0.15	19.35	-2.66	-2.39	2.542	0.449	0.449	3.09	96.62	99.73	7.98	
0.1	0.8	0.1	18.90	-2.66	-2.21	2.691	0.299	0.299	3.09	96.86	99.78	8.11	
0.05	0.9	0.05	18.45	-2.66	-2.03	2.841	0.150	0.150	3.08	97.11	99.82	8.24	
0.1	0.45	0.45	25.20	-1.63	-4.73	1.645	1.346	1.346	3.08	97.16	99.84	7.51	
0.2	0.4	0.4	23.40	-2.07	-4.01	1.794	1.196	1.196	3.10	96.61	99.73	7.51	
0.3	0.35	0.35	21.60	-2.52	-3.29	1.944	1.047	1.047	3.12	95.99	99.61	7.52	
0.4	0.3	0.3	19.80	-2.96	-2.57	2.093	0.897	0.897	3.14	95.28	99.47	7.52	
0.5	0.25	0.25	18.00	-3.41	-1.85	2.243	0.748	0.748	3.16	94.48	99.30	7.52	
0.6	0.2	0.2	16.20	-3.85	-1.13	2.392	0.598	0.598	3.20	93.56	99.11	7.52	
0.7	0.15	0.15	14.40	-4.30	-0.41	2.542	0.449	0.449	3.23	92.48	98.88	7.51	
0.8	0.1	0.1	12.60	-4.75	0.30	2.691	0.299	0.299	3.28	91.21	98.60	7.49	
0.9	0.05	0.05	10.80	-5.19	1.02	2.841	0.150	0.150	3.33	89.68	98.26	7.46	

Table F.4 The results of integrated system of two-step of hydrotreating and GSR with various selectivity of DO reaction pathways from triolein. (*Continued*).

Selectivity of DO		Heating	Cooling	Utility	Electricity	MER	Total MER	Thermal efficiency	Total efficiency
DCO ₂	HDCO	HDO	(MJ/h)	(MJ/h)	(kW)	(MJ/h)	(MJ/h)	(%)	(%)
1	0	0	3,203	3,660	124	3,114	3,811	96.70	85.60
0	1	0	3,203	3,895	187	3,023	5,148	94.16	82.41
0	0	1	3,203	4,972	313	2,142	7,108	94.70	82.86
0.5	0.5	0	3,203	3,780	156	3,066	4,483	95.39	83.89
0.5	0	0.5	3,203	4,324	219	2,631	5,470	95.64	84.07
0	0.5	0.5	3,203	4,440	250	2,589	6,136	94.44	82.63
0.45	0.45	0.1	3,203	3,901	172	2,974	4,748	95.32	83.77
0.4	0.4	0.2	3,203	4,021	188	2,883	5,012	95.24	83.66
0.35	0.35	0.3	3,203	4,140	203	2,794	5,274	95.17	83.56
0.3	0.3	0.4	3,203	4,262	219	2,701	5,539	95.10	83.45
0.25	0.25	0.5	3,203	4,382	235	2,609	5,802	95.03	83.35
0.2	0.2	0.6	3,203	4,502	250	2,519	6,066	94.96	83.24
0.15	0.15	0.7	3,203	4,619	266	2,430	6,327	94.90	83.15
0.1	0.1	0.8	3,203	4,742	282	2,335	6,591	94.83	83.04
0.05	0.05	0.9	3,203	4,863	297	2,244	6,855	94.77	82.94
0.45	0.1	0.45	3,203	4,281	216	2,670	5,438	95.49	83.91
0.4	0.2	0.4	3,203	4,238	213	2,710	5,407	95.35	83.74
0.35	0.3	0.35	3,203	4,194	209	2,751	5,373	95.20	83.58
0.3	0.4	0.3	3,203	4,153	207	2,788	5,342	95.05	83.41
0.25	0.5	0.25	3,203	4,110	203	2,827	5,310	94.90	83.24
0.2	0.6	0.2	3,203	4,068	200	2,866	5,279	94.75	83.07
0.15	0.7	0.15	3,203	4,025	197	2,905	5,247	94.61	82.91
0.1	0.8	0.1	3,203	3,981	194	2,946	5,213	94.46	82.74
0.05	0.9	0.05	3,203	3,938	190	2,985	5,181	94.31	82.58
0.1	0.45	0.45	3,203	4,360	237	2,643	5,902	94.65	82.90
0.2	0.4	0.4	3,203	4,285	225	2,692	5,672	94.86	83.16
0.3	0.35	0.35	3,203	4,207	213	2,745	5,441	95.08	83.43
0.4	0.3	0.3	3,203	4,130	200	2,797	5,210	95.29	83.70
0.5	0.25	0.25	3,203	4,053	188	2,848	4,977	95.52	83.98
0.6	0.2	0.2	3,203	3,974	175	2,902	4,745	95.74	84.26
0.7	0.15	0.15	3,203	3,898	163	2,952	4,514	95.96	84.54
0.8	0.1	0.1	3,203	3,820	150	3,005	4,281	96.20	84.86
0.9	0.05	0.05	3,203	3,740	137	3,059	4,047	96.45	85.23

APPENDIX G

Lower heating value

The lower heating value of fuel was defined as amount of heat release from fuel combustion at 25 °C of initial temperature and returning the temperature at 150 °C, which the latent heat of vaporization of water is not recovery. Aspen plus⁷¹ was used for simulation in order to define lower heating value of fuel and compared to literature review⁶⁰⁻⁶¹. However, literature review reported lower heating value of diesel, BHD and palm oil equal 43.1 MJ/kg⁷⁸, 42-44 MJ/kg⁶ and 36.543 MJ/kg⁷⁹, respectively.

Table G.1 Lower heating value of fuel.

Fuel	Lower heating value (LHV)	
	(MJ/kg)	(MJ/kmol)
Tripalmitin	36.28	29,242.75
Triolein	40.44	32,592.17
C ₁₅ H ₃₂	43.39	9,199.50
C ₁₆ H ₃₄	43.36	9,799.62
C ₁₇ H ₃₆	43.34	10,400.88
C ₁₈ H ₃₈	43.31	11,001.93
H ₂	118.79	237.57

APPENDIX H

Heat integration of integrated system

H.1 Example of heat integration of integrated system of single-step of hydrotreating and propane steam reforming with decarboxylation pathway from tripalmitin

Energy loads in each of the heat exchangers are presented in Table H.1. Summarization of temperature and heat recovery is presented in Table H.2. Heat exchanger network and heat flow after heat integration of the integrated system of single-step of hydrotreating and PSR from tripalmitin are shown in Figure H.1. Heat integration can recover heat equal to 1,355.7 MJ/h, which presents a 71% saving and the remaining required utility equals 1,081.7 MJ/h.

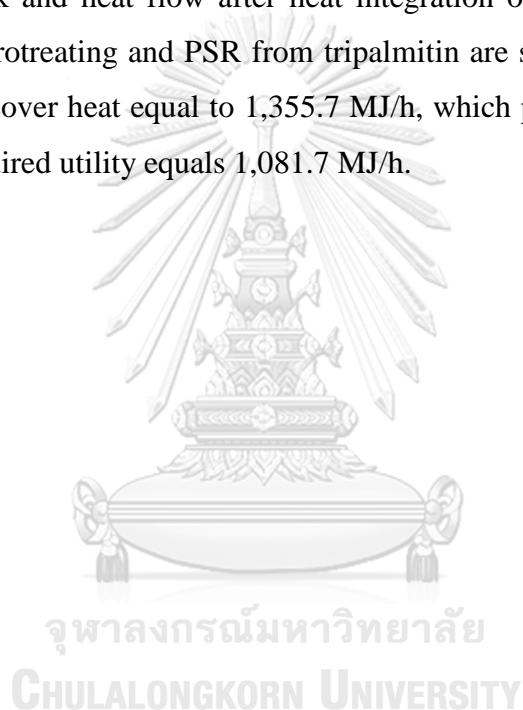


Table H.1 Energy loads in each of heat exchangers of integrated system of single-step of hydrotreating and PSR from tripalmitin.

No.	Heat exchanger	Stream name	Type	Inlet temperature (°C)	Outlet temperature (°C)	mCp (MJ/°C.h)	Enthalpy (MJ/h)
1	CL-1	S3	Hot	977.4	300.0	0.27	183.1
2	CL-2	S8	Hot	296.3	117.0	2.49	445.5
3	CL-3	S10	Hot	117.0	30.0	0.37	32.0
4	CL-7	PD-4	Hot	677.0	40.0	1.10	698.1
5	CL-8	S59	Hot	596.5	30.0	0.44	250.3
6	HT-1	S4	Cold	29.0	300.0	1.88	510.5
7	HT-6	S52	Cold	24.3	677.0	1.29	845.1
8	R-101	SM1	Hot	300.0	299.5	850.35	425.2
9	R-104	S53	Cold	677.0	677.5	806.50	403.2
Total							3,793.2

Table H.2 Summarization of temperature and heat recovery for each of heat exchangers after heat integration of integrated system of single-step of hydrotreating and PSR from tripalmitin.

No.	Heat exchanger	Hot stream	Cold stream	Hot inlet temperature (°C)	Hot outlet temperature (°C)	Cold inlet temperature (°C)	Cold outlet temperature (°C)	Load (MJ/h)
1	E-101	S3	S52	977.4	635.7	605.7	677.0	92.4
2	E-102	PD-4	S52	677.0	66.6	24.3	609.1	668.9
3	E-103	PD-4	Cooling utility	66.6	40.0			29.2
4	E-104	S3	S52	635.7	325.5	24.3	580.0	83.8
5	E-105	S8	Cooling utility	296.3	117.0			445.5
6	E-106	S59	S4	596.5	403.4	254.7	300.0	85.3
7	E-107	S59	Cooling utility	403.4	30.0			165.0
8	E-108	S10	Cooling utility	117.0	30.0			32.0
9	E-109	SM1	S4	300.0	299.5	29.0	254.7	425.2
10	E-110	Heating utility	S53			677.0	677.5	403.2
11	E-111	S3	Cooling utility	325.5	300.0			6.9
Heat recovery								
Heating utility								
Cooling utility								
Total utility								
Saving (%)								
								1,355.7
								403.2
								678.5
								1,081.7
								71.5

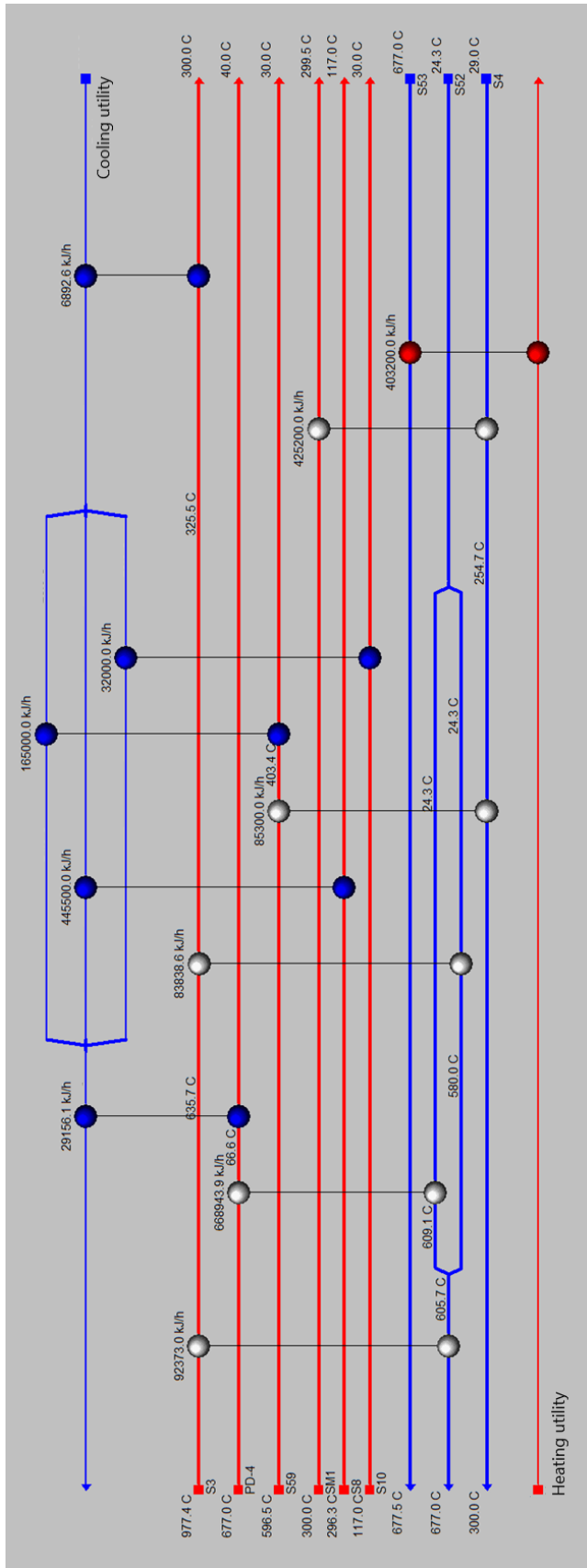


Figure H.1 Heat exchanger network and heat flow after heat integration of integrated system of hydrotreating and PSR from tripalmitin; (1) hot stream = red; (2) cold stream = blue.

H.2 Example of heat integration of integrated system of single-step of hydrotreating and propane steam reforming with decarboxylation pathway from triolein

Energy loads in each of the heat exchangers are presented in Table H.3. Summarization of temperature and heat recovery is presented in Table H.4. Heat exchanger network and heat flow after heat integration of the integrated system of single-step of hydrotreating and PSR from triolein are shown in Figure H.2. Heat integration can recover heat equal to 1,342.5 MJ/h, which presents a 66% saving and the remaining required utility equals 1,407.2 MJ/h.



Table H.3 Energy loads in each of heat exchangers of integrated system of single-step of hydrotreating and PSR from triolein.

No.	Heat exchanger	Stream name	Type	Inlet temperature (°C)	Outlet temperature (°C)	mCp (MJ/°C.h)	Enthalpy (MJ/h)
1	CL-1	S3	Hot	951.4	300.0	0.54	351.7
2	CL-2	S8	Hot	297.3	126.0	2.80	480.5
3	CL-3	S10	Hot	126.0	30.0	0.55	52.4
4	CL-7	PD-4	Hot	677.0	40.0	1.21	768.4
5	CL-8	S59	Hot	604.9	30.0	0.49	281.5
6	HT-1	S4	Cold	28.6	300.0	1.19	322.7
7	HT-6	S52	Cold	24.9	677.0	1.42	928.5
8	R-101	SM1	Hot	300.0	299.5	931.57	465.8
9	R-104	S53	Cold	677.0	677.5	881.21	440.6
Total							4,092.0

Table H.4 Summarization of temperature and heat recovery for each of heat exchangers after heat integration of integrated system of single-step of hydrotreating and PSR from triolein.

No.	Heat exchanger	Hot stream	Cold stream	Hot inlet temperature (°C)	Hot outlet temperature (°C)	Cold inlet temperature (°C)	Cold outlet temperature (°C)	Load (MJ/h)
1	E-201	S3	S52	951.4	715.0	665.1	677.0	16.9
2	E-202	S3	S53	951.4	756.5	677.0	677.4	91.3
3	E-203	PD-4	S52	677.0	241.8	159.6	647.1	525.0
4	E-204	PD-4	Cooling utility	241.8	40.0			243.4
5	E-205	S59	Cooling utility	604.9	30.0			281.5
6	E-206	S10	Cooling utility	126.0	30.0			52.4
7	E-207	S3	S4	751.0	335.9	259.0	300.0	48.7
8	E-208	S3	S52	751.0	290.0	159.6	721.0	194.8
9	E-209	S8	Cooling utility	297.3	126.0	-25.0	-24.2	480.5
10	E-210	SM1	S52	300.0	299.8	24.9	159.6	191.8
11	E-211	Heating utility	S53			677.0	677.5	349.3
12	E-212	SM1	S4	299.8	299.5	28.6	259.0	274.0
Heat recovery								
Heating utility								
Cooling utility								
Total utility								
Saving (%)								
								1,342.5
								349.3
								1,057.8
								1,407.2
								65.6

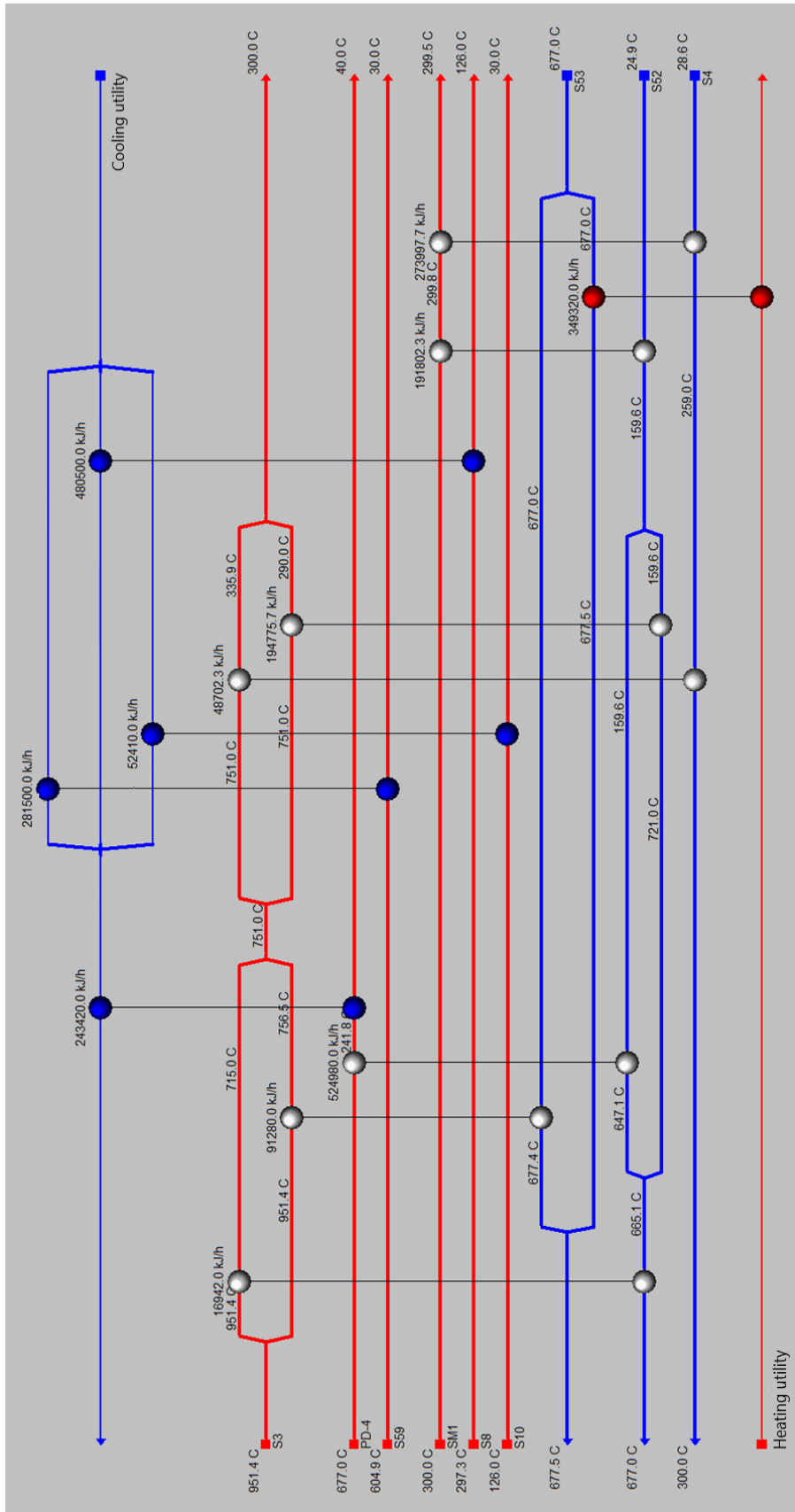


Figure H.2 Heat exchanger network and heat flow after heat integration of integrated system of single-step of hydrotreating and PSR from triolein; (1) hot stream = red; (2) cold stream = blue.

VITA

NAME Miss Siriporn Boonsuk

DATE OF BIRTH 26 January 1990

PLACE OF BIRTH Prachin Buri

INSTITUTIONS ATTENDED Chulalongkorn University

HOME ADDRESS 192 Tadsanavitee road, Tumbon Namuang, Aumphur Muang,
Prachin Buri, 25000

PUBLICATION The 2018 Pure and Applied Chemistry International Conference
(PACCON 2018) : DESIGN AND PERFORMANCE
EVALUATION OF SUSTAINABLE PROCESS COMBINING
HYDROTREATING AND HYDROGEN GENERATION FOR
BIOJET FUEL PRODUCTION FROM PALM OIL



จุฬาลงกรณ์มหาวิทยาลัย
CHULALONGKORN UNIVERSITY